UNIVERSITÀ DI PARMA

Dottorato di Ricerca in

Scienze della Terra

Ciclo XXX

Magmatic processes within the plumbing system of the Marsili seamount (Southern Tyrrhenian Sea): constraints from the phenocryst cargo of the sampled lavas

Coordinatore: Prof. Fulvio Celico

Relatore: Prof. Teresa Trua

Correlatore: Prof. Andrea Marzoli

Studente:

José Virgilio Correia da Fonseca

Abstract

This dissertations represents the work developed during the three years of the PhD program. The aim of the project was the study of the Marsili basalts and their phenocryst cargo to further characterise the plumbing system of this large volcano and consequently to give further insights into the dynamics occurring in a back-arc basin context.

A variable number of magmatic reservoirs was identified for each sample and the complexity of these magmatic structures is described through the interactions between the products of each reservoir (i.e. magmatic crystals and magmas). The samples showing a larger compositional range for both olivine and clinopyroxene crystals suggest that the magmatic plumbing systems are made of heterogeneous mushes, where the crystals record the input of magmas with variable differentiation degrees and within variable timescales.

Most primitive olivine crystals overlap the compositions related to a peridotitic source, while only few crystals show deviated compositions towards the pyroxenitic end-member. Overall, the variations found for the Marsili olivine crystals overlap those from the Aeolian Arc (Zamboni et al. 2017). However, magma composition and diffusional reequilibration due to magma mixing may have significantly influenced the olivine compositions.

The trace element compositions from the clinopyroxene crystals overlap the previous published data, with one sample showing OIB-like compositions, and the other three samples overlapping with the IAB compositions. However, two of the IAB basalts contain clinopyroxene crystals with variable LREE/HREE, suggesting that the two compound may have fed these two magmatic systems, although in significantly different proportions.

Geospeedometry tests show that most of the samples are lavas that carried olivine crystals with variable residence times. Samples show variable re-equilibrium periods, where the larger ranges are found for samples within the ridge's summit (from few days to a decade). Moreover, the olivine crystals from the samples with more differentiated compositions have compositional profiles with similar zoning patterns and lower variable re-equilibrium periods, varying from 100 to 300 days, suggesting that in these relatively acid systems the magma inputs are less frequent.

Contents

Introduction

Volcanology

Since early human times, societies with variable cultural and religious background have been fascinated by volcanic activity due to its magnificence and the risks it represents. The great agricultural potential of volcanic fields allow the prosper of several cultures, despite the hazardous environment. As a consequence of this interest in volcanic areas, many years of volcanological observations lead us to the understanding that the volcanoes are one of the most complex and fascinating natural events.

Volcanos are a marvellous and dangerous expression of thermal energy release from the Earth's interior, which is an evidence of the dynamic system that is Earth. The distribution of the volcanos on the Earth's surface generally follow the tectonic plate boundaries, where divergent or convergent forces generate specific geodynamic environments. These different stress fields reflect the mechanical behaviour on the lithosphere, which is the relatively thin rigid layer representing the outer solid shell of the planet (Moores & Twiss, 1995). The lithosphere is constituted by the crust and upper mantle.

Oceanic crust is mainly formed at mid-ocean ridges (MORs). This geodynamic environment is responsible for the highest magma and crust production and occurs along divergent plate boundaries (Paterson and Ducea, 2015). In this environment, the lithosphere is thin due to the high thermal gradients and strong extensional rate. Consequently, the mantle rocks, generally of peridotitic composition, melt due to high temperatures at anomalously low pressures. This process is called decompression melting (Winter, 2010) and is intrinsically associated with MORs volcanism. Along the constructive boundaries, the fissural volcanism is the most recurrent, especially those within oceanic crust. As new lithosphere is formed, it is pushed away from the ridge by ridge push forming a symmetric pattern (Moores & Twiss,1995; Turcotte & Schubert, 2002). While newly formed lithosphere is hot, it cools down, and it thickens, as it is pushed away from the MOR. Since the volume of the earth is constant, the older lithosphere needs to be destroyed. The older lithosphere is denser than the asthenosphere below, making it negatively buoyant. When the lithosphere starts to sink, a subduction zone is formed. This zone that separates two plates of different age or composition is called a destructive boundary. (Turcotte & Schubert, 2002). Above the subducted slab, the fluids released from it move towards shallower depths and interact with the mantle wedge, this will lead to locally lowering the solidus (fusion temperature) of the mantle rocks and melting them.

These magmas move upwards due to their positive buoyancy and form the arc volcanism. The volcanoes located above the subduction zone are usually parallel to the trench. Depending on how the subducted slab sinks, local divergent forces may induce the opening of new basins behind the arcs, called back-arc basins. Here, as in the MORs, new oceanic crust may form, possibly creating new plate.

Subduction zones are the second biggest producer of magma, right after the mid ocean ridge systems. The mechanisms responsible for the eruption of the magmas in the subductions zones are significantly different from the MORs. While the magma production on the later depend mainly on the mantle rocks exhumation due to convection, the arc volcanism depends on the magma production due the presence of relatively anomalous quantities of fluids in the mantle. It is important to say that part of the magmas produced in the mantle do not erupt. A recent study estimated that only less than 10% of the magmas produced in intra-oceanic arcs and mid-ocean ridges erupt (Paterson and Ducea, 2015). This means that most of the magmas are stored within the crust. The storage in the mid-ocean ridge systems contributes mainly for the creation of new lithosphere due to the ridge push. In contrast, in the arc settings, the distribution of the ascending magmas does not depend significantly on diverging forces, vertical accretion of the crust occurs and consequently the volcanic islands rise.

Magmatic systems' dynamics

The plumbing systems that feed the volcanos might differ from one geodynamic context to another. Their mechanisms depend on variables such as the magma production rates, crustal thickness and the stress fields. Therefore, it is important to understand the structure of the volcanic feeding system, which is one of the most discussed topics in geology.

Geophysical studies about the structure of sub-volcanic systems have failed to demonstrate the existence of big reservoirs, mainly filled with magma. Moreover, physical models show that this kind of melt-rich reservoirs are difficult to form and maintain (Cashman et al. 2017; references therein). However, the anomalous seismic velocities that characterize the mid to lower-crust below volcanoes are suggested to be a consequence of magma accumulation in the form of sills, dykes and possible melt-rich reservoirs (Lees, 2007). Furthermore, studies of continental arc systems suggest that the presence of approximately 10% of melt within the crust can explain the low velocities registered below the volcanoes (e.g. Huang et al., 2015; Kiser et al., 2016). These environments with low percentages of melt are thought to correspond to magma mushes (Crystal mushes are crystal networks through which melt is distributed), as first suggested by Marsh (1996) for the Hawaiian plumbing system. They are dynamic multiphase systems that

depend on the mafic magma input, magma segregation and heat loss (e.g. Cashman et al., 2017; Cooper, 2017). More recently, with the combined results from geophysics, petrology and geochemistry, the feeding systems below the volcanoes are thought to be

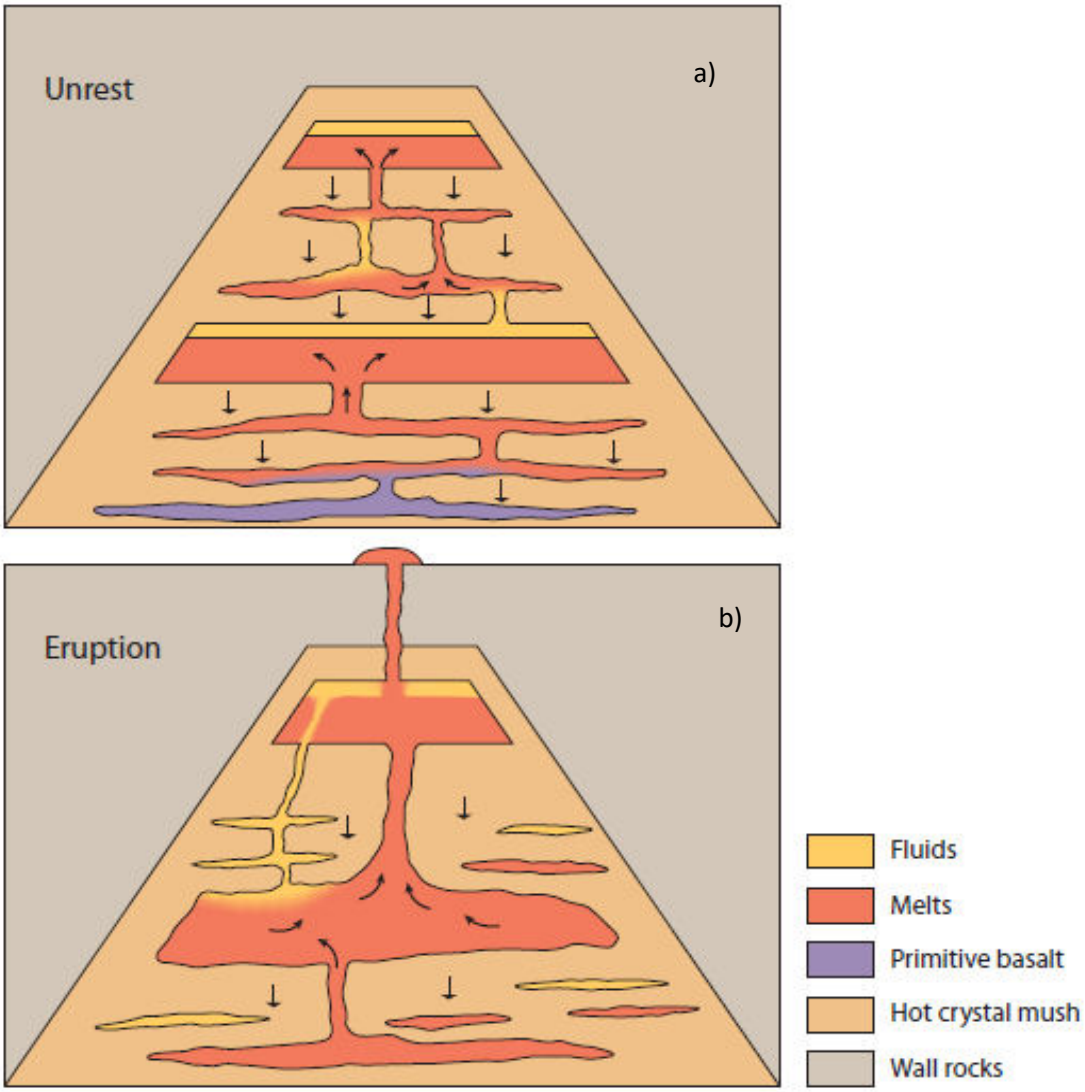

Fig. 1 - Schematic cartoon of transcrustal magmatic mush system. a) Unrest state: magmatic dynamics responsible for differentiation processes between the reservoirs within the system; b) Eruption state: destabilization of the system leads to eruption of the magmas. Adapted from Sparks and Cashman (2017).

transcrustal (Cashman et al., 2017; Sparks and Cashman, 2017). According to this model, mushes storage the magmas underneath the volcanoes, which is consistent with the general absence of large magma chambers (Fig. 1).

Annen et al. (2015) suggest that mushes result from the differentiation of melts transported within the crust by complexes of dykes and sills, and they ultimately may connect and initiate an erupt. If these mushes are not continuously fed or if they do not connect with other magma bodies, they will form plutons. Magma eruptions generally result from magma segregation from deep reservoirs and/or mush disruption, which may carry mush fragments

(antecrysts, glomerocrysts) to the surface. Kahl et al. (2011) described the magmatic dynamics below Etna as interactions between different reservoirs prior to eruption. These assumption were based on melt and olivine compositions, which shows the variability of compositions as a consequence of post-mixing diffusive re-equilibration. These kind of olivine antecrysts and glomerocrysts are a proxy of the open system character of such magmatic systems. The transcrustal plumbing system model also can explain the formation of batholitic bodies in more silicic systems, by the assemblage of small incremental magma batches over millions of years.

The timescale of these processes have been studied in the last decades (Fig. 2) (e.g. Hawkesworth et al., 2004; Turner and Costa, 2007; Zellmer et al., 2011) and the results, together with geophysical studies, are now available to create models that are consistent with the activity of the volcanoes (e.g. Kahl et al., 2015; Viccaro et al., 2016). The timescale studies are based on two main technics: U-series studies (e.g. Turner et al., 2003); and also, major and trace elements and isotopic diffusion through crystal lattice (e.g. Costa et al., 2008). Each technic gives insight about different timescales. While the U-series decay suggests that magmatic systems usually present crustal activity of 10^3 to 10^5 years (e.g. Hawkesworth et al., 2004; Turner and Costa, 2007), diffusion studies generally show significantly smaller ages, in the order of days to years, which might represent the magma mixing events prior to eruption.

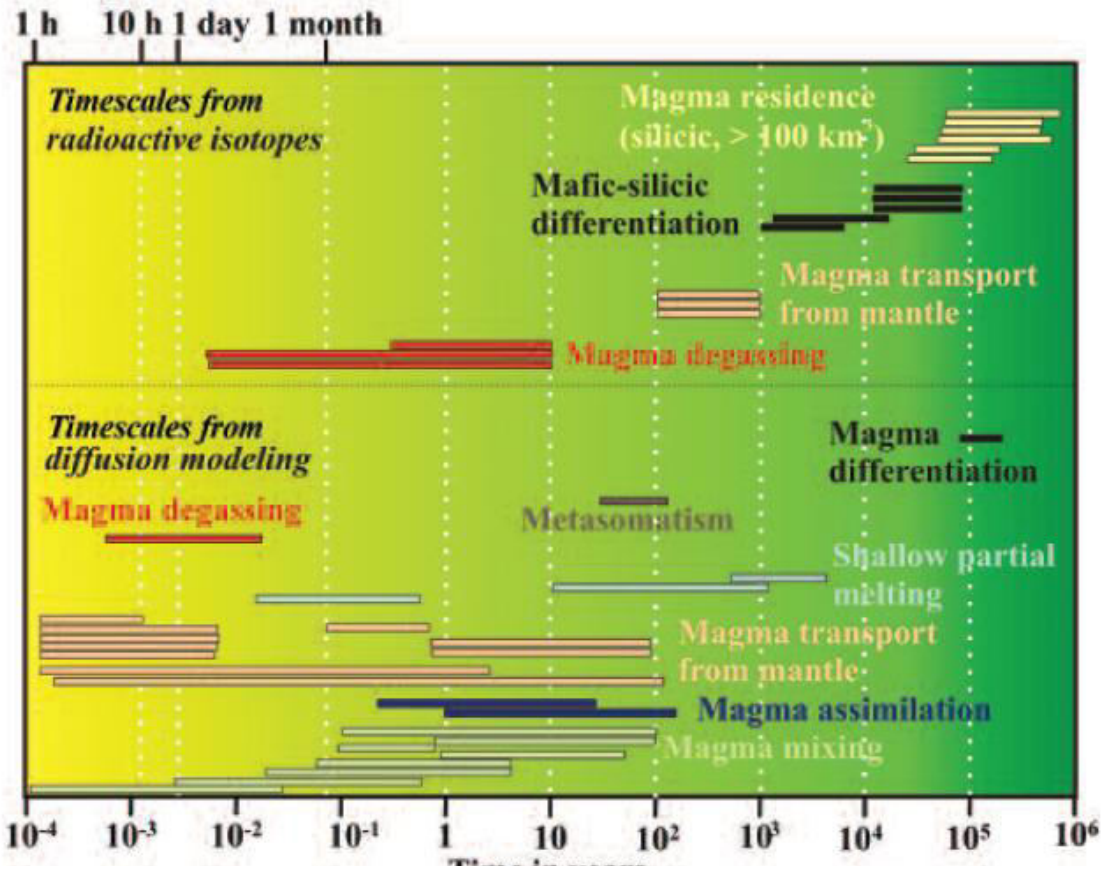

Fig. 2 - Summary of the timescales determined from radioactive isotopes and from diffusion modelling for different magmatic processes. Adapted from Turner & Costa, 2007.

The study of the physical, chemical and temporal dynamics within magmatic systems give further perspectives of how these natural systems work. Moreover, these studies contribute directly to the characterization of the variable geodynamic environments and possible transition cases. The Marsili volcano might indeed be one of these cases, and thus, the description and characterization of this magmatic structure in a complex geodynamic context is one of the main motivation for the work presented in this thesis.

Geological Setting

From the Oligocene, the convergence rate between the Africa and Eurasia plates was slower than the extension rate caused by the subduction of the Africa plate (Fig. 3). After the formation of the Alpine Orogen, the subduction trench started to retreat towards south and the back-arc extension started at ~ 30 Ma with the opening of the Liguro - Provençal basin in the central Mediterranean Sea (e.g., Kastens et al., 1988; Faccenna et al., 2004; Panza et al., 2007; Chiarabba et al., 2008). This phase of the extension was active until ~ 16 Ma and caused the asymmetrical opening of the basin and the counterclockwise ~ 40° rotation of the Sardinia-Corsica block, creating a triangular-shaped basin. Furthermore, the first eruption of a calcalkaline magmas occurred within this basin margins (e.g., Panza et al., 2007). The end of this first opening phase came with the collision with the Adria-Apulian plate and formation of the Apennine Orogen (Chiarabba et al., 2017; references therein).

After the rotation of the Sardinian block, the Calabrian block started drifting apart at 12-10 Ma (Kastens et al., 1988; Faccenna et al., 2014). During this second extension phase the first opening of the Tyrrhenian basin occurs. From 10 to 5 Ma the E-W back-arc extension caused drifting and further oceanization in the Vavilov basin (6 – 4 Ma; Kastens et al., 1988). This phase was mostly controlled by the rupture of the subducted slab below the Sicily channel (Faccenna et al., 2004), which lead to a faster consumption of the Ionian slab relatively to the African slab. The tearing also caused the entering of African mantle material into the mantle wedge, which might be the process responsible for the eruption of alkaline lavas in Tunisia, Sardinia and southern Tyrrhenian (e.g., Faccenna et al., 2004).

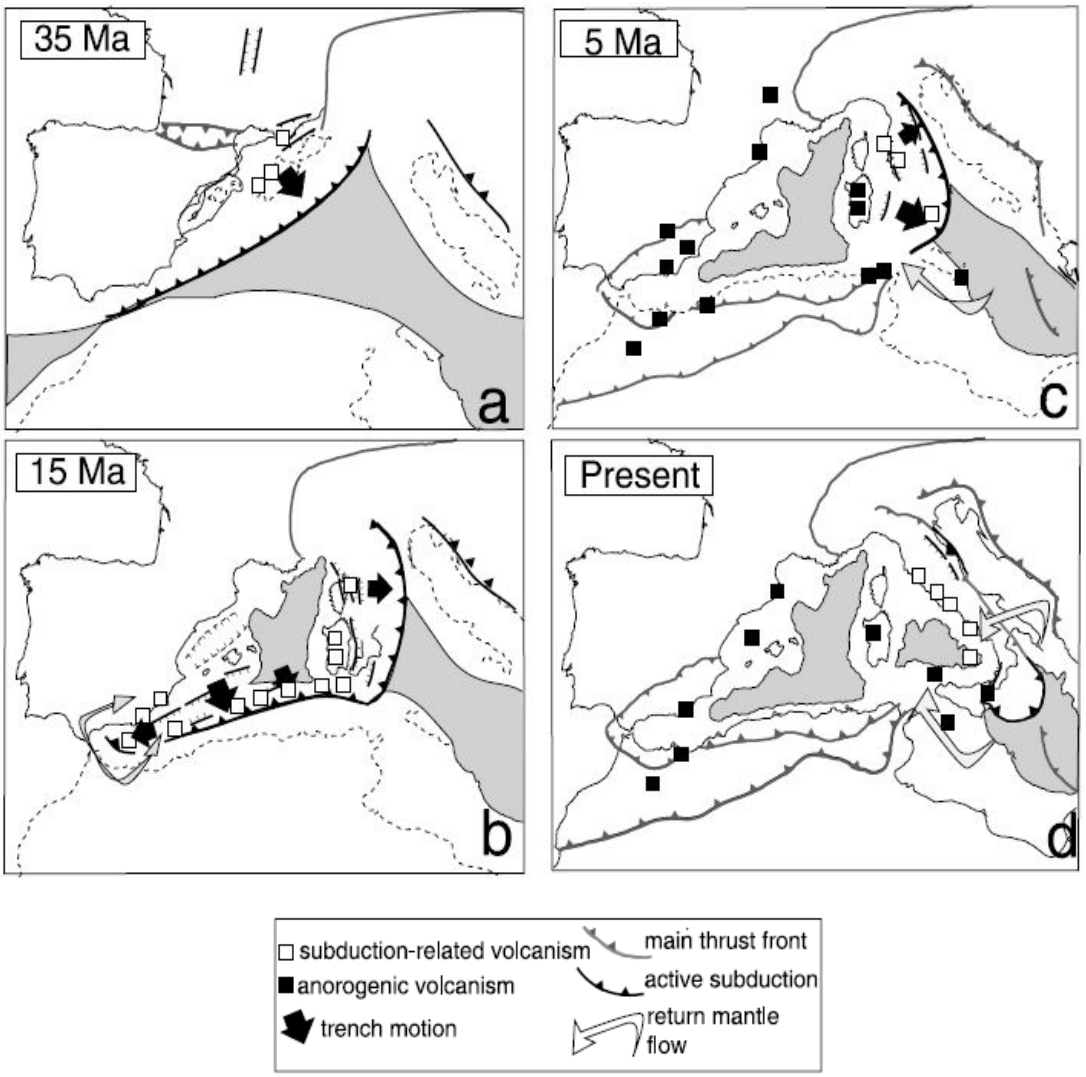

Fig. 3 - Reconstruction of the evolution of the Mediterranean region in relative (Eurasia fixed) reference frame in four stages, from 35 Ma to present-day. Deep basin domains are marked in grey. (a) First back arc extension phase with the retreat of the trench; (b) rotation of the Sardinian-Corsica block and beginning of the rifting between the eastern margin of Sardinia and Calabrian block; (c) first slab tearing event under the Sicily channel and formation of the Tyrrhenian sea with the opening of the Vavilov basin; (d) present day picture, illustrating both slab tears and both Vavilov and Marsili basins open. Adapted from Faccenna et al. (2004).

At circa 2.5 Ma, the subduction rate was inhibited at the trench by the resistance created by the Apulian continental lithosphere, which in turn, caused a strong deformation of the subduction panel (Panza et al., 2007; Chiarabba et al., 2008; Chiarabba & Palano, 2017). The mechanical contrast between the Apulian and the Ionian slab induced a new rupture between the subducted slabs at circa 2.5 Ma (Chiarabba & Palano, 2017), which consequently led to a faster sink of the Ionian slab and reactivation of the extension in the Tyrrhenian basin, with the migration of the trench towards south-east (Fig. 4). With further rollback of the narrow Ionian slab, a new rifting phase started, with ocean crust forming in the Marsili Basin at 1.9 – 1.7 Ma (Kastens et al., 1988; Marani & Trua., 2002). This extension phase was characterized by ultrafast spreading of the Marsili basin and drifting of Calabria, and it ceased or lowered significantly at

circa ~1 Ma (Chiarabba et al., 2008, 2017; Faccenna et al., 2004, 2011). The Aeolian Arc formed at 1 - 0.5 Ma and the subduction stopped its retreat when Calabria reached its recent position (Beccaluva et al., 1995).

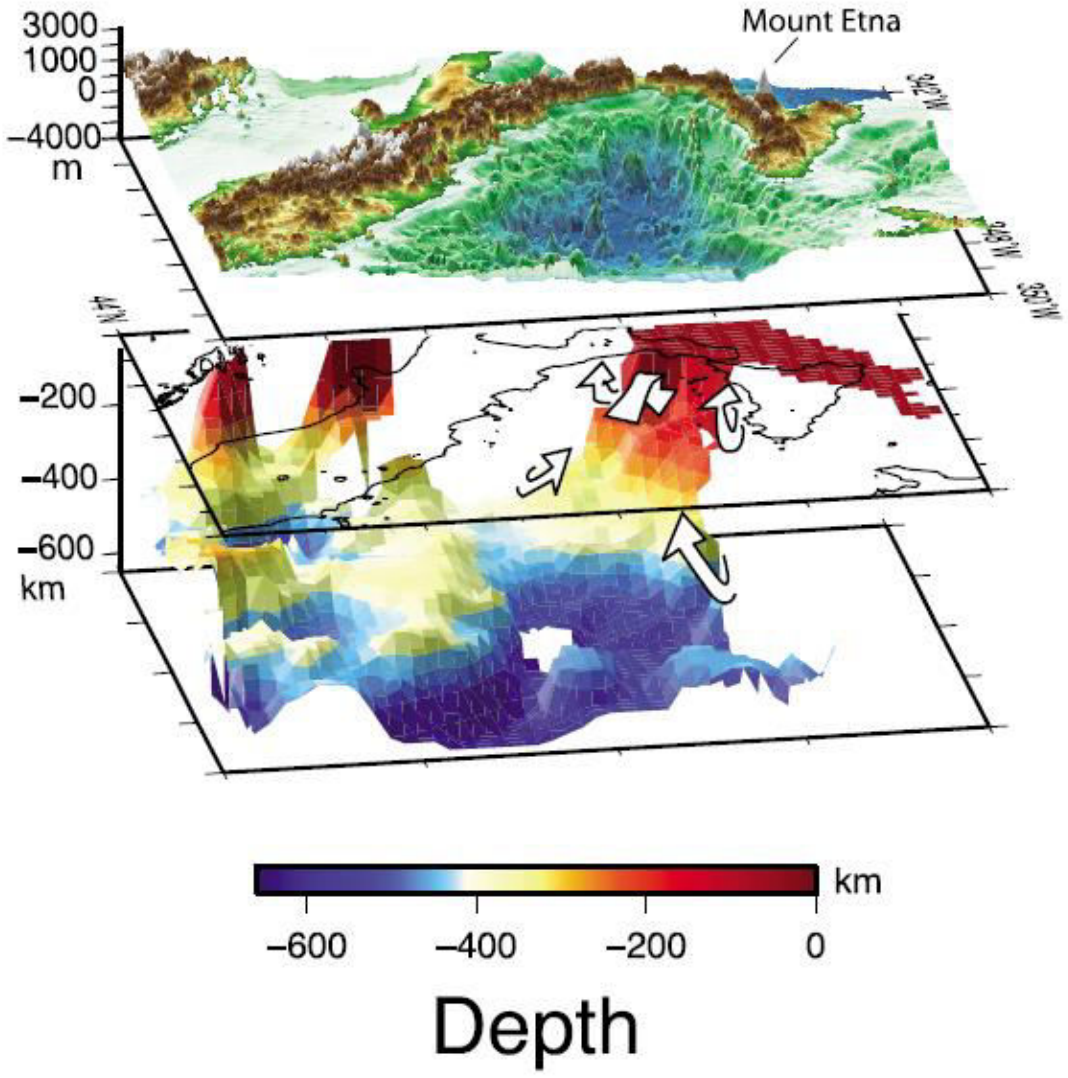

Fig. 4 - Recent numerical model for the shape and distribution of the subducted material under the Italian Peninsula and Tyrrhenian Sea. Arrows represent the mantle movements caused by the opening of the two slab windows, with consequently African asthenosphere inflow into the mantle wedge. Adapted from Faccenna et al. (2004).

Magmatism in the Tyrrhenian area has a large compositional variability, which could reflect the tectonic processes related with the formation of this back-arc system. Compositions vary from tholeiitic (mid-ocean ridge basalts (MORB) to arc-tholeiites) to calcalkaline (medium-K basalts to shoshonites) and lesser Na-transitional compositions with alkaline affinity (Beccaluva et al., 1995; Trua et al., 2011). While the calcalkaline and tholeiitic compositions might be related to the subduction-related fluids and passive mantle ascent during the rifting episodes, the alkaline-like compositions are thought to derive from: (1) the flow of OIB-like

mantle rocks into the mantle wedge through the slab windows formed during the roll-back process; or (2) by decompression melting of the same enriched mantle along the transform faults (e.g., Etna), with no mantle plume contribution (e.g., Panza et al., 2007; Chiarabba et al., 2008).

Ocean island basalts (OIB) compositions found in the Tyrrhenian area are related to recent volcanism that occurred while the Marsili basin was opening. They outcrop in the eastern margin of Sardinia (1.8 Ma years old) and Vavilov seamount (0.73 – 0.1 Ma years old) (Kastens & Mascle, 1990). One sample with OIB alkaline affinity was also dragged from the Marsili summit and its compositions resemble those of the Etna and Ustica volcanoes (Trua et al., 2011). These occurrences of OIB-like volcanism are related to the slab tearing that caused the opening of the Marsili basin, and it may reflect the effect of the toroidal mantle flow above the subducted Ionian slab.

Marsili

The volcano

The Marsili volcano is found in the axial zone of the Marsili back-arc basin (Fig. 5). This volcano has a circle-shaped basin covering ~ 8 km^2 with an average depth of 3.5 km from the sea level. The volcanic structure was formed during the last 0.7 Ma and it is a seamount elongated 60 km NNE-SSW with a main width of 20 km and 3.5 km of maximum height, where the summit is at ca. 0.5 km below the sea level (Marani & Trua, 2002). Marani & Trua (2002) suggest that the vertical accretion of the volcano occurred as a consequence of the continuous magma supply within the basin while the extension rate lowered.

The crustal thickness around the volcano is ca. 7 km and the lithosphere thickness is < 30 km (Pontevivo & Panza, 2006). Geophysical studies show that the upper mantle below the Marsili basin is characterized by low seismic velocities, suggesting up to 10% of melt within the mantle rocks (Panza, 2007). This corroborates the hypothesis that the Marsili seamount was formed upon a relatively strong mantle magma flux focused on the axial ridge of the Marsili basin (Marani & Trua, 2002). Furthermore, asthenospheric mantle inflow below the back-arc and arc systems may have increased the melt supply under the Marsili volcano, favouring the vertical accretion of the volcano (Trua et al., 2011; Trua et al., 2018).

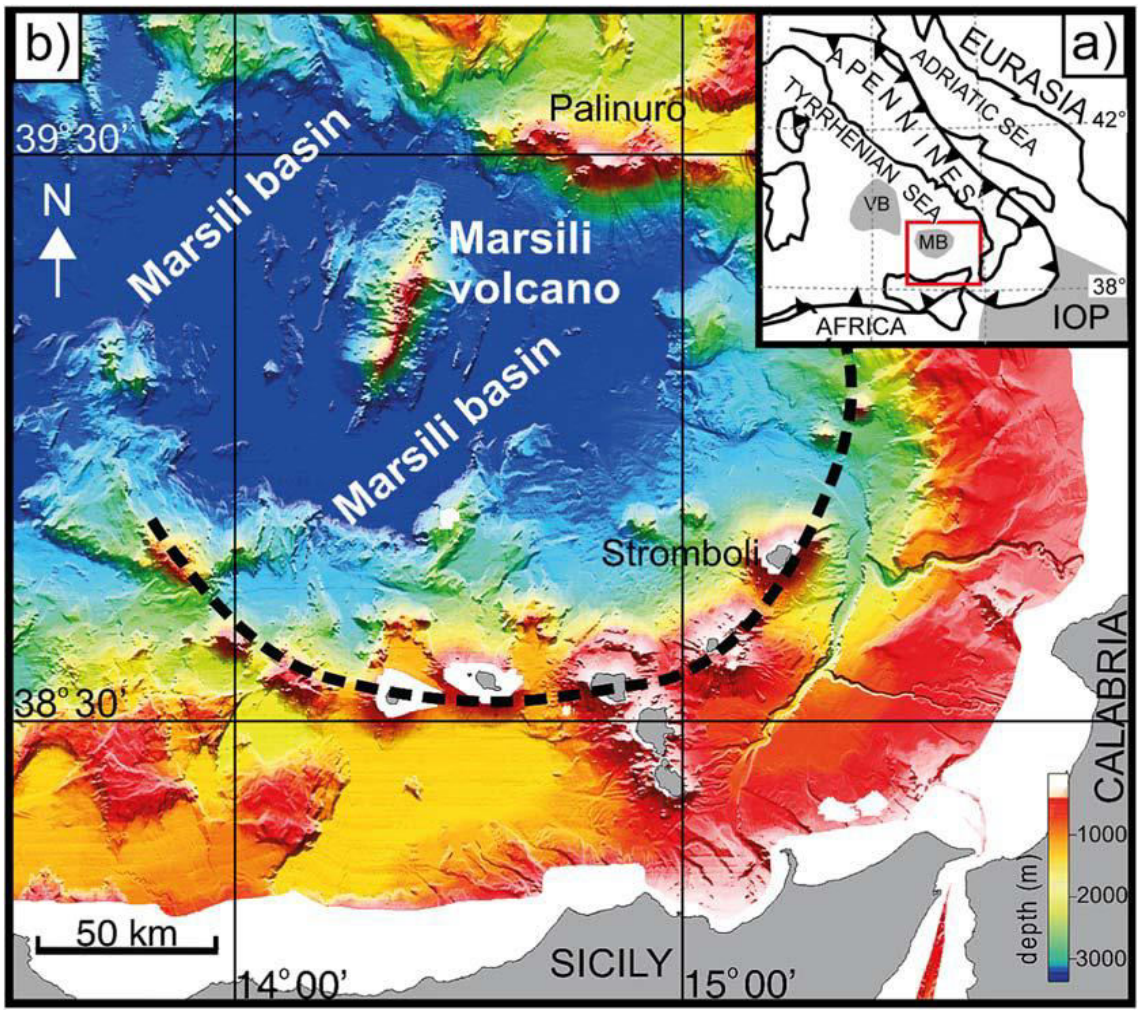

Fig. 5 - (a) Tectonic setting of the Tyrrhenian back-arc basin and respective sub-basins Vavilov (VB) and Marsili (MB); (b) Geographical setting of the Marsili basin and volcano. Modified from Trua et al. (2018).

Below the different areas that belong to the Marsili seamount are described (Fig. 6).

Axial zone

The axial portion of the volcano is the highest part of the seamount. This linear region of lower gradient stretches for ~30km and is ~1km wide, closely bounded by the 1000 m isobaths. The summit is characterized by linear arrangements of several cones forming different segments, similarly to those found in MOR ridges (Marani & Trua, 2002). The central and northern segments are formed by linear elongated cones, while the southern one is formed by a sequence of circular-based cones. The summit zone is limited to the north by a large circular cone, which represents the highest point of the volcano (~500 m). The rift zone continues to the northern and southern flanks of Marsili. In both these areas, the rift zone progressively widens downslope, reaching a width of ~5 km toward the base of the volcano.

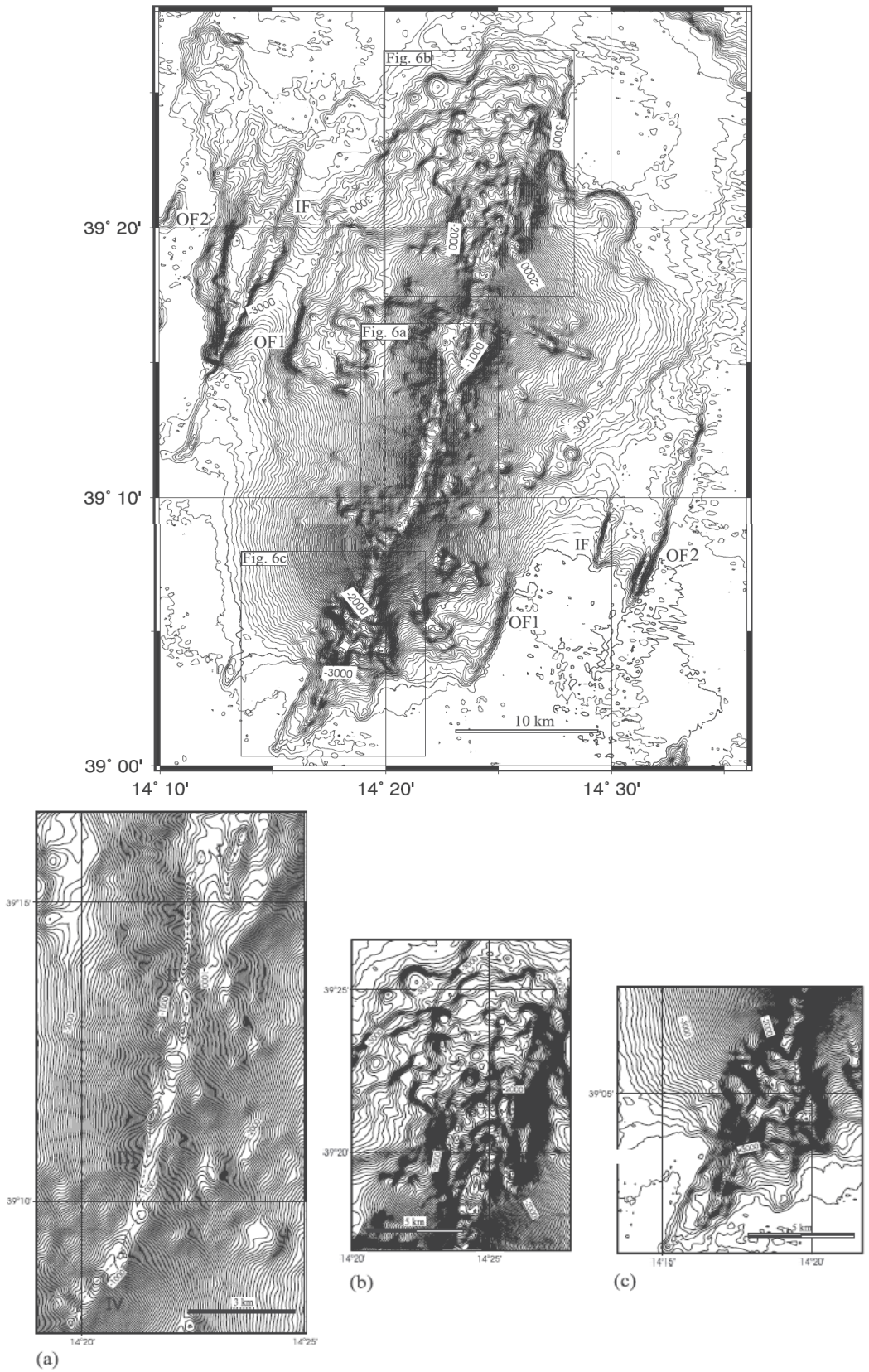

Fig. 6 - Bathymetric map of the Marsili seamount. IF (inward facing) and OF (outward facing) refer to the fault sets forming horst and graben structures (see Marani & Trua (2002) for further details). (a) zoom in of the axial segment of the summit; (b) zoom of the northern flank; (c) zoom in of the southern sector. Modified from Marani & Trua (2002).

Seamount Flanks

The flanks of the seamount have different features along the whole extension and they are limited by the isobaths at 1000 m and 3000 m. While the northern half of the seamount has asymmetrical irregularities, the southern half shows roughly concave symmetrical slopes. The flanks are often found to be disturbed by fields of circular volcanic cones that presumably represent the latest stages of volcanism. These cone fields are more extensive in the northern flank, where they sit on plateaus. The northern elevation is limited to the east by a steep scarp, which is thought to be the result of faulting or the headwall of a large flank failure event (Marani and Trua, 2002).

The south-eastern flank is morphologically comparable to the northern and the western tips, although to a smaller scale. A smaller field of volcanic cones is limited to the south by the ridge by an important scarp to the west, separating it from the featureless south-west flank. The south-eastern slope has an irregular morphology when compared to the south-western slope, and shows a higher number of isolated volcanic cones than its opposite flank.

Basin Floor Faults

Basin floor faults are present in the basin close to the seamount. They are represented by two symmetrical sets of faults parallel to the general trend of the summit axis. Each is composed of two faults forming a horst and graben set.

Marsili's Magmatism

Samples from drill holes within the Marsili basin have arc-like affinity, contrasting with the Vavilov basin, which oceanic crust is formed by MORB (Kastens et al., 1988). The large data set of lavas (Fig. 7) used to characterize the volcano Marsili was sampled during MAR98 and TIR2000 CNR cruises (Marani et al., 1999; Trua et al., 2011). The lavas sampled on the Marsili volcano have IAB compositions (medium-k basalts and basaltic andesites to high-k andesites). An OIB-like lava that was sampled in the summit of the ridge (Fig. 8).

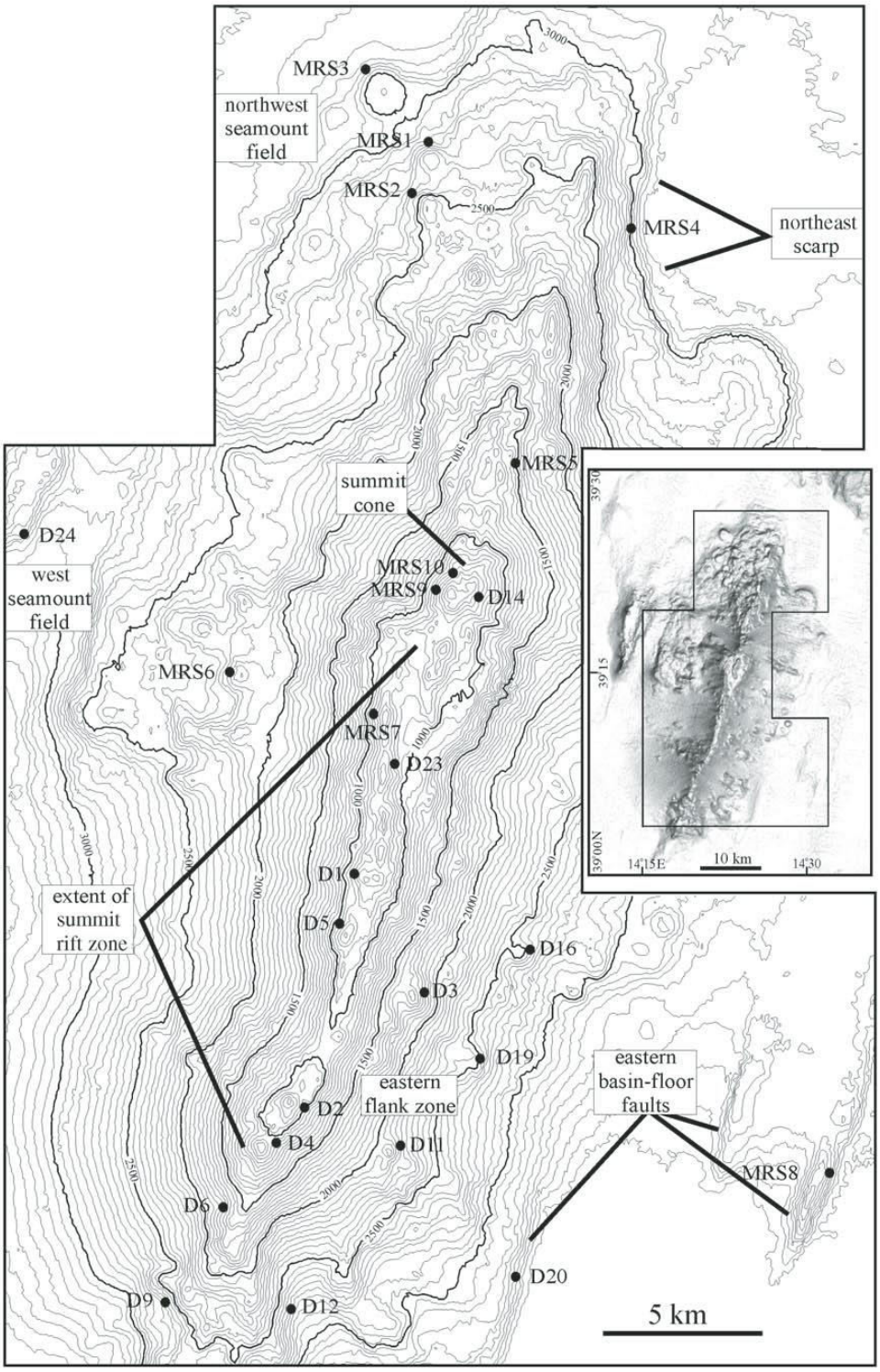

Fig. 7 - Bathymetrical map of the Marsili Seamount and location of the sampled lavas during the MAR98 and TIR2000 CNR cruises (Marani et al., 1999; Trua et al., 2011). Adapted from Trua et al. (2011).

Figure 9 contains basaltic lavas that show significant variability of the major elements. This was explained by Trua et al. (2002), and this paper also shows the presence of two IAB compositions, one represented by the basalts with olivine + plagioclase, and the other

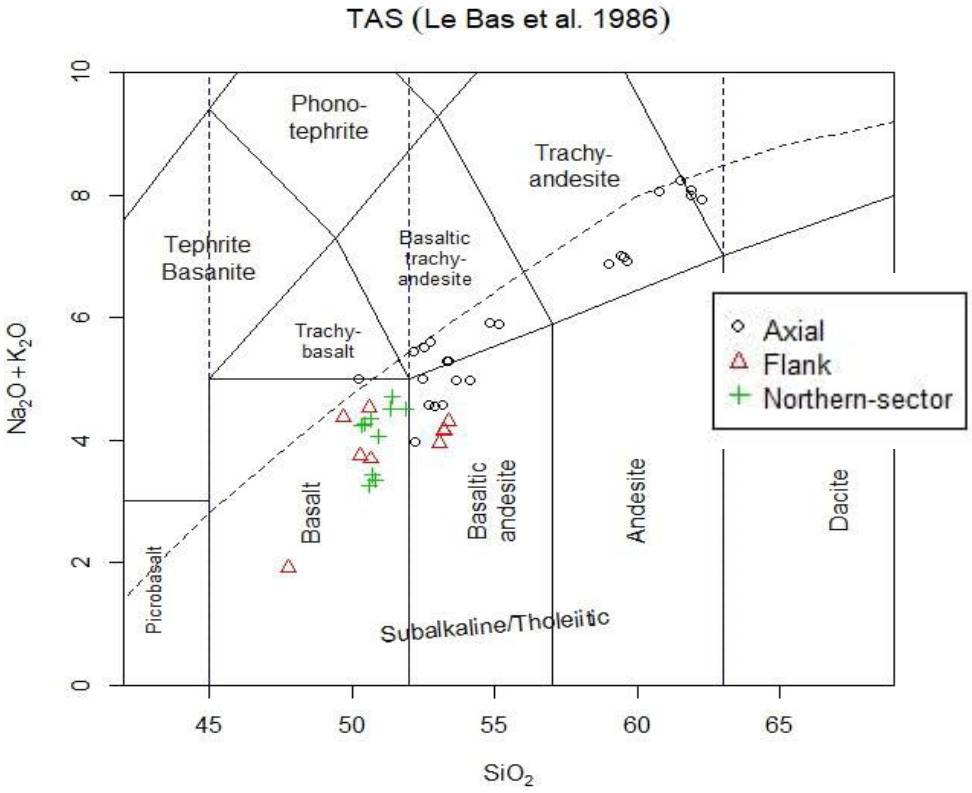

Fig. 8 - Total alkalis vs SiO_2 plot for the Marsili lavas taken from Trua et al., (2011).

represented by the basalts with olivine + clinopyroxene + plagioclase. The second composition is assumed to be the parental magmas of the basaltic andesites and andesitic lavas that might form due to large extents of fractional crystallization (up to 80%; Trua et al., 2002).

The lavas sampled in the northern flank are the less differentiated relatively to the whole Marsili data set and they are the less porphyritic (porphyritic index (PI) < 20%). Macrocrysts (here considered as crystals larger than 0.5 mm) mostly occur isolated, rarely in glomerocrysts. The lavas with only olivine + plagioclase crystals (MRS1E and MRS3) were sampled only in the northern flank, relatively close to the other lavas that have clinopyroxene, see Figure 7. The lavas with clinopyroxene in the phenocryst assemblage have higher whole rock (WR) CaO contents (wt %) and lower TiO_2 and Na_2O for similar SiO_2 contents relatively to the samples MRS1E and MRS3. The samples from the eastern flank are mainly basalts, with only few basaltic andesites, and generally have slightly higher PI (10<PI<20). Macrocrysts here occur either isolated or in glomerocrysts of variable mineral assemblages. The sample D12D1 has a higher PI = 25% and has composition resembling a cumulate rock. This sample will be described later.

Most of the lavas were sampled in the axial portion of the volcano. While the majority of the lavas from the summit are calcalkaline, one sample has an alkaline OIB-like composition.

All the samples range from basaltic to andesitic compositions and basaltic-andesites dominate the population. All the samples present similar petrographic characteristics, with PI varying between 10 and 20% and macrocrysts occurring either isolated or in glomerocrysts with different dimensions. Both basalts and basaltic andesites have plagioclase + clinopyroxene + olivine, the last is more abundant in the basalts. Amphibole was found in one basaltic andesite lava. The andesites were sampled on the highest cone at the northern part of the ridge and its phenocryst assemblage is composed by plagioclase, clinopyroxene Fe-Ti oxides and rare olivine crystals. Orthopyroxene is present in the most SiO_2 rich andesites.

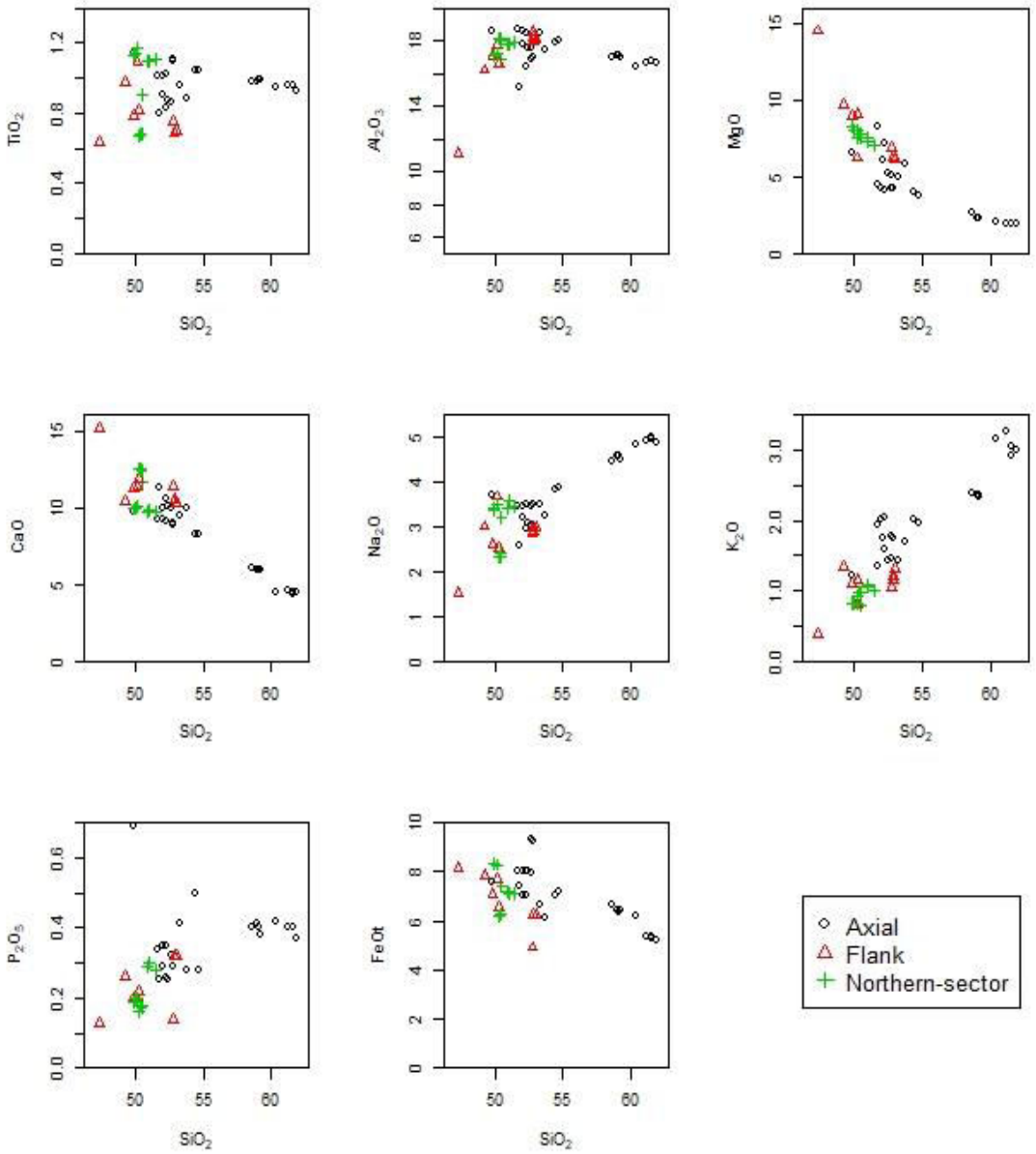

Fig. 9 - SiO_2 vs major elements for all the Marsili lavas from Trua et al. (2011). Symbols represent the three main sectors in the Marsili as described in the text.

Few lavas were sampled in within the basin floor faults and although, they are significantly altered they have a calcalkaline basaltic composition (not showed).

While the IAB lavas of Marsili display similar compositions to those from the Aeolian Arc, the OIB-like sample shows isotopic and trace element compositions similar to the Ustica, Prometeo and also to the Etna (Trua et al., 2011).

All Marsili lavas are enriched in light rare earth element (LREE). The primitive mantle-normalized incompatible trace-element patterns for all, with exception of one sample, are typical of IAB magmas, showing strong depletions in Nb and an enrichment in K and Pb relative to the rest of the plotted elements (Fig. 10). The trace elements patterns for the basaltic andesites and andesites are subparallel to the basalts patterns, extending to slightly higher abundances of these elements, which corroborates the previous suggestion that fractional crystallization controlled the evolution of some of the Marsili lavas (Trua et al., 2002).

Olivine-hosted melt inclusions from Marsili are in agreement with the observations from the whole-rock compositions of the host lavas. Overall, this compositional variability proves that both IAB and OIB melts entered the in the plumbing system of the Marsili (Trua et al., 2010). The range of compositions was produced by mixing between the OIB mantle component and the MORB mantle wedge, with both mantle components variably affected by the subduction-related metasomatism (Trua et al., 2011).

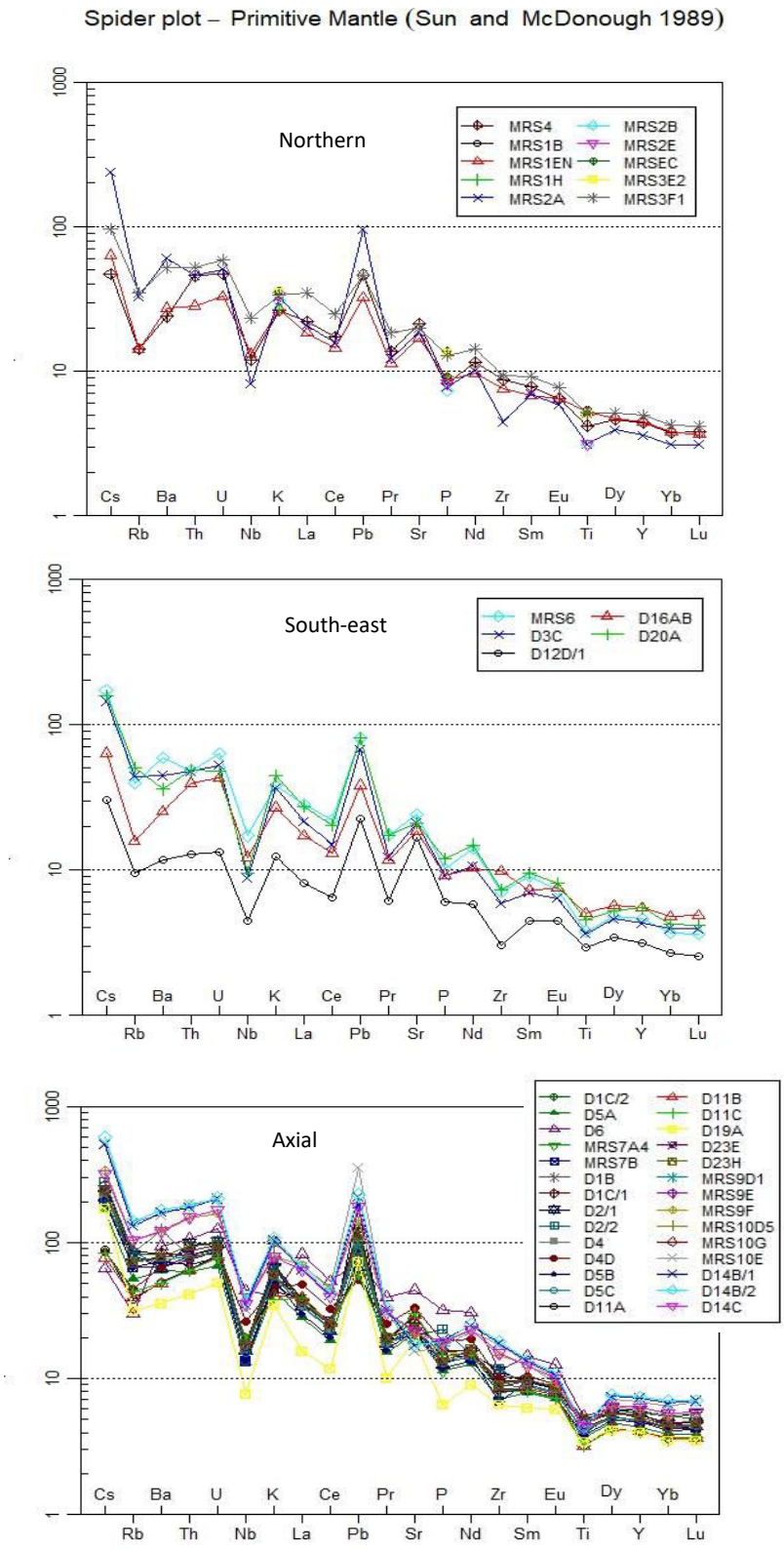

Fig. 10 - Incompatible trace elements of the Marsili lavas (Trua et al., 2011) normalized to primitive mantle composition (Sun & McDonough, 1989).

Objectives

The aim of this dissertation is to study with more detail the plumbing system of the volcano Marsili using olivine and clinopyroxene crystals from a group of basaltic lavas samples during the MAR98 and TIR2000 cruises (Trua et al., 2014; references therein), representing the whole extension of the volcano, both geographical and geochemically.

Olivine and clinopyroxene crystals record the first magmatic dynamics within the more mafic reservoirs and may also register the mixing between more felsic compositions within the magmatic system. Trua et al. (2014) showed that within the Marsili lavas there are variable compositions and suggest the main differentiation processes and where they occur within the Marsili plumbing system. However, the study of a larger number of samples with the use different geothermobarometric models associated to the composition variability is lacking.

New trace element compositions from clinopyroxene crystals will allow to further study the variability of the parental melts in two more samples and will be compared to the major elements to better describe the differentiation processes.

Olivines will also be used to test the timescales of the magmatic processes within the plumbing system. Using multi-elemental profiles from the olivine crystals, the zoned profiles will be modelled to study the variability of re-equilibrium periods associated to the magma mixing episodes prior to the eruption.

Samples and Methodology

Samples description

The olivines and clinopyroxenes used to study the Marsili's plumbing system in this work are from eight lavas, covering the whole length of the ridge. In Fig. 7 it is possible to see the location of each sample, covering the northern flank (MRS1E, MRS2A and MRS4), the axial portion (D4, D5A and D6) and the south-east flank (D12D2 and D16AB). The majority of the samples are IAB medium-k calcalkaline basalts. The exceptions are D6 which is an OIB-like medium-k basalt and D4, which is an IAB high-k basaltic andesite, respectively (Trua et al., 2011). Two thin sections of each samples MRS1E, D5A and D16AB were used, while for samples MRS2A, MRS4, D4, D6 and D12D1 only one thin section was used. The pairs of thin sections for each of the MRS1E, D5A and D16AB are referred in Table 1.

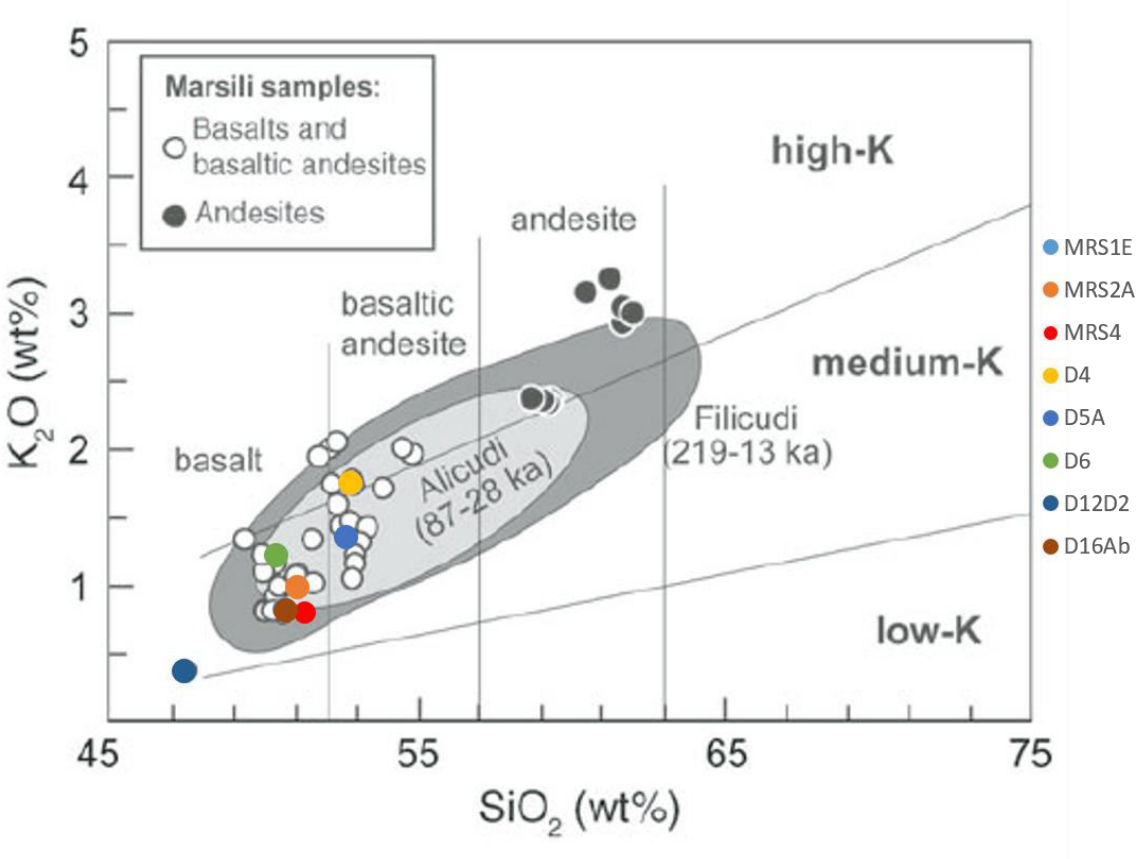

Fig. 11 - K_2O vs. SiO_2 plot for all the Marsili samples, putting in evidence (colour) the studied samples. Modified from Trua et al. (2011).

Table 1 - Studied samples in this dissertation with the respective number of crystals of each mineral phase analysed. The porphyric index is reported for each sample, calculated with at least 1000 counts per thin section. Macrocryst assemblage based on porphyric index. The pairs MRS1En-MRS1Em, D5A(1)-D5A(2) and D16AB(1)-D16AB(2) represent the pairs of thin sections from the samples MRS1E, D5A and D16AB, respectively.

Sample name	*Position*	*Classification*	*Porphyric index*	*Macrocrysts*	*Nº analysed Ol*	*Nº analysed Cpx*
MRS1En and MRS1Em	Northern flank	Basalt	15%	Ol (5%) – Plg (10%)	8	-
MRS2A	Northern flank	Basalt	19%	Ol (6%) – Plg (11%) – Cpx (2%)	5	3
MRS4	Northern flank	Basalt	10%	Ol (5%) – Plg (2%) – Cpx (3%)	4	-
D4	Axial portion	Basalt andesite	28%	Ol (3%) – Plg (20%) – Cpx (5%)	6	-
D5A(1) and D5A(2)	Axial portion	Basalt	34%	Ol (5%) – Plg (14%) – Cpx (15%)	12	4
D6	Axial portion	Basalt	16%	Ol (5%) – Plg (10%) – Cpx (1%)	5	2
D12D2	South-eastern flank	Basalt	37%	Ol (9%) – Plg (21%) – Cpx (7%)	7	3
D16AB(1) and D16AB(2)	South-eastern flank	Basalt	23%	Ol (2%) – Plg (14%) – Cpx (7%)	10	3

These eight samples represent the less differentiated lavas sampled on Marsili and the whole chemical variability. The samples have different major element compositions for similar SiO_2 contents (Fig 12). Some of these differences might be a consequence of the high content of macrocrysts in the samples, and the sample D12D2 is the best example of that. However, different major element contents in samples with lower porphyric index might be a consequence of petrological processes. All Marsili lavas are enriched in light rare earth element (LREE). However, the subduction signature is variable for samples having similar SiO_2 content. Indeed, the lower abundances of High Field Strength Elements (HFSE) coupled with the higher positive Pb anomaly in sample MRS2A suggest that the mantle source supplying this magma was more depleted and had a stronger subduction signature compared with the sample MRS1E (Trua et

al., 2011). Only the sample D6 (OIB-like) shows trace element patterns more enriched when comparing to the rest of the data set. Sample D12D2 has the poorest composition (Fig. 12), which is in agreement with its contrasting major elements composition. The trace elements patterns for the basaltic andesites and andesites are subparallel to the basalts patterns, extending to slightly higher abundances of these elements which corroborates the previous suggestion that fractional crystallization controlled the evolution of some of the Marsili lavas

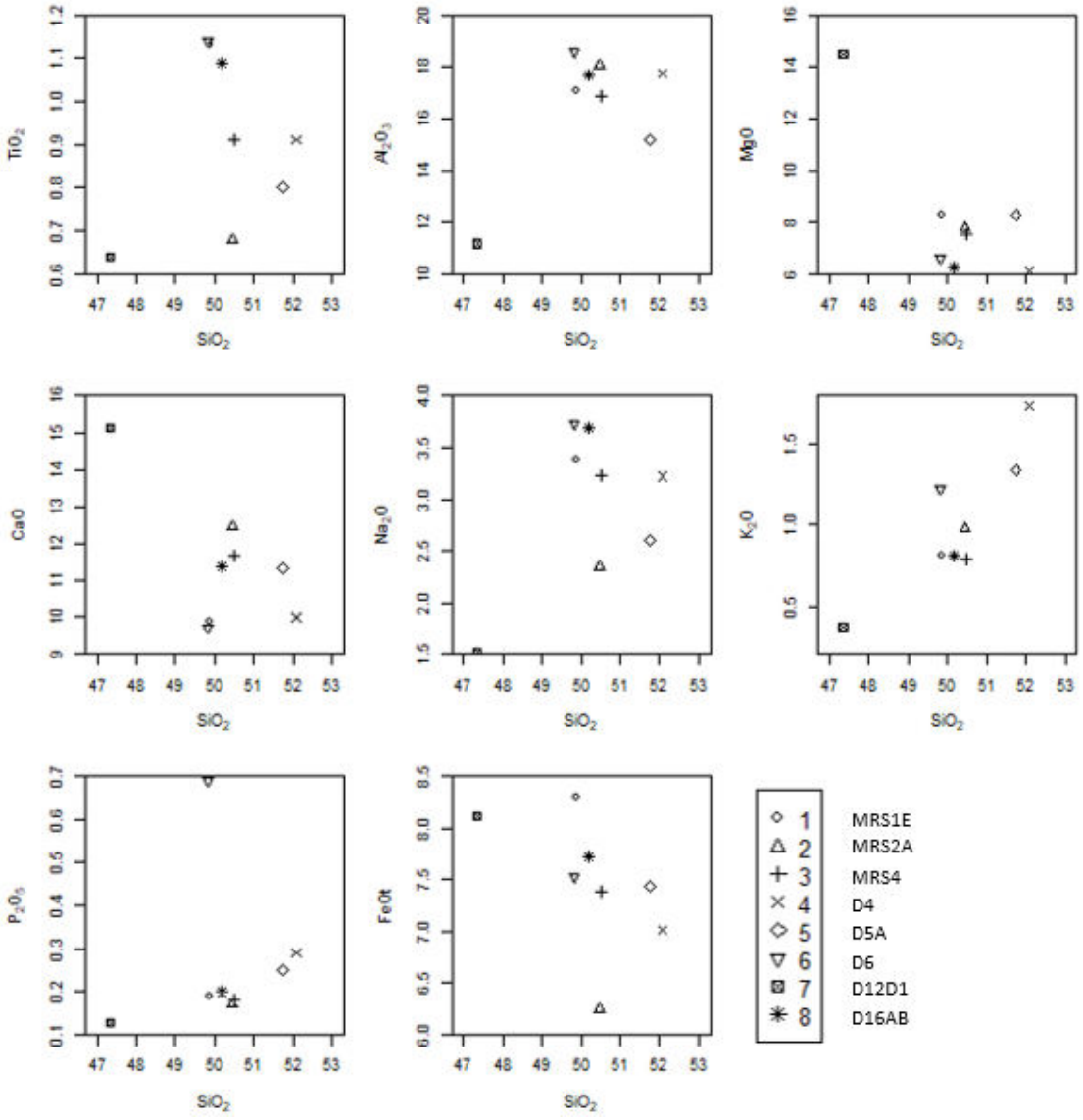

Fig. 12 – Major elements vs SiO_2 contents of the whole rock compositions of the lavas chosen for this dissertation. These samples represent the compositional variability found in the Marsili lavas (Fig. 9). Data from Trua et al. (2011).

(Trua et al., 2002). Olivine-hosted melt inclusions from Marsili are in agreement with the observations from the whole-rock compositions of the host lavas (Trua et al., 2010). On one hand, Marsili IAB samples have olivine-hosted melt inclusions with compositions similar to the IAB lavas from the Marsili and the Aeolian Islands. On the other hand, the olivine-hosted melt inclusions from the sample D6 confirmed the OIB-like composition observed by the whole-rock.

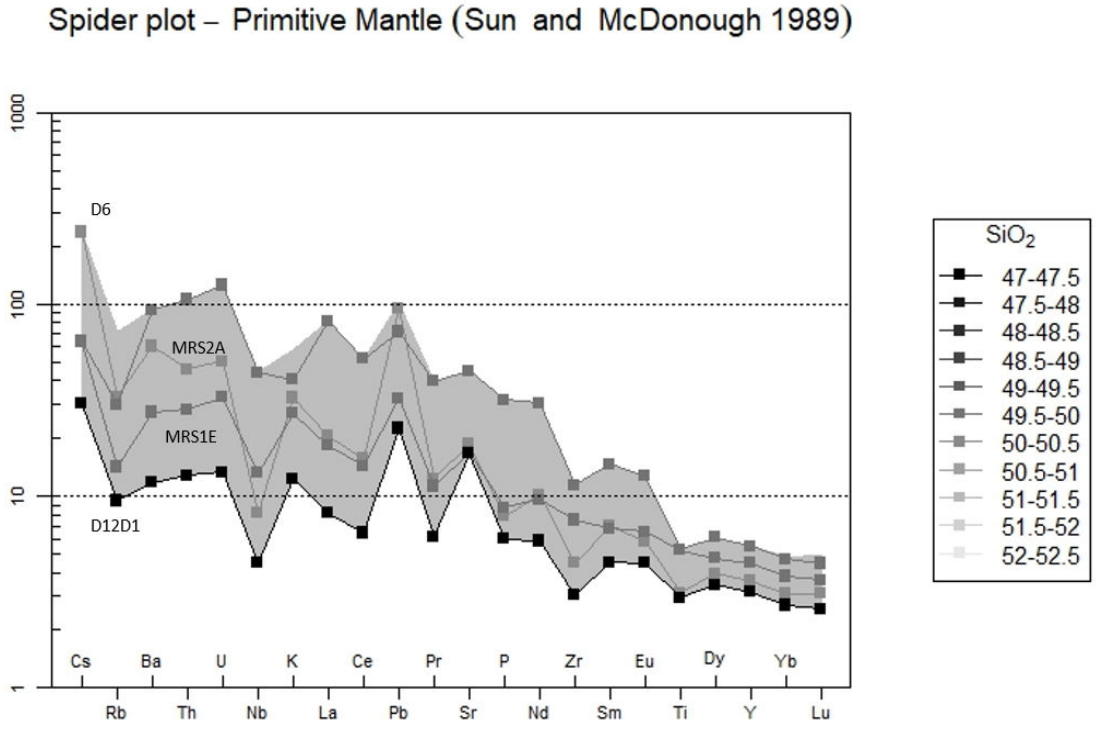

Fig. 13 - Rare earth elements (REE) of the lavas D6, MRS1En, MRS2A and D12D2 normalized to the chondrite composition (Nakamura 1974). Grey field represents the field occupied by all the chosen Marsili samples (Trua et al., 2011). Samples with darker colour have lower SiO_2 wt% contents.

Methodology

Major element mineral chemistry in the olivine and clinopyroxene crystals was determined at "Istituto di Geoscienze e Georisorse" of the National Research Council (IGG-CNR) at the Padua (Italy) branch with a CAMECA SX50 electron microprobe (EMP) equipped with four wavelength dispersive spectrometers (WDS) and one energy dispersive spectrometer (EDS). Analytical conditions were: 15 kV accelerating voltage, 15 nA beam current, peak counting times 15 s, and about 2 μm focused electron beam. Standards were natural silicates and metals of known composition. Precision was better than 1% for oxide content higher than 10 wt.%, and better than 3% for oxide content less than 10 wt.%.

Trace element mineral composition was determined by laser ablation inductively coupled plasma mass spectrometry (LA–ICP-MS) at the Dipartimento di Biologia Ecologia e

Scienze della Terra, University of Calabria (Italy). The equipment was a combination of a New Wave Research UP213 solid-state Nd-YAG laser probe (213 nm) (LA) and an Elan DRCe (Perkin Elmer) ICP-MS. In the analysed crystals, more than one ablation point and/or core–rim sections were performed. Ablation spots with 40 μm of diameter were analysed on polished sections (80 μm thick) at a constant repetition rate of 10 Hz and fluence of ~20 J/cm2. The SRM612 glass by NIST (National Institute of Standard and Technology) was used as an external standard, using 43Ca or 29Si as internal standards, depending on the analysed mineral. In each analytical sequence the USGS reference sample BCR-2Gwas analysed together with the unknowns for quality control. Precision and accuracy are better than 5% and 10%, respectively.

To determine the crystallographic orientation of olivine EBSD analysis was applied. As a first step the thin sections were Syton polished to remove the mechanical damage generated during previous mechanical polishing (Flynn & Powell, 1979; Prior et al., 1996). Subsequently the samples were carbon coated applying a 20 nm thin film to prevent electrical charging problems. One EBSD analysis per grain was performed manually at the Department of Mineralogy and Petrology, University of Padova (Italy), using a CamScan MX2500 SEM equipped with an LaB6 electron source and an NordlysNano EBSD detector. An acceleration voltage of 15 kV, a filament emission current of 450 μA, and a working distance of 25 mm were used. EBSD patterns were indexed with the CHANNEL 5.0 software from Oxford Instruments. Indexing was accepted when at least seven detected Kikuchi bands were successfully simulated by the HKL- reflector file for olivine. Each collected data point was plotted in a stereo plot using the Mambo component of the CHANNEL 5.0 software in order to measure the angle between chemical profile and axes.

Results

Mineral Compositions

Marsili olivine and clinopyroxene crystals show a wide compositional range that varies from sample to sample. In general the olivine crystals with higher fosterite (Fo = Mg# = (Mg/(Mg+Fe^{2+})); calculated using olivine compositions) are in equilibrium with the host sample. However, the majority of the crystals have lower Fo contents (Fig.).

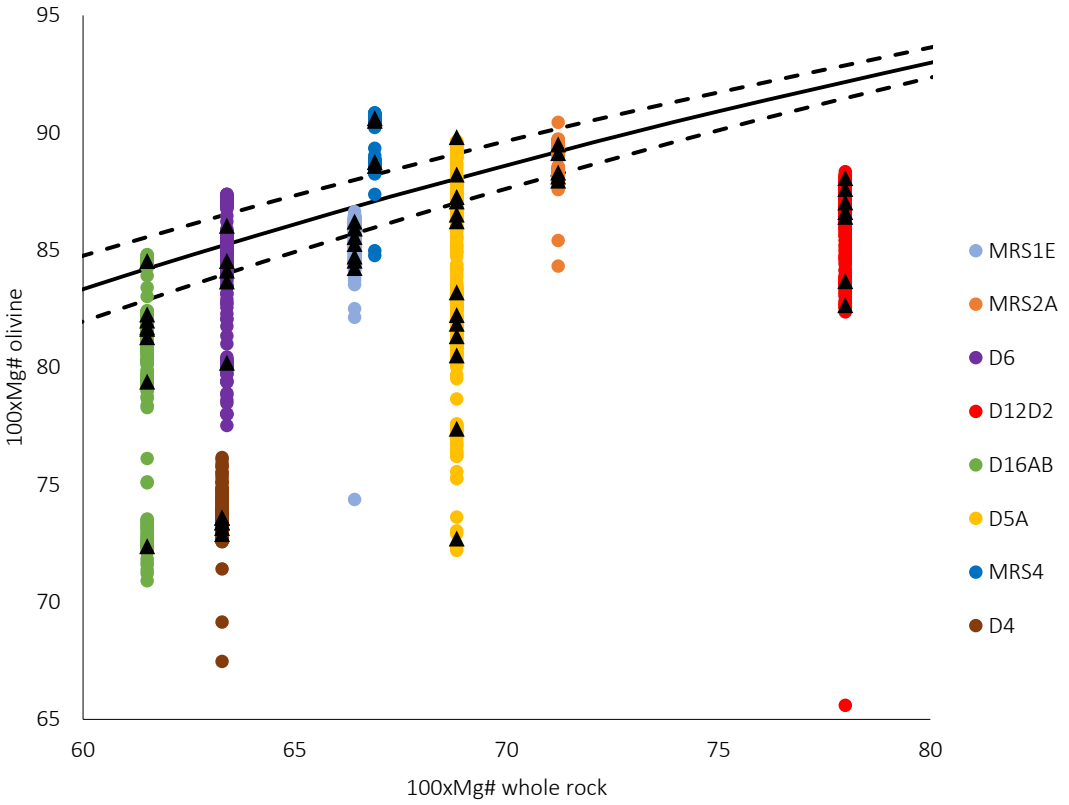

Fig. 14 – Equilibrium plot between olivine crystals and respective host samples. Coloured dots represent the whole data set obtained from the compositional profiles of the olivines. Black triangles represent core compositions from the analysed crystals. Mg# = Mg/(Mg+Fe), where Fe for olivine is Fe^{2+} and Fe for whole rock is Fe^{2+} using FeO/Fe2O3 = 0,9

MRS1E

Olivines

MRS1En olivine crystals are subhedral to anhedral and are isolated from other crystals. Thin section MRS1Em shows instead less olivine (core with Fo86) as a single crystal and more glomerocrysts of olivine (Fo84.5) and olivine + plagioclase. Core compositions from two thin sections (MRS1En and MRS1Em) vary between Fo86 and Fo84. The compositional profiles have different geometries, generally showing normally zoned rims with Fo84.5 (Fig. 15). Few crystals

present reversed zoning before the normal zoned rims. The compositions on these reversely zoned profiles fall within the range of compositions of the plateaus presented by the other crystals. NiO profiles show flat geometries and due to the analytical error it is difficult to say whether the rims are zoned or not as is Fo (Fig. 16). Only (2) Ol9 shows a profile normally zoned for NiO. The decrease of NiO starts from 400 μm (core as starting point) while the zoning for Fo starts from about 300 μm. Olivine (1) Ol1 shows a slight increase in NiO from core to rim towards the compositions of the rest of the crystals. CaO instead shows that core compositions range between 0.3 and 0.2 wt. % and rims register 0.25 wt. %. Crystals with core compositions of Fo86 show CaO concentrations varying from 0.22 to 0.26 wt. % and crystals with Fo84.5 core compositions yield ca. 0.25 wt. % CaO (Fig. 16).

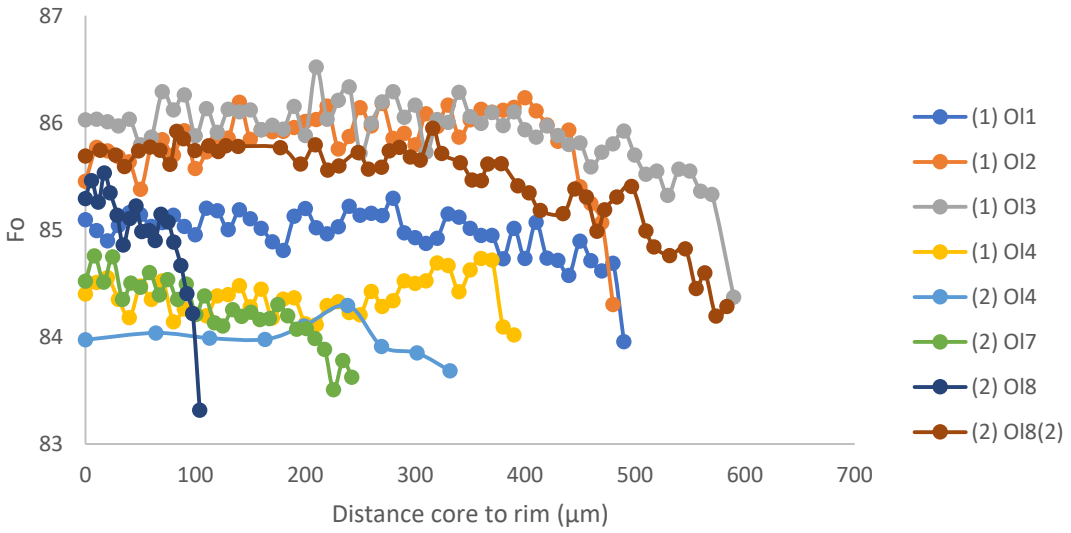

Fig. 15 - Fo profiles from core to rim of the analysed olivine crystals from MRS1En (1) and MRS1Em (2).

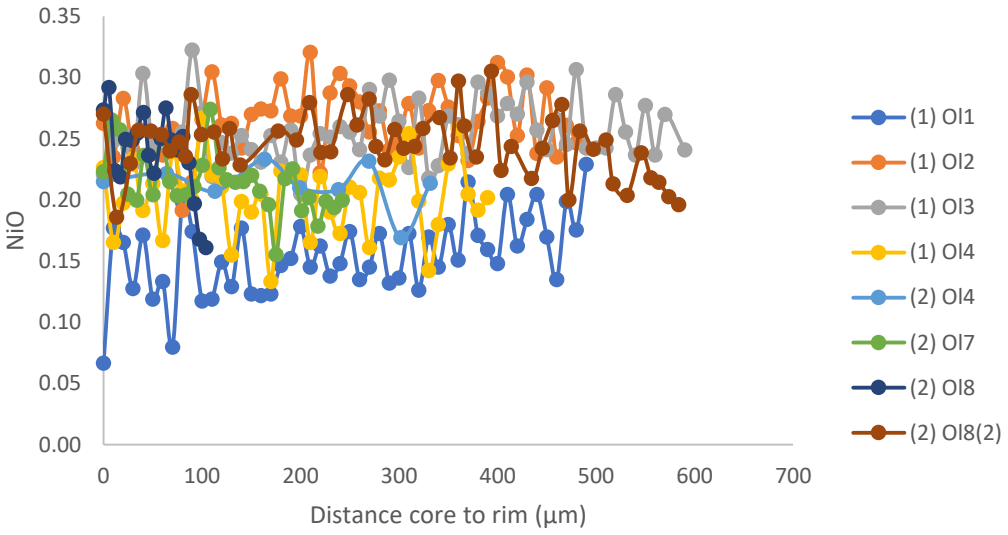

Figure 1 - NiO profiles from core to rim of the analysed olivine crystals from samples MRS1E (1) and MRS1Em (2).

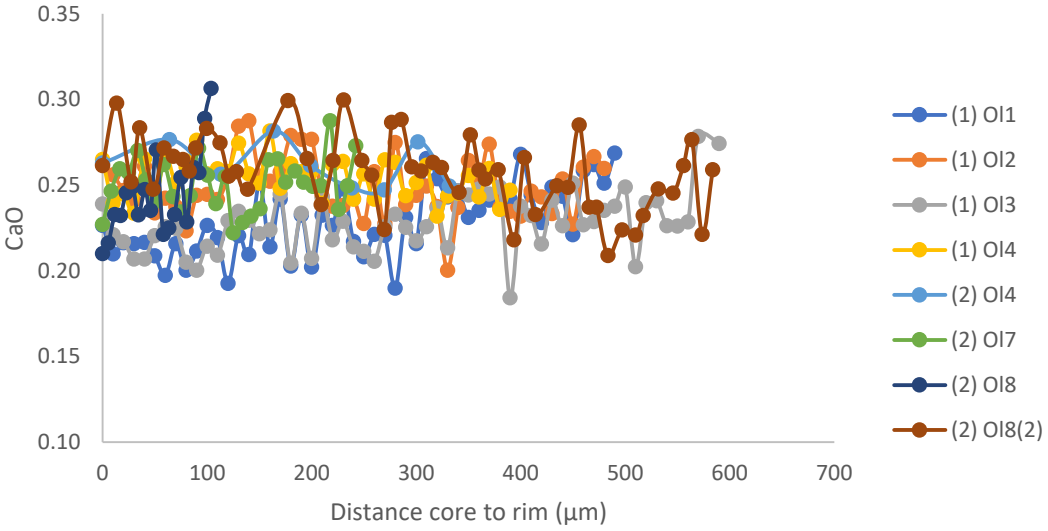

Fig. 16 - CaO profiles from core to rim of the analysed olivine crystals from samples MRS1E (1) and MRS1Em (2).

Considering the plot Fo against NiO (Fig. 17), most of the crystals form a positive trend, probably related to a general liquid line of descent (l.l.d.). However, (1) Ol1 shows a lower content of NiO for what would be expected for its Fo value according to the l.l.d. represented by the other olivines.

CaO vs. Fo contents lack a good correlation. While the crystals with Fo > 85 are scattered and do not follow a unique l.l.d., crystals with Fo bellow 85 present a shallow negative correlation between CaO and Fo.

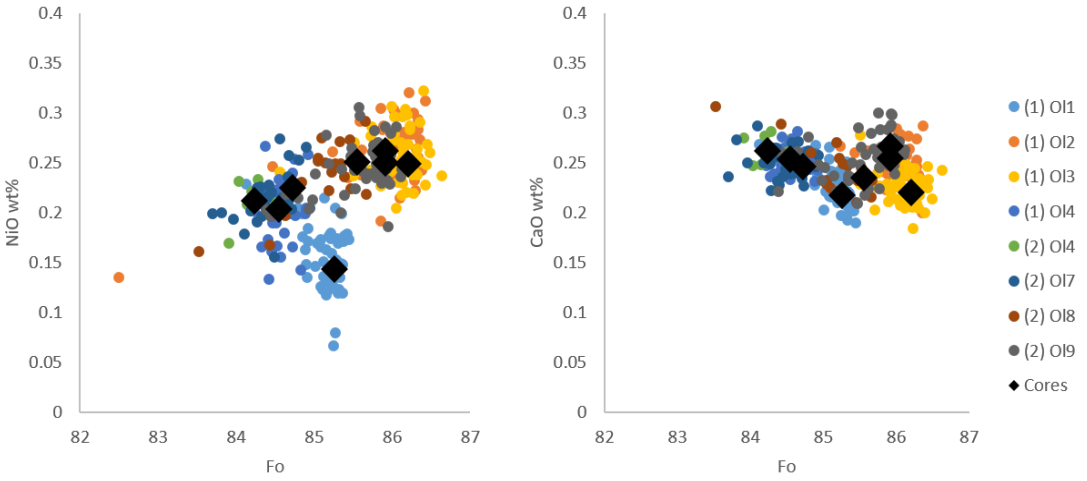

Fig. 17 - NiO vs. Fo and CaO vs. Fo for the olivine crystals from MRS1E and MRS1Em. Black Diamonds ent the average compositions of the crystals' cores.

MRS2A

Olivines

Olivine crystals in sample MRS2A present two groups of different Fo values and these groups of crystals present different textures, with the first group (Fo89.5) given by isolated crystals and the second (Fo88) represented by crystals associated to clinopyroxene and plagioclase in a glomerocryst. One of the crystals forming the Fo89.5 group is reversely zoned from the core almost to the rim, while the last 30 microns are normally zoned. The rest of the crystals, from both clusters, show flat Fo profiles (Fig. 18). NiO profiles (Fig. 19) are similar to those of Fo. Instead, CaO profiles are flat (Fig. 20) except for a slight increase from 0.20 to 0.25 wt. % at about 20-30 microns from the rims.

NiO wt% vs. Fo (Fig. 21) present a positive trend, while CaO wt% does not show important variations with Fo, forming a rather flat, slightly negative trend. The olivine Ol3, with higher Fo content in the core, shows NiO and CaO contents slightly different from the rest of the crystals.

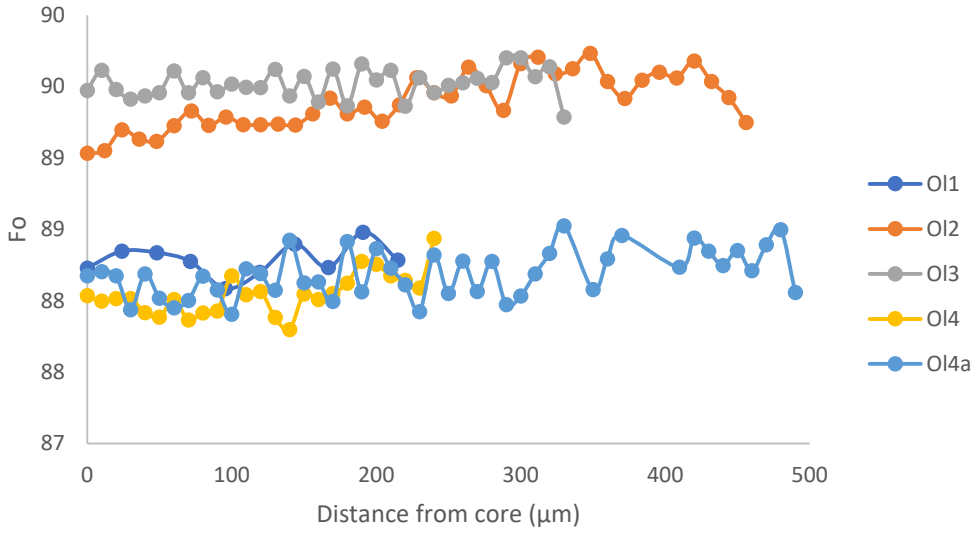

Fig. 18 - Fo core to rim profiles for the olivine crystals from MRS2A.

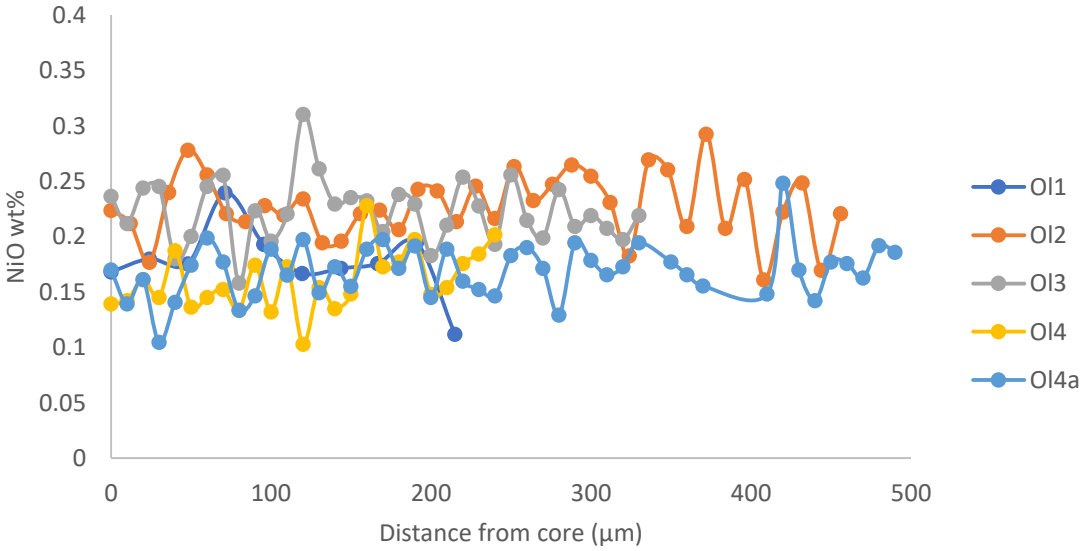

Fig. 19 - NiO core to rim profiles for the olivine crystals from MRS2A.

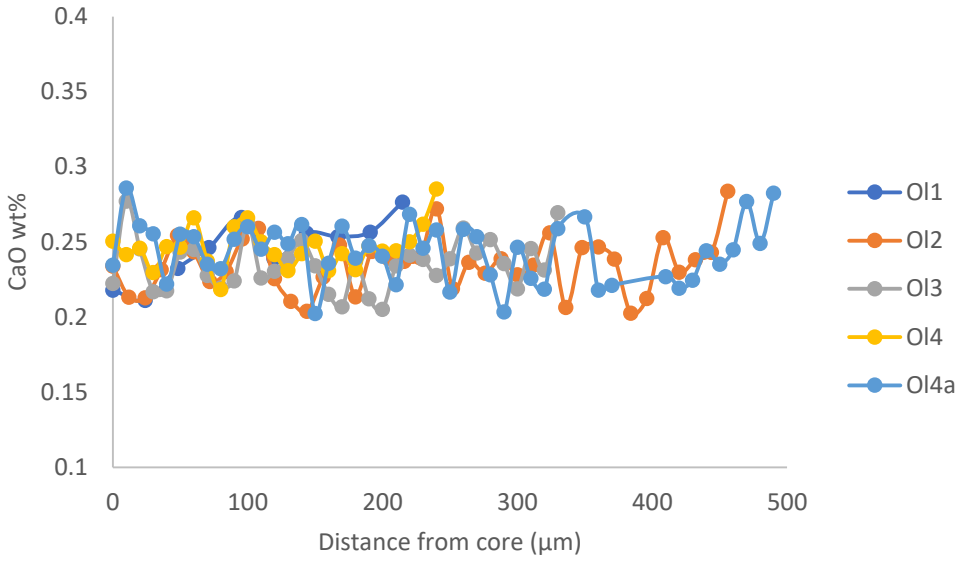

Fig. 20 – CaO core to rim profiles for the olivine crystals from MRS2A.

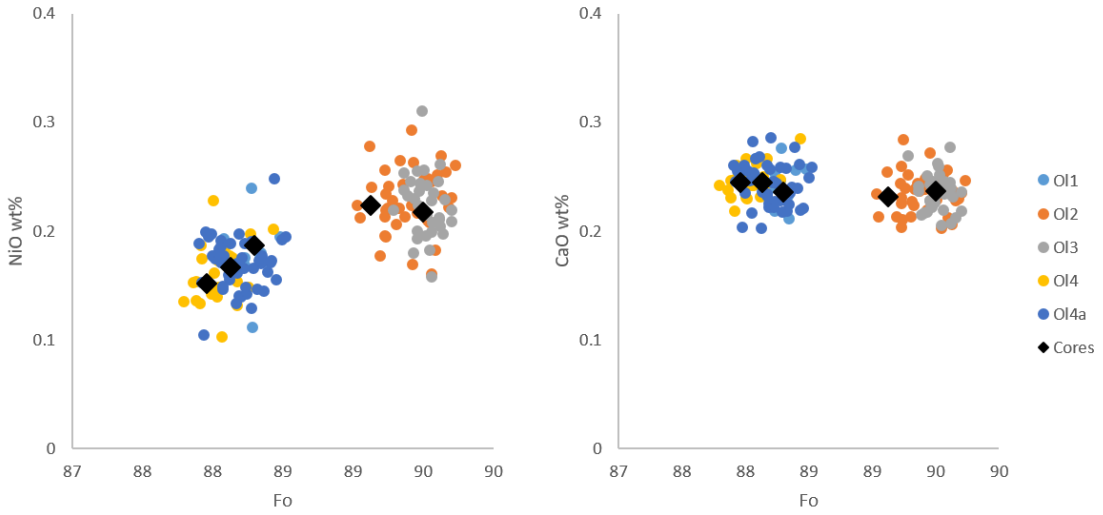

Fig. 21 - NiO vs. Fo and CaO vs. Fo for the olivine crystals from MRS2A. Black diamonds represent the average compositions of the crystal cores.

Clinopyroxenes

All the analysed clinopyroxene crystals are zoned with compositions ranging from $Wo_{48-44}En_{49-45}Fs_{9-6}$ and Mg#89.5 to Mg#84 (Mg# = 100*(Mg/(Mg+Fe^{tot})). Crystals show concentric zoning with rather abrupt compositional changes, although no sector zoning is observed. Rim compositions is Mg#87.5 for all crystals but one (Mg#89.5) (Fig. 22). TiO_2 wt% (Fig. 24) correlates negatively with Mg# while Cr_2O_3 (Fig. 23) correlates positively, and Al_2O_3 (Fig. 25) instead shows

some variability when compared with Mg#. The Al_2O_3 variability will be investigated in the thermobarometer chapter to understand whether these differences depend on the composition of the system or on the intensive variables.

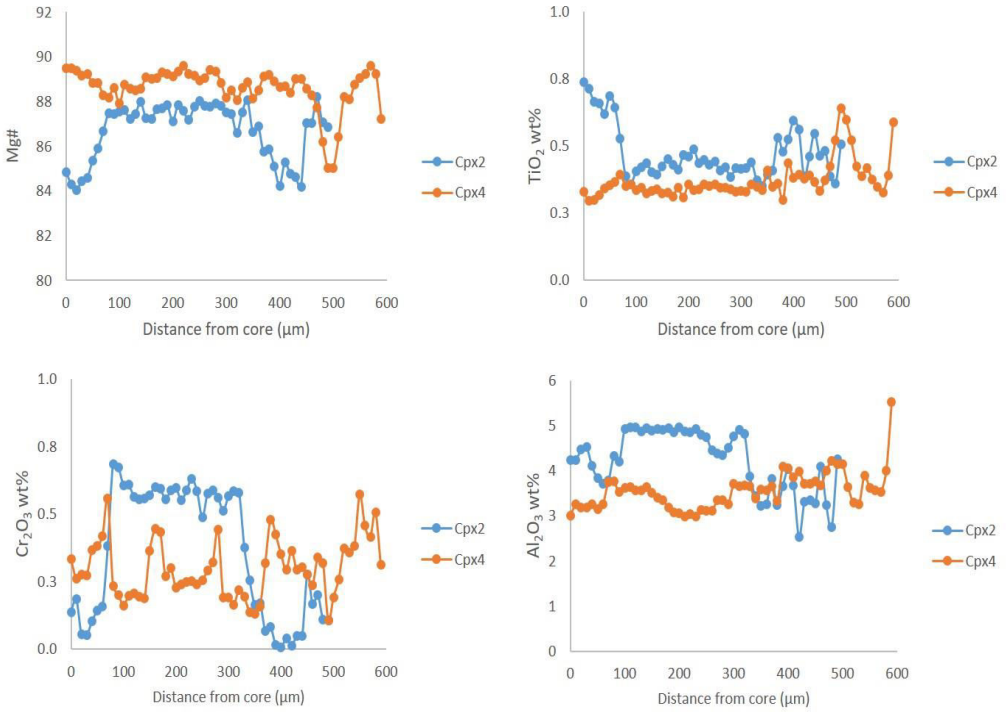

Fig. 22 – Clinopyroxene core to rim compositions of crystals from sample MRS2A.

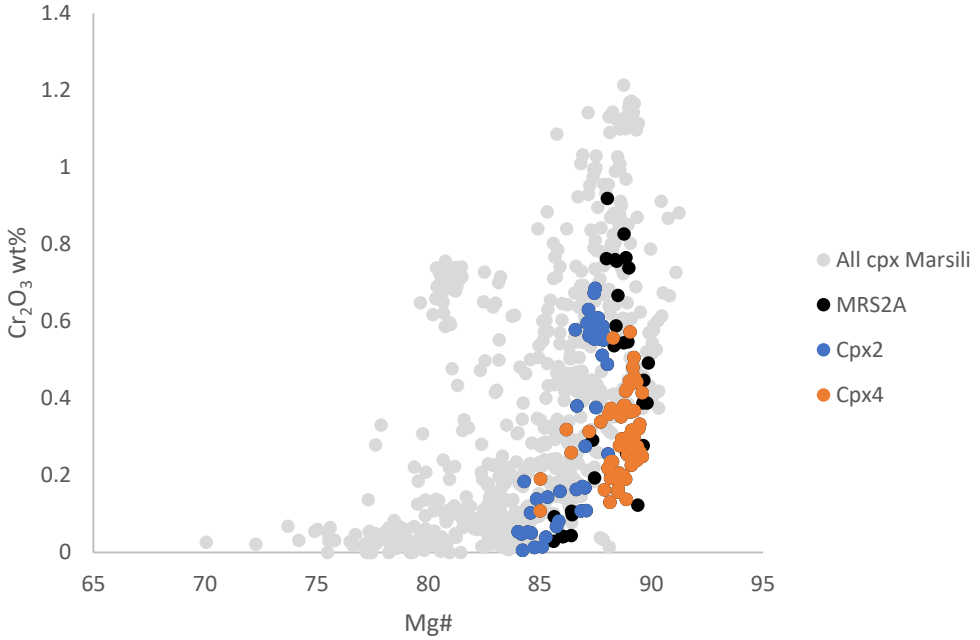

Fig. 23 - Cr_2O_3 contents of the clinopyroxene crystals from the sample MRS2A. Black dots represent the clinopyroxenes from this sample from Teresa Trua (personal communication).

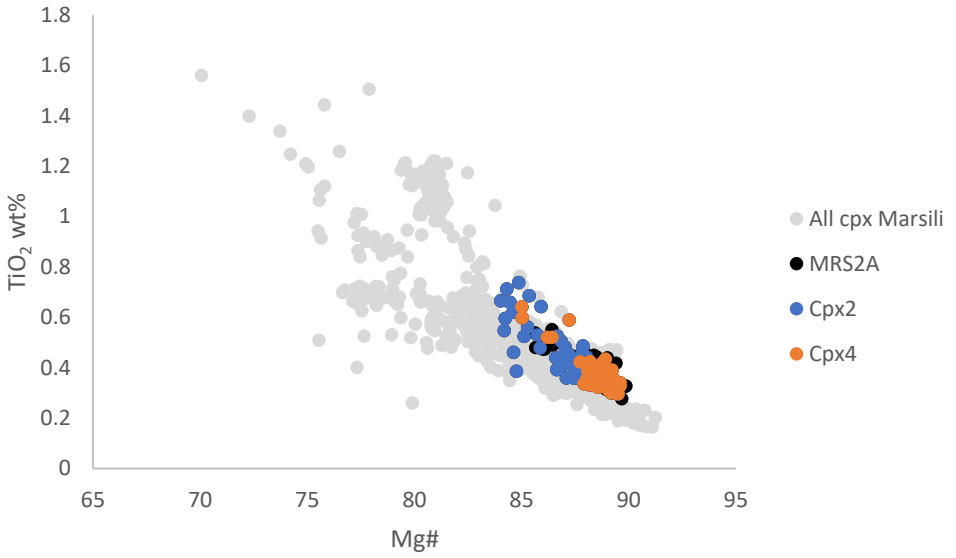

Fig. 24 – TiO_2contents of the clinopyroxene crystals from the sample MRS2A. Black dots represent the clinopyroxenes from this sample from Teresa Trua (personal communication).

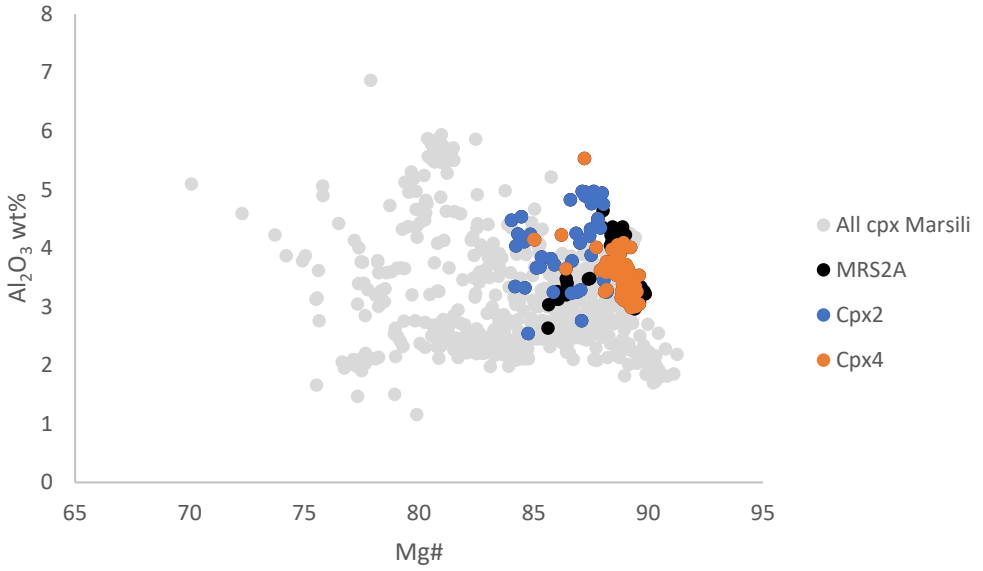

Fig. 25 - Al_2O_3 vs. Mg# for the clinopyroxenes from the sample MRS2A. Black dots represent the clinopyroxenes from Teresa Trua (Personal communication).

MRS4

Olivines

MRS4 olivine crystals are euhedral and isolated in the matrix. These crystals have two different core compositions of Fo90.5 and Fo88.5 (Fig. 26). All the four crystals are isolated except for one (Fo88.5) which is associated with a clinopyroxene crystal. Fo profiles are mostly flat and both crystals with Fo88.5 present normally zoned rims towards Fo85.

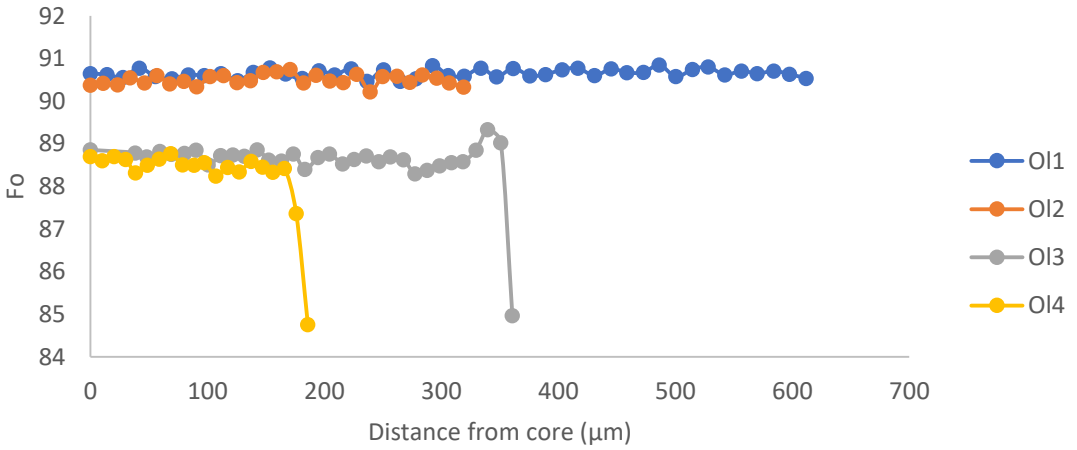

Fig. 26 - Fo core to rim profiles of the olivine crystals from the sample MRS4.

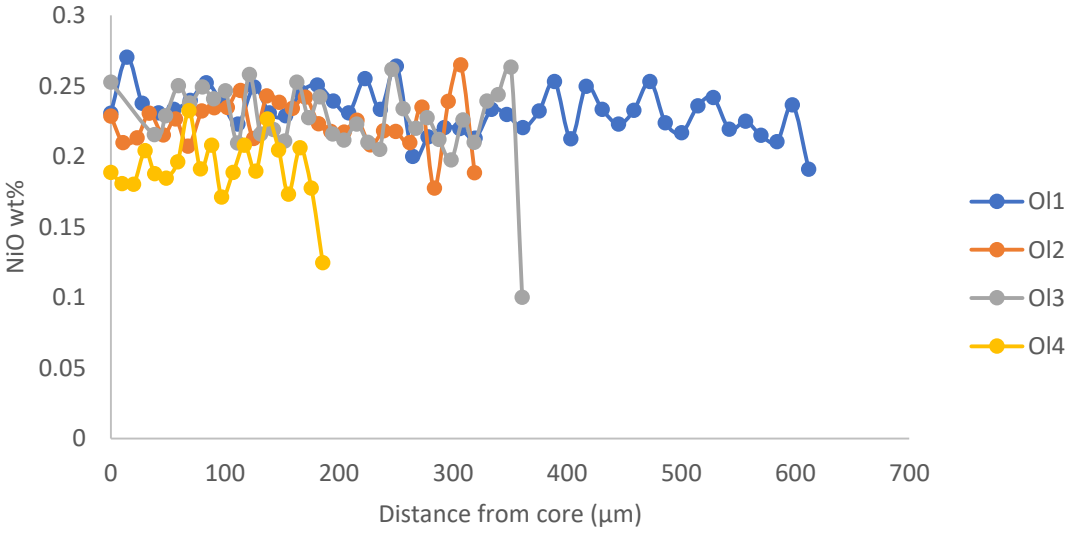

Fig. 27 - NiO core to rim profiles of the olivine crystals from the sample MRS4.

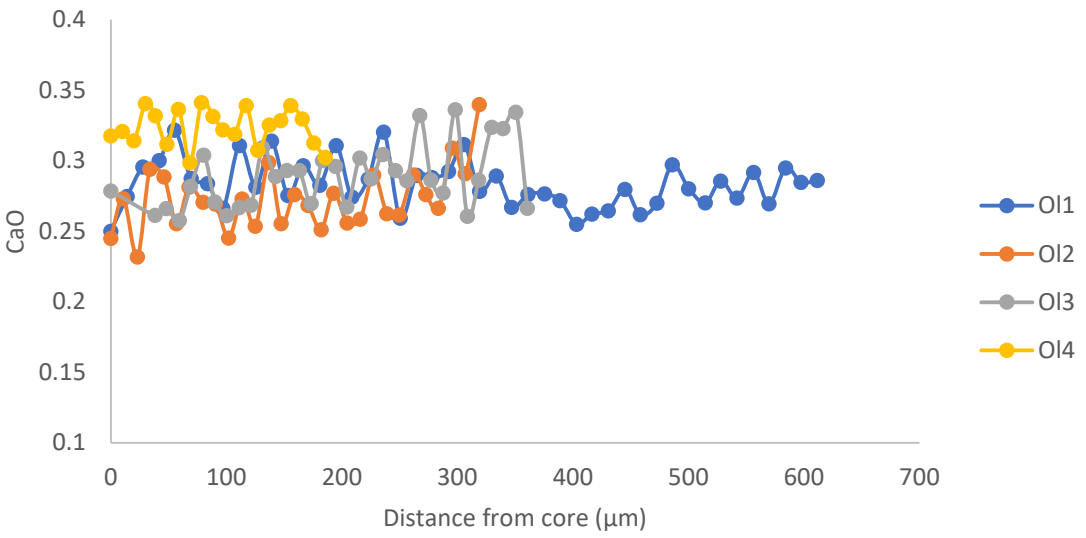

Fig. 28 - CaO core to rim profiles of the olivine crystals from the sample MRS4.

NiO contents plotted against Fo (Fig. 27) show that the crystals with Fo88.5 in the core present slightly different NiO contents, where Ol3 has the same NiO as Ol1 and Ol2, and Ol4 presents a lower NiO content. Cao contents are not correlated to Fo values (Fig. 28), in particular, Ol4 has slightly higher CaO than Ol3 despite their identical Fo. + It is noteworthy that Ol3 and Ol4, although presenting variable core NiO and CaO contents, present similar rim compositions.

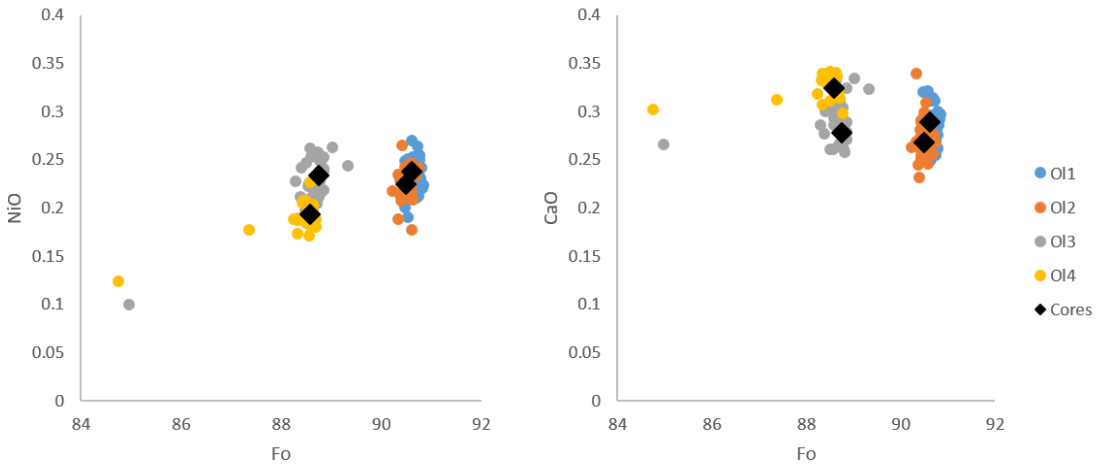

Fig. 29 - NiO vs. Fo and CaO vs. Fo for the olivine crystals from MRS4. Black diamonds represent the average compositions of the crystals' cores.

D4

Olivines

D4 olivines are compositionally similar, with all the cores clustering at Fo74-73 (Fig. 30). All the compositional profiles from core to rim show gradually zoned rims towards Fo76-74.5. All the analysed crystals are part of a glomerocryst with clinopyroxene and plagioclase. NiO (Fig. 31) and CaO (Fig. 32) profiles are always flat at fairly low values. Plots of NiO and CaO vs Fo (Fig. 33) show again the compositional similarity of the olivine crystals from this sample.

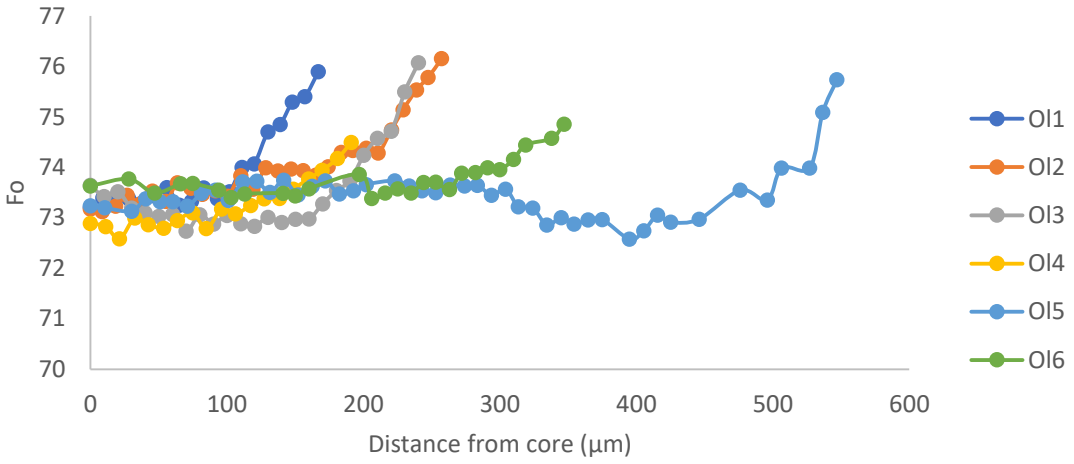

Fig. 30 - Fo core to rim profiles from for the olivine crystals from the sample D4.

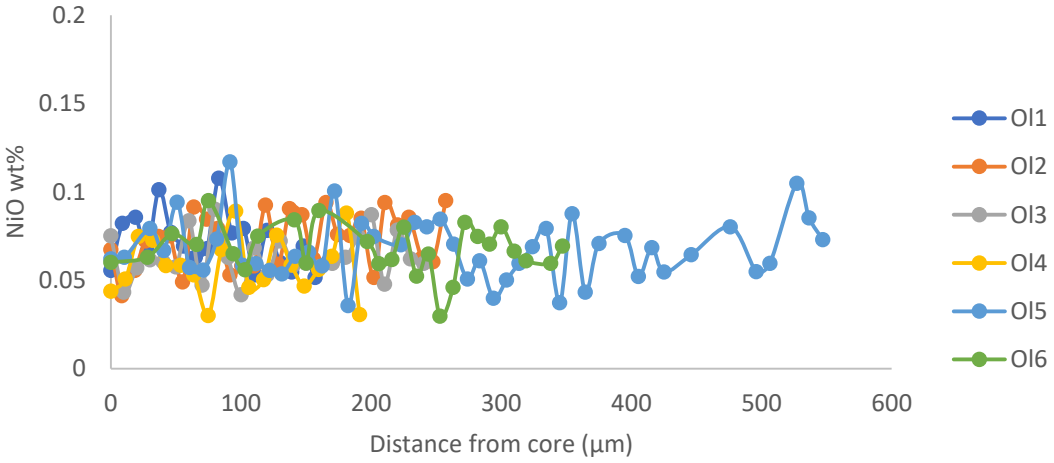

Fig. 31 – NiO core to rim profiles from for the olivine crystals from sample D4.

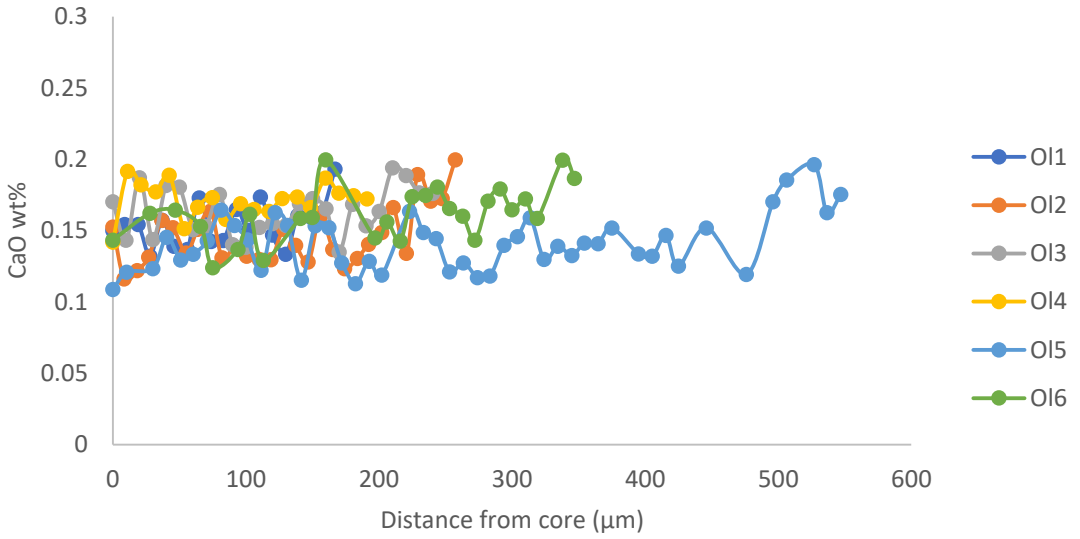

Fig. 32 - CaO core to rim profiles for the olivine crystals from the sample D4.

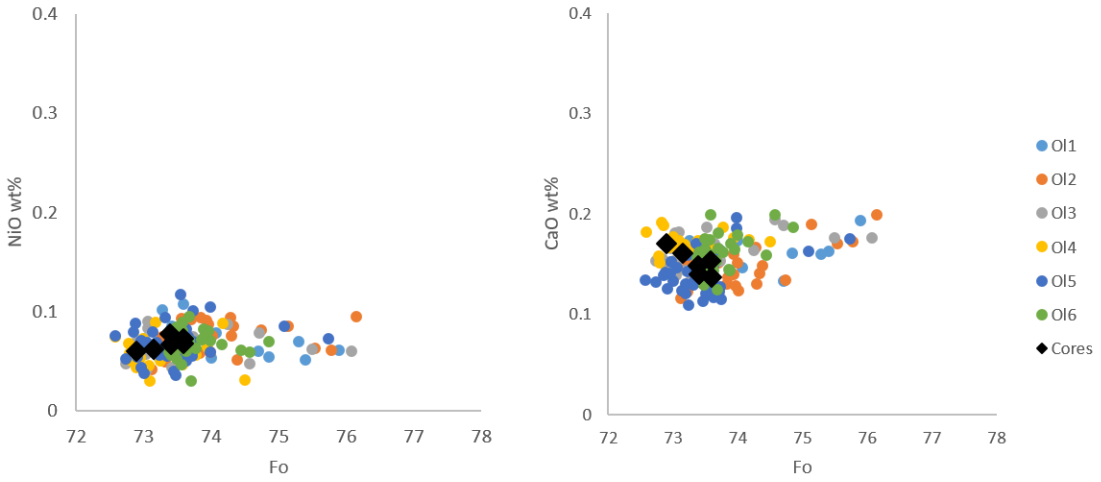

Fig. 33 - NiO vs. Fo and CaO vs. Fo for the olivine crystals from D4. Black diamonds represent the average compositions of the crystals' cores.

D5A

Olivines

D5A olivine crystals have the largest compositional variety. Olivine core compositions can be divided in 3 main groups: Fo90-86, Fo83-80, and Fo78-76. Zoning profiles are quite variable, with most of the crystals presenting normally zoned rims towards Fo83-80 and Fo77-75.5 (Fig. 34). Some of the crystals present reversely zoned patterns within the profile from core

to rim, with Fo varying within the range of Fo of its groups (e.g. (2) Ol2, (2) Ol4). Olivines with higher Fo contents are present either as isolated crystals or as mono-mineralic glomerocrysts. The rest of them usually form multi-mineralic glomerocrysts together with clinopyroxene and plagioclase.

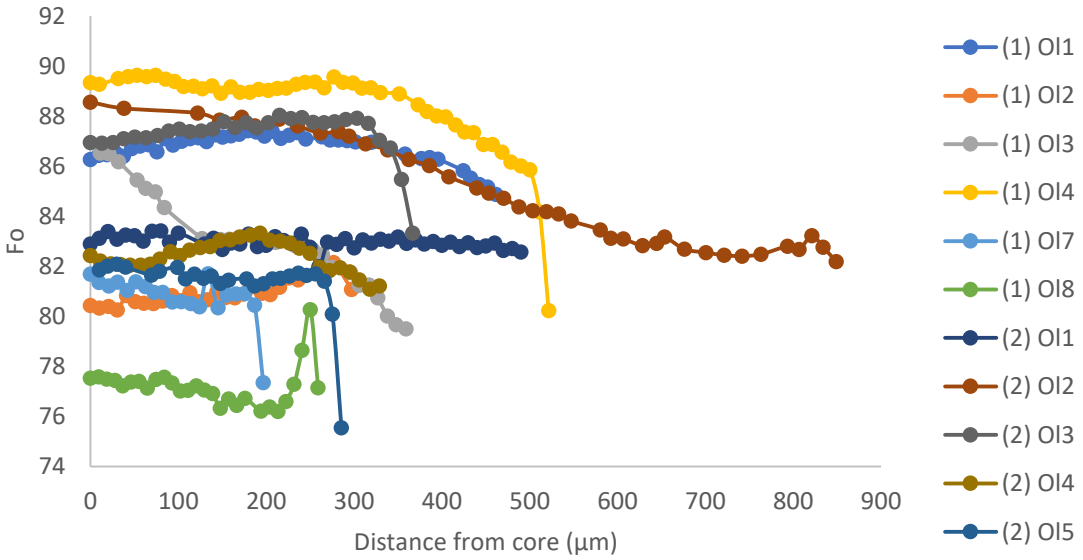

Fig. 34 - Fo core to rim profiles from core to rim for the olivine crystals from the sample D5A. The Fo profile of the olivine (1) Ol1 is from rim to rim.

NiO profiles show similar geometries compared to Fo, with the crystals with higher Fo values presenting evidently zoned profiles, while the crystals with lower Fo values present flat NiO profiles (Fig. 35). CaO profiles are generally flat from core to rim (Fig. 36). Only the crystal (2) Ol2 and (1) Ol3 show an evident variation of CaO from the core to the rim.

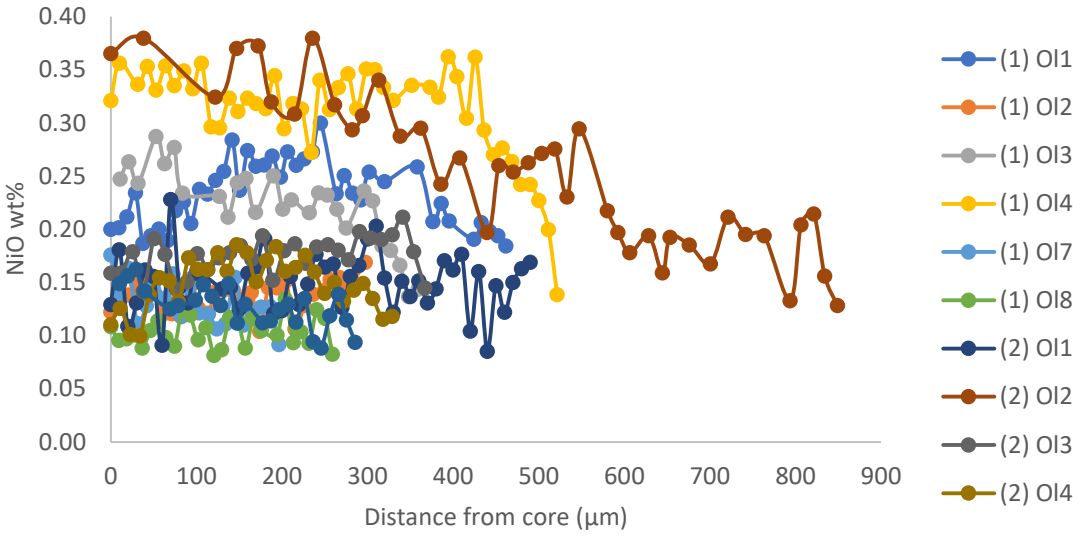

Fig. 35 - NiO core to rim profiles for the olivine crystals from the sample D5A. The NiO profile of the olivine (1) Ol1 is from rim to rim.

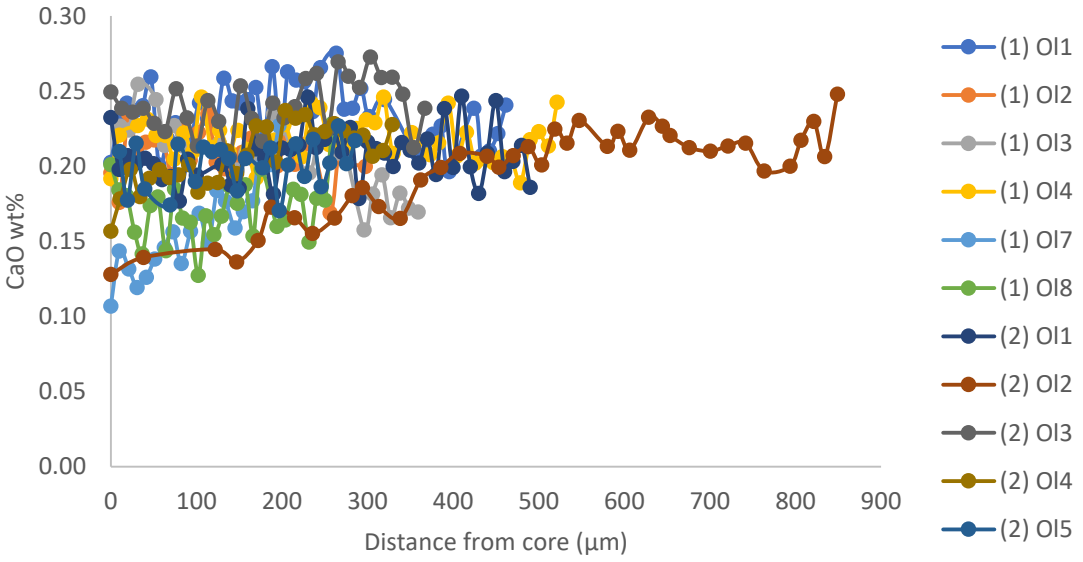

Fig. 36 - CaO core to rim profiles for the olivine crystals from the sample D5A. The CaO profile of the olivine (1) Ol1 is from rim to rim.

NiO vs. Fo variations are well correlated (Fig. 37). Crystals with Fo>85 present some heterogeneities but crystals with Fo<85 are quite homogeneous. Moreover, the crystals with Fo>85 form a steeper trend (stronger Ni/Fo decrease) compared to the crystals with Fo<85. It is interesting to see that the trend formed by all the data is much more variable than the trend formed by the core compositions. While the core average compositions present a curved trend, the crystals (1) Ol3 and (2) Ol2 form a linear trend. Also the CaO vs. Fo plot shows a good correlation, although presenting some variability for two of the three groups of crystals (Fo88-86 and Fo83-80) (Fig. 37). Most of the crystals describe a positive trend, while two crystals ((1)

Ol7 and (2) Ol2) show lower Ca contents than expected according with the general trend of the rest of the crystals. The trends defined by all the data points from these two crystals show that with the decrease of Fo, CaO increases towards the concentrations of the rest of the crystals with similar Fo.

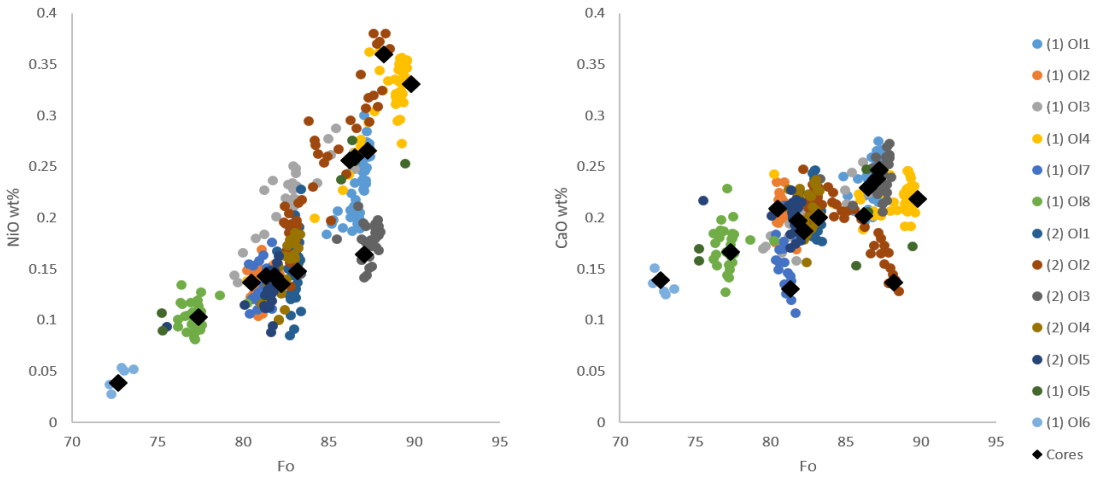

Fig. 37 - NiO vs. Fo and CaO vs. Fo for the olivine crystals from D5A. Black diamonds represent the average compositions of the crystals' cores.

Clinopyroxenes

Clinopyroxene crystals are generally included in glomerocrysts formed either by only clinopyroxene ($Mg\#_{90-86}$), by clinopyroxene + olivine ± plagioclase, or by clinopyroxene + plagioclase. Compositions vary largely, i.e., $Wo_{48-41}En_{49-42}Fs_{12-5}$ and Mg#90 to Mg#77. Rim compositions vary from Mg#88.5 to Mg#83 (Fig. 38). Compositional profiles show that all crystals were in contact with different magmas during crystallization, with oscillatory zoning possibly representing cyclic recharges of magma. TiO_2 (Fig. 40) presents a clear negative correlation with Mg#, while Cr_2O_3 (Fig. 39) correlates positively with Mg#. Al_2O_3 (Fig. 41) correlates negatively with Mg# but it is significantly more scattered than TiO_2 and Cr_2O_3.

Trace element compositions were obtained for a relatively large set of clinopyroxenes (Fig. 39; including data from Teresa Trua, personal communication). The clinopyroxenes from the sample D5A present a slight depletion for LREE (light rare earth elements) comparing to HREE (heavy rare earth elements) when normalised to the Chondrite (Sun & Mcdonough, 1989). Patterns are not complete for most of the analysed points and HREE generally show larger

analytical errors. $Ce/Dy_{(N)}$ was used to describe the variations between LREE and HREE, and the analysed crystals vary from 1.25 to 0.54. N-MORB-normalised trace elements (Sun & Mcdonough, 1989) present rather flat incompatible elements patterns with important negative anomalies for Nb, Sr, Zr and Ti (Fig.). $Ce/Y_{(N)}$ ratio was calculated to describe the behaviour of these patterns and the analysed clinopyroxenes range from 3.45 to 0.95.

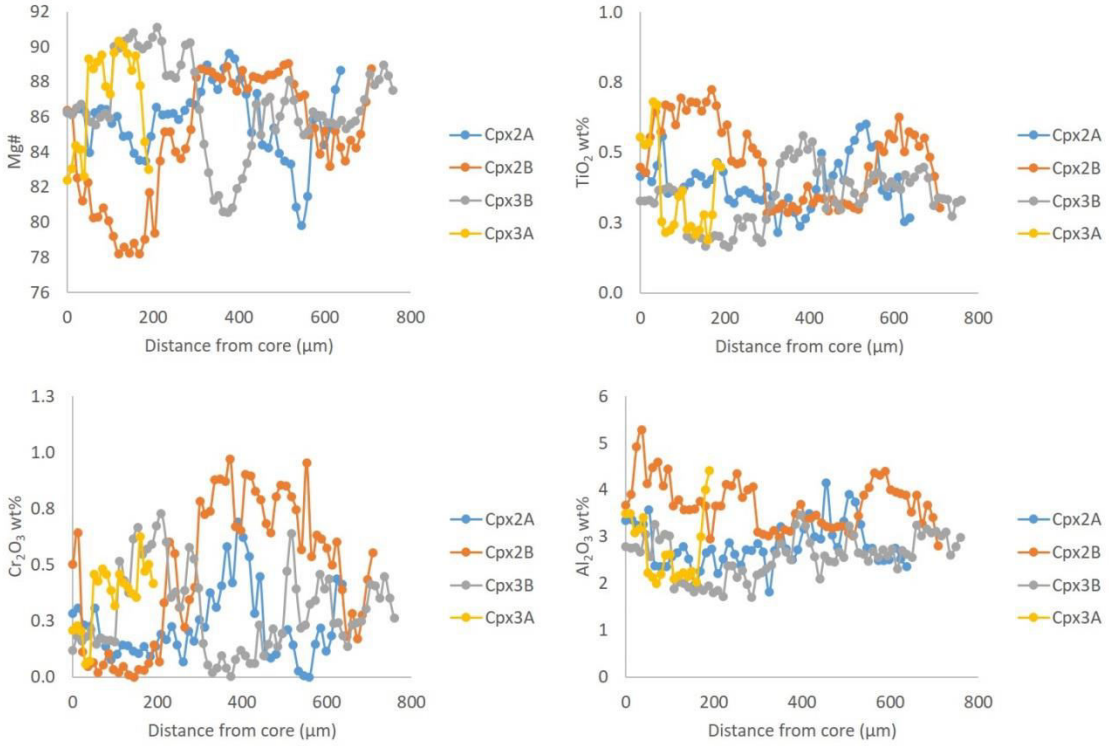

Fig. 38 - Compositional profiles of Mg#, TiO_2, Cr_2O_3 and Al_2O_3 (wt. %) from core to rim of the clinopyroxene crystals from D5A.

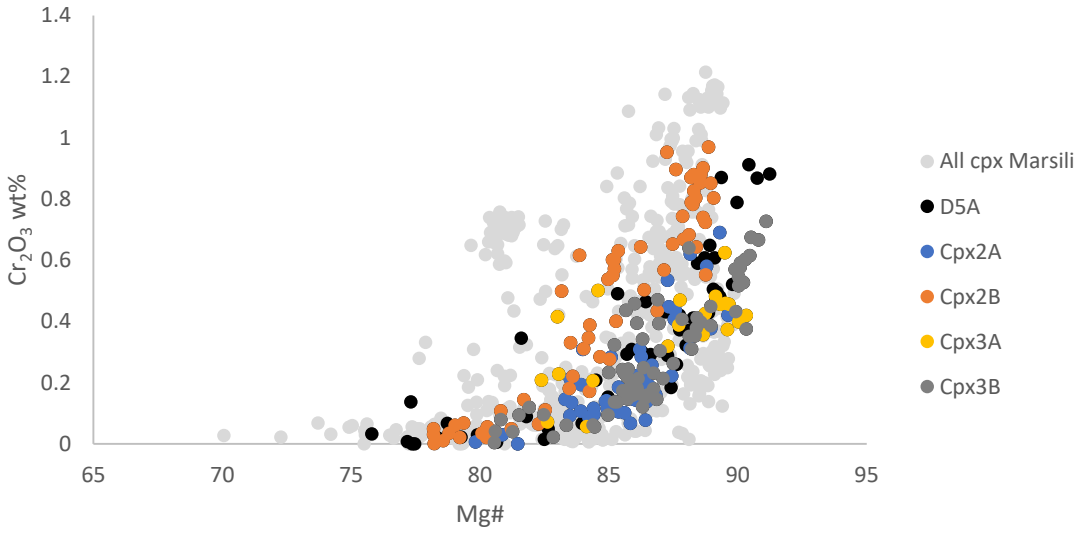

Fig. 39 . Cr_2O_3 vs. Mg# for the clinopyroxenes from the sample D5A. Black dots represent clinopyroxene crystals in D5A from Teresa Trua (Personal communication).

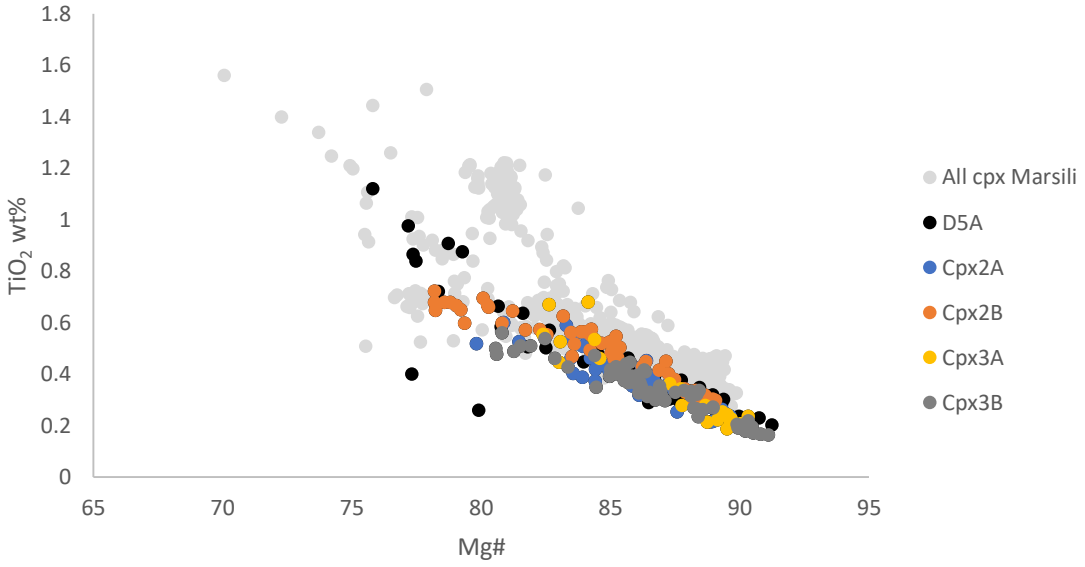

Fig. 40 - TiO_2 vs. Mg# for the clinopyroxenes from the sample D5A. Black dots represent clinopyroxene crystals in D5A from Teresa Trua (Personal communication).

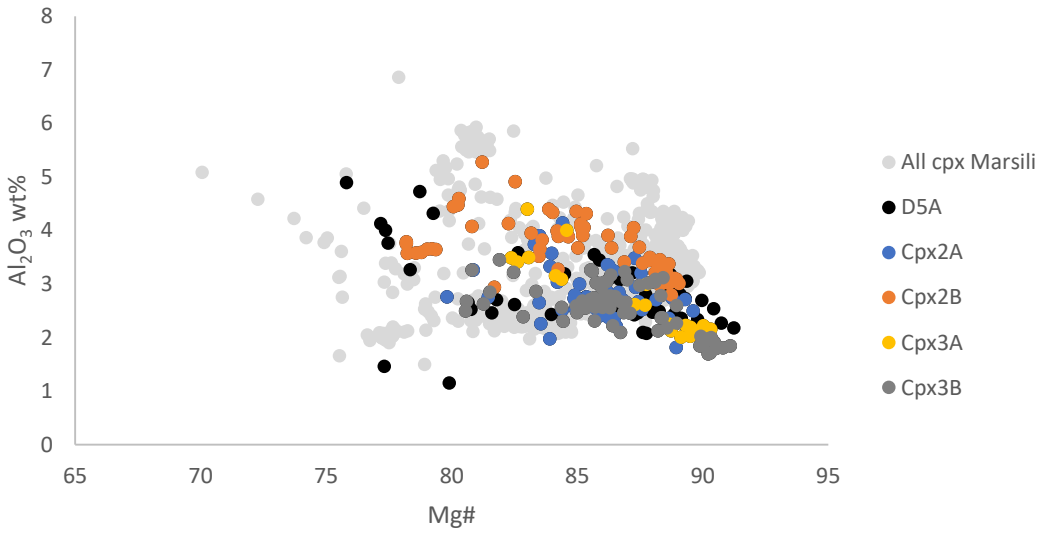

Fig. 41 - Al_2O_3 for the clinopyroxenes from the sample D5A. Black dots represent clinopyroxene crystals in D5A from Teresa Trua (Personal communication).

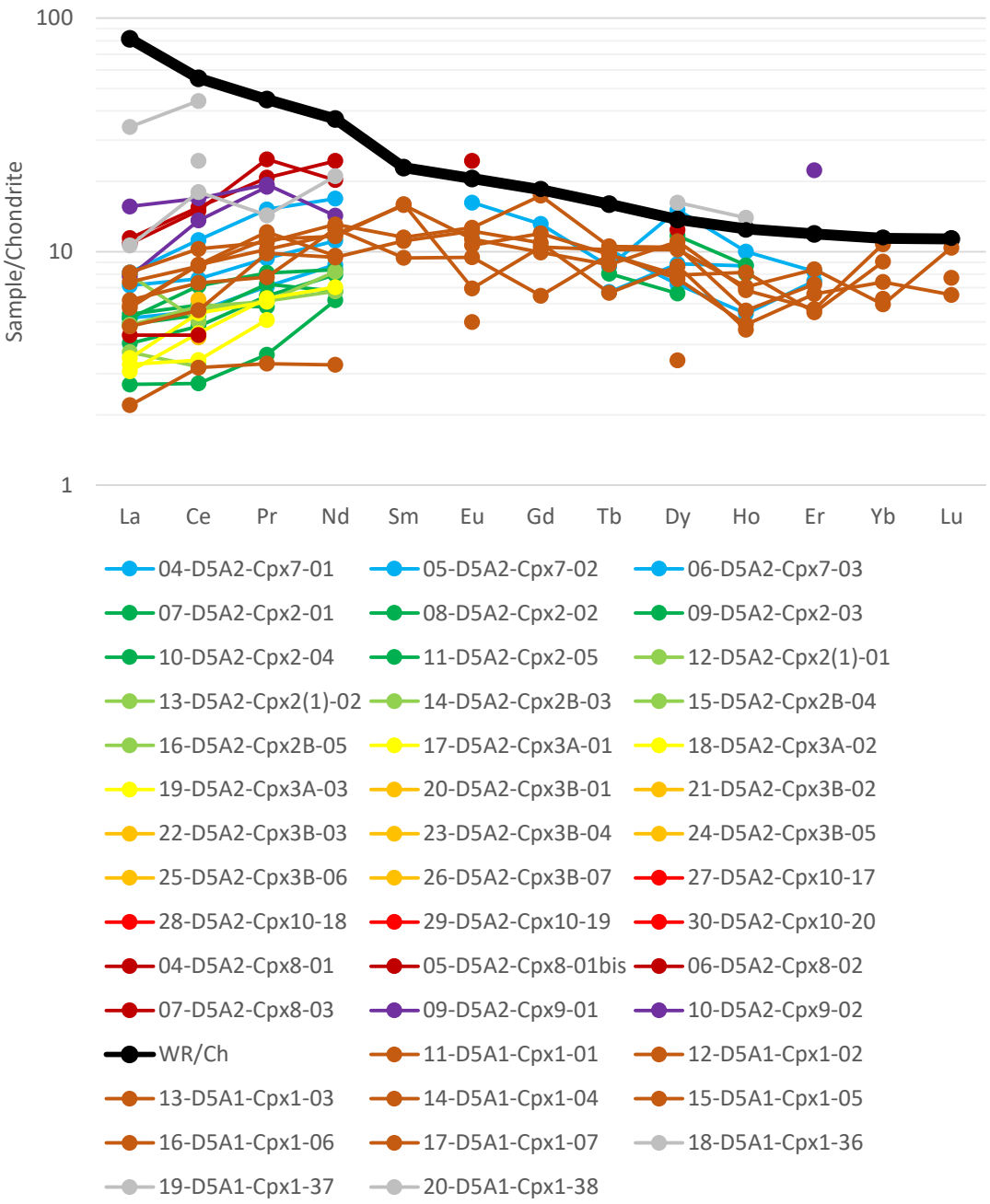

Fig. 42 - Rare earth elements from clinopyroxenes from D5A normalised to Chondrite (Sun & Mcdonough, 1989). *Black line represents the whole rock composition* (Teresa Trua & Marani, 2011). *Each colour represents a different crystal. Crystals Cpx2A, Cpx2B, Cpx3A and Cpx3B correspond to the compositional profiles shown above. The rest of the crystals are represented as black diamonds in Fig. 39, 40 and 41.*

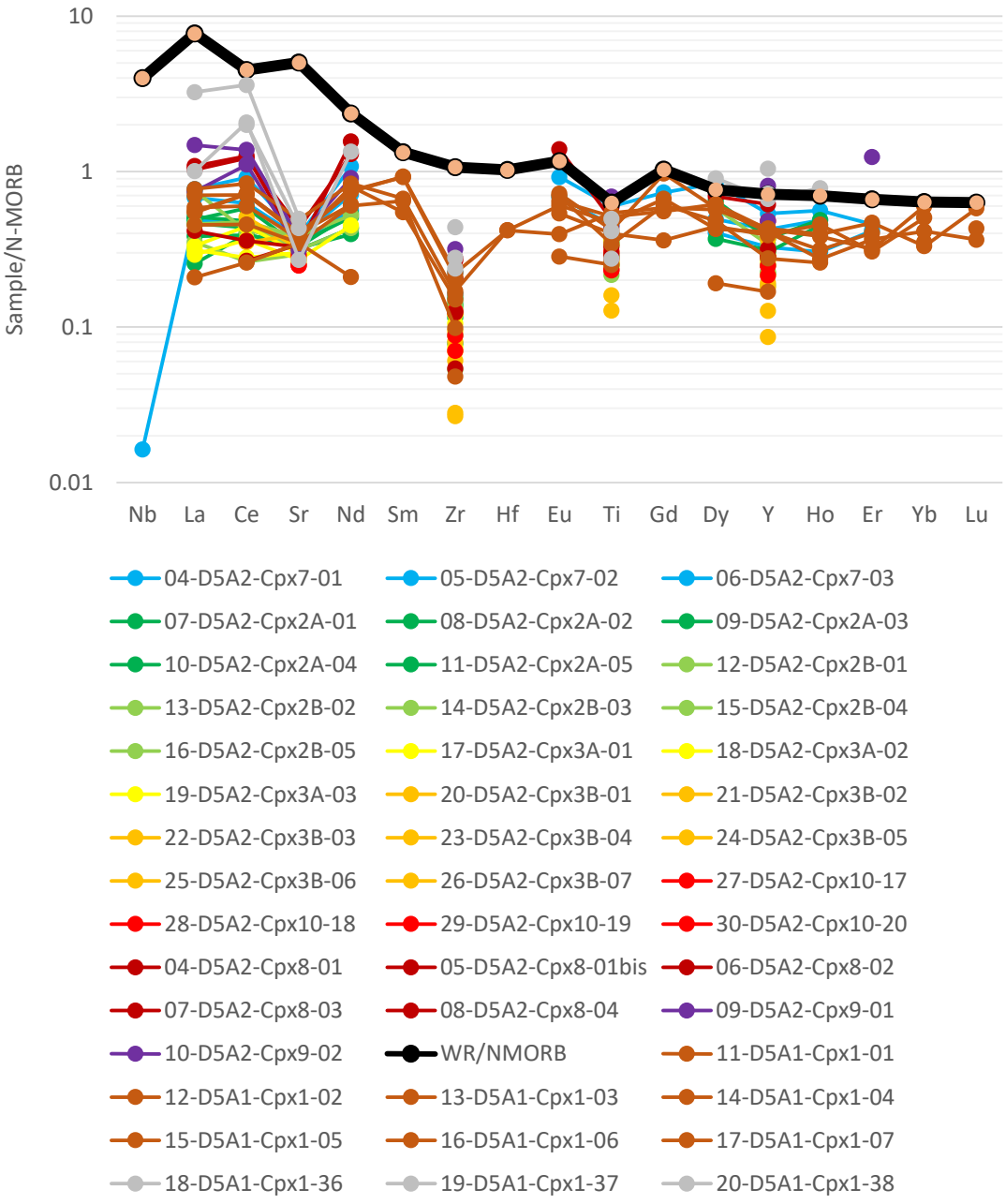

Fig. 43 - Incompatible elements from clinopyroxenes from D5A normalised to N-MORB (Sun & Mcdonough, 1989). *Black line represents the whole rock composition* (Teresa Trua & Marani, 2011). *Each colour represents a different crystal. Crystals Cpx2A, Cpx2B, Cpx3A and Cpx3B correspond to the compositional profiles shown above. The rest of the crystals are represented as black diamonds in Fig. 39, 40 and 41.*

D6

Olivines

D6 olivine crystals have subhedral to euhedral textures and generally are isolated from other crystals. Olivine Ol1 is significantly at least two times larger than the other olivine crystals. One crystal has a core plateau at Fo86; three crystals that vary their core and mantle compositions between Fo84.5 and Fo83.5; and a last crystal with Fo80 in the core and Fo77 closer to the rim (although the rim registers Fo80). All the five profiles show relatively simple geometries, with all the crystals presenting a plateau in the centre of the crystals and normal zoning towards the rim. The crystal Ol4 shows a more complex rim geometry, with a reverse zoning following the described normal zoning. All the crystals have zoned rims range from Fo81.5 to 80.

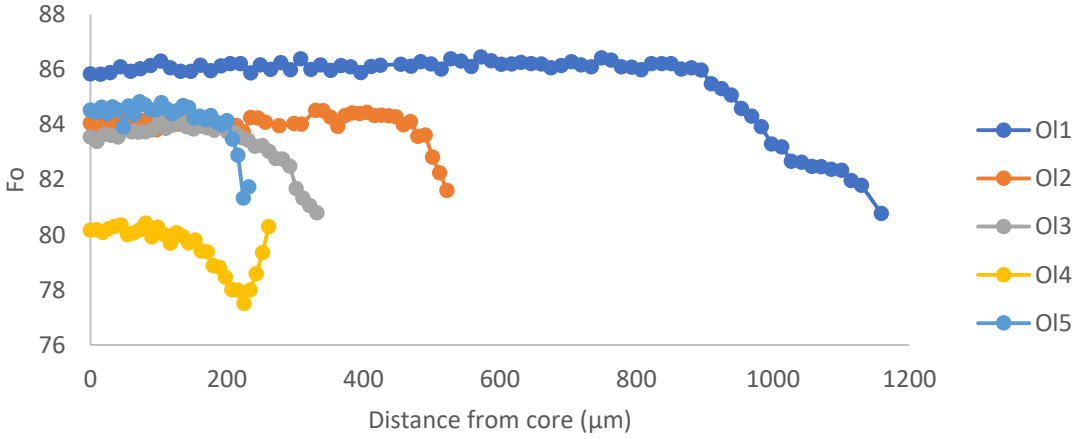

Fig. 44 - Fo core to rim profiles of the olivine crystals from the sample D6.

NiO (wt. %) profiles are similar to Fo profiles (Fig. 45), with the rims of most of the crystals presenting normal zoning. CaO profiles (Fig. 46) instead show reversely zoned rims for all the crystals (0.21 – 0.25 wt. %). NiO vs. Fo shows that crystals with core Fo84 present variable NiO contents, although the general trend positive (Fig. 47). CaO vs Fo shows that the olivines with the Fo84 again present variable CaO contents (Fig. 47). The general trend formed by all crystals is negative.

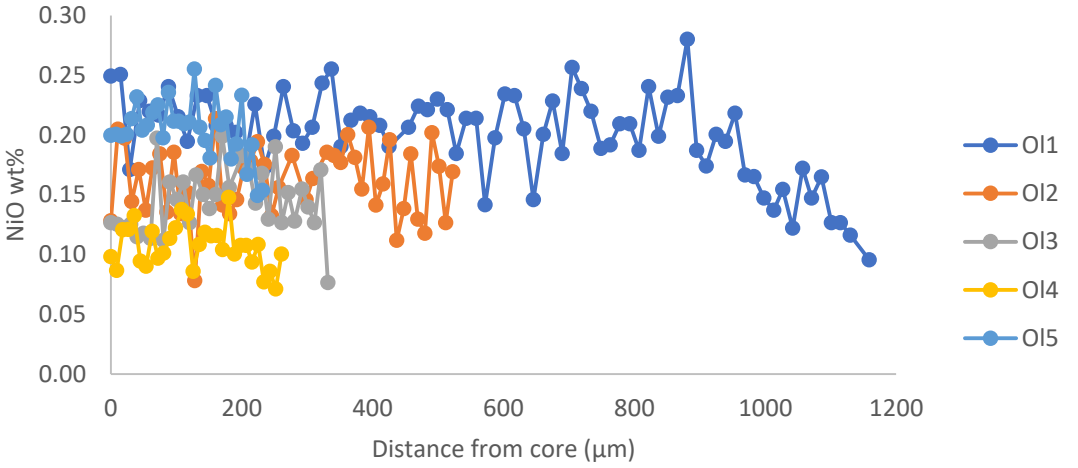

Fig. 45 - NiO core to rim profiles for the olivine crystals from the sample D6.

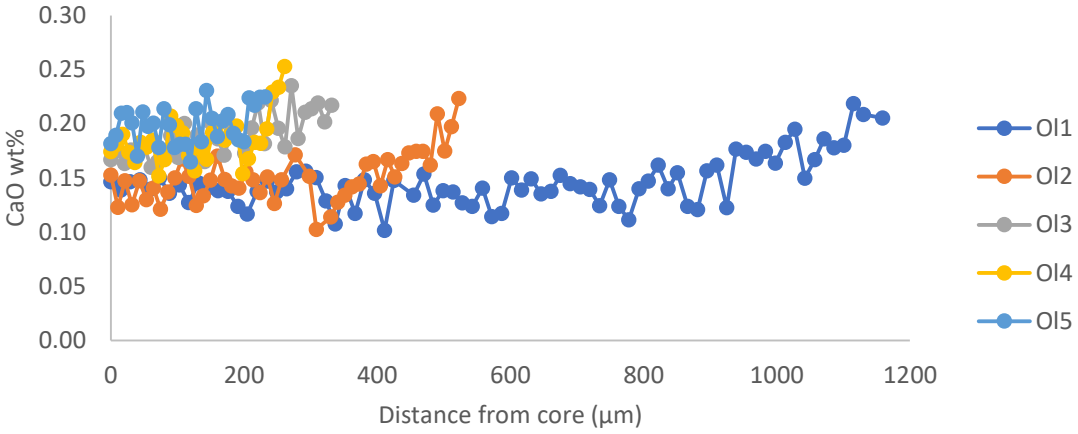

Fig. 46 – CaO core to rim profiles for the olivine crystals from the sample D6.

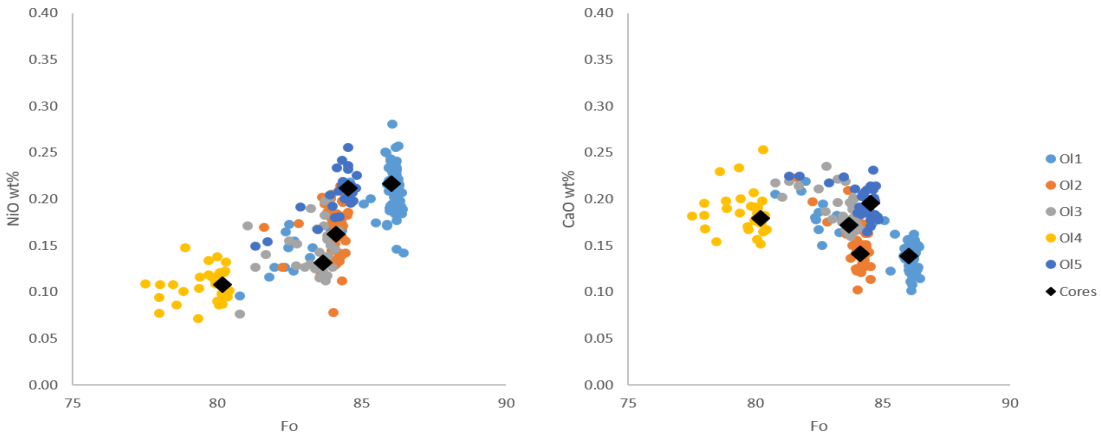

Fig. 47 - NiO vs Fo and CaO vs. Fo for the olivines from D6. Black diamonds represent the average compositions of the crystals' cores.

Clinopyroxenes

D6 clinopyroxenes ($Wo_{49-46}En_{44-40}En_{13-9}$) present cores with Mg#80 and compositional profiles are slightly different, with Cpx1 presenting flat profiles for all the elements and Mg# while Cpx2 presents gradually different compositions from core to rim (Fig. 48). Cr_2O_3 (Fig. 49) and Al_2O_3 (Fig. 51) vs Mg# show that the two analysed crystals are compositionally distinct, although TiO_2 (Fig. 50) is similar for both. Moreover, these clinopyroxenes have the highest Al_2O_3O and TiO_2 contents compared to the other samples.

Trace element analyses show parallel profiles with no significant variability. The compositions overlap those already published for this sample (Trua et al., 2014) and no significant differences were found from core to rim. Chondrite-normalised (Fig. 52) $Ce/Dy_{(N)}$ for these two clinopyroxenes vary from 2.78 to 1.92, showing a general enrichment of LREE comparing to HREE. N-MORB-normalised incompatible elements (Fig. 53) show important negative anomalies for Nb, Sr, Zr and Ti (Fig.). The $Ce/Y_{(N)}$ for D6 ranges from 5 to 3.38.

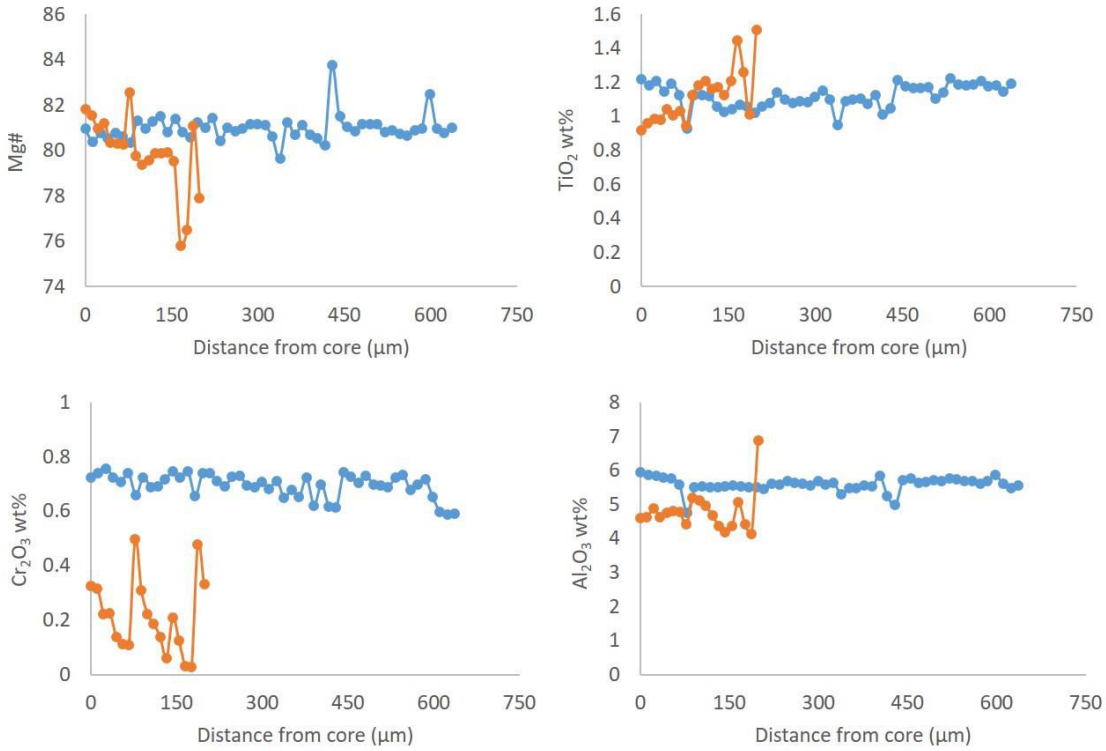

Fig. 48 - Compositional profiles of Mg#, TiO_2, Cr_2O_3 and Al_2O_3 (wt. %) from core to rim of the clinopyroxene crystals from D6.

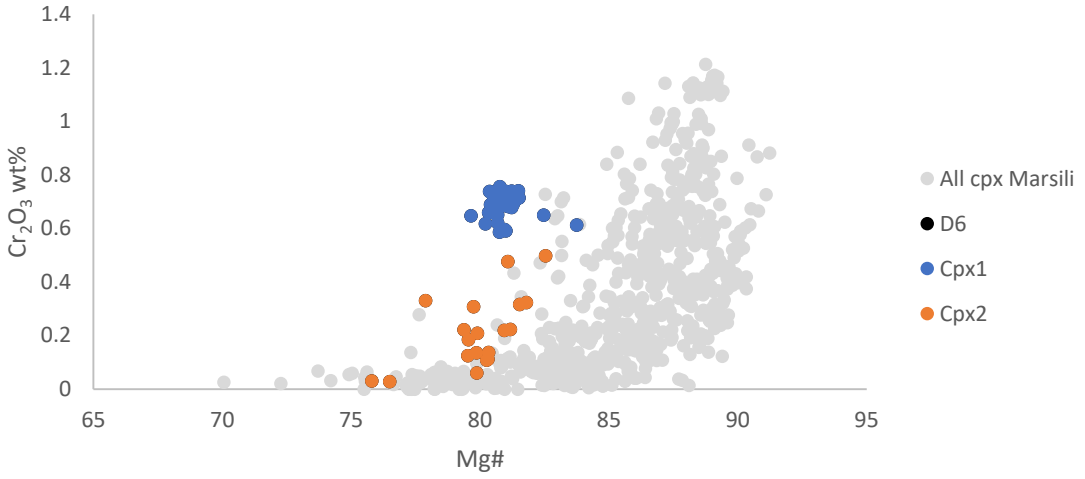

Fig. 49 - Cr_2O_3 vs. Mg# for the clinopyroxene crystals from the sample D6.

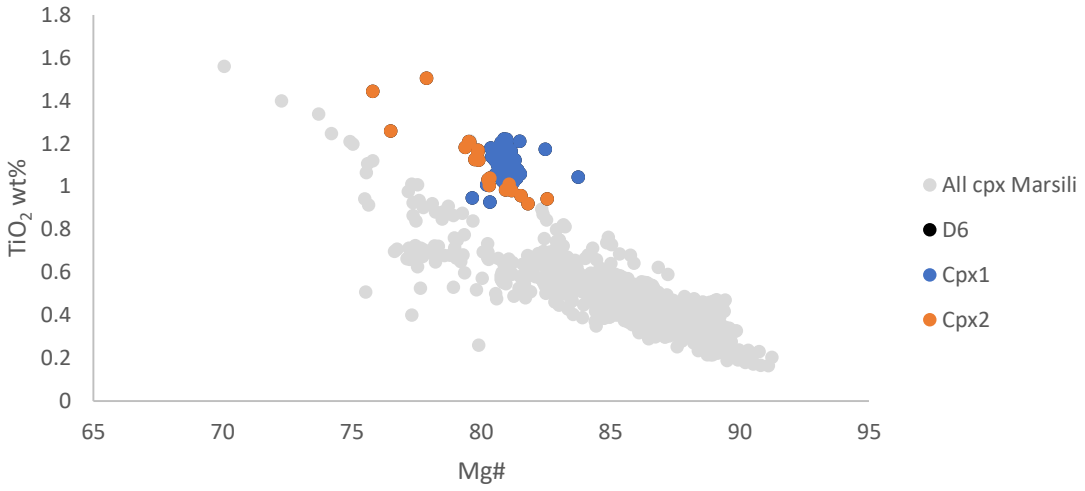

Fig. 50 - TiO_2 vs. Mg# for the clinopyroxene crystals from D6.

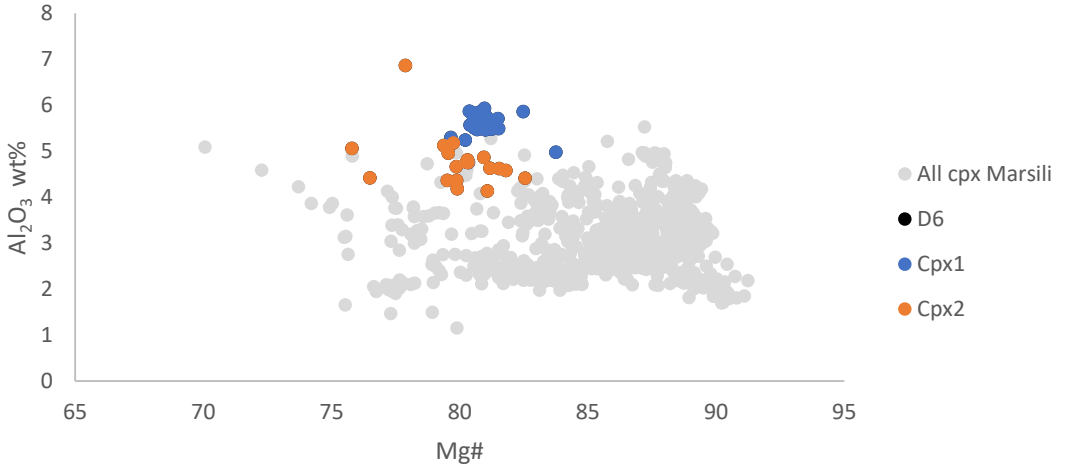

Fig. 51 - Al_2O_3 vs. Mg# for the clinopyroxene crystals from D6.

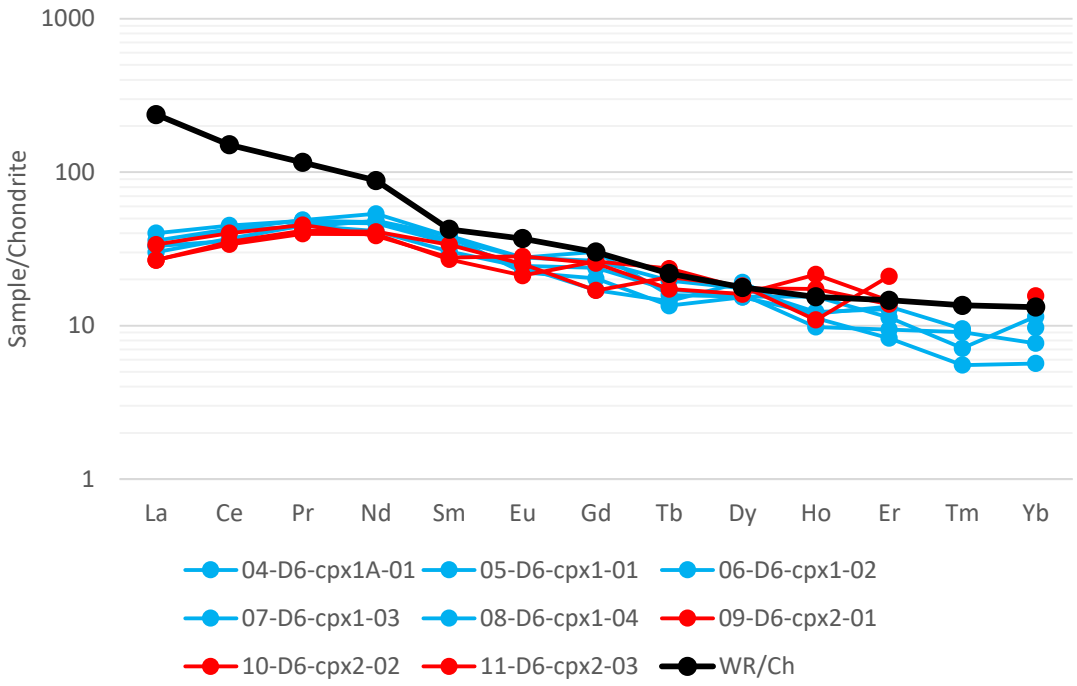

Fig. 52 - Rare earth elements from clinopyroxene crystals from D6 normalised to Chondrite (Sun & Mcdonough, 1989). *Black line represents the whole rock composition* (Trua et al., 2011). *Each colour represents a different crystal.*

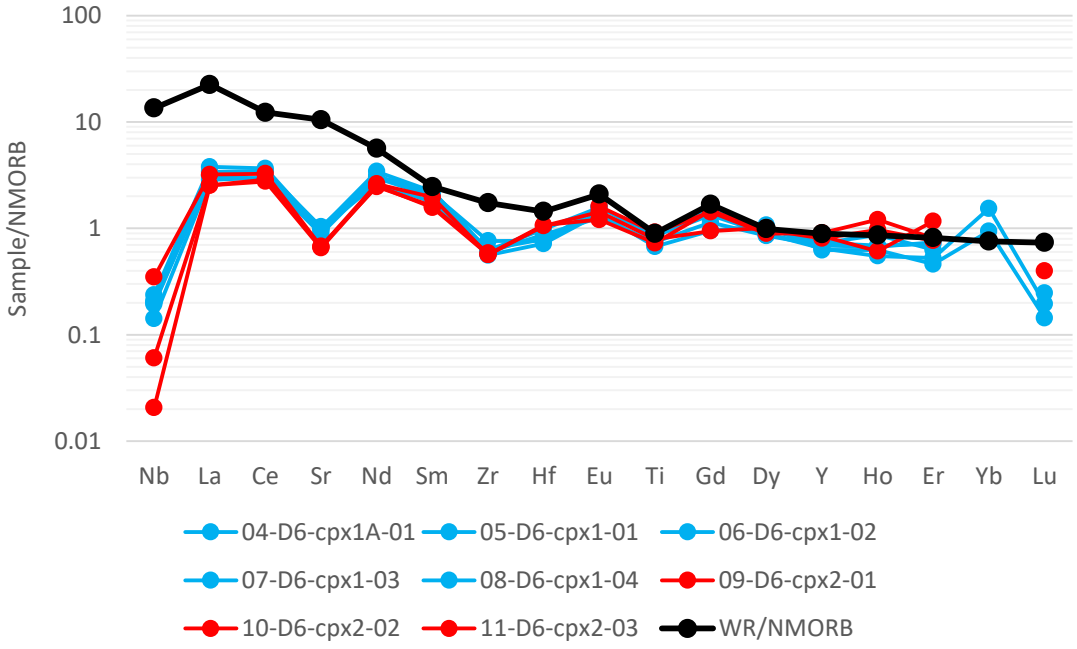

Fig. 53 - Incompatible elements from clinopyroxene crystal from D6 normalised to N-MORB (Sun & Mcdonough, 1989). *Black line represents the whole rock composition* (Trua et al.,, 2011). *Each colour represents a different crystal.*

D12D2

(Note: this sample is sometimes called D12D1 during the dissertation)

Olivines

Olivine crystals from D12D2 have two main core composition groups, with the first ranging from Fo88 to Fo86 and the second from Fo83.5 to Fo82.5 (Fig. 54). Compositional profiles have different geometries but are consistent. The first group of crystals show normally zoned profiles. On the contrary, crystals with Fo83 within the core have profiles zoned in a more complex way, with a mix of reversed and normally zoning geometries. Rim compositions vary from Fo84.5 to Fo83 apart from one crystal, which shows a rim of Fo85.5. Apart from Ol7, the NiO profiles (Fig. 55) of the analysed olivines present similar geometries to the Fo profiles. However, changes in Ni contents are observed closer to the rim of the crystals than Fo variations. For example, Ol4 starts the reversed zoning for Fo at 300 μm, while for NiO, the same reserved zoning starts at ca. 400 μm. CaO (Fig. 56) presents flat profiles for olivines with Fo88-86 cores, while those with Fo83.5-82.5 cores present zoned rims towards higher CaO contents, overlapping the CaO contents of the rest of the crystals. NiO vs. Fo (Fig. 57) shows that all the crystals form simple trend. CaO shows similar contents for all crystals ranging from Fo88 to Fo86, while it is significantly lower in the more differentiated olivines (Fig. 57).

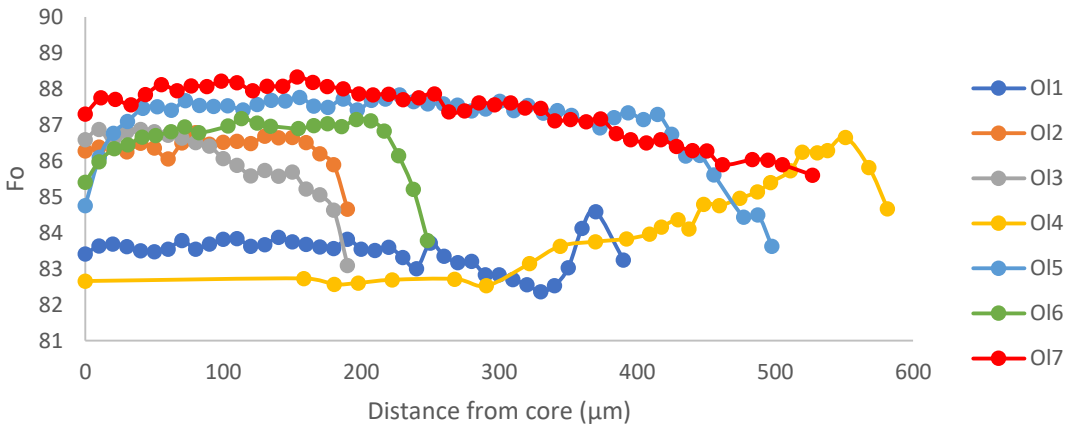

Fig. 54 - Fo core to rim profiles of the olivine crystals from the sample D12D2. Ol5 is a profile from rim to rim.

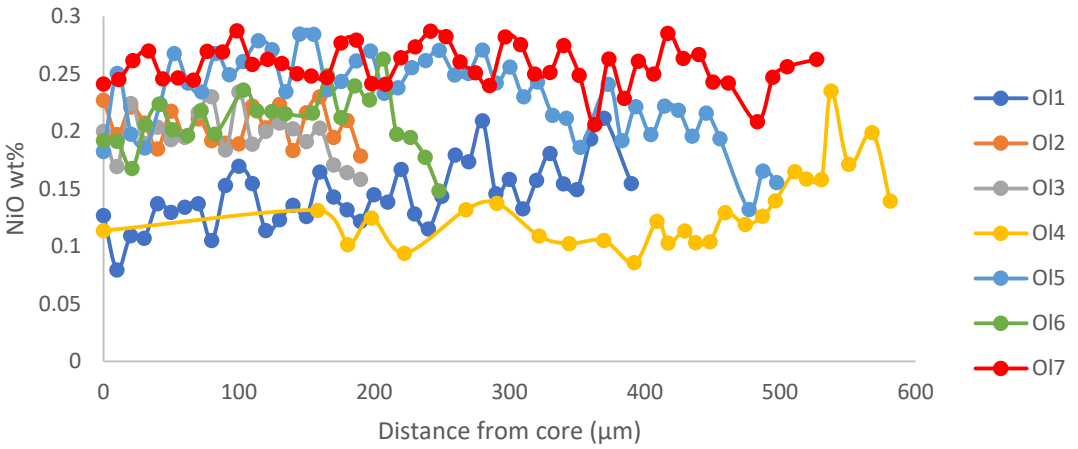

Fig. 55 - NiO core to rim profiles for the olivine crystals from the sample D12D2. Ol5 is a profile from rim to rim.

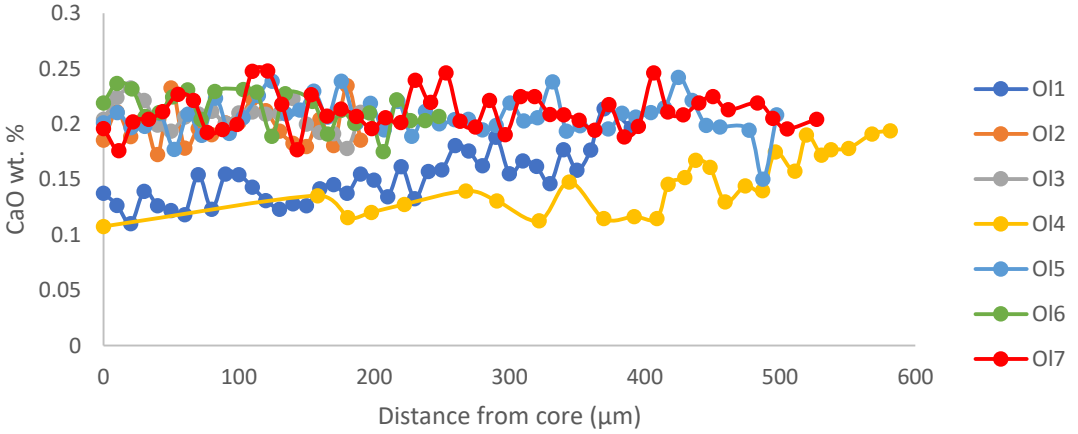

Fig. 56 - CaO core to rim profiles for the olivine crystals from the sample D12D2. Ol5 is a profile from rim to rim.

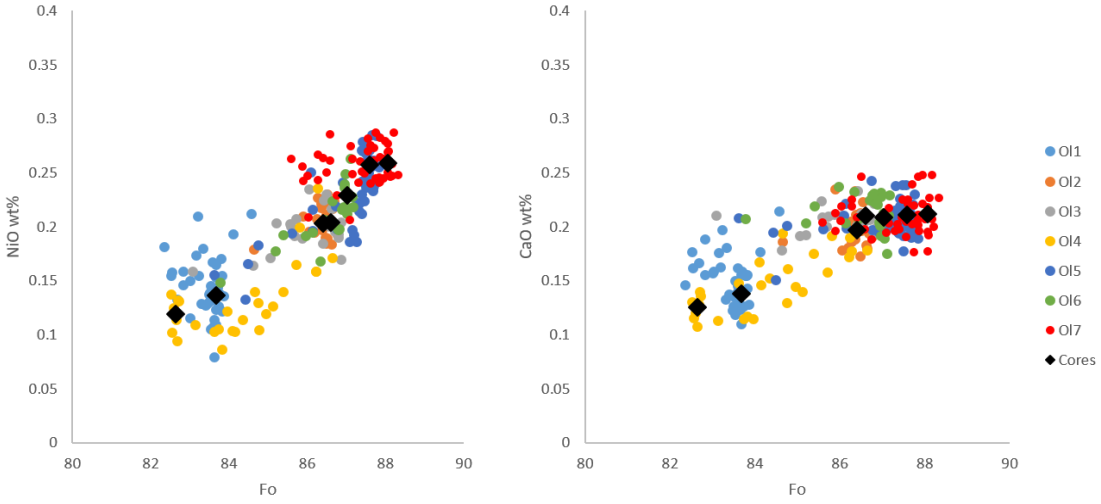

Fig. 57 - NiO vs. Fo and CaO vs. Fo for the olivine crystals from D12D2. Black diamonds represent the average compositions of the crystals' cores.

Clinopyroxenes

Clinopyroxene crystals are usually euhedral. Three different groups of crystals are observed: 1) crystals with more than 1 mm length, with no sign of disequilibrium; 2) crystals ranging from 1mm to 0.5 mm length, generally isolated or inter-crystallized with plagioclase, with cores showing resorption textures; 3) micro-phenocrysts, less than 0.5 mm, that are usually isolated or occur in small mono-mineralic clusters. The analysed crystals ($Wo_{48-39}En_{49-46}Fs_{12-6}$) range from Mg#89 to Mg#82. Compositional profiles present variable oscillatory geometries with compositional plateaus observed at Mg#89, Mg#87, Mg#84.5 and Mg#82.5 (Fig. 58). Rim compositions are homogeneous (Mg#87.5-86.5). TiO_2 (Fig. 60) contents correlate negatively with Mg#, while Al_2O_3 (Fig. 61) and Cr_2O_3 (Fig. 59) correlate positively.

Trace elements were analysed in the three described crystals and the obtained compositions overlap the compositions already reported for the clinopyroxenes from this sample (Trua et al., 2014). The present analysis present the trace elements variations within the crystal (from core to rim). Chondrite-normalised rare earth elements show variable contents that correlate negatively with Mg# (not shown). $Ce/Dy_{(N)}$ range from 1.79 to 0.65 and no significant Eu anomaly was found (Fig. 62). N-MORB-normalised incompatible elements (Sun & Mcdonough, 1989) patterns with important negative anomalies for Nb, Sr, Zr and Ti (Fig. 63). $Ce/Y_{(N)}$ range from 3.06 to 1.29, with the higher values corresponding to the lower Mg# contents in the crystal Cpx4, interpreted to be an antecryst.

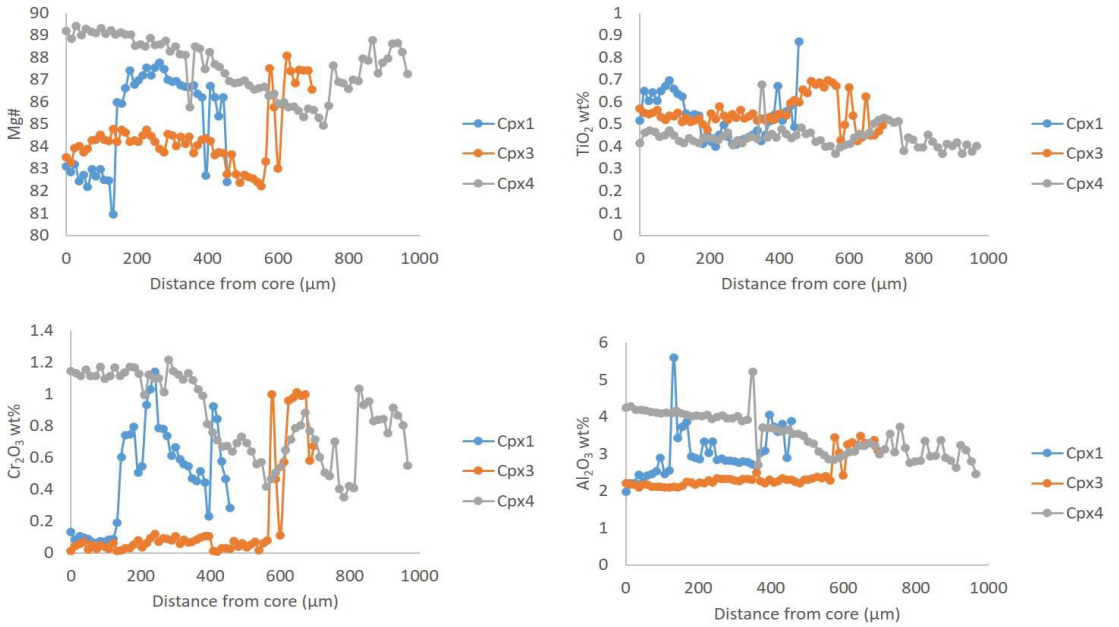

Fig. 58 - Compositional profiles of Mg#, TiO_2, Cr_2O_3 and Al_2O_3 from core to rim of the clinopyroxene crystals from D12D2.

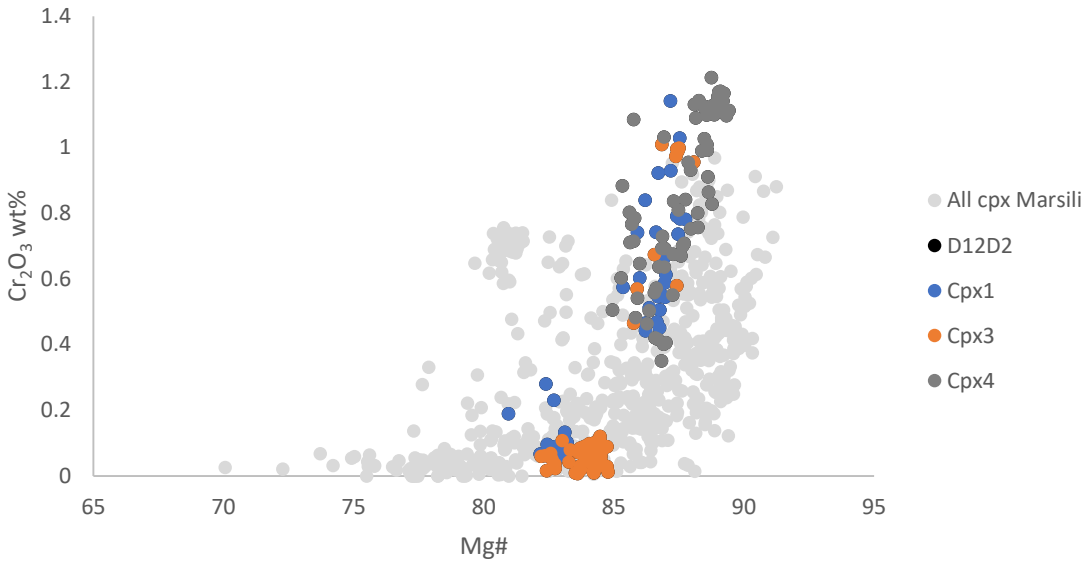

Fig. 59 - Cr_2O_3 vs. Mg# for the clinopyroxene crystals from the sample D12D1.

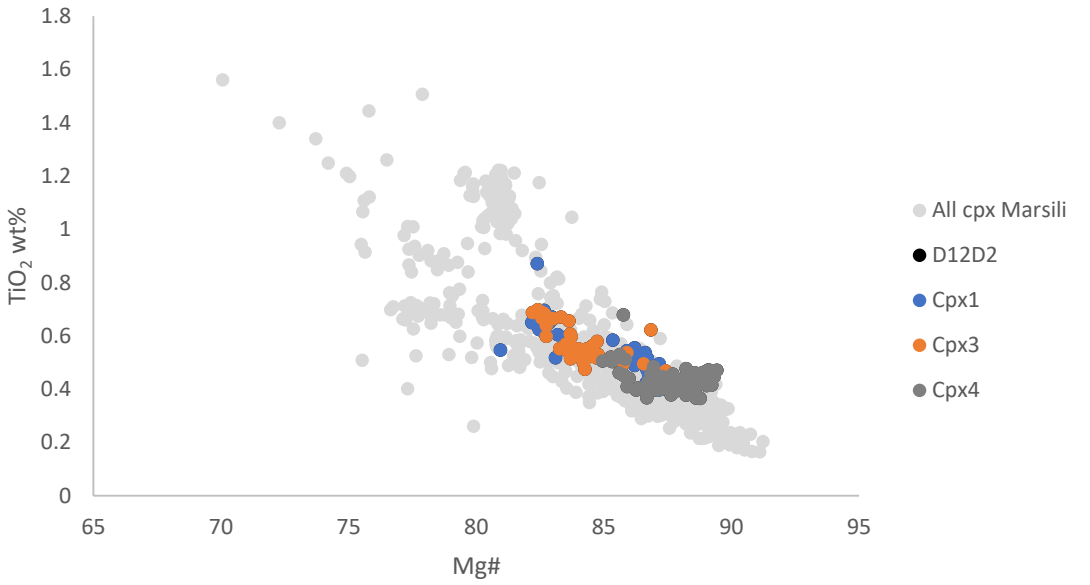

Fig. 60 - TiO_2 vs. Mg# for the clinopyroxene crystals from D12D2.

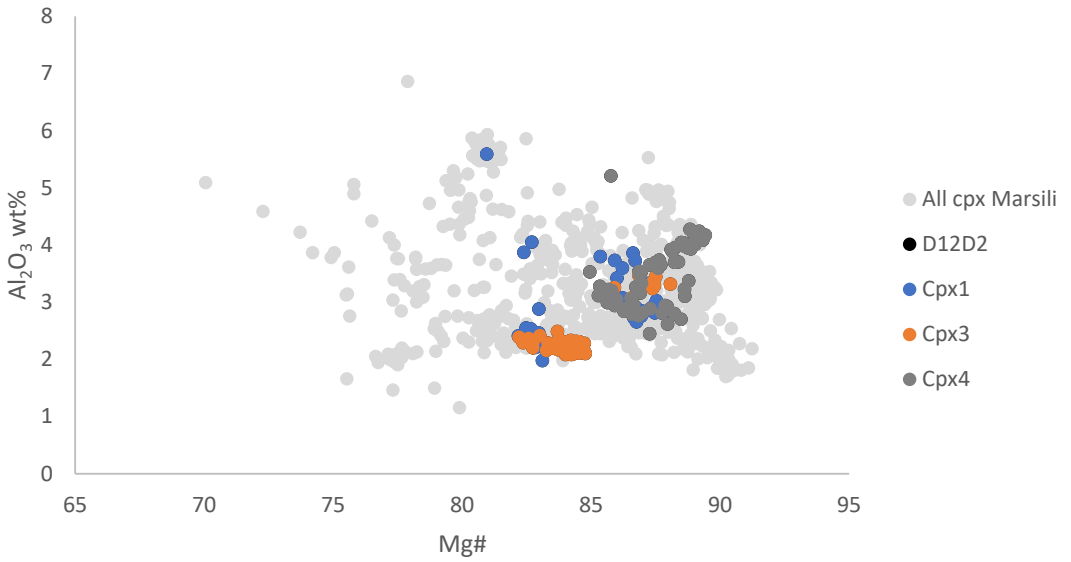

Fig. 61 - Figure 2 - Al_2O_3 vs. Mg# for the clinopyroxene crystals from D12D2.

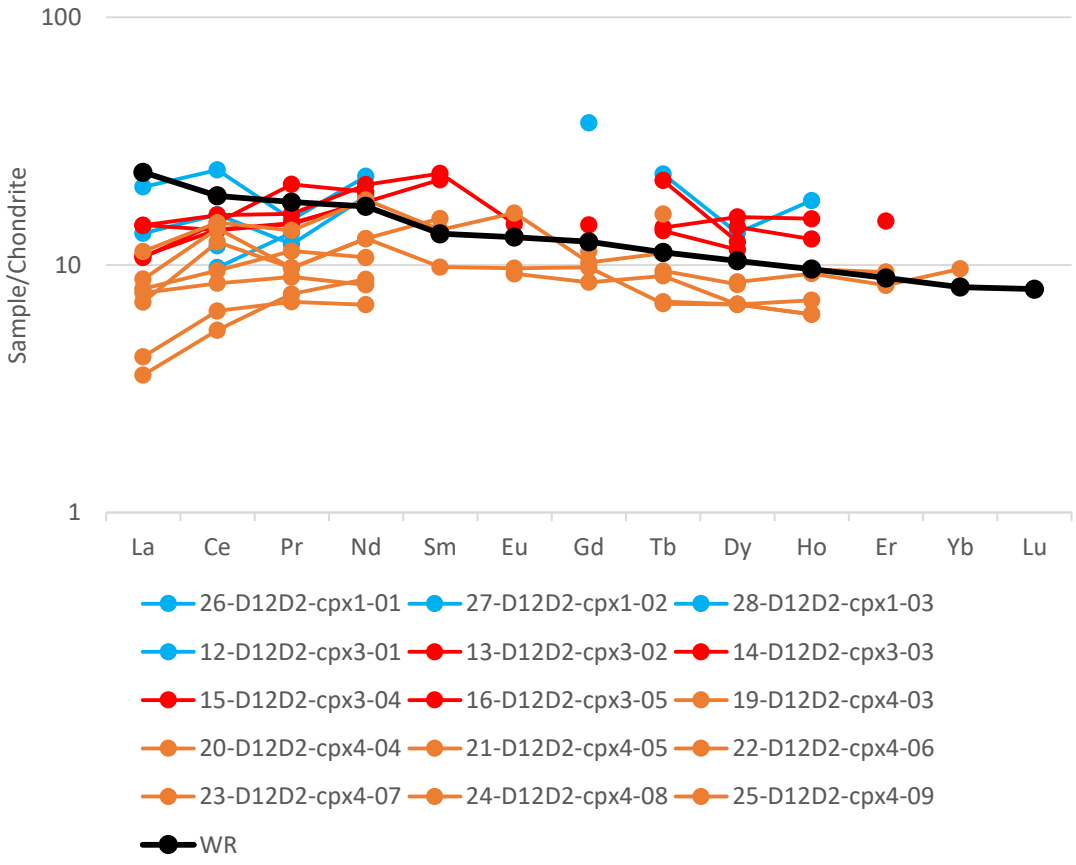

Fig. 62 - Rare earth elements from clinopyroxenes from D12D2 normalised to Chondrite (Sun & Mcdonough, 1989). *Black line represents the whole rock composition* (Trua et al., 2011). *Each colour represents a different crystal.*

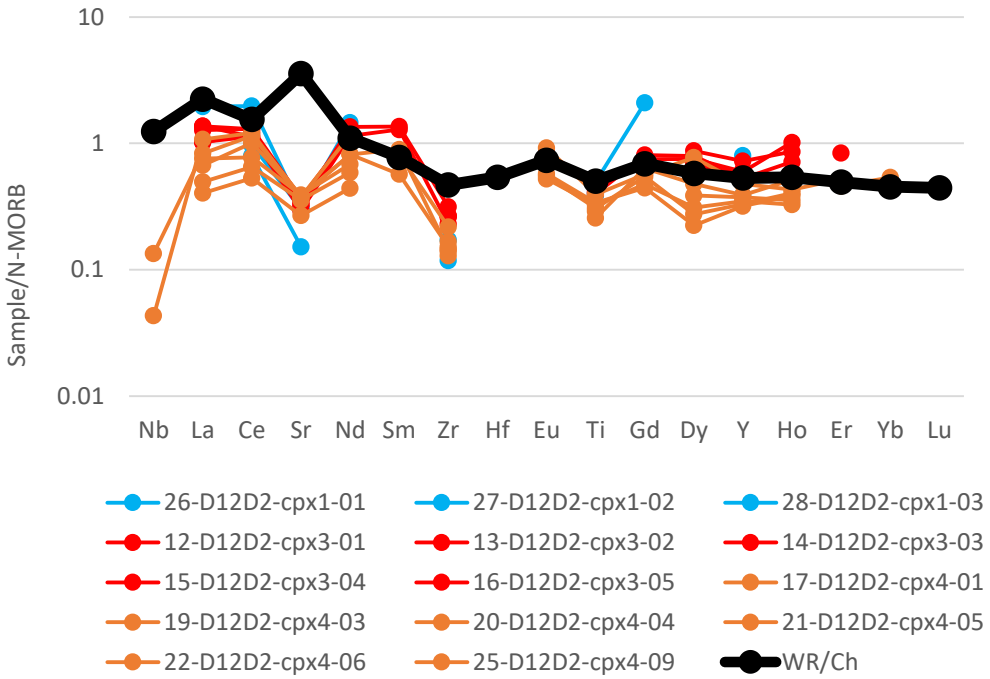

Fig. 63 - Rare earth elements from clinopyroxenes from D12D2 normalised to N-MORB (Sun & Mcdonough, 1989). *Black line represents the whole rock composition* (Trua et al., 2011). *Each colour represents a different crystal.*

D16AB

Olivines

Olivine crystals from sample D16AB show three main groups of compositions (Fig. 64). One olivine presents a core composition of Fo84.5; a group of olivine crystals with cores ranging from Fo82 to Fo80, showing distinct zoning profiles for Fo; and a last olivine crystal has Fo72 at the core and an oscillatory profile towards the rim. Rim compositions fall within the compositional ranges of the second group of crystals (Fo82-80). NiO profiles (Fig. 65) show that apparently NiO does not vary from core to rim in these crystals apart from (1) Ol1 and (1) Ol2 that are normally zoned towards the rim. CaO profiles (Fig. 66) show constant contents within the crystals. Only (2) Ol3 presents a zoned profile with CaO increasing towards the rim, reaching the composition of the rest of the crystals.

The NiO vs. Fo plot (Fig. 67) shows that the crystals form a positive trend with low NiO variation (0.1 to 0.05 wt.%). (2) Ol3 has NiO slightly higher compared to the trend formed by the rest of the crystals. CaO vs. Fo (Fig. 67) present positive correlation and the CaO content of this sample is higher than in most other samples within this Fo range (Fo85-70). One of the crystals

shows a significantly lower CaO content, plotting below the trend defined by the rest of the crystals of this sample, but overlapping the crystals from other samples.

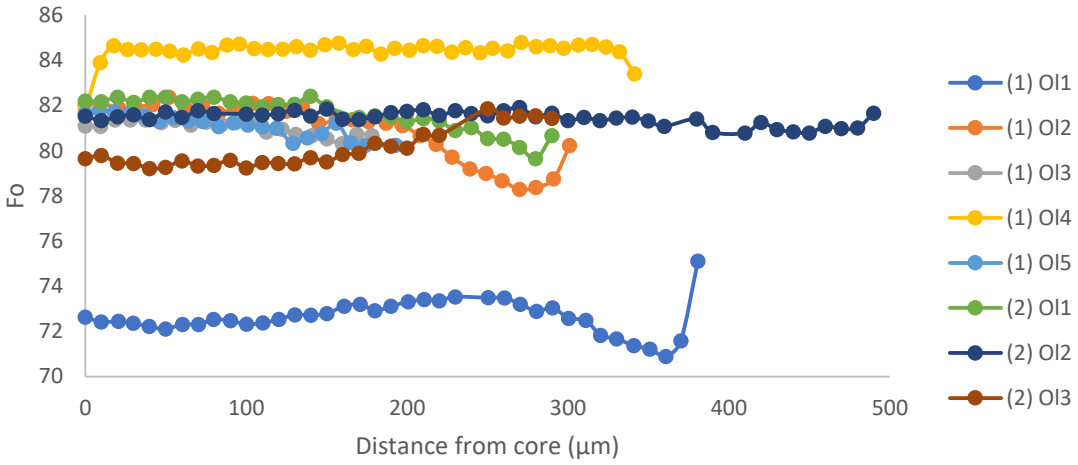

Fig. 64 - Fo profiles of the olivine crystals from the sample D16AB. The Fo profile of the crystal (1) Ol4 is from rim to rim.

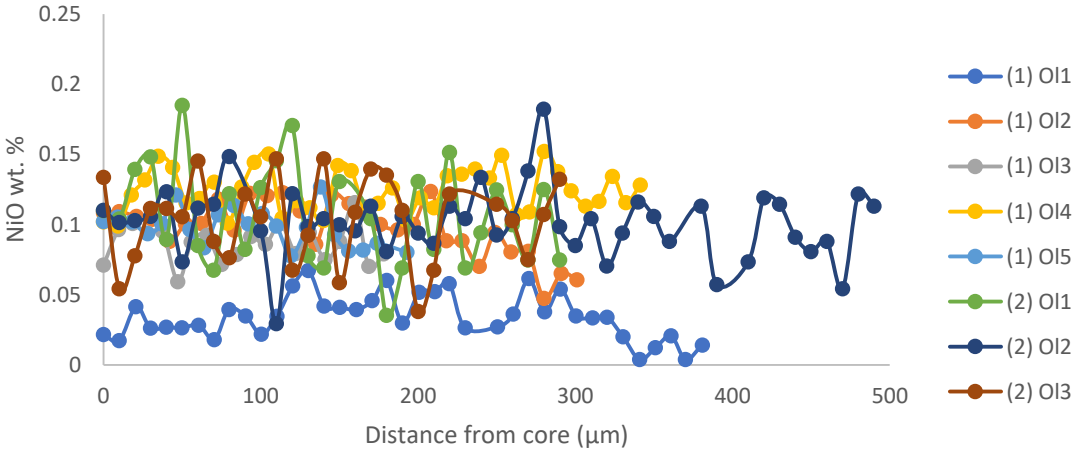

Fig. 65 - NiO profiles of the olivine crystals from the sample D16AB. The NiO profile of the crystal (1) Ol4 is from rim to rim.

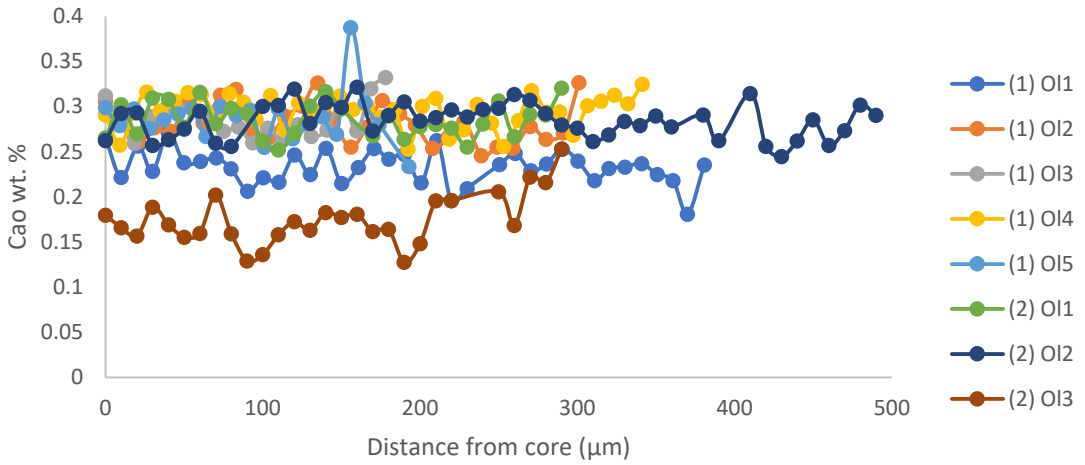

Fig. 66 - CaO profiles of the olivines from the sample D16AB. The NiO profile of the crystal (1) Ol4 is from rim to rim.

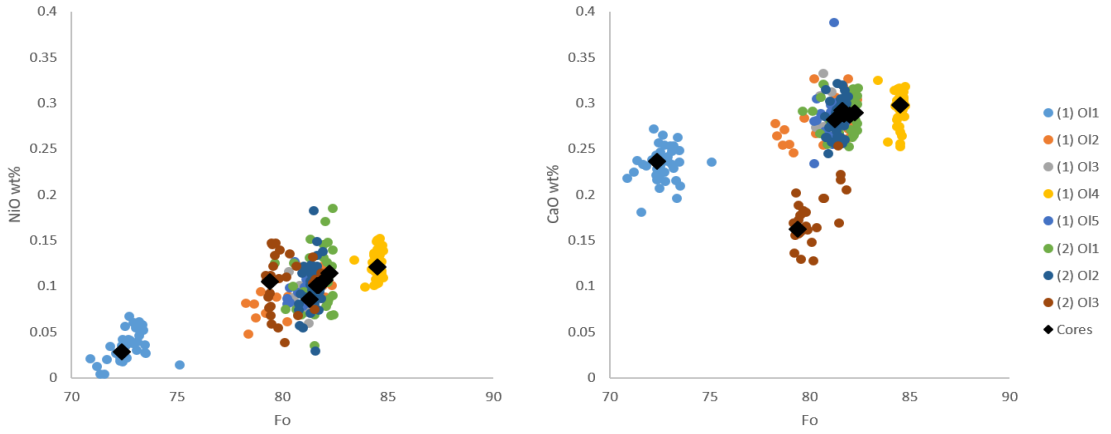

Fig. 67 - NiO vs. Fo and CaO vs. Fo for the olivine crystals from D16AB. Black diamonds represent the average compositions of the crystals' cores.

Clinopyroxenes

Clinopyroxene crystals show variable compositions, with most of the samples plotting between Mg#86 and Mg#80. Oscillatory profiles are common and the maximum range of variations ranges between Mg#86 and Mg#70 (Fig. 68). TiO_2 and Cr_2O_3 correlate negatively and positively, respectively, with Mg# and Al_2O_3 tends to scatter, suggesting only a slightly positive correlation. One of the analysed crystals, presenting a spongy texture probably due to disequilibrium crystallization, presents higher TiO_2 contents than expected for the Mg# of this crystal, overlapping the TiO_2 contents of clinopyroxenes from sample D6.

Trace elements in this clinopyroxene crystals shows less enrichment for LREE than for HREE comparing to the rest of the samples, although these compositions overlap the rest of the

clinopyroxenes from Marsili IAB lavas. Chondrite-normalised rare earth elements for the analysed crystals show relatively low $Ce/Dy_{(N)}$ values (0.6 to 0.37). The same is observed for N-MORB-normalised incompatible elements ($Ce/Y_{(N)}$ = 1.20 to 0.64).

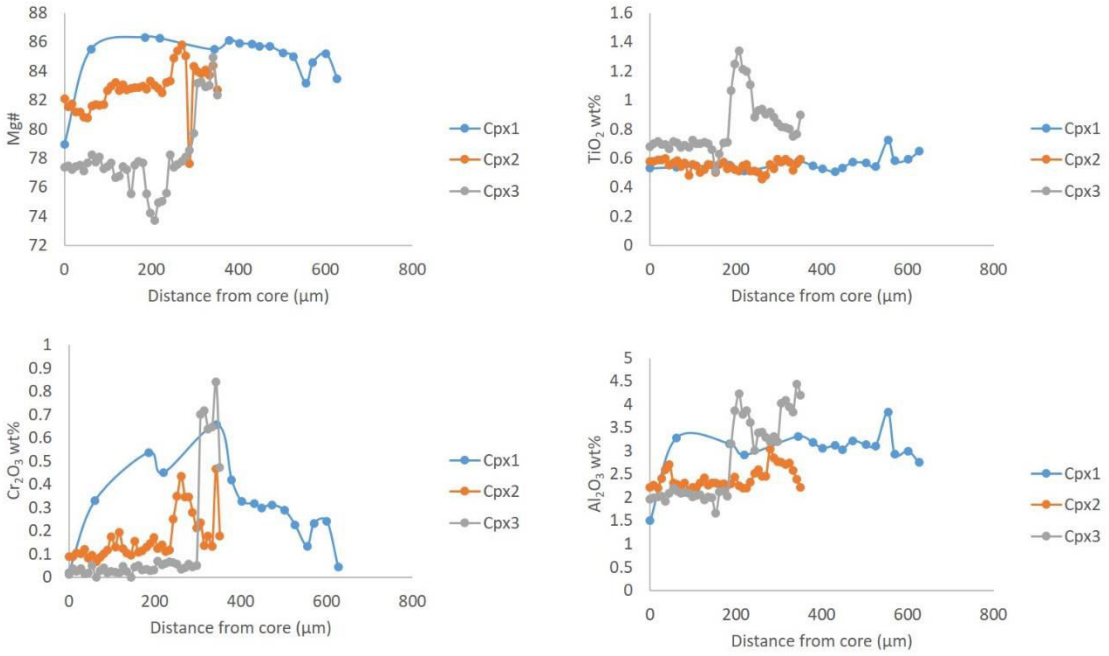

Fig. 68 - Compositional profiles of Mg#, TiO_2, Cr_2O_3 and Al_2O_3 from core to rim of the clinopyroxene crystals from D12D2.

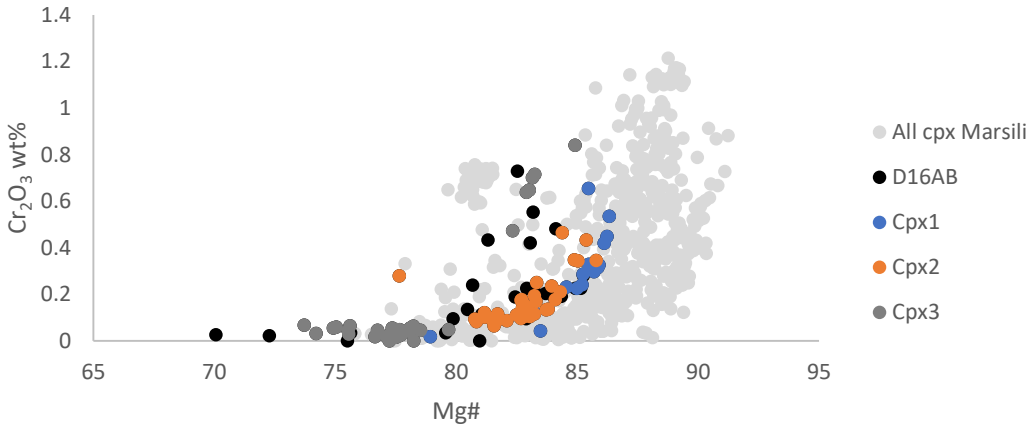

Fig. 69 - Cr_2O_3 vs. Mg# for the clinopyroxene crystals from the sample D16AB. Black dots represent clinopyroxene crystals in D16AB from Teresa Trua (Personal communication).

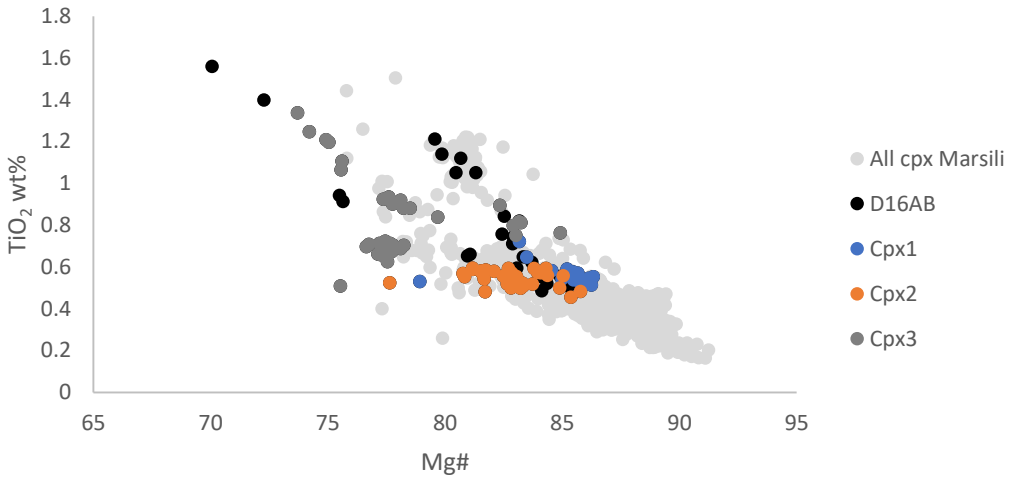

Fig. 70- TiO_2 vs. Mg# for the clinopyroxene crystals from the sample D16AB. Black dots represent clinopyroxene crystals in D16AB from Teresa Trua (Personal communication).

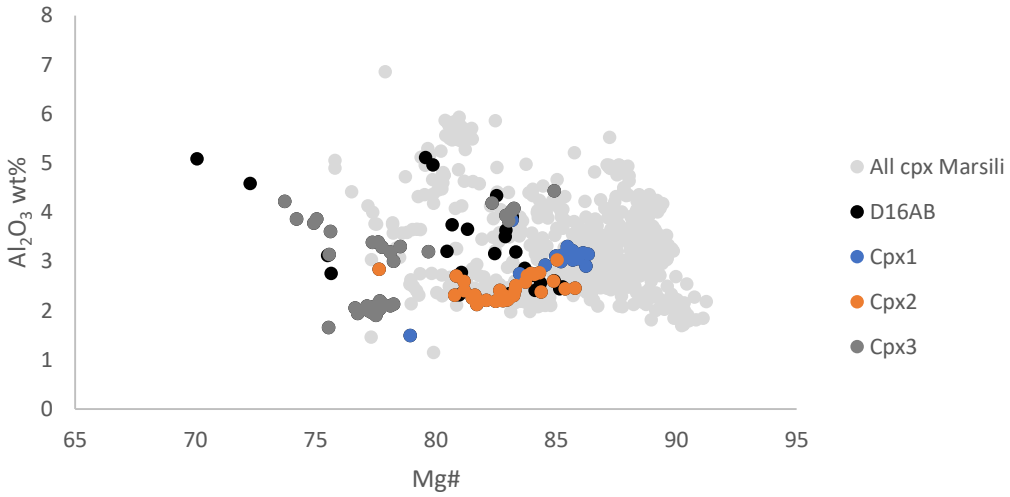

Fig. 71 - Al_2O_3 vs. Mg# for the clinopyroxene crystals from the sample D16AB. Black dots represent clinopyroxene crystals in D16AB from Teresa Trua (Personal communication).

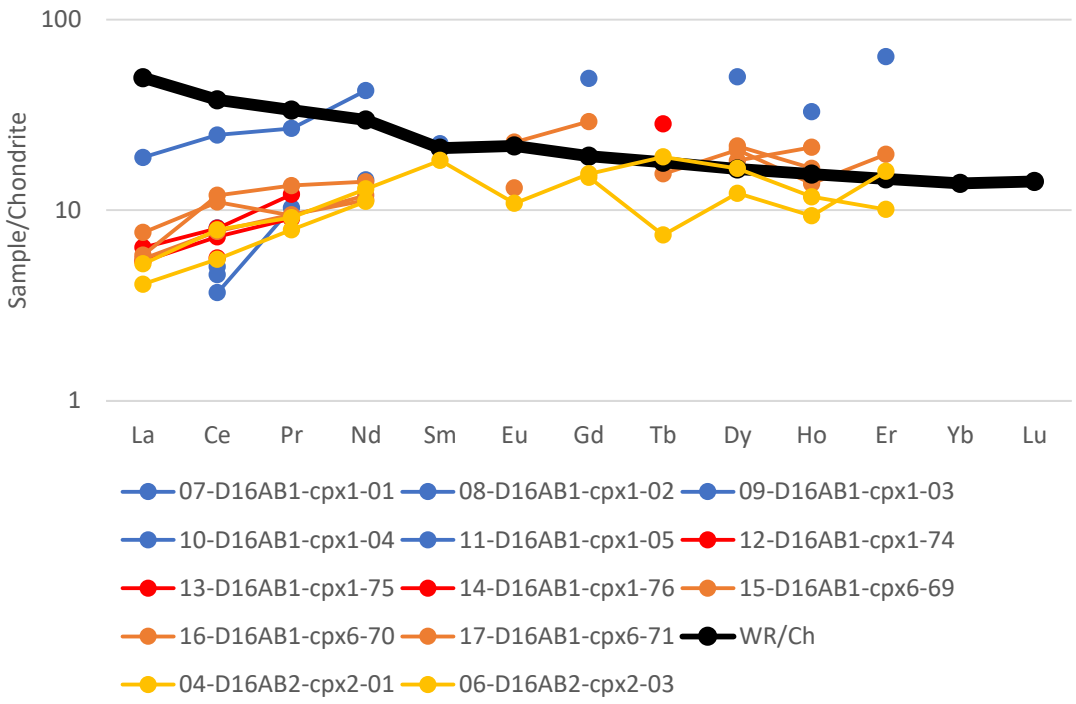

Fig. 72 - Rare earth elements from clinopyroxenes from D16AB normalised to Chondrite (Sun & Mcdonough, 1989). Black line represents the whole rock composition (Trua et al., 2011). Each colour represents a different crystal. Crystals D16AB2-Cpx2 is Cpx2 and correspond to the compositional profiles shown above. The rest of the crystals are represented as black diamonds in Fig. 69, 70 and 71.

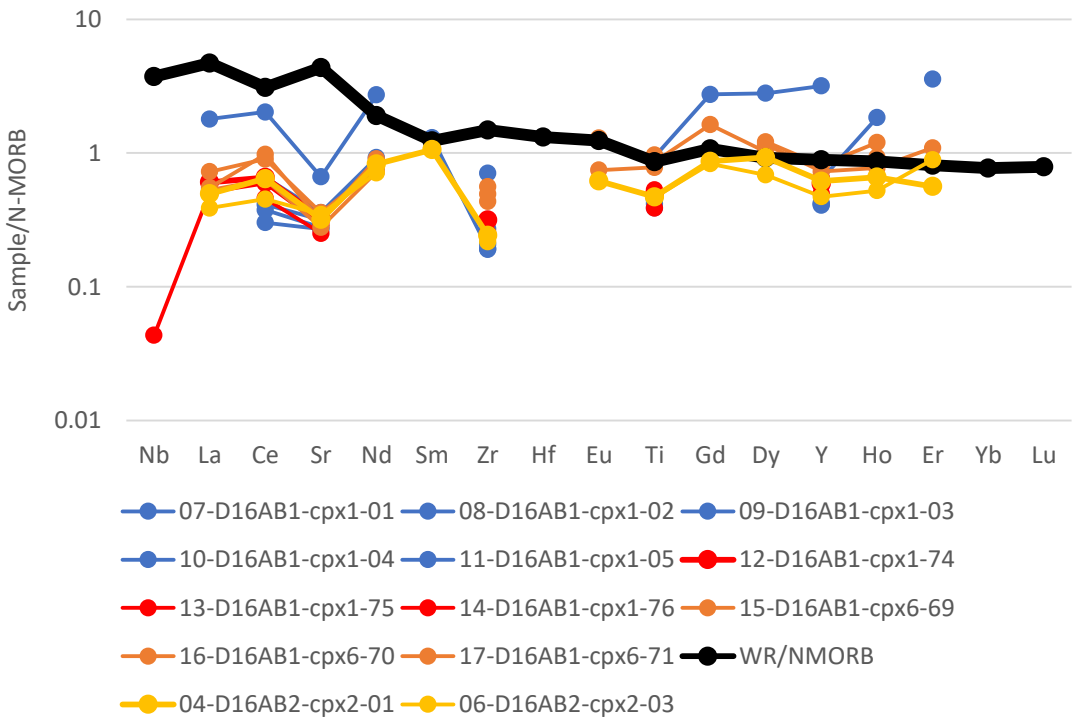

Fig. 73 - Incompatible elements from clinopyroxenes from D16AB normalised to N-MORB (Sun & McDonough, 1989). Black line represents the whole rock composition (Trua et al., 2011). Each colour represents a different crystal. Crystals D16AB2-Cpx2 is Cpx2 and correspond to the compositional profiles shown above. The rest of the crystals are represented as black diamonds in Fig. 69, 70 and 71.

Parental Melts

Olivines

Ni values in Marsili olivine crystals' cores fit the liquid line of descent (l.l.d.) modelled for olivine fractionation published by Zamboni et al. (2017) after Herzberg (2011). This model shows two liquid lines of descent for Ni concentrations in olivine fractionation (Fig. 74): (1) ol+ cpx; and (2) ol only.

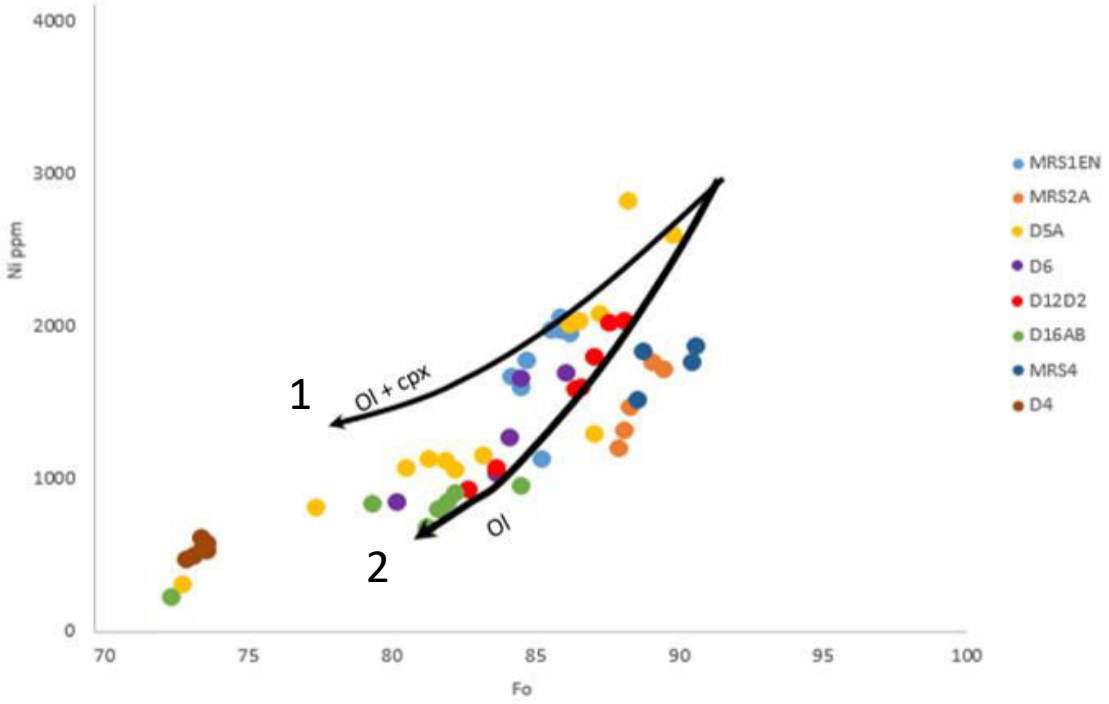

Fig. 74 – Ni (ppm) vs Fo plot of all the olivine crystals' core compositions from Marsili. The black arrows represent two different fractionation trends starting from a peridotitic melt: (1) ol + cpx fractionation and (2) ol fractionation. Model from Zamboni et al. (2017) after Herzberg (2001).

MRS1E olivine crystals overlap the modelled l.l.d. for ol + cpx cotetic. However, cpx crystals are not present in this sample. A possible explanation for this behavior is a significant control of the olivine compositions by diffusive reequilibration. Lynn et al. (2017) shows the importance of the diffusion processes as a factor that contribute to modify the initial composition of the olivine crystals as a consequence of the distinct diffusion velocities of each diffusion cation ($D_{Fe\text{-}Mg} \sim D_{Mn} > D_{Ni} >> D_{Ca}$; D is the diffusion coefficient between olivine and melt).

Olivine crystals from sample MRS1E show both normal and reversely zoned compositional profiles and this might be a consequence of magma mixing, and consequently diffusional reequilibration of the olivine compositions. It is important to have in mind that almost all the studied lavas have zoned olivine crystals. Moreover, the olivine crystals from the sample MRS1E present stronger zoning, although, this sample has limited Fo range (Fo_{86}-Fo_{84}).

The trend defined by the olivine crystals with Fo<85 from D5A and D16AB is significantly shallower than the modelled l.l.d. for olivine-only fractionation, even though Ni contents are lower than those modelled for the fractionation of the cotetic ol + cpx. This could be due to a significant olivine fractionation prior to the cotetic fractionation of ol + cpx. D5A shows this process where olivines from Fo90 to Fo85 show a steeper l.l.d. than olivines with Fo<85. Mixing and diffusional reequilibration might also have contributed to generate these flat patterns, but to a lesser extent in respect to the cotetic fractionation of olivine plus clinopyroxene. Otherwise Ni contents would still be flat but higher, as it happens for MRS1E.

Olivine crystals from MRS4 and MRS2A have lower Ni contents than what is expected according to the liquid line of descent from Herzberg (2011). Putirka (2011) suggests that temperature and pressure may have a strong control on the partition of Ni into olivine, and an example of this is the high Ni content of olivine crystals from Hawaii. Zamboni et al. (2017) found that the different Ni content within the Aeolian olivine crystals might not depend significantly on T, since in the arc environment is not hot enough to justify such differences. The input of hotter mantle in the mantle wedge below Marsili and the Aeolian arc could have an impact in the melting zone. The sample D6 (OIB-like composition) has slightly higher Ni values in respect to the average Marsili for a given Fo, but do not show significant differences, as it would be expected for a hotter mantle source (Putirka et al., 2011). This suggests that the observed differences in Ni might not depend significantly on temperature anomalies. Alternatively, magmas with higher polymerization and/or contents of SiO_2 can influence the Ni contents in olivine compositions because they cause higher partition coefficients for nickel in the olivine (e.g., $D_{NiOl/melt}$ = 7.5–12.5 for basaltic melts; Wang & Gaetani, 2008). Fosterite contents of the olivine crystals analysed from the samples MRS2A and MRS4 are the highest within the complete dataset. (Fo_{88}-Fo_{91}) and these crystals are not in equilibrium with respective bulk rock composition. Comparing to MRS1E, the REE of MRS2A pattern is slightly more enriched and this could be an evidence of a lower melting rate and consequently lower SiO_2. Samples MRS1E, MRS2A and MRS4 have different major elements content for similar SiO_2 (Fig. 12). However, small differences may influence the Ni contents. H_2O content in the magma influences its polymerization degree and this also may influence the Ni partition coefficient (Wang & Gaetani,

2008). Olivine's crystals from most of the Marsili's sample apparently show evidence of different H_2O content, namely MRSA2 and MRS2A contain evidence of lower H_2O contents. Therefore, the SiO_2 influence on the olivine's Ni partition seems to be plausible explanation for the variability of Ni within the crystals with higher forsterite contents (>Fo_{85}), of Marsili' samples. For lower fosterite contents the Ni contents is the result a mix of differentiation processes, such as multi-phase fractionation and diffusional reequilibration.

A different hypothesis to explain variable contents of Ni in olivines is the existence of different source lithologies in the mantle, varying from a peridotite to a pyroxenite (formed by reaction of partial melts of eclogite with peridotite; Sobolev et al. 2007). Sobolev et al. (2007) suggest that magmas may form from peridotitic and pyroxenitic mantle rocks in variable proportions, and higher the percentages of pyroxenite component is, higher Ni content will be in olivine. This model could explain that the differences of Ni contents found within the Marsili olivine crystals were given by variable percentages of a pyroxenite source as suggested for the Aeolian Islands (Zamboni et al., 2017).

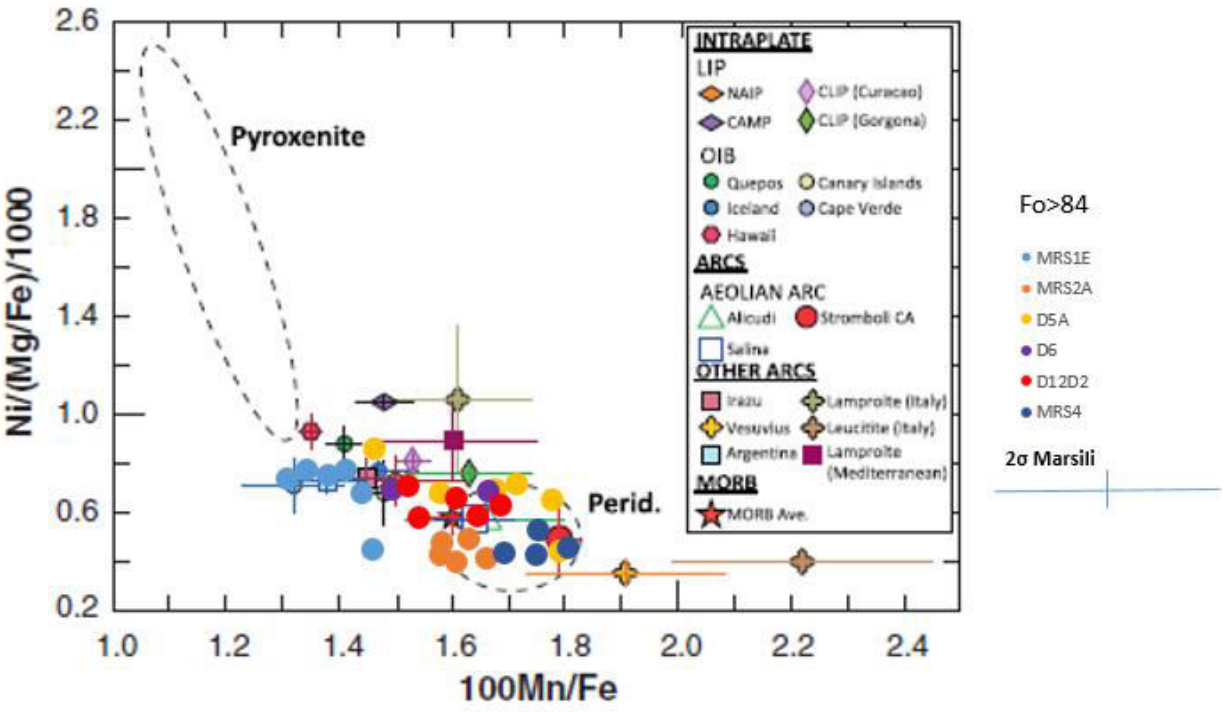

*Fig. 75 – Ni/(Mg/Fe)/1000 vs 100*Mn/Fe plot of the Marsili olivine core compositions from crystals with >Fo84. The two fields pyroxenite and Peridot. (Peridotite) represent the compositional end-members. Adapted from Zamboni et al., 2017).*

Ni/(Mg/Fe) and Mn/Fe ratios calculated with olivine compositions were used by Sobolev et al. (2007) to discriminate between the end members peridotite and pyroxenite. The authors use these ratios because of the low influence that fractionation has over them. Among the

Marsili olivines, only sample MRS1E and few other crystals almost overlap the pyroxenite compositions. In fact, when plotting Ni/(Mg/Fe) against Mn/Fe (Fig. 75), MRS1E olivines plot away from the rest of the Marsili data, closely overlapping the pyroxenite field due to slightly higher Ni/(Mg/Fe) and higher Mn/Fe.

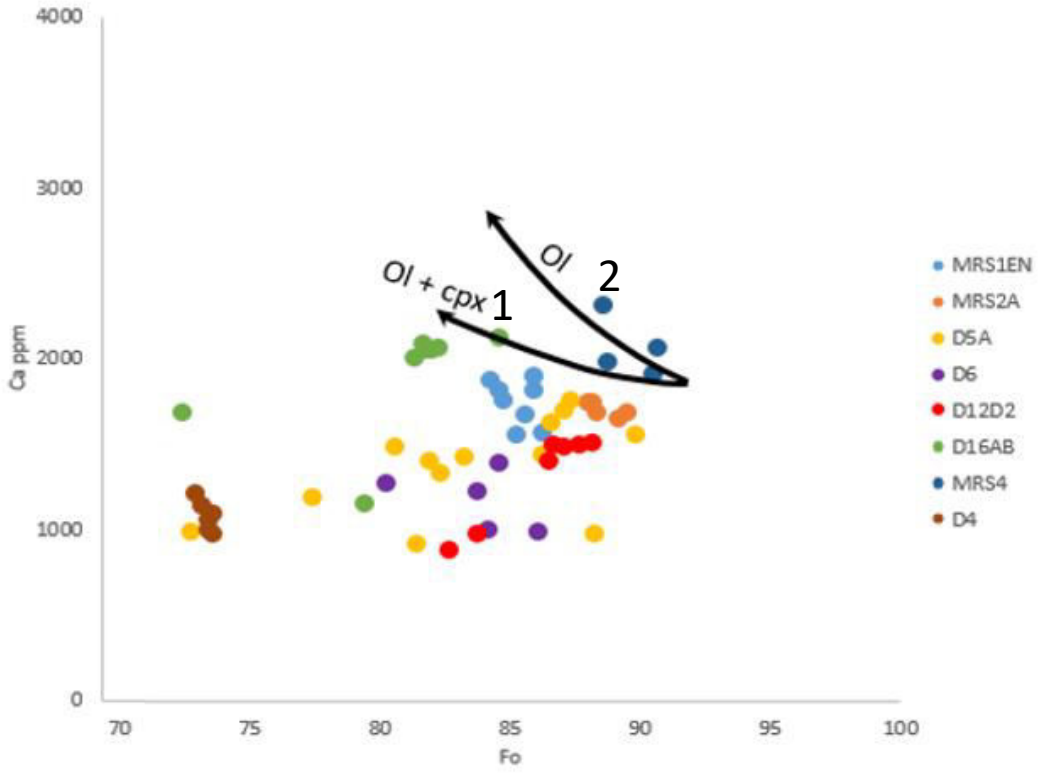

Fig. 76 - Ca (ppm) vs Fo plot of all the olivine crystals' core compositions from Marsili. The black arrows represent two different fractionation trends starting from a peridotitic melt: (1) ol + cpx fractionation and (2) ol fractionation. Model from Zamboni et al. (2017) after Herzberg (2001).

The overlap of the Marsili olivines in the peridotite and pyroxenite fields is an interesting feature and could give insights of the Petrogenesis of the parental magmas from which these olivine crystals crystalized. However, as it was suggested before, the composition of the olivine crystals from the sample MRS1E might depend strongly on diffusive reequilibration. Ni diffuses slowly compared to the couple Mg-Fe within the olivine structure, which would result in higher Ni compositions for olivines that reequelibrated with more differentiated melts relatively to those from which they crystallized. For Mn it may be the opposite. Mn and Fe contents in olivine correlate positively during olivine fractionation. In the case of diffusional reequilibration, $D_{Mg\text{-}Fe}$ is similar to D_{Mn}, although the latter is slightly slower (Chakraborty, 2010). Therefore, olivine crystals that reequilibrate with more differentiated melts would have higher Ni and lower Mn contents. Following this hypothesis, the higher Ni and lower Mn contents of the olivine crystals

from the sample MRS1E could depend mostly on diffusional reequilibration, instead of lithological source differences. To better understand the distributions of the Marsili olivine composition and the process controlling it, chemical analysis with a higher definition are needed to study the matter.

Ca contents in Marsili olivine crystals vary more than Ni contents and generally plot below the fractionation models (Fig. 76). The l.l.d. calculated by Herzberg (2011) shows that Ca in olivine should gradually increase either with olivine-only or ol + cpx fractionation in an anhydrous system. Marsili data show flat to decreasing Ca content with decreasing forsterite, contrasting significantly with the anhydrous models. Since Ni shows a significant role of olivine fractionation for higher Fo values, in an anhydrous scenario, it would lead Ca to increase significantly with fractionation. However, this is not what the results show. A flat/decreasing l.l.d. could be explained by the increase of water in the melt or by significant fractionation of plagioclase. Alternatively**,** Zamboni et al. (2017) suggested that the lower Ca content in the olivine crystals from the Aeolian Islands relatively to the anhydrous model (similar to Marsili olivine; not shown) might be associated to content of H_2O in the melt. According to Gavrilenko et al. (2016) the partition coefficient for Ca between olivine and melt depends on the water content, and thus, the Kd for Ca decreases with increasing H_2O contents. MRS2A and MRS4 are among the less differentiated lavas. On one hand, the Ca content in the olivine crystals is higher than the average (Fig. 76). On the other hand, plagioclase crystals analysed in these two samples are among the samples that have the highest Ca contents (An80-An95) among all the crystals analysed by Trua et al. (2018). Fractionation of calcic plagioclase decreases with increasing H_2O content (Nelson & Montana, 1992). Therefore, the low H_2O content can explain the Ca contents in both olivine and plagioclase, in MRS2A and MRS4 samples. The same does not apply well to the other samples. Although not quantified, H_2O could be the main process controlling the Ca compositions of the Marsili olivine crystals.

In summary, the different compositions of the Marsili olivine crystals may be controlled by differentiation processes (crystal fractionation and diffusive reequilibration) and by compositional differences between the magmas feeding the Magmatic system. However, the extent of the control of each process is still not quantified.

Clinopyroxenes

The trace elements (TE) analysis show that the majority of the clinopyroxene crystals have low concentrations and thus, together with some instrumental limitations, some of the analysed elements present a large variability, with sigma-1 error generally varying from 5 to 20%. The Chondrite-normalised (Sun & McDonough, 1989) REE patterns of the analysed clinopyroxenes overlap those already published (Trua et al., 2014), distinguishing two main groups: D6 with clinopyroxene TE compositions related to a OIB-like magma and the rest of the samples (D5A, D12D2 and D16AB) with a IAB TE pattern (Fig. 77). The $Ce/Dy_{(N)}$ ratio, representative of a Light REE (LREE) vs. Heavy (H)REE ratio ranges from 2.78 (D6) to 0.37 (D16AB). Cpx from these two samples show a narrow range of $Ce/Dy_{(N)}$, with D6 varying from 2.78 to 1.92 and D16AB ranging from 0.6 and 0.37. D5A and D12D2 present a larger $Ce/Dy_{(N)}$ range (D5A from 1.25 to 0.54; D12D2 (1.79 to 0.65; (Fig. 77)).

N-MORB normalized (Sun & McDonough, 1989) incompatible element patterns are similar to those already published for Marsili clinopyroxene crystals (Trua et al., 2014; not shown). The $Ce/Y_{(N)}$ ratio used as proxy for very to moderately incompatible elements shows systematic differences among the samples, i.e. $Ce/Y_{(N)}$ for D6 ranges from 5 to 3.38, D16AB from 1,20 to 0.64, D12D2 ranging from 3.06 to 1.29 and D5A from 3.45 to 0.95. The highest $Ce/Y_{(N)}$ (3.45 to 2.77) in D5A were obtained in one specific crystal. This crystal shows low Al_2O_3 and TiO_2 for its Mg# when compared with the rest of the crystals, overlapping the compositions of the orthopyroxene present in some Marsili andesites. This crystal also presents a spongy texture, carved of inclusions suggesting that it was in disequilibrium and the contrasting compositions might be due to this, possibly. The clinopyroxene crystals from D12D2 and D5A that present $Ce/Dy_{(N)}$ and $Ce/Y_{(N)}$ similar to the clinopyroxenes from D6 also show similar trace element patterns, with about 60% lower trace elements contents compared to D6 clinopyroxene crystals. The fact that these two samples show a larger variety for trace elements than D6 and D16AB, could suggest the contributions of melts with significantly different compositions in these plumbing systems but further information would be necessary to confirm the processes responsible for the variability.

Using the partitioning coefficients for clinopyroxene and melt proposed by Kajacz & Halter (2007) as used before by Trua et al. (2014), sample D6 presents an equilibrium melt that overlaps the OIB-type patterns from Ustica and Etna melt inclusions (Trua et al., 2014; references therein). The melts in equilibrium with the clinopyroxene crystals from the other three samples instead overlap the compositions obtained from the melt inclusions in olivines

from Marsili IAB basalts (Trua et al., 2014; Trua et al., 2010). The new data corroborates the presence of the input of two different melts in the Marsili system, where apparently the OIB-like melt is represented only by the sample D6. However, the variations in the $Ce/Y_{(N)}$ in the samples D5A and D12/D2 suggest that these OIB-like melts may have also entered in the IAB magmatic systems, although in a significantly lower proportion comparing to the IAB melts.

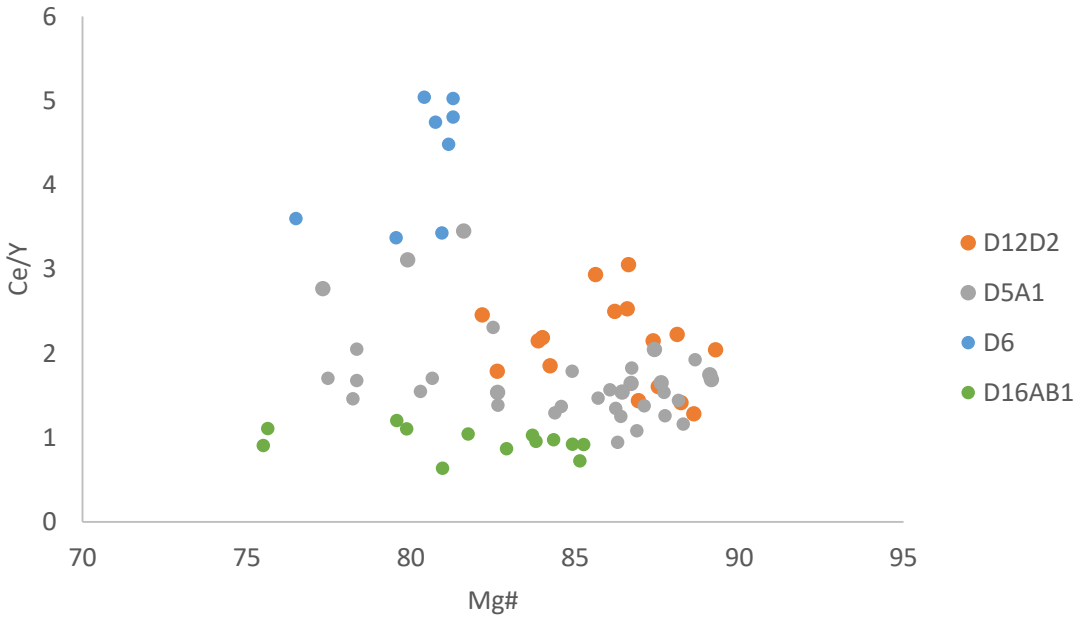

Fig. 77 - Plot of the $Ce/Y_{(N)}$ vs. Mg# for the clinopyroxenes analysed in the samples D5A, D6, D12D2 and D16AB.

Differentiation processes from clinopyroxenes

Plotting the $Sr/Sr^*_{(N)}$ ($Sr_{(N)}/((Ce_{(N)}+Nd_{(N)})/2)$) against Mg# shows a general positive trend for all four samples (Fig. 78). While the clinopyroxenes from D12D2 and D16AB show a good correlation between these two parameters, D5A shows a larger variety. Taking a closer look to the variation within each crystal in this sample, two of the crystals show similar values of $Sr/Sr^*_{(N)}$ for different Mg#. Since Sr is incompatible in clinopyroxene and compatible in plagioclase (Zajacz & Halter, 2007), Sr trace element variations are fundamentally controlled by plagioclase fractionation. Such plagioclase control may explain the general positive trend between Sr/Sr* and Mg#. On the other hand, most of the analysed crystals with high Mg# present a constant

Sr/Sr* for most of range of Mg#, suggesting that plagioclase did not co-crystalize significantly with clinopyroxene and olivine during the first stages of clinopyroxene crystallization. D6 also shows constant Sr/Sr* values of ca. 0.3 and there is no variation with its Mg# (Fig. 78).

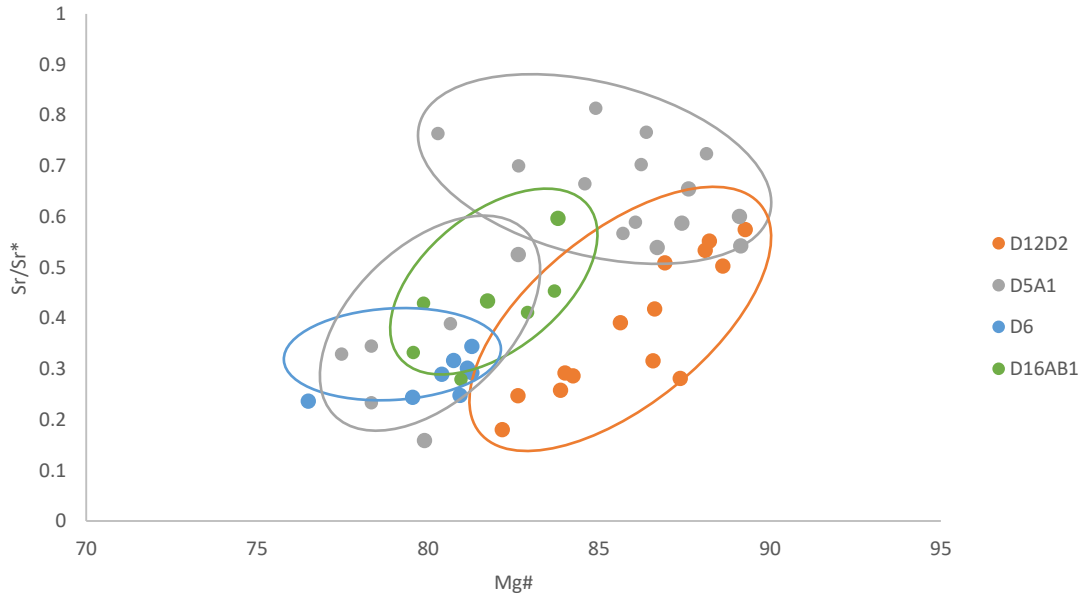

Fig. 78 - Plot of Sr/Sr vs. Mg# for the analysed clinopyroxene crystals from the four studied samples. The fields are coloured with the same colour of the sample they represent.*

Samples, D5A, D12D2 and D16AB show similar Sr/Sr* for their higher Mg# clinopyroxenes, while all four samples converge to similar low Sr/Sr* in low-Mg clinopyroxenes. The different Sr/Sr* vs Mg# trend displayed by D5A and D12D2 could be explained by co-crystallization of clinopyroxene + plagioclase in D12D2, while in D5A plagioclase crystallization was delayed after clinopyroxene crystallization. Clinopyroxenes of sample D16AB show a decreasing Sr/Sr* and Mg# from compositions similar to the most evolved ones of D5A that could already have crystallized mafic minerals mainly.

The lack of significant Eu and Sr anomalies in the whole-rock and melt inclusion trace element compositions point to a negligible plagioclase fractionation (Trua et al., 2010; Trua & Marani, 2011). However, the Sr/Sr* from the analysed clinopyroxene crystals suggests that plagioclase played a role in the differentiation of the melts related to some of the studied samples. The plagioclase present in the Marsili basalts were already studied (Barca & Trua, 2012; Trua et al., 2014) and the authors found that the Ba vs. Sr contents suggest a plagioclase-poor crystallization path. According to the new clinopyroxene trace element compositions, the Marsili

basalts may have differentiated along different crystallizations paths, although presenting similar final mineral assemblages. These different crystallization paths might be the result of different magmatic conditions, such as different H_2O contents (as suggested by the olivines) and/or different crystallization temperature and pressures, according to the results reported in the Geo-thermobarometry chapter.

Magmatic environments and plumbing system structure

Geothermobarometry models

Previous studies of geothermobarometry (e.g. Trua et al., 2014; Trua et al., 2002) already gave some constrains on the intensive variables acting in the Marsili magmatic system. The model based on the equilibrium between olivine and spinel (Ballhaus et al., 1991), applied to olivines and their spinel inclusions from samples ranging from basalts to basaltic andesites yielded temperatures from 1130 °C to 970 °C and oxygen fugacity from 1.5 to 2.5 log units above the QFM (quartz-fayalite-magnetite) buffer. The thermobarometer based on the composition of amphibole (Ridolfi et al., 2010) applied to the amphiboles found in one of the basaltic andesite samples resulted in temperatures of 910-1000°C and pressures of 2 to 4 kbar. The hygrometer from the same model estimates 4-6 wt% of H_2O, which is slightly higher than the 3-4wt% H_2O estimated with the plagioclase-liquid hygrometer (Lange et al., 2009). The oxygen fugacities obtained from the amphibole composition range from 0.3 to 1.5 log units above the NNO (nickel-nickel oxide) buffer. MELTS models (Ghiorso & Sack, 1995) succeeded in predicting crystallization of minerals with similar compositions as those found in the Marsili samples for these oxygen fugacities and pressures. Pressures close to 3kbar correspond to ca. 10km of depth which is close to the estimated Moho depth (e.g. Pontevivo & Panza (2006)) of 11km.

In order to characterize the intensive variables for each studied sample we used different models. These are based on thermodynamic data to estimate temperature, pressure, and oxygen fugacity based on the whole-rock, olivine, and clinopyroxene compositions, assuming equilibrium among whole-rocks, olivine and clinopyroxene. Estimating these intensive variables for each sample helps not only to better describe the structure and properties of each of these plumbing systems but is also a fundamental input for geospeedometry calculations,

since the diffusion of the cations present both in the melt and in the crystals strongly depends on the intensive variables, especially temperature.

We chose to use three different modelling approaches, i.e., MELTS on whole-rock data; clinopyroxene and olivine vs whole-rock geo-thermobarometry (Putirka, 2008); the composition of the clinopyroxene crystals (Putirka, 2008) and olivine-clinopyroxene geothermometry (Loucks et al., 1996). This choice is not only aiming to compare the different models that complement one another. Moreover, the considered models cannot be applied to all the studied samples (e.g., some lack clinopyroxene crystals or whole-rock data are not representative of magmatic liquid compositions as some whole-rock compositions are influenced by crystal accumulation and high percentage of phenocrysts).

Since this study is based on olivine and clinopyroxene compositions, the equilibrium conditions between these phases is the most important proxy for temperature calculations. Loucks et al. (1996) is the preferred tool to estimate different conditions in the sub-magmatic systems by using the potential equilibrium found between these two minerals within different reservoirs, both pre- and sin-eruption. Moreover, sin-eruption temperatures are quite relevant for geospeedometry models that estimate the conditions when the mixing of different melts occurred and crystals re-equilibrated with the new compositions. MELTS tests, when applicable, are used to further constrain P-T-fO2-H2O conditions. The models from Putirka (2008) are used to test equilibrium between whole-rock and crystals and to test if the clinopyroxene crystals within each sub-system present significant compositional/structural differences, based on the temperature and pressure results obtained.

In the next paragraphs we discuss the results obtained for each model and then we present a final discussion integrating all the results.

Clinopyroxene-olivine geothermometry (Loucks, 1996)

Introduction

The thermometer published by Loucks (1996) is based on the partitioning of Fe/Mg between olivine and clinopyroxene, which is temperature-dependent. This thermometer applies well to the here studied Marsili samples and different approaches are possible. First, as suggested by the author, the thermometer might be applied to the compositions of the rims of the crystals which record the composition before the eruption of the magma. Second, the geothermometer might be used to predict the temperature of all the magmatic reservoirs represented in each samples by calculating the potential equilibrium between olivine and

clinopyroxene. To do so we tested the equilibrium between each phase and hypothetical melt in equilibrium with it, and then compared with the natural dataset.

This geothermometer have some limitations. If one or both mineral phases show disequilibrium textures, then the equilibrium temperature cannot be calculated. If one of the minerals is zoned towards the rim but the other is not, then the equilibrium is only given in the case that the first came to equilibrate with the second's equilibrium conditions (antecrysts and xenocrysts). Otherwise, contrasting mineral zoning could just be the result of different diffusion rates, resulting in compositions that might not be in equilibrium (e.g. in case of mixing just before the eruption). The errors associated to the model itself are quite low (±6 °C on the calculated equilibrium crystallization temperature) and are in fact negligible compared to uncertainties related to possible (and unconstrained) lack of equilibrium. It is therefore difficult to estimate the error and for this reason, when possible, we present a temperature range given by the different compositions.

The first approach we applied is to consider the compositional ranges recorded by the rims of the crystals and test the equilibrium between pairs of crystals. In most of the samples, especially those with a large amount of phenocrysts, both olivines and clinopyroxenes tend to yield a limited range of rim compositions, which might be interpreted as the compositions resulting from mixing before the eruption of the magma. The first temperature to be calculated is the one given by the extremes of the compositional range: the lowest composition in case of normal zoning and the highest composition in case of reversed zoning. A test to check if the compositional extremes are given by disequilibrium crystallization (e.g. fast cooling rates) or by equilibrium crystallization is to apply the model to the rest of the rim compositions within the range. Temperatures should not change significantly in case of equilibrium crystallization when using pairs of different compositions.

The second approach we applied is to use the Fe/Mg Kd between olivine and melt and clinopyroxene and melt to calculate the potential equilibrium between olivines and clinopyroxenes and then compare this to the observed compositions. In all studied samples, olivine crystal cores display one or more dominant compositions. Assuming these ranges of compositions as a proxy of the magmatic reservoirs, and assuming the $\mathrm{KD}_{\mathrm{Fe/Mg}}^{\mathrm{ol/melt}}$ as 0.3, it is possible to calculate the Mg# of the melt in equilibrium with such cluster. Then, it is possible to calculate the Mg# of the clinopyroxenes in equilibrium with the resulting melt by using the Kd Fe/Mg between clinopyroxene and melt. According to different authors (e.g. Putirka, 2008) the $\mathrm{KD}_{\mathrm{Fe/Mg}}^{\mathrm{cpx/melt}}$ equals about 0.27±0.03, even if it should be considered that the $\mathrm{KD}_{\mathrm{Fe/Mg}}^{\mathrm{cpx/melt}}$ is temperature dependent. For a range of temperatures varying from 1100 and 1250 °C, the Kd

varies from 0.257 to 0.29, respectively. The results are then compared with the composition of the clinopyroxenes present in the samples, from core to rim. By using this approach it is possible to access to the temperatures in the reservoirs that in the system, prior to the mixing event associated to the eruption.

The model requires the $KD_{Fe/Mg}^{ol/cpx}$ to be calculated by using Fe^{2+}/Mg from both olivine and clinopyroxene. As said before, the clinopyroxenes in Marsili samples show all high values of calculated Fe^{3+}. The temperature calculated considering Fe^{2+} are significantly lower than those calculated considering Fe^{total} and the latter are much closer to the results obtained with the other thermometers. If the Mg# for the clinopyroxenes is calculated using Fe^{2+} only, the resulting Mg# appears too high to be in equilibrium with most olivines present in the samples. Since Fo vs NiO variations of olivines suggest that olivine was the main fractionating phase during the first steps of differentiation of the parental magmas, it is not expected that clinopyroxenes were in equilibrium with melts with higher Mg# than those in equilibrium with the olivines. Furthermore, Mollo et al., 2013 show that Fe^{3+} calculated from clinopyroxene EPMA data are inconsistent with those obtained, e.g., with Mossbauer spectroscopy and thus suggest to use Fe^{total}. Therefore, the Mg# for the clinopyroxenes and the $KD_{Fe/Mg}^{ol/cpx}$ are calculated using total iron.

Putirka (2008)

Introduction

Putirka (2008) presents many equilibrium models based on equilibrium between liquid and olivine, clinopyroxene or plagioclase, or between two distinct pyroxenes or plagioclases. With the data available in this study (whole-rock compositions from Trua & Marani, 2011, and olivine and clinopyroxene analyses) it is possible to apply the thermometry models based on olivine-liquid equilibrium and thermobarometry based on clinopyroxene composition. However, the equilibrium between the whole-rock the mineral phases is limited to a few samples, considering that the analysed bulk compositions might not represent a plausible approximation of the parental melt from which the minerals crystallized, as already said above. To test the equilibrium between the whole-rock compositions and the minerals found in each sample we used the $KD_{Fe/Mg}^{ol/melt}$ (0.3±0.03) and the $KD_{Fe/Mg}^{cpx/melt}$ (0.27±0.03) suggested by Roeder and Emslie (1973) and Putirka (2008). We use the temperature calculations based on the equilibrium between melt and olivine only for samples MRS1E, D6 and MRS2A. The thermobarometer based on the composition of the clinopyroxenes first suggested by Nimis (1995) and modified by Putirka (2008) is applicable to all the samples but one (MRS1E) since it depends only on the

compositions of the clinopyroxenes. The barometer considers Fe^{3+} as input parameter. Therefore, we changed the equation to depend on the total iron. However, the calculated pressures do not vary significantly comparing to the original equation. A large number of point-analyses in samples D5A, MRS2A and D16AB's clinopyroxenes yielded negative pressures and were discarded. The results are averaged for each sample/group of results and 1-sigma errors are considered.

The thermodynamic equilibrium model from (Mollo et al., 2013), based on the comparison between the predicted DiHd value calculated from the liquid (i.e. whole-rock) composition and the observed DiHd from the analysed clinopyroxenes is used to test for equilibrium conditions. Most of the samples are in equilibrium with their crystals, although plotting slightly above the 1:1 line (which represents the equilibrium ideal compositions; not shown). This suggests that these crystals may be in equilibrium with the bulk composition of the rock, but would only saturate with slightly different compositions.

MELTS approach

Introduction

MELTS (Ghiorso & Sack, 1995) is a software based on a thermodynamic database developed for modelling differentiation processes in magmatic systems $_2$-H_2O paths. Many works (e.g.(Teresa Trua et al., 2002)(Teresa Trua et al., 2002)(Teresa Trua et al., 2002)(Teresa Trua et al., 2002)(Trua et al., 2002)(Trua et al., 2002) Trua et al., 2002; Kahl et al., 2014) use this approach to model the intensive variables for which the crystal compositions found in their samples are in equilibrium. For Marsili samples this approach was already used to estimate magmatic conditions for each sample (e.g., Trua et al., 2002) and for defining calculated fractionation paths in comparison with observed ones. Although it is a powerful tool for modelling magmatic systems, in the case of Marsili, the lack of liquid compositions that may be used as an approximation of a parental melt for each sample limits the use of this approach for most of the studied samples. The MELTS tests are thus applied to samples MRS1E, D6, MRS2A and MRS4 and the results are discussed below.

Results

MRS1E

The bulk rock composition of the sample MRS1E was used as an approximation of the parental melt. With H_2O varying from 1 to 2wt%, pressure varying from 1 to 2kbar and oxygen fugacity varying from QFM to NNO buffers, the results are quite satisfying. Olivine with Fo86 is obtained for 1wt% H_2O and 1-2kbar for the NNO buffer at 1220-1200^{o}C (liquidus). Modelling fractional crystallization with the same initial conditions shows that olivine with Fo84 crystalizes at 1180-1165^{o}C. Clinopyroxenes do not fractionate above 1150^{o}C in all the models. Therefore, above 1150^{o}C the mineral assemblage obtained above 1150^{o}C by the MELTS models fits the mineral assemblage of the sample (ol + plg + oxides). Using 2wt% of H_2O also gives olivine compositions that fit the compositions found in the sample. Although, using a water content higher than 1% makes clinopyroxenes to be in equilibrium before plagioclase, which does not correspond to the observed paragenesis.

D6

The bulk composition was used as an approximation of a parental melt. In this sample, olivines range from Fo86 to Fo80, pressure I set to 2 to 4 kbar, H_2O from 1 to 2wt% and oxygen fugacity buffer from QFM to NNO. For most of the models, the olivine is the first mineral crystalizing with a composition of Fo84 from 1190 to 1170^{o}C. Olivine with Fo80 follows at temperatures ranging from 1140 to 1130^{o}C. Clinopyroxene (Mg#80) is in equilibrium with the magma at 1145 (at 2 kbar) or 1170^{o}C (at 4kbar, 1wt% H2O and NNO buffer). The model at 4 kbar predicts clinopyroxene crystalizing before plagioclase. Since the clinopyroxene is a rare mineral in the sample comparing to olivine and plagioclase, it might be plausible to assume that the P was below 4 kbar. However, given the lack of an Eu anomaly in the clinopyroxene compositions, plagioclase did not fractionate significantly before the crystallization of the clinopyroxene. Assuming that P varies from 2 to 3kbar, temperatures for olivines with Fo84 range from 1180^{o}C to 1187^{o}C, olivines with Fo80 are in equilibrium with the magma at 1130^{o}C to 1137^{o}C and clinopyroxene reaches the liquidus at 1150-1167^{o}C.

MRS2A

Using the whole rock composition as an approximation of its parental melt, the results are not completely satisfying. At 1-2wt% H_2O, 1-3kbar and QFM-NNO buffer, olivines crystalizes

with maximum Fo86 and clinopyroxenes with Mg#84, i.e. at low values compared to the natural sample (Fo89.5 and Mg#89). Applying a high oxygen fugacity (NNO+2) it is possible to achieve Fo87 olivine composition, but the clinopyroxenes crystalizing do not register a Mg# higher than 84.5. This suggests that the bulk rock composition may not represent an approximation of a parental melt for the crystals analysed in this sample possibly due to an open system differentiation process (e.g., magma mixing) before eruption that changed the composition of the melt. In fact, some of the analysed clinopyroxenes register zoned bands with Mg#84.

MRS4

Sample MRS4 is the sample with highest Fo olivines, with cores ranging from Fo90.5 to Fo88 and rims from Fo90 to Fo84. The same problem was found as for MRS2A and thus the models do not succeed in predicting crystal compositions comparable to the observed ones.

Mass balances

Since the idea is to model the conditions of the system from which these crystals fractionated, we tried to model the liquids in equilibrium with the olivines and clinopyroxenes in the samples MRS2A and MRS4. To do so, we used a simple model for mass balance between a melt and olivine and/or clinopyroxene, using as starting compositions the whole rock and the compositions of an olivine and a clinopyroxene representative of the analysed crystals. The model is given by the following expression:

$$C^i = \frac{\left(\left(F \times C_l^i\right) + \left((F-1) \times C_s^i\right)\right)}{100},$$

where F is the fraction of melt, i is the element (expressed in its oxide), C_l^i and C_s^i are the concentrations of the oxides in the liquid and in the solid phase, respectively, expressed in wt.%. In order to calculate a liquid in equilibrium with the crystals from each sample we considered a reversed fractional crystallization, where crystals with a chosen composition are added to the bulk liquid composition. This approach was also used by Albert et al. (2014). Only olivine and clinopyroxene were considered in this model based on the suggested crystallizations paths lacking significant plagioclase fractionation by Trua et al. (2014).

Testing the mass balance model with the sample MRS2A, different percentages of olivine and/or clinopyroxene were added to the liquid and then I used the software MELTS to verify if the obtained compositions were able to predict the same compositions as those found in the analysed crystals. Adding at least 5% of olivine (Fo89) to the whole rock composition

allows MELTS to predict the precipitation of olivines with the same composition at temperatures of ca. 1250 ºC. To predict the precipitation of clinopyroxenes with Mg#88-89 it was necessary to add at least 20% of this mineral phase (Mg#89) to the whole-rock composition, at temperatures of ca. 1235 ºC. The best fitting model was to use the whole-rock composition adding 5% of olivine Fo89 and 20% of clinopyroxene with Mg#89 at 2kbar and NNO conditions, with the resulting olivines Fo89 and clinopyroxenes Mg#88 crystallizing at 1270 ºC and 1230 ºC, respectively.

The model was also tested for the sample MRS4 by adding different amounts of olivine and clinopyroxene. The best fit was given by a mass balance with the whole rock composition and 10% of olivine (Fo90) and 20% of clinopyroxene (Mg#87) for 2kbar and NNO oxygen buffer. Calculated temperatures for olivine with Fo90 was 1315 ºC, 1235 ºC for clinopyroxene with Mg#87.5 and 1200 ºC for Mg#84, following the fractional crystallization model.

Discussion

Overall, the models converge to similar results. Since not all the thermometers are applicable to all samples, we use the samples with results for all the models (MRS2A and D6) to calibrate their use.

The different models show different temperatures, with MELTS and Loucks (1996) predicting the higher temperatures compared to those obtained following Putirka (2008) (Table 2). The results for MRS2A yielded by MELTS were calculated using compositions obtained by mass balance models, and so these results must be considered as estimates. Moreover, taking into account the model of cpx-melt equilibrium based on DiHd values, MRS2A clinopyroxenes are rather in disequilibrium with the whole-rock composition, which corroborate the use of mass balances as a plausible way to recalculate an approximate equilibrium magma. Loucks (1996) predicts temperatures quite close to those obtained with MELTS. The results from the mineral-whole-rock model of Putirka (2008) predict instead systematically lower temperatures, arguing possibly for a lack of equilibrium between whole-rock and minerals and thus favoring the approach of recalculating such melt composition. The clinopyroxene-based model predicts systematically lower temperatures too for all samples. Therefore, this thermometer accounts for different P-T crystallization conditions for distinct clinopyroxene crystals of a single sample. Interestingly, also the model of Loucks (1996) predicts different crystallization temperatures for distinct clinopyroxene crystals of single samples.

Table 2 - Temperatures resulting from all the thermometers applied to the Marsili samples

	MELTS	Putirka (2008)			Loucks (1996)
		Melt (Beattie)	Olivine-melt	Cpx	
MRS1E	**Fo86** – 1220-1200°C **Fo84** – 1180-1165°C	1220 - 1227°C	**Fo85** – 1195-1200°C	X	X
MRS2A	**Fo89** – 1250-1270°C **Mg#89** - 1230°C	1182 - 1188°C	**Fo89** – 1160 - 1166°C	1160°C	**Fo88 – Mg#89** Core - 1200°C **Fo88 – Mg#87.5** Rim - 1245°C
MRS4	**Fo90** – 1315°C **Mg#89** – 1235°C **Mg#87** - 1200°C	1190 - 1200°C	X	1158°C	1230°C 1225°C
D4	X	X	X	1139°C	**Core** – 1145-1155°C **Rim** – 1170°C
D5A	X	X	X	1150 - 1140°C 1098°C	1190-1195°C 1180-1185°C 1175-1160°C
D6	**Fo84** – 1187-1180°C **Fo80** – 1137-1130°C **Mg#80** – 1167-1150°C	1190 - 1185°C	**Fo84** – 1158-1152°C	1140°C	**Fo77-Mg#80** - 1175°C
D12/D2	X	X	X	1174°C 1160 - 1143°C 1134°C	1190°C 1165-1155°C 1180°C
D16AB	X	X	X	1160 - 1143°C 1125°C	1188-1180°C

Taking a closer look to the results obtained for D6, and reminding that the whole-rock composition of this sample successfully predicted the compositions found in the sample when using MELTS, the different models seem to converge to similar temperatures. Again, the models from Putirka (2008) predict temperatures slightly lower than the other models, but the differences are not as great as for MRS2A. Taking into account these differences, the use of different models might be a good test to evaluate how good a whole-rock composition can be used as proxy of a parental melt for thermometry calculations.

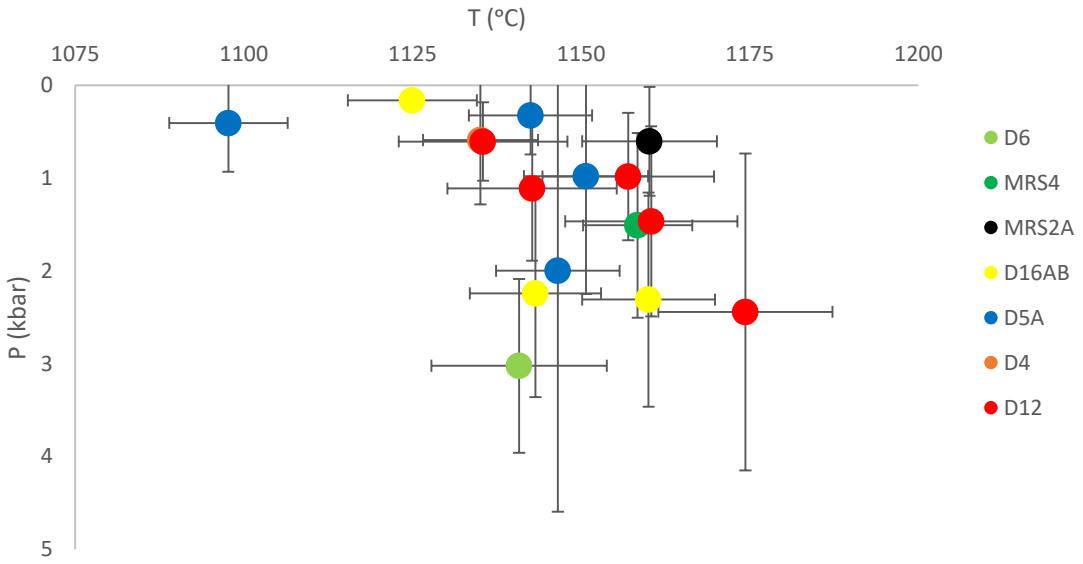

Fig. 79 - Temperature vs. Pressure for the Marsili samples. Values obtained are from the model using the composition of the clinopyroxene crystals (Putirka, 2008, following Nimis et al., 1995).

The thermometer and barometer based on the clinopyroxene compositions succeed to predict both temperature and pressure for all the samples with clinopyroxene crystals with variable precisions (Fig. 79). Temperatures vary roughly between 1200 °C and 1100 °C which is within the range of temperatures obtained with the other thermometers. The majority of the samples show no correlation between Mg# and calculated T but some present clusters. The pressures obtained using this model vary from 4 to 0 kbar. This pressure range is within the results already published for Marsili samples. Moreover, although the model itself presents a large error (±2.6 kbar), it is possible to distinguish more or less complex magmatic plumbing systems. D6 is the only sample presenting higher pressure of 3 kbar, representing a depth of ca. 10 km, which corresponds to the depth of the Moho (e.g., Trua et al., 2014). All other samples plot mostly below 2 kbar, suggesting that most of the magmatic reservoirs are within the intermediate-shallow crust. MRS2A and MRS4, two of the most primitive samples, present low pressures, below 2 kbar (as consistent also with MELTS). These two samples were sampled in the northern part of the base of Marsili. Instead, samples picked at the summit present at least two different groups of pressures, suggesting that the most primitive magmas represented by these crystals settled at deep crustal levels while more evolved melts probably resided at shallower levels, where the analysed crystals recorded compositions that represent the mixing of these magmas. Moreover, plotting the results from core to rim for some crystals shows that pressure and temperature change within the profile.

The temperatures obtained from the thermometer based on the equilibrium between olivine and clinopyroxene are generally higher than those from the thermometer of Putirka (2008) after Nimis (1995). However, both models predict that temperatures do not vary much within the Marsili samples and temperature variability within each magmatic sub-system do not vary more than 50°C.

Identification of the magmatic environments

MRS1E

The two groups of crystals might represent two different reservoirs that interacted before the eruption. However there are no evidences to say that these two reservoirs were placed at different depths or had significantly different intensive variables. The analysed crystals have different core compositions but vary within a small range. The complex geometries of the zoned compositional profiles and the differences in NiO wt% suggest that the different crystals represent different magmatic environments where crystals grew and latter mixed, before ascending towards the surface.

MRS2A

Olivine crystals in sample MRS2A present two groups of different Fo values and these groups of crystals present different textures, with the first group (Fo89.5) given by single crystals and the second (Fo88) represented by crystals associated to clinopyroxene and plagioclase. Clinopyroxenes instead present a larger range of compositions. The olivines calculated to be in equilibrium with the Mg# range obtained for clinopyroxenes (Mg#89.5-84) range from Fo88 to Fo84-83 (see Geothermobarometry models). This suggests that olivines with Fo89.5 represent a more mafic melt that entered in the reservoir represented by the olivines with Fo88 and the clinopyroxenes + plagioclase, probably corresponding to a crystal mush of. The lack of zoning in the olivines might suggest that the slightly more mafic melt sampled the glomerocrysts from the mush column while ascending.

MRS4

Given that clinopyroxenes present a larger range of compositions compared to olivine crystals, the latter may represent a magma that entered the reservoir where the clinopyroxene crystals resided, probably in a mush system, given the variable clinopyroxene compositions. Indeed, these olivine crystals are zoned towards the rim with Fo85 which would be in equilibrium with some of the clinopyroxenes. After that, the magma carrying the olivine crystals with Fo90.5 entered the reservoir and triggered the eruption. Thus, two mixing events are identified: the first given by the normal zoning of the olivines with lower Fo in the core, and the last, given by the most mafic olivine crystals with no sign of diffusion.

D4

The crystals analysed in this sample represent a single reservoir probably formed by a crystal mush, where different magmas interacted. Clinopyroxene crystals within a glomerocryst have oscillatory compositions. Olivine instead show core compositions rather invariable, comparing to the rims, which are reversely zoned. This suggest that before the eruption the input of a more mafic magma entered the system, disaggregating the mush in different glomerocrysts and allowing for olivine crystals to re-equilibrate with it. This is the only mixing event recorded by the olivine crystals, although clinopyroxene compositions oscillate. The contrasting zoning patterns may suggest that different magma batches interacted within the reservoir, with long recharging intervals.

D5A

Olivines with higher Fo contents are present either as single crystals or as mono-mineralic glomerocrysts and thus they represent a specific reservoir. Moreover, the l.l.d. given by NiO vs. Fo for olivine cores with Fo>85 overlaps the l.l.d. modelled for olivine-only fractionation (e.g. Gavrilenko et al., 2016) and the modelled Mg# of clinopyroxenes in equilibrium with these olivines does not match with the compositions presented by the analysed clinopyroxene crystals. These olivines have compositional profiles that suggest the interconnection between different magmatic environments with slightly different compositions prior to the ascent towards the shallower reservoirs.

The olivines with Fo83-80 in the core, together with the clinopyroxene crystals may represent the biggest reservoir in this sub-magmatic system. These olivine crystals have normal to reversely zoned profiles and few crystals show more complex profiles (i.e. compositional steps bounded by either abrupt or gradual compositional changes), implying the presence and mixing of magmas with different ratios of differentiation. Part of these crystals with Fo83-80 core compositions have rims with lower Fo contents (Fo77-77.5). The olivine with Fo77 the core is part of a glomerocrysts with clinopyroxene and plagioclase and it probably was part of a mush that was desegregated when the more mafic magma entered the system.

Apparently, there are different mixing events recorded in the olivine compositions. These crystals have compositions that might represent continuous interactions within a single reservoir and multiple reservoirs.

D6

D6 crystals suggest two main reservoirs, the first being the one containing the compositions Fo84.5-83.5 and the second the one containing the olivine (Fo80-78) and the clinopyroxene crystals. Both groups show isolated crystals, suggesting that no important mush disaggregation occurred unlike for samples MRS2A, D5A and D16AB. Both reservoirs are represented by olivine crystals with some major element variability and with compositional profiles that show some re-equilibrium dynamics, suggesting that both reservoirs contained magmas with different degrees of differentiation that gradually mixed. The clinopyroxene crystals might have crystallised in the shallower reservoir (with Fo80-78), due to their late appearance in the crystallization assemblage (equilibrium with the lowest Fo contents found). The crystals show lesser major and minor elements variations. However, Cr and trace elements vary from Cpx1 to Cpx2, with the latter showing slightly lower Cr and $Ce/Y_{(N)}$. These differences suggest that these crystals may have crystallised from slightly different magmas, but clearly crystallised separately, and it resembles the behaviour of the olivines minor elements as pointed above. Overall, the analysed crystals suggest an immature magmatic system, where magma percolated through fractures rather than a crystal mush. This also explains the slightly higher pressure obtained with these clinopyroxene crystals, suggesting that these magmas fractionated the olivine and clinopyroxene crystals before reaching the crystal mush that may characterize the crust below Marsili (e.g. Trua et al., 2014).

D12D2

The core compositions and the profile geometries of the olivine crystals suggest that the main crystallization reservoirs were two. These reservoirs were affected by at least two episodes of recharge in order to explain the profiles with gradual zoning profiles contrasting to those with abrupt zoning in the rim. Clinopyroxene compositions, although showing oscillatory zoning profiles, present similar rim compositions that may have be in equilibrium with olivines with Fo86-84. Olivine with Fo>85 show a NiO vs. Fo trend that overlaps the l.l.d. given by olivine fractionation with lesser (or none) clinopyroxene fractionation. The fact that the majority of the clinopyroxene crystals present resorption textures and intergrowth of plagioclase, is probably because the clinopyroxene and plagioclase crystals resided where the magma resulting from only olivine fractionation (Fo>85) batched, generating disequilibrium conditions. Considering all the profiles from this sample, it seems that Ol7 and Ol4, the bigger crystals, represent magmas that mixed and the resulting magma is the magma from which the crystals Ol2, 3, 5, 6 crystallised and after that the magma moved towards a shallower reservoir where it mixed with a slightly more felsic magma (with Ol1) and then erupted.

D16AB

Most of the analysed crystals, either olivine or clinopyroxene, are part of glomerocrysts, sometimes with plagioclase too. Among the analysed olivine crystals, only two crystals are isolated, and these crystals have core compositions of Fo84 and Fo72. All the other crystals belong to the group with Fo ranging from Fo82 to Fo80 and present zoned profiles, either normal or reversed. Clinopyroxenes instead present different textures, and the analysed crystals are either isolated or, mostly, in glomerocrystic aggregates of different mineral assemblages, from clinopyroxene only, to clinopyroxene + olivine or with minor plagioclase. This suggests that this sample, as already seen for D5A, derives from a heterogeneous mush where different magmas with different compositions interacted. Given the olivine rim compositions, all ranging between Fo82 and Fo80, and considering that the crystal with a core of Fo84 presents an abrupt change in the rim, it is suggested that the arrival of this less differentiated magma (in equilibrium with Fo84 olivine) may have triggered the eruption. The olivine and clinopyroxene crystals with lower Mg# might represent a shallower reservoir where the magma carrying the rest of the analysed crystals passed without effective mixing.

Timescales in the Marsili plumbing system

Introduction

Using the software DIPRA (Girona & Costa, 2013), which allows to model the compositional profiles to estimate the timescales of the diffusion processes when olivine crystals re-equilibrate with a different magma, a set of crystals from each sample was tested. With this modelling approach it is possible to estimate the timescales of the processes responsible for the variable zoning geometries.

The modelling approach was to use 1D composition profiles (from core to rim) analysed in different euhedral olivine 2D sections. The majority of the compositional profiles were obtained perpendicular to a crystal face to minimise errors related with the orientation of the transverse. After that, the crystals were oriented by using the EBSD technic (Prof. Richard Spiess, University of Padova) in order to measure the angles between the transverse and the crystal axes. The angles between the transverses and the crystal axes are reported in Table 3.. Unfortunately, the minor elements analysed in the olivines present a significant variability due to analytical errors. Thus, the compositional variations in some profiles are within the error, making it difficult if not impossible to compare clearly the behaviour of Fo and the minor elements.

After that, the modelled T, P and fO_2 (reported in the Geothermobarometry Models chapter) were used together with the transverse orientation in the program DIPRA to model the timescales associated with the diffusion profiles. The results are reported in Table 4.

Table 3 – angles between the analysed compositional traverse and the crystal axis.

	Olivine	α [100]	β [010]	γ [001]
MRS1E	**(2) Ol9**	116	82	27
MRS4	**Ol3**	135	52	79
	Ol4	170	92	78
D4	**Ol1**	20	105	102
	Ol2	30	114	73
	Ol3	105	25	71
	Ol4	100	165	80
	Ol5	20	73	102
	Ol6	68	158	97

D5A	**(1) Ol1**	93	37	127
	(1) Ol3	135	47	78
	(1) Ol4	22	85	65
	(1) Ol4(2)	88	78	11
	(1) Ol8	82	168	84
	(2) Ol2	155	66	92
	(2) Ol3	105	156	72
	(2) Ol5	95	6	89
D6	**Ol1**	15	102	80
	Ol2	102	58	145
	Ol3	102	144	56
	Ol4	96	159	70
	Ol5	148	103	63
D12D2	**Ol1**	71	157	83
	Ol2	78	155	100
	Ol4	20	107	115
	Ol5	35	80	122
	Ol6	153	65	96
D16AB	**(1) Ol1**	75	145	60
	(1) Ol4	122	34	80
	(2) Ol1	156	102	57
	(2) Ol3	143	48	115

Olivine profiles description

MRS1E

One crystal ((2) Ol9; MRS1Em) was used for this sample. The Fo profile shows normal zoning towards the rim (Fo84.5) after a core plateau at Fo86 (Fig. 80). NiO profile seems flat, although presenting a smooth normal zoning in the last ca. 100 μm. CaO does not show any variation from core to rim.

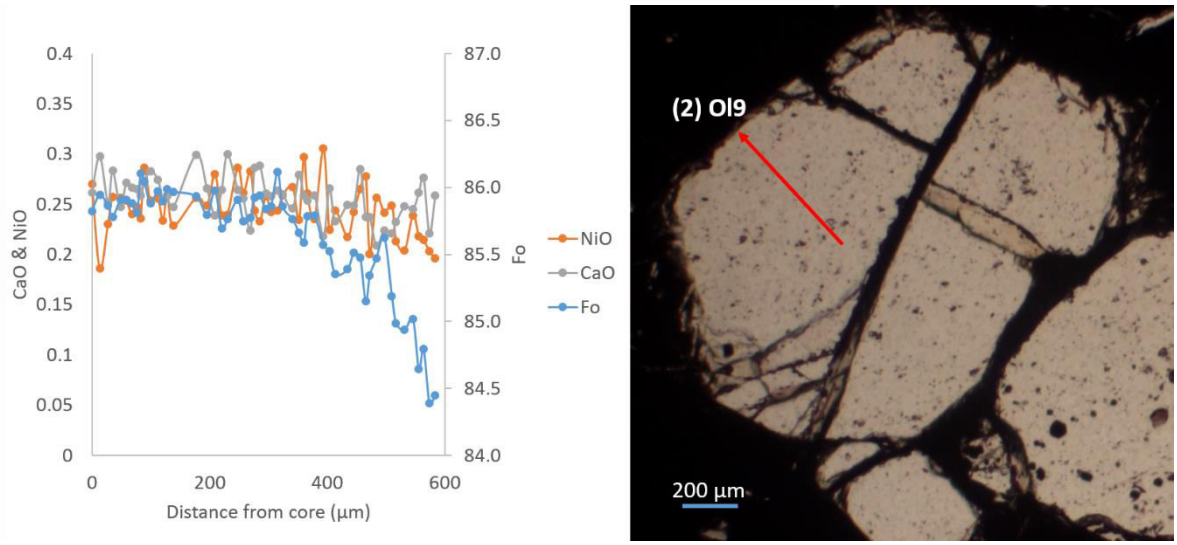

Fig. 80 - Fo, NiO and CaO profiles from core to rim for olivine (2) Ol9 from MRS1Em.

MRS4

Two crystals from this sample were oriented (Ol3 and Ol4). Ol3 is twice the size of Ol4. Although, both crystals show compositional plateaus followed by abrupt decrease of Fo and NiO. Ol3 presents a shoulder before the Fo decrease (e.g. Lynn et al., 2017) and this feature is not easily modelled with DIPRA. The transverse obtained for Ol4 has a short length (200 µm) but presents a simple normally zoned profile, and thus it was used to estimate the timescales, apparently quite short due to the abrupt compositional change (Fig. 81).

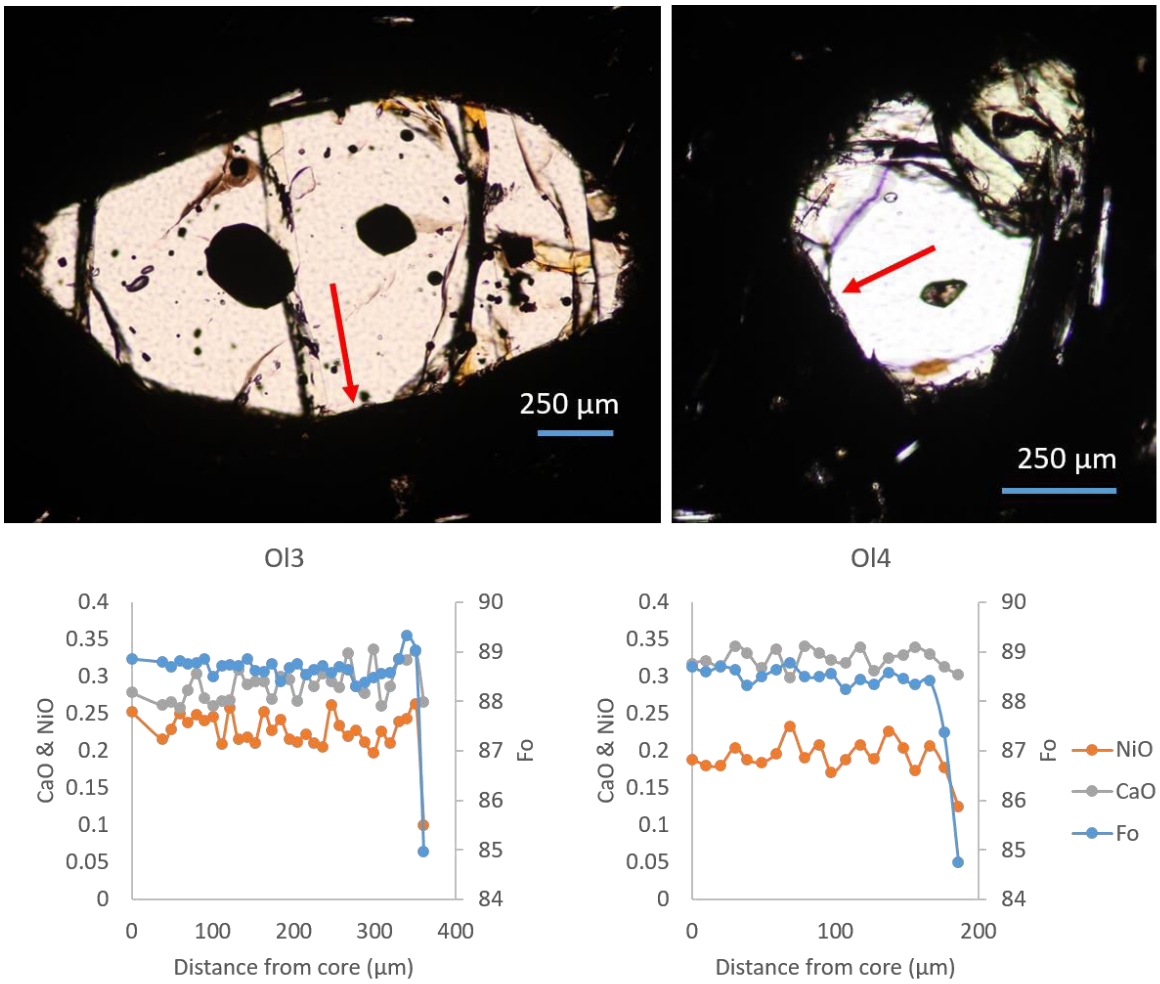

Fig. 81 - Fo, NiO and CaO profiles from core to rim for olivines Ol3 and Ol4 from sample MRS4.

D4

All the olivines from this sample present similar reversed Fo profiles (Fig. 82). The crystal with Fo73.5 first re-equilibrated with a melt in equilibrium with Fo73 (which corresponds to the core compositions of some of the rest of the crystals from this sample) and then, all the crystals re-equilibrated with a melt less differentiated, explaining the almost constant Fo86 in the rims.

To test if the zoning found in the studies crystals was due to diffusion, a second transverse was obtained for the olivine Ol3 (Fig. 83), perpendicular to the first transverse but his time not perpendicular to a crystal face, but exactly from the core to a crystal angle. Both profiles are reversely zoned but the geometries contrast, with the second transverse showing a larger length of zoning and a more gradual increase of Fo. This could be explained by the fact that the faces of the crystals might diffuse along a principal diffusional flux, while the angles are exposed

to different fluxes (Costa & Chakraborty, 2004), resulting in a more evolved diffusion profile and consequent overestimation of the timescales. Therefore, the reversely zoned profiles are assumed to depend mainly on diffusion, and therefore these crystals were used to estimate the timescales acting in this magmatic sub-system.

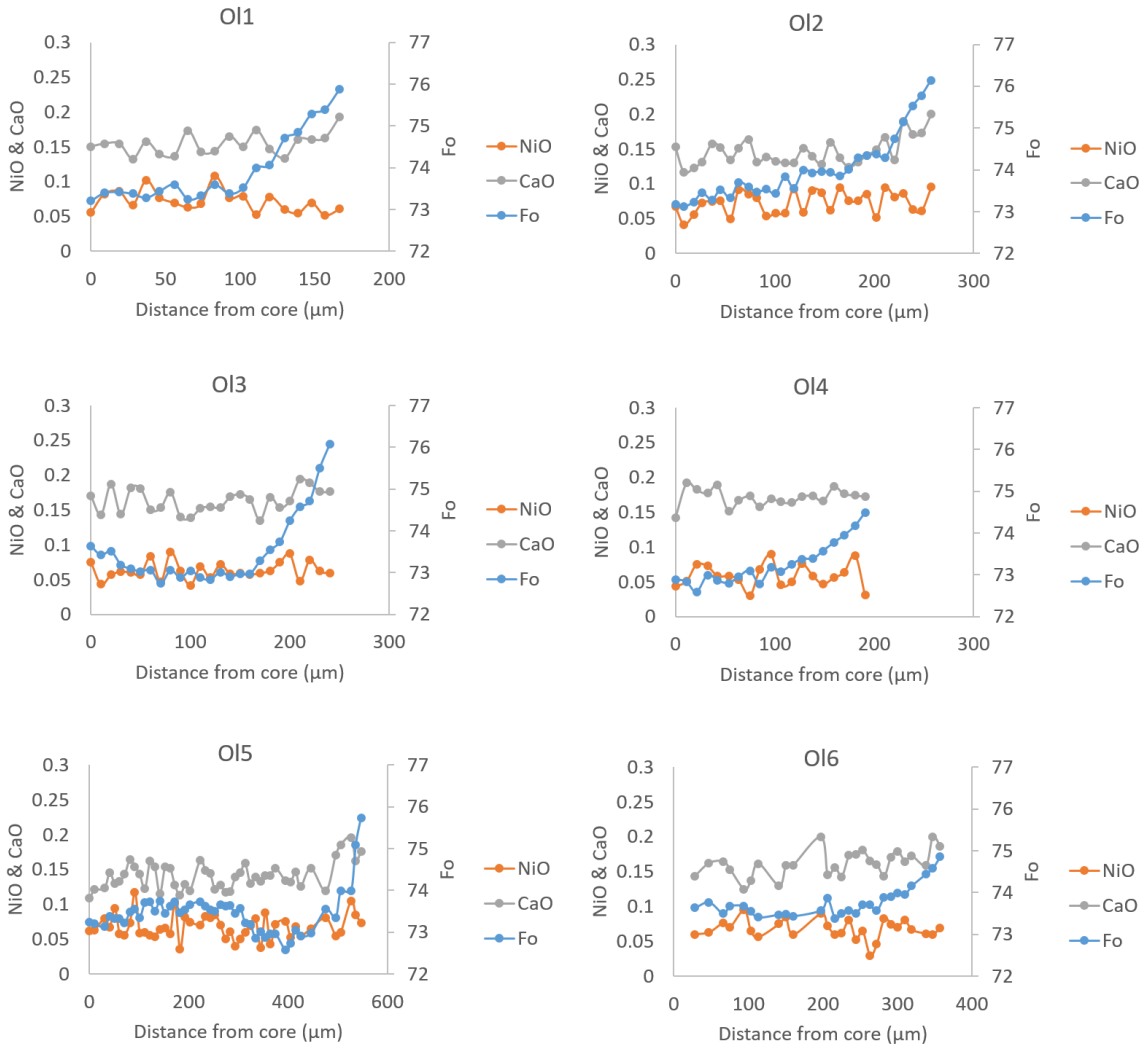

Fig. 82 - Fo, NiO and CaO profiles from core to rim for olivines from sample D4

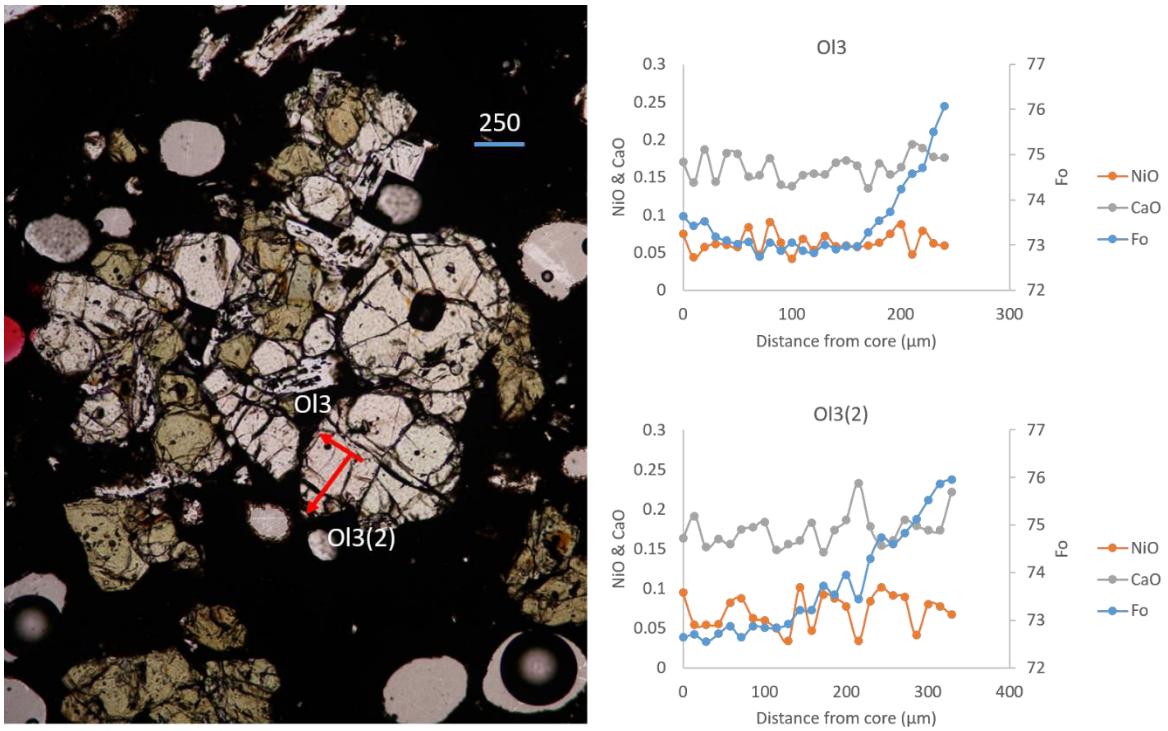

Fig. 83 - Fo, NiO and CaO profiles from core to rim along two perpendicular transverses in the crystal Ol3.

D5A

Sample D5A has the greater variety of profiles with different geometries and compositional ranges. The first evidence to assume diffusion as the main process responsible for the variable geometries presented by these compositional profiles is that the compositions shown by the cores, compositional steps and rims of these crystals, all repeat among the analysed crystals. Most of the crystals with core compositions varying from Fo90 to Fo86 are larger than the rest of the crystals with lower Fo and show variable profiles' geometries varying between this Fo range. This suggests that these crystals come from the deepest reservoir that makes part of the magmatic sub-system and that probably the timescales associated with the mixing episodes occurring in this reservoir are longer than in the rest of the plumbing system. Further geothermobarometer studies are need to support this hypothesis. (1) Ol3 is a particular example of these crystals from this deeper reservoir. According to the Fe concentration map and habit of the crystal it is possible to see that this crystal is formed by two different parts, probably two former crystals that grew parallel to each other till they came together, forming a single crystal. The Fe compositional map shows a clear asymmetric zoning pattern. The two black circles in Fig. 84(c) represent the presumed cores of the two crystals. The area around these two cores shows variable gradual decrease of Fe, depending on the direction. Paying special

attention to lowermost part of the crystal (not covered by the EPMA transverses), the angles of the crystal show a significant more smooth zoning towards the core comparing to the crystal face, which suggests that the zoning occurred mainly due to diffusion.

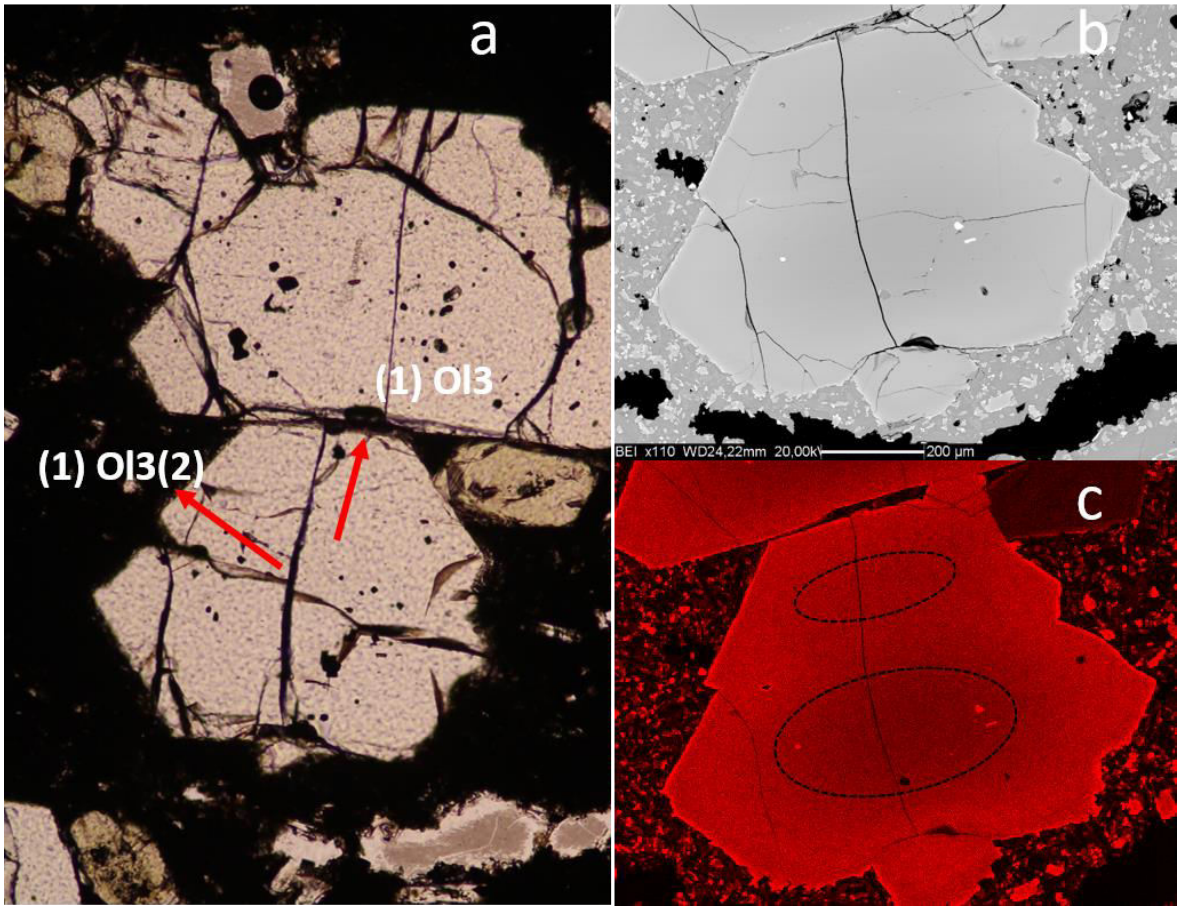

Figura 84 - Olivine (1) Ol4 from sample D5A. (a) Picture obtained with a optical microscope, where the two transverses (1) Ol4 and (1) Ol4(2) where analysed with EPMA. (b) Backscatter image of the same crystal obtained with SEM. (c) Fe (iron) compositional map in red scale (darker colours represent lower Fe contents) obtained with SEM, clearly showing the asymmetry of the compositional zoning. The two dark circles represent the former cores of the crystals now forming (1) Ol3. All the used instruments were from the Department of Geosciences, University of Padova.

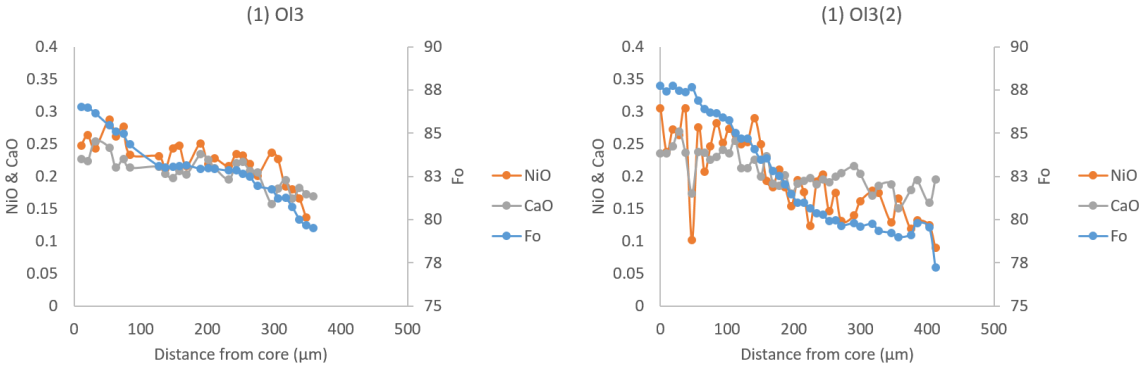

Fig. 85 - Fo, NiO and CaO for the two transverses analysed in the olivine (1) Ol3.

The compositional profiles obtained for to different directions in the crystal show contrasting geometries (Fig. 85). (1) Ol3 presents three different compositions, from an initial Fo86.6 towards a plateau of Fo83 and then an abrupt decrease towards Fo79.5 at the rim. Instead, the transverse (1) Ol3(2) show an initial composition of Fo88 and from here Fo decreases gradually to Fo80, with the last microns closer to the rim showing a shoulder, ending in an abrupt decrease to Fo77. Concluding, the transverse (1) Ol3 represents in the first 100 µm the result of the diffusion between the core of the two different crystals, while the rest of the profile is the plateau representing the core of the upper crystal and the normal zoning towards Fo79.5. The transverse (1) Ol3(2) instead registers initially the core composition of the lowermost crystal and the rest of the profile represents the diffusion between this core and the rim of Fo79.5. The diffusion responsible for this profile might have been influenced from different fluxes, contrarily to what is registered in the transverse (1) Ol3. Therefore, the latter ((1) Ol3) is ideal for geospeedometry calculations, while the former ((1) Ol3(2)) is not.

(1) Ol4 is another good example of the effects of diffusion occurring within the plumbing system and it might be used to study the magma transport dynamics (Fig. 84). Comparing the two transverses analysed perpendicularly (both from the core towards the rim), although the core and rim compositions are equal, the profiles in between vary significantly. The transverse (1) Ol4(2) shows a longer profile with a smooth decrease of Fo from the core (Fo90) to a compositional step (Fo85) that almost goes till the rim. The transverse (2) Ol4 shows a rather different geometry, presumably resulting from diffusion between two compositional steps (Fo90 and Fo85). The last microns of each profile represent the contact of this crystal with a more differentiated melt in equilibrium with olivine Fo80. Although the two profiles have different geometries, they may be both tested for geospeedometry calculations.

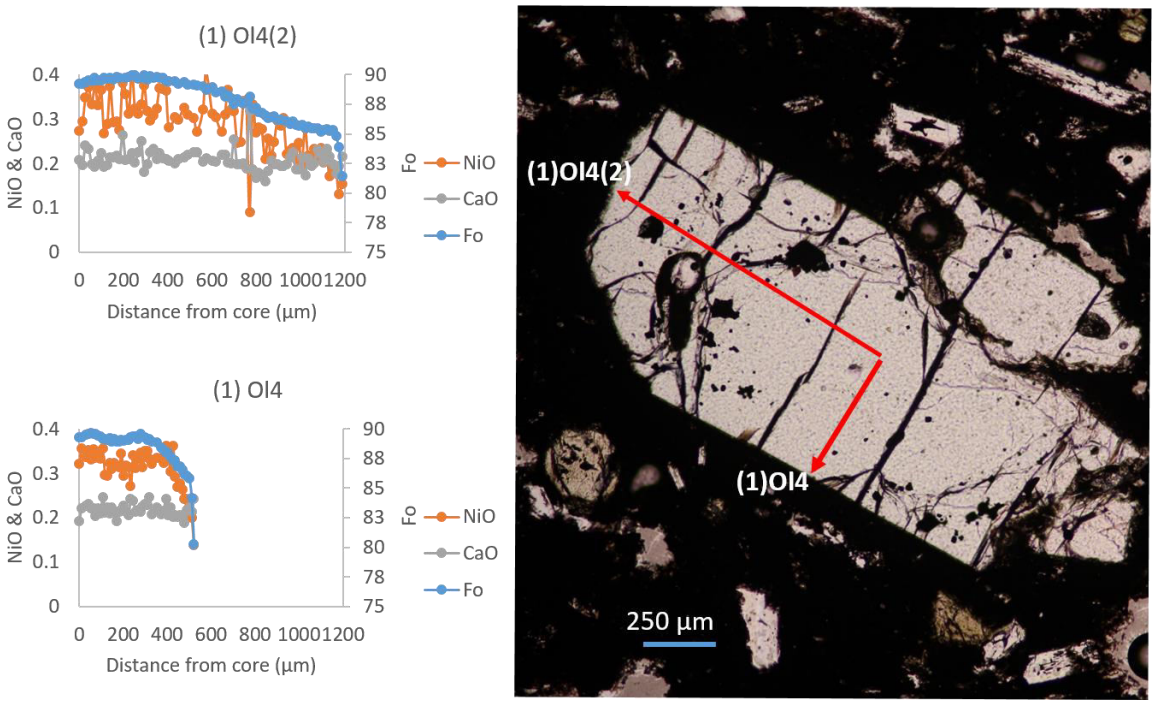

Fig. 86 - Fo, NiO and CaO profiles obtained from the two transverses analysed from Olivine (1) Ol4. The picture to the right shows the crystal and the position of the two transverses.

The rest of the chosen crystals (Fig. 87) are assumed to have zoned profiles mainly due to diffusion processes and are used to estimate the timescales on the magma transport between the identified reservoirs. Crystals with Fo>85 presenting compositional profiles with variable geometries within a similar range might represent the recharge of more mafic magma in its reservoir. The geothermobarometers applied to the compositions considered to natural from this reservoir point for temperatures of about 1190 ºC and pressures of about 1 kbar. Olivine (1) Ol1 presents a curved profile from rim to rim, and rim compositions vary (Fo86.3 and Fo84.9). The shape of this profile could be the result of a completely modified geometry due to a long re-equilibration period (Costa et al., 2008). The last ca. 50 µm of the profile show a steeper decrease of Fo till Fo84.5. Using the entire profile it was not possible to fit a single diffusion curve. This suggests that the steeper part of the profile might be the result of a secondary diffusional process that occurred after the main re-equilibration episode. Therefore, to model this profile, the last 50 µm were not used, and the resulting profile is assumed to go from rim to rim with rim compositions of Fo86.3 and Fo85.8.

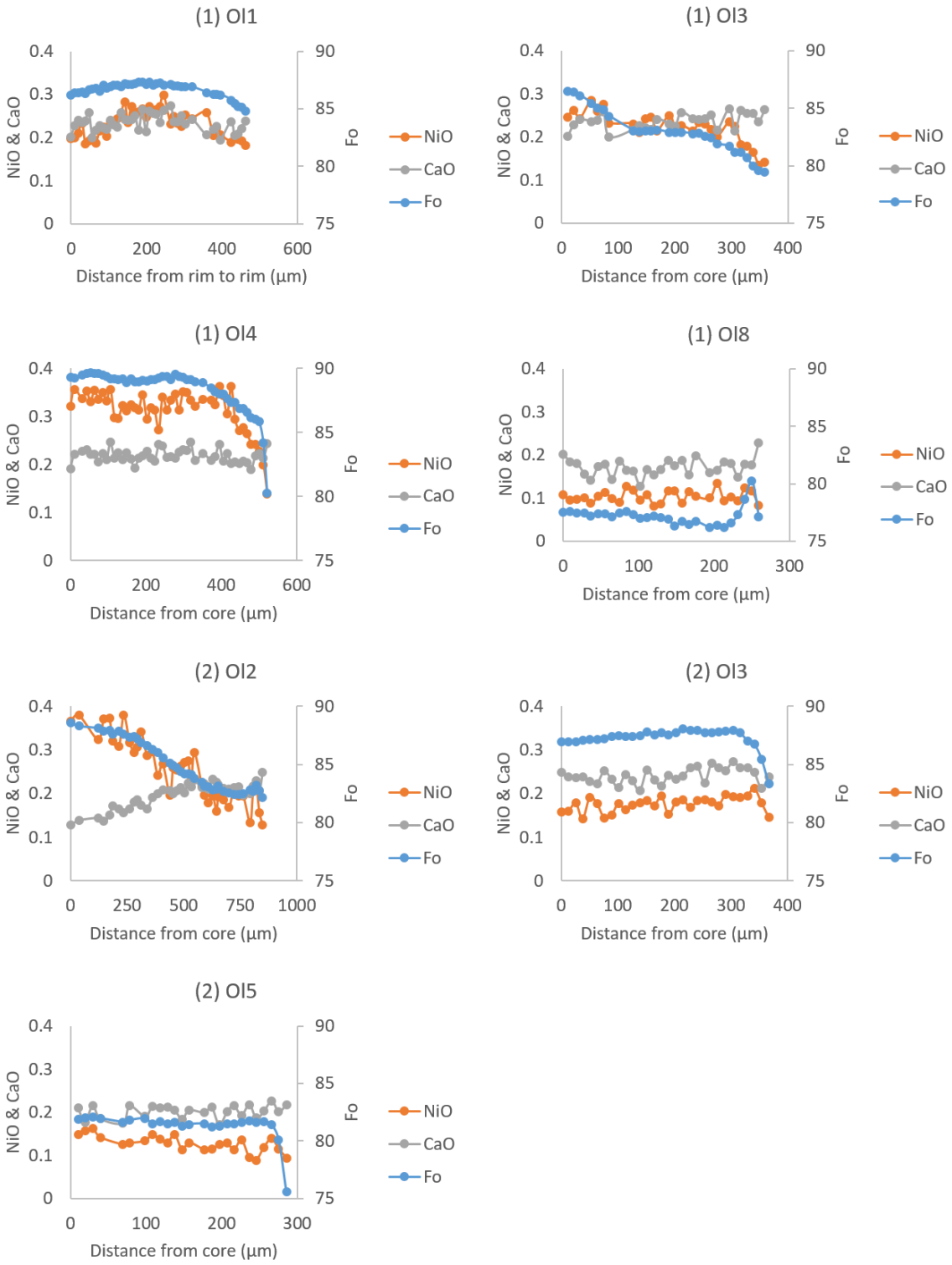

Fig. 87 - Fo, NiO and CaO profiles for olivines from sample D5A. Olivine (1) Ol1 represents the profile from rim to rim.

The modelling strategy used was to take out the last microns of the profile where the Fo decreases abruptly from Fo85.5 to Fo80. This part of the profile, i.e. the rim, might represent the contact between this crystal and the shallower reservoir, where the abrupt Fo decrease

represents a significantly shorter re-equilibrium period in the reservoir with compositions ranging from Fo86-85. Therefore, the profile from the core till the point where the composition decreases to Fo85.5 was used. Thus, this part of the model is comparable with the profile obtained perpendicularly. Similarly to (1) Ol4, (1) Ol4(2) shows a core composition of Fo90, a mantle composition of Fo85.5 and a rim composition of Fo80. The rim shows again an abrupt Fo decrease and this part of the profile was not used here. Therefore, both profiles can be used to estimate the timescales associated to the residence times within the deepest reservoir. The diffusion models applied to the two profiles were different. While for (1) Ol4 a simple initial and final composition were fixed (representing a crystal with a constant composition that re-equilibrates with the melt), the profile (1) Ol4(2) was modelled using a compositional step (as assuming that the initial crystal with a constant composition recrystallized when in contact with a melt with a different composition and then the cations diffused from one part of the crystal to the other). Considering that the profile (1) Ol4(2) shows a flat shape with Fo85.5 before the abrupt decrease towards the rim, this part of the crystal is useful to infer the timescales on this latter re-equilibrium episode.

Most of the rim compositions converge to Fo83-80 and as suggested before, this range of compositions is considered to correspond to a reservoir. The thermobarometry calculations show that temperature here ca. 1180 ^{o}C and pressures of about 0.5kbar.

Olivine (2) Ol3 shows a reversed zoning from the core (Fo87) till almost the rim (, where here instead the Fo shows a steep decrease towards Fo83. Due to the shape of the reversely zoned profile, this part of the crystal was not modelled. Probably that shape is given by the diffusion between two parts of the crystal with different compositions (this is also apparently seen in the CaO profile) but the Fo and NiO profiles show that significant diffusion occurred to hide the initial core composition. Therefore, only the rim is used.

Olivine (2) Ol2 shows a core composition of Fo88.5 and a rim composition of Fo82.5, with a profile similar to that of (1) Ol4(2). The rim shows a shoulder and so it was not accounted for the model, using the rest of the profile.

Olivine (1) Ol3 was already described above. The two profiles contrast and due to a better location, the profile used for geospeedometry calculations is (1) Ol3. If the first 100microns are not accounted, the rest of the profile shows a plateau at Fo83 followed by a normal zoning patter towards Fo79.

Olivine (1) Ol8 shows a core composition of Fo77.5 and from here the Fo slightly decreases to Fo76. The rim instead shows a shoulder pattern towards Fo80. Since the shoulder pattern might hide the real Fo content in the rim for the normal zoning registered from the core

to the shoulder, this profile is used to estimate only the timescales involved in the re-equilibration hat formed the reverse zoning.

The last olivine from this sample used for geospeedometry modelling is (2) Ol5. This olivine shows a plateau at Fo81.5 and an abrupt normal zoning patter towards Fo75.5. This zoning pattern represents the contact between the magmas from the reservoir 2 and 3, as seen by the olivine (1) Ol8, but on the contrary, here the crystals is normally zoned. The thermobarometer predicted for this third reservoir temperatures of 1170°C and low pressures as for the reservoir 2 (0.5 kbar).

D6

Olivines from this sample present similar zoning patterns, independently of the core composition (Fig. 88). The composition of the rims is rather constant, suggesting that all the crystal rims were in equilibrium with the same melt at the moment of the eruption. Using the thermobarometers, the reservoir where this magma mixing occurred is estimated to be at ca. 3 kbar with temperatures of about 1180 °C.

The only crystal with a significantly different zoning pattern is Ol4, which shows a normal zoning pattern from Fo80 to Fo77.5 and for the last 40 µm the Fo content increases abruptly towards Fo80. This crystal might be used to estimate the diffusion period responsible for the first part of the profile, i.e., normal zoning pattern.

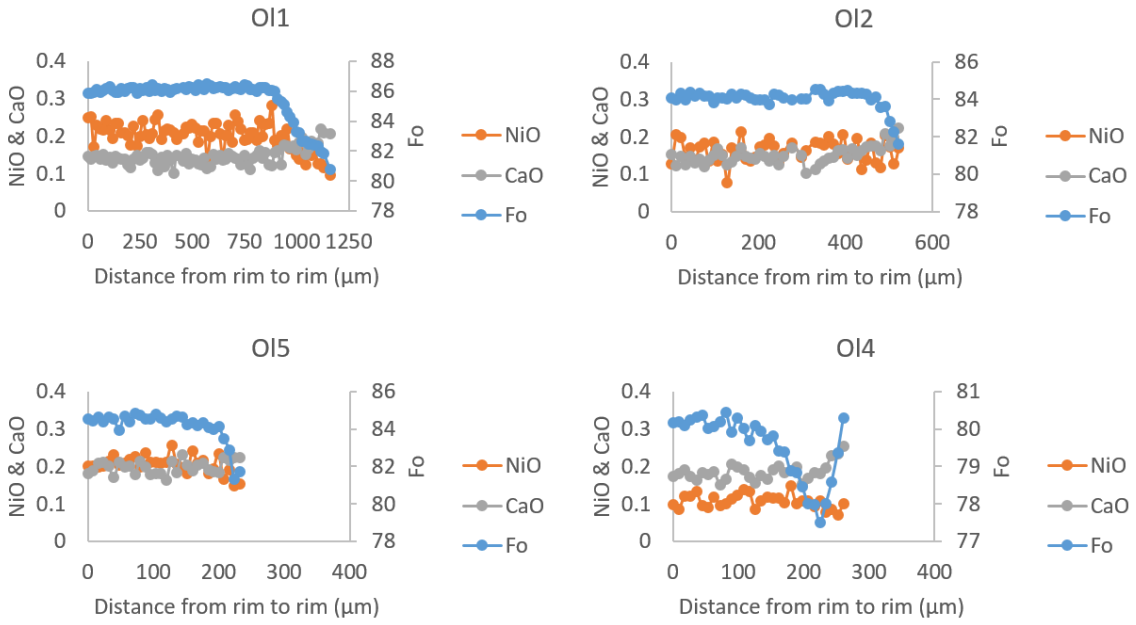

Fig. 88 - Fo, NiO and CaO profiles of the oriented olivines from the sample D6.

D12D2

As for sample D6, olivines from sample D12D2 (Fig. 88) present similar rim compositions, although the zoning patterns differ. According to the results obtained with the thermobarometers, the temperatures obtained with the crystals with more differentiated compositions are ca. 1180 °C at pressures of ca. 1.5 - 1 kbar. Ol5 shows the highest Fo content in the core among these crystals. The zoning pattern differs for the two rims and this could be the consequence of the sectioning of the crystals, sometimes responsible for compositional profiles that do not correspond to the real ones (Shea et al., 2015). The approach used to model this profile was to set two different rim compositions (corresponding to the rims of the crystal) and the core composition as initial composition. Although the rims show different zoning patterns, the diffusion model applied fitted well the analysed profile.

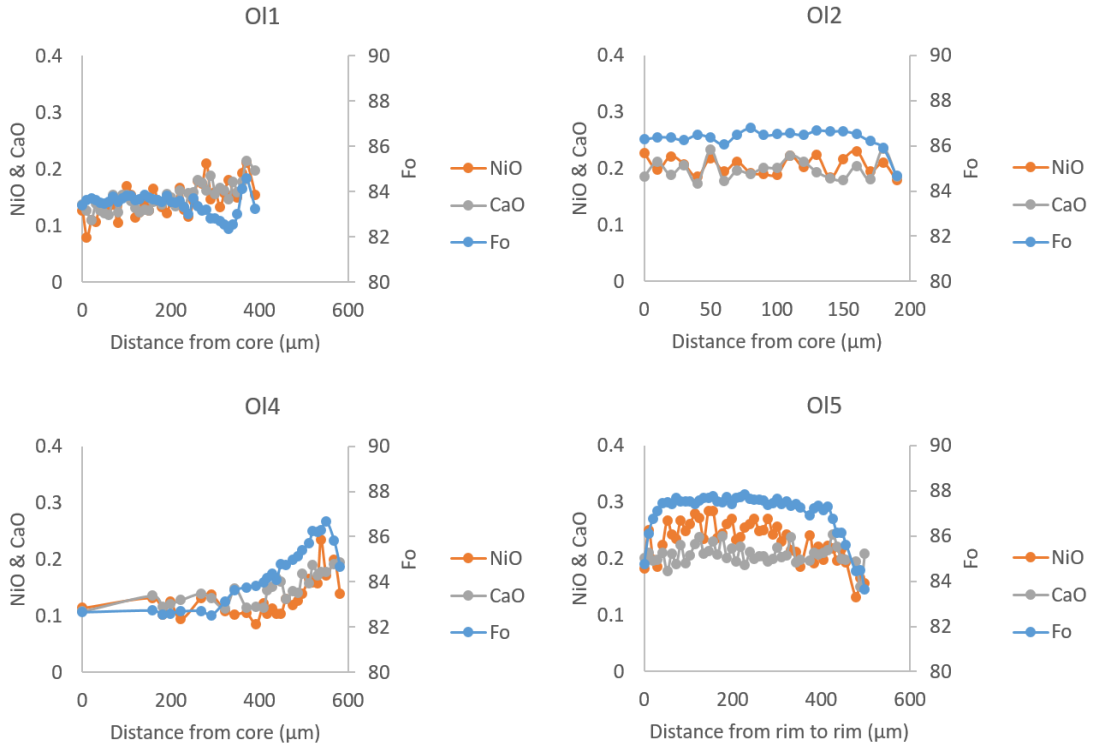

Fig. 89 - Fo, NiO and CaO profiles of the oriented olivines from the sample D12D2.

Ol1 and Ol4 have lower core compositions (Fo83.5 and Fo82.5, respectively). Ol1 shows a plateau that towards the rim decreases gradually to Fo82.5 and then forms a shoulder. The approach applied to this profile was to consider only the normal zoning before the shoulder pattern and thus estimate the timescales of magma movements within this reservoir. Ol4 instead shows a larger profile with a reversely zoned pattern from a core of Fo82.5 towards a maximum of Fo86.5. After this peak, Fo decreases abruptly to Fo84.5. The model approach used

to model this profile was not to count with the last 30 microns where the profile is normally zoned, but to use only the reversely zoned profile.

D16AB

Olivines from the sample D16AB have a relatively small compositional range (Fig. 90). Apart from (1) Ol1, the rim compositions of the olivines from this sample converge to Fo81.5-80. This suggests that the zoning patterns shown by these crystals were probably formed on similar physical conditions. The thermobarometers predicted a pressure of circa 2 kbar for the main reservoir (Fo82-80) and temperatures of circa 1180 °C. The crystals from the shallower reservoir instead resulted in predicted pressures of 0.5 kbar and temperatures similar to the deeper reservoir. Starting from the highest Fo compositions, (1) Ol4 is the only olivine with Fo84.5 at the core. The profile from rim to rim shows a plateau that changes only at the rims with an abrupt Fo decrease towards Fo83.5 and Fo81.8. The modelling approach was to fix the core and rims compositions and the model fitted well the olivine profile.

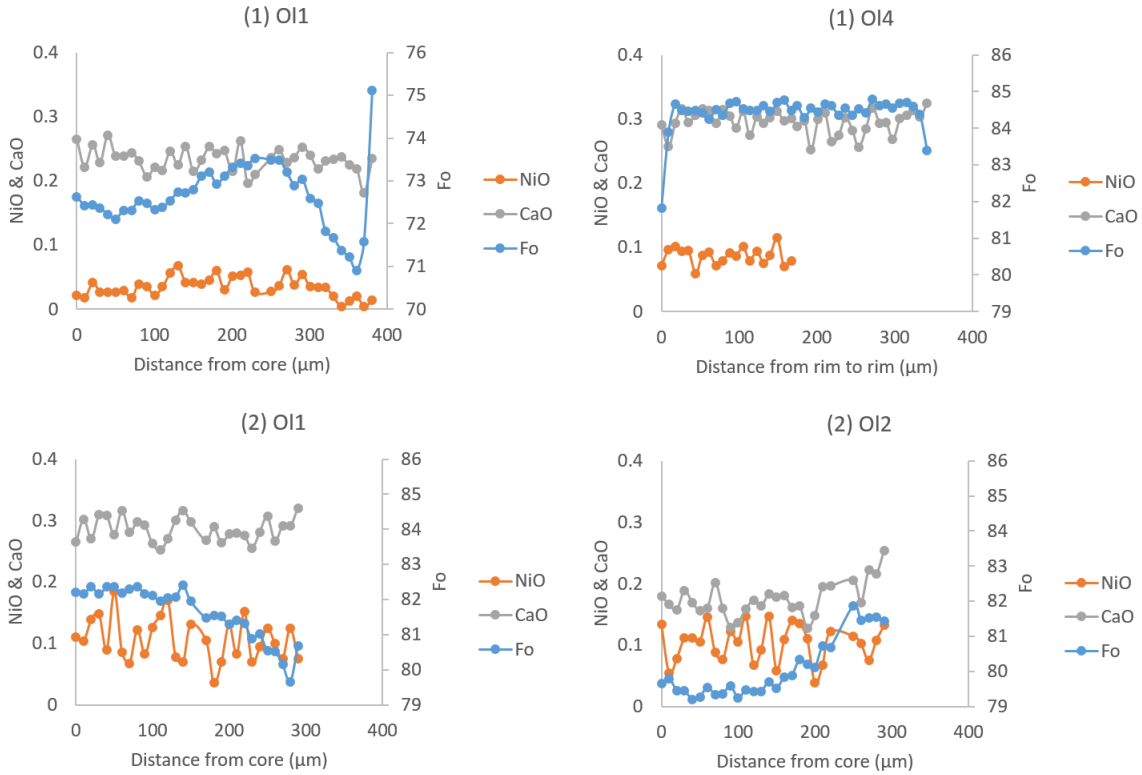

Fig. 90 - Fo, NiO and CaO profiles of the oriented olivines from the sample D16AB.

Olivine (2) Ol1 presents a normally zoned profile from core to rim, from Fo82 towards Fo79.5. The last 10 μm show a slight increase in Fo but this data point was not included in the profile for diffusion modelling. Although, the traverse is not perpendicular to a crystal face. Instead it is perpendicular to a crystal angle. This means that modelling this profile could result in overestimation of the real time it would take for the crystal to achieve such pattern (e.g. Shea et al., 2015). The only model that fitted the profile was an hypothetic profile with two compositional steps, and a different rim composition as initial boundaries (Fig. 91).

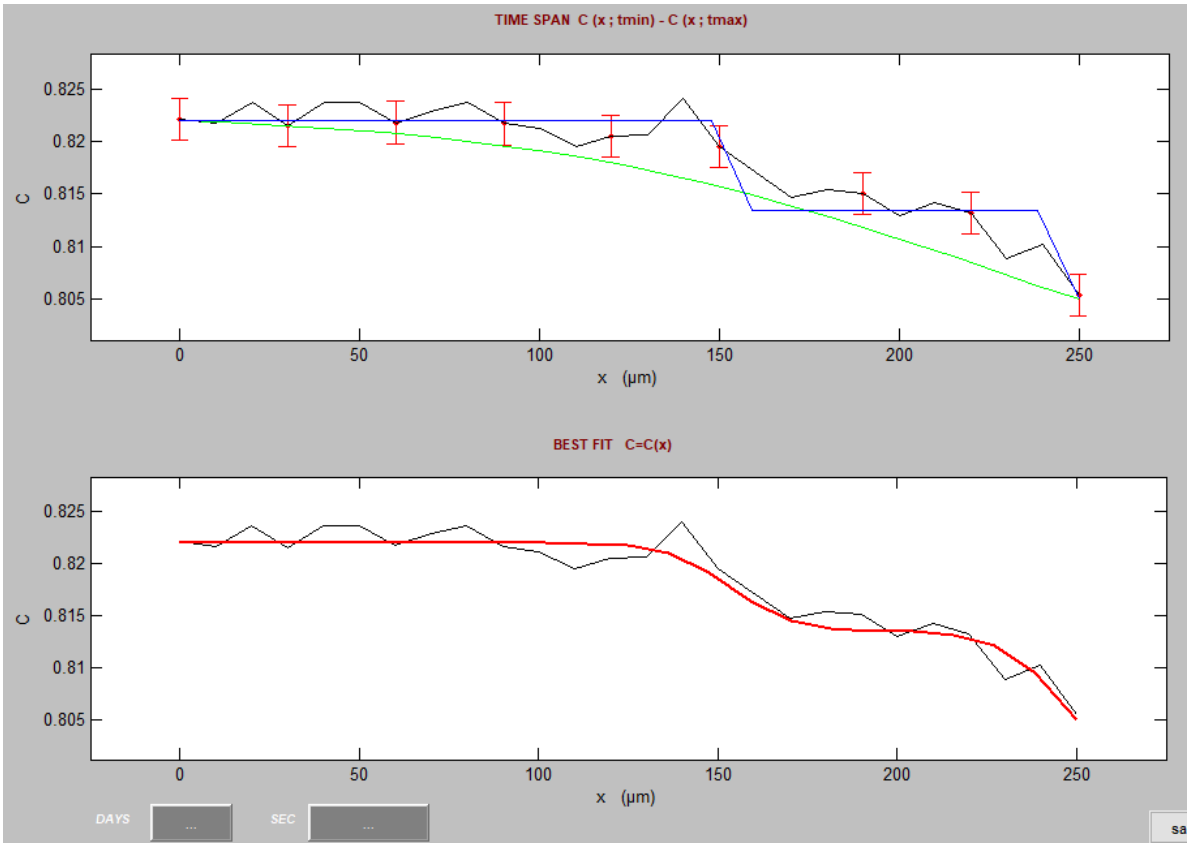

Fig. 91 - Results of the diffusion modelling of (2) Ol1 with DIPRA (Girona & Costa, 2013). *The image above: black line represents the analysed Fo profile for (2) Ol1; blue line represents the initial conditions of the calculated model; green line represents the profile resultant from diffusion of the blue line after 278 days. The image bellow: black line represents the analysed Fo profile for (2) Ol1; redline represents the best fit obtained from the diffusion of the blue line, resulting in 10 days.*

The olivine (1) Ol1 shows the lower core composition found in the sample (Fo72) and the neither the core nor the rim compositions are overlapped by any of the other crystals. The Fo profile shows an oscillating pattern that might reflect the magma dynamics in the shallower reservoir (0.5 kbar). To model this profile, the last 40 μm were not used because they show an abrupt Fo increase (from Fo70.5 to Fo75), which could rather represent the rise and mixing of

the magma. To fit the model two compositional steps were used plus a fixed rim composition (Fo72, Fo73 and Fo70.5, respectively).

Results

Table 4 - Results from Geospeedometry modelling using DIPRA. The results (in days) are presented with the respective model error.

Sample	Ol	Core Fo	Rim Fo	Days	erro-days	erro+ days	est. error %
MRS1EM	Ol9	85.8	84.5	282	94	91	33
MRS4	Ol3	88.5	84.7	3	2.6	0.33	49
	Ol4	88.4	84.7	9	3	3	33
D5A	(1) Ol1	87.1	85.8	448	33	42	8
	(1) Ol3	82.9	79	384	31	64	12
	(1) Ol4	89.1	85.5	1935	330	327	17
	(1) Ol4(2)	89.8	85.3	1121	146	73	10
	(1) Ol4(2)	85.4	81.5	4	3	2	63
	(1) Ol8	76.5	80.2	20	5	12	43
	(2) Ol2	88.4	82.4	4031	337	259	7
	(2) Ol3	87.6	83.1	65	8	20	22
	(2) Ol5	81.5	75.2	6	4	3	58
D6	Ol1	86	82.9	629	58	61	9
	Ol2	84.8	83.2	46	16	17	36
	Ol4	80	77.5	144	50.93	32.41	29
	Ol5	84	81.3	19	10	10	53
D16AB	(1) Ol1	73.5	70.5	124	12	10	9
	(1) Ol4	84	83	5	5	3	80
	(2) Ol1	82	80.5	10	3	25	140
	(2) Ol3	79.4	81.8	194	14	37	13
D12D2	Ol1	83.5	82	463	60	114	19
	Ol2	86.3	84.7	23	15	11	57

	Ol4	82.7	86.7	1594	94	158	8
	Ol5	87.4	83.5	225	24	27	11
D4	Ol1	73.3	75.9	168	19	18	11
	Ol2	73	76.2	213	20	40	14
	Ol3	72.8	76	120	35	35	29
	Ol4	72.9	74.5	289	47	25	12
	Ol5	73.6	74	188	35	57	24
	Ol6	74	75	264	97	61	30

Table 4 shows the results for the geospeedometry models using DIPRA (Girona & Costa, 2013). Although the number of olivines used by sample may be not statistically representative, the results together give a preliminary idea of the timescales associated to the magmatic dynamics within the plumbing system of the Marsili. The results vary from a few days to a maximum of a decade, but the majority of the results range from a few days to 500 days.

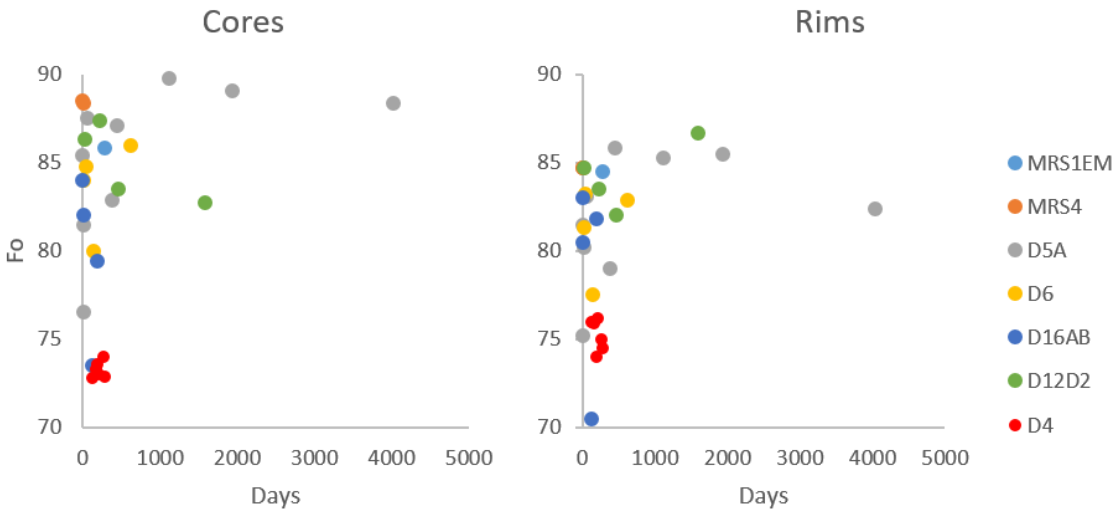

Fig. 92 - Fo contents for core (left) and rim (right) vs. the results obtained from diffusion modelling with DIPRA. Each data point represents a profile and each colour a sample.

Plotting the calculated diffusion periods against the core compositions (i.e. the initial plateau composition) shows that the crystals showing higher residence periods in reservoirs with different conditions from the initial equilibrium conditions are the crystals with Fo>85 (Fig. 85).

D5A olivines with core Fo higher than Fo88 show the highest times retrieved. The corresponding rim compositions of these crystals have similar compositions, although with variable re-equilibrium times. This variability might represent different magma batches

recharging the system, specifically the reservoir with a composition in equilibrium with Fo85-86. Moreover, this reflects the higher volume of magma entering in this system, as suggested above. The rim plot shows the composition at which the crystals re-equilibrate and for how long. The first observations is that the higher rim Fo contents show more variable retrieved times. This suggests that the magma input in the less evolved systems might be higher comparing to the more felsic ones.

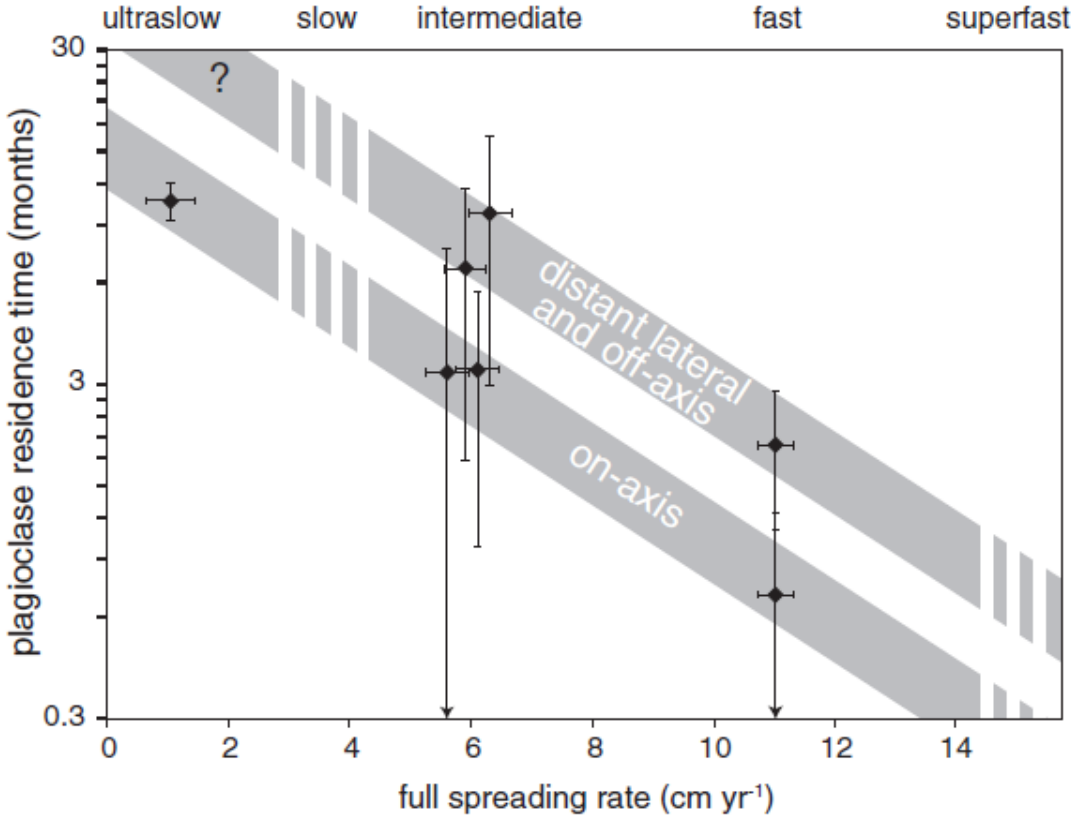

Fig. 93 – Residence times calculated with plagioclase crystals as a function of spreading rate and the proximity to the axis of the MOR. Adapted from Zellmer et al. (2012).

Overall, the majority of the samples have crystals showing only a few days of diffusion re-equilibration, probably associated with the last mixing episode prior to the eruption. Instead, D4 olivines present slightly longer times, from 100 to 300 days, similar to the olivine (1) Ol1 from D16AB with the lower rim composition registered (Fig. 92). This different behaviour might be related with the more acid compositions and the smaller flux of more mafic magma input in such reservoirs. According to Zellmer et al. (2012), the residence times of plagioclase phenocrysts within the crustal magmatic system depend on the spreading rate (Fig. 93). This has direct implications on understanding the feeding rates of the magmatic systems and magma accumulation in the crust. According to the results obtained by modelling timescales in the Marsili plumbing system, the last residence times recorded by the olivine compositions before the eruption of the carrying magmas are in general less than 150 days and it overlaps with the

fast-spreading ridge record (Zellmer et al., 2012; Fig. 93). The timescales referring to magmatic dynamics within a reservoir are greater than the timescales obtained for magmatic transport from one reservoir to another. The residence times of these mixing events within a reservoirs may be underestimated due to the limitations of the modelling approach. However, they still suggest that existing magma reservoirs that make part of the Marsili plumbing system connect long before the eruption, transporting magma at different rates.

Summary

The geodynamic environment in which the Marsili back-arc basin and volcano formed is complex, starting from the formation of the formation of oceanic crust in the centre of the basin and further formation of the strongly elongated inflated-volcanic seamount, probably formed due to the input of mantle material under the basin, inducing a strong magma production (Trua & Marani, 2011; Trua et al., 2002). The study of phenocryst cargo of the Marsili basalts served to further characterise the plumbing system of this large volcano and to give further insights into the dynamics occurring in a back-arc basin context. Several olivine and clinopyroxene crystals from eight basalts sampled along the volcanic ridge were used to identify and describe the magmatic structures of the plumbing systems represented by each sample, characterizing the physical and chemical variability within each sample and between samples.

Olivine (major and minor elements) and clinopyroxene (minor and trace elements) were also used to characterize the diversity of the magmas entering in the Marsili plumbing system, giving further insights to the variability already pointed using isotopic and trace element data (e.g. Trua et al., 2011). The olivine present similar compositions found in the Aeolian Islands (Zamboni et al., 2017), ranging from the compositions characterised as representative of a peridotitic source towards the compositions from typical of a pyroxenitic source (Sobolev et al., 2007), but never overlapping the latter ones. However, variable water contents, melt compositions and diffusional reequilibration might explain the differences between olivine crystals. Further studies with high precision compositions are necessary to confirm these observations and to better characterize the composition variability of the crystals from primitive magmas. Trace element compositions from the clinopyroxene crystals overlap results already published (Trua et al., 2014). The calculated melts in equilibrium with the clinopyroxenes from the sample D6 overlap the compositions from OIB-like lavas, while the rest of the samples overlap the compositions obtained from olivine-melt inclusions in the IAB Marsili basalts. Some

of the analysed samples although present a higher LREE/HREE variability, suggesting that probably these two end-members may have entered in these plumbing systems in variable proportions. To further confirm this, more clinopyroxene compositions with higher precision are needed and melt inclusions from olivine and clinopyroxenes crystals might be analysed from these samples.

A variable number of reservoirs was identified for each sample and the complexity of these magmatic systems might correlate directly with the flux of magma input in each system. The geothermobarometers used in this study estimate that the identified reservoirs reside at variable pressures (i.e. depths) ranging from 0.5 to 3 kbar and temperatures may vary from 1250 to 1150 ^{o}C. The crystals from the lavas sampled in the southern part of the summit of the volcano present higher compositional variability and the larger range of pressures and temperatures. Here, up to three different reservoirs were identified. Some of these reservoirs, the olivines and clinopyroxenes modelled to be in equilibrium present compositional profiles with zoned and oscillatory patterns, suggesting open-system differentiation processes. The textures from the lavas in these samples show several glomerocrysts with plagioclase and some clinopyroxene crystals presenting disequilibrium textures. These observations suggest that these crystals and crystal clusters might represent mush structures that might have been desegregated prior to the eruption. Conversely, the lavas sampled from the northern part of the volcano, out of the summit, have crystals with lower composition variabilities and lower porphyritic indexes.

The zoned profiles found in most of the olivines from the majority of the samples were modelled with the geospeedometry technic, using the software DIPRA (Girona & Costa, 2013). The average timescales retrieved from the olivine crystals range from a few days to a ca. two years. Samples show variable re-equilibrium periods, where the larger ranges are found for samples within the ridge's summit (from few days to a decade). Moreover, the samples with more differentiated compositions present lower variable re-equilibrium periods, varying from 100 to 300 days, suggesting that in these relatively more felsic systems the magma inputs are less frequent.

The timescales retrieved associated to the compositional descriptions and reservoir identifications might also correlate with seismic activity, as already suggested and observed by a large variety of authors (e.g. Albert et al., 2016; Kahl et al., 2014; Kahl et al., 2017; Viccaro et al., 2016). The larger re-equilibrium periods obtained by the Marsili are related with the cyclic magma recharges of the deeper and less differentiated reservoirs for the samples in the summit, but also related to the replenishment of the shallower mush zoned. Here, the mush desegregation and magma transport may generate the seismic activity temporally correlated

with the retrieved timescales and therefore this is an important technic to apply in areas with a risk of geohazards, such as the Marsili volcano.

References

Albert, H., Costa, F., & Martí, J. (2016). Years to weeks of seismic unrest and magmatic intrusions precede monogenetic eruptions. *Geology*, *44*(3), 211–214. https://doi.org/10.1130/G37239.1

Ballhaus, C. B., Berry, R. F., & Green, D. H. (1991). High pressure experimental calibration of the olivine-orthopyroxene-spinel oxygen barometer - implications for redox conditions in the Upper mantle. *Contributions to Mineralogy and Petrology*, *107*, 27–40.

Barca, D., & Trua, T. (2012). Magma emplacement at anomalous spreading ridge : Constraints due to plagioclase crystals from basalts of Marsili seamount (Southern Tyrrhenian back-arc) Marsili seamount sampling. *Journal of Volcanology and Geothermal Research*, *241–242*, 61–77. https://doi.org/10.1016/j.jvolgeores.2012.06.021

Costa, F., & Chakraborty, S. (2004). Decadal time gaps between mafic intrusion and silicic eruption obtained from chemical zoning patterns in olivine, *227*, 517–530. https://doi.org/10.1016/j.epsl.2004.08.011

Costa, F., Dohmen, R., & Chakraborty, S. (2008). Time Scales of Magmatic Processes from Modeling the Zoning Patterns of Crystals. *Reviews in Mineralogy and Geochemistry*, *69*(14), 545–594. https://doi.org/10.2138/rmg.2008.69.14

Gavrilenko, M., Ozerov, A., Kyle, P. R., Carr, M. J., Nikulin, A., Vidito, C., & Danyushevsky, L. (2016). Abrupt transition from fractional crystallization to magma mixing at Gorely volcano (Kamchatka) after caldera collapse. *Bulletin of Volcanology*, *78*(7). https://doi.org/10.1007/s00445-016-1038-z

Ghiorso, M. S., & Sack, R. O. (1995). Chemical mass transfer in magmatic processes IV. A revised and internally consistent thermodynamic model for the interpolation and extrapolation of liquid-solid equilibria in magmatic systems at elevated temperatures and pressures. *Contributions to Mineralogy and Petrology*, *119*(2–3), 197–212. https://doi.org/10.1007/BF00307281

Girona, T., & Costa, F. (2013). DIPRA: A user-friendly program to model multi-element diffusion in olivine with applications to timescales of magmatic processes. *Geochemistry, Geophysics, Geosystems*, *14*(2), 422–431. https://doi.org/10.1029/2012GC004427

Herzberg, C. (2011). Identification of source lithology in the Hawaiian and Canary Islands:

Implications for origins. *Journal of Petrology*, *52*(1), 113–146. https://doi.org/10.1093/petrology/egq075

Kahl, M., Chakraborty, S., Pompilio, M., & Costa, F. (2014). Constraints on the nature and evolution of the magma plumbing system of Mt. Etna volcano (1991-2008) from a combined thermodynamic and kinetic modelling of the compositional record of minerals. *Journal of Petrology*, *56*(10), 2025–2068. https://doi.org/10.1093/petrology/egv063

Kahl, M., Viccaro, M., Ubide, T., Morgan, D. J., & Dingwell, D. B. (2017). A branched magma feeder system during the 1669 eruption of Mt Etna: Evidence from a time-integrated study of zoned olivine phenocryst populations. *Journal of Petrology*, *58*(3), 443–472. https://doi.org/10.1093/petrology/egx022

Kastens, K., & Mascle, J. (1990). The Geological Evolution of the Tyrrhenian Sea: An Introduction to the Scientific Results of ODP Leg 107. *Proceedings of the Ocean Drilling Program*, *107*(1986), 3–26. https://doi.org/10.2973/odp.proc.sr.107.187.1990

Kastens, K., Mascle, J., Auroux, C., Bonatti, E., Broglia, C., Channell, J., … Torii, M. (1988). ODP Leg 107 in the Tyrrhenian Sea: Insights into passive margin and back-arc basin evolution. *Bulletin of the Geological Society of America*, *100*(7), 1140–1156. https://doi.org/10.1130/0016-7606(1988)100<1140:OLITTS>2.3.CO;2

Lange, R. A., Frey, H. M., & Hector, J. (2009). A thermodynamic model for the plagioclase-liquid hygrometer/thermometer. *American Mineralogist*, *94*(4), 494–506. https://doi.org/10.2138/am.2009.3011

Loucks, R. R. (1996). A precise olivine-augite Mg-Fe-exehange geothermometer. *Contributions to Mineralogy and Petrology*, *125*(2–3), 140–150. https://doi.org/10.1007/s004100050211

Lynn, K. J., Garcia, M. O., Shea, T., Costa, F., & Swanson, D. A. (2017). Timescales of mixing and storage for Keanakāko'i Tephra magmas (1500–1820 C.E.), Kīlauea Volcano, Hawai'i. *Contributions to Mineralogy and Petrology*, *172*(9). https://doi.org/10.1007/s00410-017-1395-4

Mollo, S., Blundy, J. D., Iezzi, G., Scarlato, P., & Langone, A. (2013). The partitioning of trace elements between clinopyroxene and trachybasaltic melt during rapid cooling and crystal growth. *Contributions to Mineralogy and Petrology*, *166*(6), 1633–1654. https://doi.org/10.1007/s00410-013-0946-6

Mollo, S., Putirka, K., Misiti, V., Soligo, M., & Scarlato, P. (2013). A new test for equilibrium based on clinopyroxene-melt pairs: Clues on the solidification temperatures of Etnean alkaline melts at post-eruptive conditions. *Chemical Geology*, *352*, 92–100. https://doi.org/10.1016/j.chemgeo.2013.05.026

Nimis, P. (1995). A clinopyroxene geobarometer for basaltic systems based on crystal-structure modeling. *Contributions to Mineralogy and Petrology*, *121*(2), 115–125. https://doi.org/10.1007/s004100050093

Panza, G. F., Peccerillo, A., Aoudia, A., & Farina, B. (2007). Geophysical and petrological modelling of the structure and composition of the crust and upper mantle in complex geodynamic settings: The Tyrrhenian Sea and surroundings. *Earth-Science Reviews*, *80*(1–2), 1–46. https://doi.org/10.1016/j.earscirev.2006.08.004

Pontevivo, A., & Panza, G. F. (2006). The lithosphere-asthenosphere system in the Calabrian Arc and surrounding seas - Southern Italy. *Pure and Applied Geophysics*, *163*(8), 1617–1659. https://doi.org/10.1007/s00024-006-0093-3

Putirka, K. D. (2008). Thermometers and Barometers for Volcanic Systems. *Reviews in Mineralogy and Geochemistry*, *69*(1), 61–120. https://doi.org/10.2138/rmg.2008.69.3

Putirka, K., Ryerson, F. J., Perfit, M., & Ridley, W. I. (2011). Mineralogy and composition of the oceanic mantle. *Journal of Petrology*, *52*(2), 279–313. https://doi.org/10.1093/petrology/egq080

Ridolfi, F., Renzulli, A., & Puerini, M. (2010). Stability and chemical equilibrium of amphibole in calc-alkaline magmas: An overview, new thermobarometric formulations and application to subduction-related volcanoes. *Contributions to Mineralogy and Petrology*, *160*(1), 45–66. https://doi.org/10.1007/s00410-009-0465-7

Shea, T., Costa, F., Krimer, D., & Hammer, J. E. (2015). Accuracy of timescales retrieved from diffusion modeling in olivine: A 3D perspective. *American Mineralogist*, *100*(10), 2026–2042. https://doi.org/10.2138/am-2015-5163

Sobolev, A. V, Hofmann, A. W., Kuzmin, D. V, Yaxley, G. M., Arndt, N. T., Chung, S.-L., … Teklay, M. (2007). The amount of recycled crust in sources of mantle-derived melts. *Science (New York, N.Y.)*, *316*(5823), 412–7. https://doi.org/10.1126/science. 1138113

Sun, S., & Mcdonough, W. F. (1989). Geological Society , London , Special Publications Chemical and isotopic systematics of oceanic basalts : implications for mantle composition and processes Chemical and isotopic systematics of oceanic basalts : implications for mantle composition and proc. https://doi.org/10.1144/GSL.SP.1989.042.01.19

Trua, T., Clocchiatti, R., Schiano, P., Ottolini, L., & Marani, M. (2010). Lithos The heterogeneous nature of the Southern Tyrrhenian mantle : Evidence from olivine-hosted melt inclusions from back-arc magmas of the Marsili seamount. *LITHOS*, *118*(1–2), 1–16. https://doi.org/10.1016/j.lithos.2010.03.008

Trua, T., Marani, M., & Barca, D. (2014). Lower crustal differentiation processes beneath a back-

arc spreading ridge (Marsili seamount, Southern Tyrrhenian Sea). *Lithos*, *190–191*, 349–362. https://doi.org/10.1016/j.lithos.2013.12.014

Trua, T., & Marani, M. P. (2011). Magmatic evidence for African mantle propagation into the southern Tyrrhenian backarc region, *2478*(16), 307–331. https://doi.org/10.1130/2011.2478(16).

Trua, T., Marani, M. P., & Gamberi, F. (2018). Magma Plumbing System at a Young Back-Arc Spreading Center: The Marsili Volcano, Southern Tyrrhenian Sea. *Geochemistry, Geophysics, Geosystems*, *19*(1), 43–59. https://doi.org/10.1002/2017GC007151

Trua, T., Serri, G., Marani, M., Renzulli, A., & Gamberi, F. (2002). Volcanological and petrological evolution of Marsili seamount (southern Tyrrhenian Sea). *Journal of Volcanology and Geothermal Research*, *114*(3–4), 441–464. https://doi.org/10.1016/S0377-0273(01)00300-6

Viccaro, M., Giuffrida, M., Nicotra, E., & Cristofolini, R. (2016). Timescales of magma storage and migration recorded by olivine crystals in basalts of the March-April 2010 eruption at Eyjafjallajökull volcano, Iceland. *American Mineralogist*, *101*(1), 222–230. https://doi.org/10.2138/am-2016-5365

Zajacz, Z., & Halter, W. (2007). LA-ICPMS analyses of silicate melt inclusions in co-precipitated minerals: Quantification, data analysis and mineral/melt partitioning. *Geochimica et Cosmochimica Acta*, *71*(4), 1021–1040. https://doi.org/10.1016/j.gca.2006.11.001

Albert, H., Costa, F., & Martí, J. (2016). Years to weeks of seismic unrest and magmatic intrusions precede monogenetic eruptions. *Geology*, *44*(3), 211–214. https://doi.org/10.1130/G37239.1

Ballhaus, C. B., Berry, R. F., & Green, D. H. (1991). High pressure experimental calibration of the olivine-orthopyroxene-spinel oxygen barometer - implications for redox conditions in the Upper mantle. *Contributions to Mineralogy and Petrology*, *107*, 27–40.

Barca, D., & Trua, T. (2012). Magma emplacement at anomalous spreading ridge : Constraints due to plagioclase crystals from basalts of Marsili seamount (Southern Tyrrhenian back-arc) Marsili seamount sampling. *Journal of Volcanology and Geothermal Research*, *241–242*, 61–77. https://doi.org/10.1016/j.jvolgeores.2012.06.021

Costa, F., & Chakraborty, S. (2004). Decadal time gaps between mafic intrusion and silicic eruption obtained from chemical zoning patterns in olivine, *227*, 517–530. https://doi.org/10.1016/j.epsl.2004.08.011

Costa, F., Dohmen, R., & Chakraborty, S. (2008). Time Scales of Magmatic Processes from Modeling the Zoning Patterns of Crystals. *Reviews in Mineralogy and Geochemistry*, *69*(14),

545–594. https://doi.org/10.2138/rmg.2008.69.14

Gavrilenko, M., Ozerov, A., Kyle, P. R., Carr, M. J., Nikulin, A., Vidito, C., & Danyushevsky, L. (2016). Abrupt transition from fractional crystallization to magma mixing at Gorely volcano (Kamchatka) after caldera collapse. *Bulletin of Volcanology*, *78*(7). https://doi.org/10.1007/s00445-016-1038-z

Ghiorso, M. S., & Sack, R. O. (1995). Chemical mass transfer in magmatic processes IV. A revised and internally consistent thermodynamic model for the interpolation and extrapolation of liquid-solid equilibria in magmatic systems at elevated temperatures and pressures. *Contributions to Mineralogy and Petrology*, *119*(2–3), 197–212. https://doi.org/10.1007/BF00307281

Girona, T., & Costa, F. (2013). DIPRA: A user-friendly program to model multi-element diffusion in olivine with applications to timescales of magmatic processes. *Geochemistry, Geophysics, Geosystems*, *14*(2), 422–431. https://doi.org/10.1029/2012GC004427

Herzberg, C. (2011). Identification of source lithology in the Hawaiian and Canary Islands: Implications for origins. *Journal of Petrology*, *52*(1), 113–146. https://doi.org/10.1093/petrology/egq075

Kahl, M., Chakraborty, S., Pompilio, M., & Costa, F. (2014). Constraints on the nature and evolution of the magma plumbing system of Mt. Etna volcano (1991-2008) from a combined thermodynamic and kinetic modelling of the compositional record of minerals. *Journal of Petrology*, *56*(10), 2025–2068. https://doi.org/10.1093/petrology/egv063

Kahl, M., Viccaro, M., Ubide, T., Morgan, D. J., & Dingwell, D. B. (2017). A branched magma feeder system during the 1669 eruption of Mt Etna: Evidence from a time-integrated study of zoned olivine phenocryst populations. *Journal of Petrology*, *58*(3), 443–472. https://doi.org/10.1093/petrology/egx022

Kastens, K., & Mascle, J. (1990). The Geological Evolution of the Tyrrhenian Sea: An Introduction to the Scientific Results of ODP Leg 107. *Proceedings of the Ocean Drilling Program*, *107*(1986), 3–26. https://doi.org/10.2973/odp.proc.sr.107.187.1990

Kastens, K., Mascle, J., Auroux, C., Bonatti, E., Broglia, C., Channell, J., … Torii, M. (1988). ODP Leg 107 in the Tyrrhenian Sea: Insights into passive margin and back-arc basin evolution. *Bulletin of the Geological Society of America*, *100*(7), 1140–1156. https://doi.org/10.1130/0016-7606(1988)100<1140:OLITTS>2.3.CO;2

Lange, R. A., Frey, H. M., & Hector, J. (2009). A thermodynamic model for the plagioclase-liquid hygrometer/thermometer. *American Mineralogist*, *94*(4), 494–506. https://doi.org/10.2138/am.2009.3011

Loucks, R. R. (1996). A precise olivine-augite Mg-Fe-exehange geothermometer. *Contributions to Mineralogy and Petrology*, *125*(2–3), 140–150. https://doi.org/10.1007/s004100050211

Lynn, K. J., Garcia, M. O., Shea, T., Costa, F., & Swanson, D. A. (2017). Timescales of mixing and storage for Keanakāko'i Tephra magmas (1500–1820 C.E.), Kīlauea Volcano, Hawai'i. *Contributions to Mineralogy and Petrology*, *172*(9). https://doi.org/10.1007/s00410-017-1395-4

Mollo, S., Blundy, J. D., Iezzi, G., Scarlato, P., & Langone, A. (2013). The partitioning of trace elements between clinopyroxene and trachybasaltic melt during rapid cooling and crystal growth. *Contributions to Mineralogy and Petrology*, *166*(6), 1633–1654. https://doi.org/10.1007/s00410-013-0946-6

Mollo, S., Putirka, K., Misiti, V., Soligo, M., & Scarlato, P. (2013). A new test for equilibrium based on clinopyroxene-melt pairs: Clues on the solidification temperatures of Etnean alkaline melts at post-eruptive conditions. *Chemical Geology*, *352*, 92–100. https://doi.org/10.1016/j.chemgeo.2013.05.026

Nimis, P. (1995). A clinopyroxene geobarometer for basaltic systems based on crystal-structure modeling. *Contributions to Mineralogy and Petrology*, *121*(2), 115–125. https://doi.org/10.1007/s004100050093

Panza, G. F., Peccerillo, A., Aoudia, A., & Farina, B. (2007). Geophysical and petrological modelling of the structure and composition of the crust and upper mantle in complex geodynamic settings: The Tyrrhenian Sea and surroundings. *Earth-Science Reviews*, *80*(1–2), 1–46. https://doi.org/10.1016/j.earscirev.2006.08.004

Pontevivo, A., & Panza, G. F. (2006). The lithosphere-asthenosphere system in the Calabrian Arc and surrounding seas - Southern Italy. *Pure and Applied Geophysics*, *163*(8), 1617–1659. https://doi.org/10.1007/s00024-006-0093-3

Putirka, K. D. (2008). Thermometers and Barometers for Volcanic Systems. *Reviews in Mineralogy and Geochemistry*, *69*(1), 61–120. https://doi.org/10.2138/rmg.2008.69.3

Putirka, K., Ryerson, F. J., Perfit, M., & Ridley, W. I. (2011). Mineralogy and composition of the oceanic mantle. *Journal of Petrology*, *52*(2), 279–313. https://doi.org/10.1093/petrology/egq080

Ridolfi, F., Renzulli, A., & Puerini, M. (2010). Stability and chemical equilibrium of amphibole in calc-alkaline magmas: An overview, new thermobarometric formulations and application to subduction-related volcanoes. *Contributions to Mineralogy and Petrology*, *160*(1), 45–66. https://doi.org/10.1007/s00410-009-0465-7

Shea, T., Costa, F., Krimer, D., & Hammer, J. E. (2015). Accuracy of timescales retrieved from

diffusion modeling in olivine: A 3D perspective. *American Mineralogist*, *100*(10), 2026–2042. https://doi.org/10.2138/am-2015-5163

Sobolev, A. V, Hofmann, A. W., Kuzmin, D. V, Yaxley, G. M., Arndt, N. T., Chung, S.-L., … Teklay, M. (2007). The amount of recycled crust in sources of mantle-derived melts. *Science (New York, N.Y.)*, *316*(5823), 412–7. https://doi.org/10.1126/science. 1138113

Sun, S., & Mcdonough, W. F. (1989). Geological Society , London , Special Publications Chemical and isotopic systematics of oceanic basalts : implications for mantle composition and processes Chemical and isotopic systematics of oceanic basalts : implications for mantle composition and proc. https://doi.org/10.1144/GSL.SP.1989.042.01.19

Trua, T., Clocchiatti, R., Schiano, P., Ottolini, L., & Marani, M. (2010). Lithos The heterogeneous nature of the Southern Tyrrhenian mantle : Evidence from olivine-hosted melt inclusions from back-arc magmas of the Marsili seamount. *LITHOS*, *118*(1–2), 1–16. https://doi.org/10.1016/j.lithos.2010.03.008

Trua, T., Marani, M., & Barca, D. (2014). Lower crustal differentiation processes beneath a back-arc spreading ridge (Marsili seamount, Southern Tyrrhenian Sea). *Lithos*, *190–191*, 349–362. https://doi.org/10.1016/j.lithos.2013.12.014

Trua, T., & Marani, M. P. (2011). Magmatic evidence for African mantle propagation into the southern Tyrrhenian backarc region, *2478*(16), 307–331. https://doi.org/10.1130/2011.2478(16).

Trua, T., Marani, M. P., & Gamberi, F. (2018). Magma Plumbing System at a Young Back-Arc Spreading Center: The Marsili Volcano, Southern Tyrrhenian Sea. *Geochemistry, Geophysics, Geosystems*, *19*(1), 43–59. https://doi.org/10.1002/2017GC007151

Trua, T., Serri, G., Marani, M., Renzulli, A., & Gamberi, F. (2002). Volcanological and petrological evolution of Marsili seamount (southern Tyrrhenian Sea). *Journal of Volcanology and Geothermal Research*, *114*(3–4), 441–464. https://doi.org/10.1016/S0377-0273(01)00300-6

Viccaro, M., Giuffrida, M., Nicotra, E., & Cristofolini, R. (2016). Timescales of magma storage and migration recorded by olivine crystals in basalts of the March-April 2010 eruption at Eyjafjallajökull volcano, Iceland. *American Mineralogist*, *101*(1), 222–230. https://doi.org/10.2138/am-2016-5365

Zajacz, Z., & Halter, W. (2007). LA-ICPMS analyses of silicate melt inclusions in co-precipitated minerals: Quantification, data analysis and mineral/melt partitioning. *Geochimica et Cosmochimica Acta*, *71*(4), 1021–1040. https://doi.org/10.1016/j.gca.2006.11.001

Appendix I – Sample MRS1En and MRS1EM

This appendix contains the major element analyses of 13 olivines. The major element compositions were obtained with EPMA and laser ablation. Each table contains the information of a single crystal. The values at the upper part of the tables represent the analyses performed in the core of the crystal and values at the bottom of the tables represent the major element composition of the rim of the crystal.

MRS1En - Ol 1												
name	**Distance (µm)**	**Na_2O**	**MgO**	**Al_2O_3**	**SiO_2**	**CaO**	**TiO_2**	**Cr_2O_3**	**MnO**	**FeO**	**NiO**	**Total**
ol1-1_1	Core - 0	-	45.76	-	39.38	0.23	0.01	0.02	0.17	14.12	0.07	**99.76**
ol1-1_2	10	0.01	45.64	0.02	39.73	0.21	0.01	-	0.22	14.14	0.18	**100.16**
ol1-1_3	20	0.01	45.76	0.03	39.56	0.22	-	0.01	0.20	14.30	0.17	**100.25**
ol1-1_4	30	-	45.49	0.04	39.67	0.22	0.01	0.00	0.22	14.04	0.13	**99.80**
ol1-1_5	40	-	45.57	0.03	39.60	0.22	0.01	-	0.24	13.91	0.17	**99.75**
ol1-1_6	50	0.02	45.33	0.03	39.57	0.21	0.01	0.01	0.19	13.91	0.12	**99.41**
ol1-1_7	60	0.02	45.83	-	39.55	0.20	0.02	0.01	0.23	14.14	0.13	**100.14**
ol1-1_8	70	0.01	45.48	-	39.41	0.22	0.03	0.03	0.22	14.01	0.08	**99.49**
ol1-1_9	80	-	45.53	0.00	39.46	0.20	0.01	0.01	0.23	13.93	0.20	**99.58**
ol1-1_10	90	-	45.63	0.01	39.41	0.21	0.03	0.05	0.20	14.11	0.17	**99.83**
ol1-1_11	100	-	45.54	0.01	39.70	0.23	0.02	0.01	0.23	14.15	0.12	**100.00**
ol1-1_12	110	-	45.51	0.00	39.17	0.22	0.03	0.02	0.18	13.91	0.12	**99.15**
ol1-1_13	120	0.01	45.68	0.01	39.68	0.19	0.02	0.02	0.18	13.99	0.15	**99.92**
ol1-1_14	130	0.00	45.82	0.03	39.40	0.22	0.01	0.02	0.24	14.17	0.13	**100.04**
ol1-1_15	140	0.03	45.64	0.04	39.36	0.21	0.01	0.01	0.22	13.92	0.18	**99.63**
ol1-1_16	150	-	45.52	0.03	39.33	0.25	0.05	0.01	0.24	13.96	0.12	**99.51**
ol1-1_17	160	0.01	45.76	0.03	39.55	0.21	-	0.03	0.19	14.19	0.12	**100.09**
ol1-1_18	170	-	45.63	-	39.37	0.24	0.01	0.01	0.24	14.23	0.12	**99.85**
ol1-1_19	180	0.01	45.68	0.02	39.35	0.20	0.02	0.01	0.23	14.36	0.15	**100.03**
ol1-1_20	190	-	45.51	0.03	39.38	0.23	0.02	0.00	0.17	13.99	0.15	**99.50**
ol1-1_21	200	-	45.87	0.02	39.71	0.20	0.03	0.03	0.24	13.96	0.18	**100.24**
ol1-1_22	210	0.04	45.48	-	39.80	0.23	0.02	0.01	0.23	14.05	0.15	**100.00**
ol1-1_23	220	-	45.60	0.02	39.63	0.23	0.03	0.01	0.21	14.17	0.16	**100.07**
ol1-1_24	230	-	45.74	0.00	39.42	0.25	-	0.01	0.27	14.08	0.14	**99.91**
ol1-1_25	240	0.02	45.65	0.01	39.78	0.22	0.01	-	0.16	13.95	0.15	**99.94**
ol1-1_26	250	-	45.92	0.02	39.29	0.21	0.03	0.01	0.17	14.12	0.17	**99.94**
ol1-1_27	260	-	45.61	0.01	39.67	0.22	0.02	-	0.20	13.97	0.14	**99.83**
ol1-1_28	270	-	45.54	0.01	39.75	0.22	0.01	0.03	0.23	13.95	0.15	**99.88**
ol1-1_29	280	-	45.57	-	39.48	0.19	0.02	-	0.17	13.83	0.17	**99.43**
ol1-1_30	290	-	45.62	0.02	39.47	0.23	0.02	-	0.21	14.17	0.13	**99.88**

Table 1: EPMA analyses of the major element composition of an olivine crystal. The dash symbol (-) represent concentration under the detection limit of the instruments.

MRS1En - Ol 1												
name	**Distance (µm)**	**Na2O**	**MgO**	**Al2O3**	**SiO2**	**CaO**	**TiO2**	**Cr2O3**	**Mno**	**FeO**	**NiO**	**Total**
ol1-1_31	300	0.03	45.51	-	39.61	0.22	0.02	0.00	0.21	14.19	0.14	**99.91**
ol1-1_32	310	0.00	45.45	0.02	39.16	0.27	0.03	0.03	0.24	14.20	0.17	**99.57**
ol1-1_33	320	0.01	45.83	0.04	39.54	0.25	0.02	0.02	0.18	14.32	0.13	**100.34**
ol1-1_34	330	-	45.56	-	39.36	0.24	0.01	0.00	0.17	13.99	0.17	**99.51**
ol1-1_35	340	0.02	45.61	0.01	39.30	0.25	-	-	0.18	14.03	0.15	**99.54**
ol1-1_36	350	0.00	45.74	0.06	39.43	0.23	0.02	0.01	0.22	14.14	0.18	**100.04**
ol1-1_37	360	0.03	45.30	0.01	39.26	0.24	0.03	0.02	0.18	14.12	0.15	**99.33**
ol1-1_38	370	0.02	45.32	0.02	39.18	0.24	0.02	-	0.20	14.11	0.21	**99.32**
ol1-1_39	380	-	45.63	0.04	39.20	0.24	-	0.04	0.21	14.44	0.17	**99.97**
ol1-1_40	390	0.00	45.47	0.02	39.20	0.24	0.03	-	0.23	14.06	0.16	**99.42**
ol1-1_41	400	0.00	45.13	0.03	39.19	0.27	0.01	0.02	0.18	14.31	0.15	**99.29**
ol1-1_42	410	-	45.30	0.01	39.40	0.24	0.02	0.02	0.22	13.95	0.20	**99.34**
ol1-1_43	420	-	45.15	0.01	39.09	0.23	0.02	0.04	0.17	14.33	0.16	**99.20**
ol1-1_44	430	-	45.33	0.02	39.66	0.25	0.00	0.02	0.23	14.35	0.18	**100.04**
ol1-1_45	440	0.01	45.39	0.04	39.22	0.24	0.01	0.02	0.24	14.52	0.20	**99.90**
ol1-1_46	450	-	45.45	0.04	39.23	0.22	0.02	0.00	0.16	14.26	0.17	**99.54**
ol1-1_47	460	-	45.15	0.03	39.23	0.26	0.02	0.01	0.21	14.31	0.14	**99.35**
ol1-1_48	470	0.01	44.70	-	39.35	0.26	0.03	0.05	0.25	14.24	0.20	**99.08**
ol1-1_49	480	-	44.85	0.01	39.09	0.25	0.01	0.01	0.18	14.27	0.18	**98.85**
ol1-1_50	490 - Rim	0.02	44.48	0.04	39.66	0.27	0.02	0.04	0.19	14.96	0.23	**99.90**

Table 1: Continuation.

MRS1En - Ol 2												
Name	**Distance (µm)**	**Na_2O**	**MgO**	**Al_2O_3**	**SiO_2**	**CaO**	**TiO_2**	**Cr_2O_3**	**Mno**	**FeO**	**NiO**	**Total**
ol2-1_1	Core - 0	-	46.06	0.02	40.04	0.26	-	0.02	0.17	13.81	0.26	**100.65**
ol2-1_2	10	-	46.16	-	40.22	0.26	0.01	0.01	0.17	13.48	0.24	**100.54**
ol2-1_3	20	-	46.15	0.01	39.69	0.25	0.03	0.01	0.15	13.54	0.28	**100.11**
ol2-1_4	30	-	46.43	0.01	40.17	0.24	0.01	0.02	0.19	13.64	0.24	**100.95**
ol2-1_5	40	-	46.25	0.02	39.85	0.26	-	0.02	0.20	13.63	0.26	**100.49**
ol2-1_6	50	-	46.03	-	40.15	0.23	0.01	0.01	0.24	13.81	0.24	**100.71**
ol2-1_7	60	-	46.02	0.03	39.66	0.24	-	0.04	0.18	13.40	0.24	**99.80**
ol2-1_8	70	0.01	46.44	0.01	39.95	0.24	-	0.00	0.15	13.50	0.26	**100.57**
ol2-1_9	80	-	46.24	0.01	39.80	0.22	-	0.03	0.17	13.58	0.19	**100.24**
ol2-1_10	90	0.01	46.21	0.01	39.90	0.24	0.01	0.04	0.19	13.30	0.21	**100.14**
ol2-1_11	100	-	46.41	0.02	39.95	0.24	-	0.01	0.25	13.69	0.27	**100.85**
ol2-1_12	110	0.01	46.40	0.04	39.89	0.24	-	0.04	0.14	13.62	0.30	**100.69**
ol2-1_13	120	-	46.20	0.03	40.01	0.26	-	0.01	0.16	13.42	0.26	**100.35**
ol2-1_14	130	0.01	46.30	0.02	39.88	0.28	-	0.03	0.17	13.43	0.26	**100.39**
ol2-1_15	140	0.01	46.45	0.01	39.79	0.29	0.01	0.04	0.20	13.06	0.24	**100.10**

Table 2: The major element composition of an olivine crystal from sample MRS1E. The dash symbol (-) represent concentration under the detection limit of the instruments.

MRS1En - Ol 2												
Name	Distance (µm)	Na_2O	MgO	Al_2O_3	SiO_2	CaO	TiO_2	Cr_2O_3	MnO	FeO	NiO	Total
ol2-1_16	150	-	46.54	-	40.20	0.26	-	0.02	0.23	13.45	0.27	**100.96**
ol2-1_17	160	0.03	46.58	0.01	39.87	0.25	0.02	0.04	0.18	13.40	0.27	**100.67**
ol2-1_18	170	-	46.26	0.06	40.06	0.26	-	0.01	0.17	13.35	0.27	**100.44**
ol2-1_19	180	-	46.61	0.01	39.86	0.28	-	0.04	0.15	13.47	0.30	**100.71**
ol2-1_20	190	0.03	46.60	0.02	40.22	0.28	-	0.05	0.14	13.43	0.27	**101.03**
ol2-1_21	200	0.01	46.51	0.02	39.85	0.28	-	0.02	0.17	13.31	0.27	**100.44**
ol2-1_22	210	0.01	46.54	-	39.92	0.24	-	0.06	0.20	13.27	0.32	**100.57**
ol2-1_23	220	0.04	46.67	0.01	39.97	0.24	0.02	0.02	0.16	13.21	0.22	**100.55**
ol2-1_24	230	-	46.61	0.03	40.13	0.24	-	0.03	0.15	13.65	0.29	**101.13**
ol2-1_25	240	-	46.56	0.03	40.12	0.24	-	0.01	0.16	13.49	0.30	**100.91**
ol2-1_26	250	-	46.48	0.01	40.00	0.23	0.02	0.03	0.21	13.12	0.29	**100.39**
ol2-1_27	260	0.01	46.64	0.01	40.20	0.26	0.01	0.05	0.19	13.38	0.28	**101.02**
ol2-1_28	270	0.03	46.57	0.03	40.20	0.23	-	0.03	0.16	13.15	0.26	**100.65**
ol2-1_29	280	-	46.53	-	40.04	0.27	-	0.01	0.17	13.49	0.27	**100.79**
ol2-1_30	290	0.01	46.60	-	39.58	0.24	-	0.04	0.23	13.40	0.24	**100.34**
ol2-1_31	300	0.01	46.29	0.01	39.86	0.24	0.01	0.03	0.21	13.45	0.25	**100.36**
ol2-1_32	310	-	46.28	-	40.10	0.25	0.01	0.05	0.20	13.14	0.28	**100.30**
ol2-1_33	320	0.01	46.43	0.02	40.00	0.24	-	0.04	0.21	13.30	0.24	**100.48**
ol2-1_34	330	0.01	46.47	0.03	39.91	0.20	-	0.00	0.21	13.09	0.27	**100.19**
ol2-1_35	340	0.01	46.57	-	39.91	0.24	0.02	0.04	0.22	13.44	0.30	**100.75**
ol2-1_36	350	0.01	46.74	0.02	40.18	0.26	0.01	0.05	0.17	13.36	0.28	**101.08**
ol2-1_37	360	0.02	46.47	0.01	39.85	0.25	-	0.03	0.17	13.17	0.25	**100.22**
ol2-1_38	370	0.01	46.40	0.02	39.96	0.27	0.01	0.05	0.20	13.15	0.23	**100.31**
ol2-1_39	380	0.01	46.43	-	39.85	0.24	-	0.05	0.21	13.13	0.26	**100.18**
ol2-1_40	390	0.02	46.49	0.01	40.02	0.23	-	0.00	0.20	13.12	0.28	**100.38**
ol2-1_41	400	-	46.45	0.04	39.94	0.23	0.01	0.01	0.20	13.01	0.31	**100.20**
ol2-1_42	410	-	46.53	0.01	39.76	0.25	0.01	0.04	0.18	13.19	0.30	**100.28**
ol2-1_43	420	-	46.50	-	40.01	0.24	0.02	0.03	0.15	13.36	0.25	**100.57**
ol2-1_44	430	-	46.67	0.02	39.87	0.23	-	0.02	0.22	13.52	0.30	**100.85**
ol2-1_45	440	-	46.51	0.01	39.52	0.25	0.02	0.03	0.11	13.46	0.24	**100.16**
ol2-1_46	450	0.01	46.28	0.04	39.91	0.23	-	0.04	0.20	13.89	0.29	**100.90**
ol2-1_47	460	0.02	46.06	0.01	39.95	0.26	-	0.09	0.21	14.00	0.24	**100.84**
ol2-1_48	470	0.03	45.93	0.05	39.63	0.27	0.02	0.09	0.19	14.18	0.26	**100.64**
ol2-1_49	480	-	45.75	0.02	39.14	0.26	0.02	0.16	0.18	15.00	0.25	**100.77**
ol2-1_50	490 - Rim	0.19	43.03	0.91	38.69	0.56	0.05	0.33	0.24	16.27	0.13	**100.41**

Table 2: Continuation.

MRS1En - Ol 3												
Name	Distance (µm)	Na_2O	MgO	Al_2O_3	SiO_2	CaO	TiO_2	Cr_2O_3	MnO	FeO	NiO	Total
ol3-2_1	Core - 0	-	46.05	0.02	40.28	0.24	-	0.04	0.17	13.16	0.22	**100.18**
ol3-2_2	10	0.03	46.18	0.04	39.70	0.22	0.02	0.02	0.18	13.18	0.25	**99.81**
ol3-2_3	20	-	46.24	0.02	39.92	0.22	0.01	0.01	0.16	13.25	0.25	**100.08**
ol3-2_4	30	0.02	46.00	0.02	39.88	0.21	0.01	0.02	0.18	13.20	0.23	**99.76**
ol3-2_5	40	0.02	46.38	0.03	40.03	0.21	0.01	0.02	0.14	13.28	0.30	**100.43**
ol3-2_6	50	0.01	46.06	-	39.86	0.22	0.01	0.03	0.14	13.45	0.24	**100.01**
ol3-2_7	60	-	46.04	-	39.83	0.23	0.02	0.02	0.15	13.36	0.25	**99.89**
ol3-2_8	70	0.01	46.38	0.02	39.95	0.22	-	0.04	0.16	12.98	0.25	**100.01**
ol3-2_9	80	0.01	46.22	0.01	39.82	0.21	0.02	0.02	0.20	13.07	0.26	**99.84**
ol3-2_10	90	0.01	46.47	0.01	39.77	0.20	0.02	0.03	0.15	13.04	0.32	**100.03**
ol3-2_11	100	-	46.32	0.02	39.92	0.21	-	0.02	0.13	13.45	0.27	**100.35**
ol3-2_12	110	0.04	46.13	-	39.66	0.21	0.01	-	0.16	13.08	0.22	**99.52**
ol3-2_13	120	-	46.31	0.01	39.78	0.23	-	0.02	0.16	13.37	0.25	**100.14**
ol3-2_14	130	-	46.22	0.05	39.98	0.23	0.01	0.02	0.21	13.06	0.24	**100.02**
ol3-2_15	140	-	46.38	0.04	39.84	0.23	0.01	0.02	0.17	13.17	0.25	**100.10**
ol3-2_16	150	0.04	46.41	0.02	39.80	0.22	0.02	-	0.18	13.15	0.24	**100.08**
ol3-2_17	160	0.03	46.33	0.02	39.80	0.22	0.01	0.04	0.16	13.36	0.23	**100.20**
ol3-2_18	170	-	46.24	-	39.83	0.24	0.01	0.03	0.21	13.23	0.25	**100.06**
ol3-2_19	180	-	46.19	0.02	39.72	0.20	-	0.02	0.19	13.27	0.23	**99.85**
ol3-2_20	190	0.01	46.33	0.02	39.90	0.23	-	0.05	0.17	13.10	0.26	**100.08**
ol3-2_21	200	0.04	46.19	0.02	39.87	0.21	0.01	0.06	0.19	13.34	0.20	**100.12**
ol3-2_22	210	-	46.25	0.02	39.84	0.24	0.01	0.03	0.12	12.72	0.24	**99.48**
ol3-2_23	220	-	46.46	0.02	39.99	0.22	0.01	0.02	0.10	13.35	0.25	**100.41**
ol3-2_24	230	-	46.13	-	39.90	0.23	0.01	0.04	0.18	12.97	0.25	**99.71**
ol3-2_25	240	-	46.30	-	39.97	0.21	-	0.00	0.17	12.89	0.26	**99.81**
ol3-2_26	250	-	46.12	0.01	39.66	0.21	0.02	0.02	0.20	13.50	0.26	**99.99**
ol3-2_27	260	-	46.29	0.02	39.87	0.21	-	0.03	0.24	13.19	0.24	**100.09**
ol3-2_28	270	-	46.46	0.03	39.95	0.23	-	0.05	0.18	13.09	0.29	**100.27**
ol3-2_29	280	0.01	46.27	0.04	40.01	0.23	-	0.02	0.17	12.93	0.27	**99.96**
ol3-2_30	290	0.02	46.23	0.02	39.88	0.23	0.01	0.03	0.16	13.20	0.30	**100.06**
ol3-2_31	300	-	45.96	-	39.87	0.22	-	0.03	0.16	12.99	0.26	**99.50**
ol3-2_32	310	0.01	46.32	0.01	40.02	0.23	-	0.03	0.14	13.60	0.23	**100.59**
ol3-2_33	320	0.01	46.46	0.01	39.92	0.24	-	0.01	0.21	13.23	0.28	**100.39**
ol3-2_34	330	-	46.37	0.02	39.98	0.21	-	0.01	0.13	13.32	0.22	**100.27**
ol3-2_35	340	-	46.27	0.02	40.04	0.25	0.02	0.03	0.16	12.95	0.23	**99.95**
ol3-2_36	350	-	46.27	0.04	40.03	0.24	0.03	0.02	0.16	13.20	0.27	**100.25**
ol3-2_37	360	-	46.33	0.01	39.88	0.25	-	0.04	0.16	13.29	0.26	**100.23**
ol3-2_38	370	0.01	46.23	-	39.82	0.24	-	0.02	0.18	13.13	0.24	**99.86**
ol3-2_39	380	0.01	46.10	0.02	39.96	0.25	-	0.04	0.17	13.23	0.30	**100.10**

Table 3: EPMA analyses of the major element composition of an olivine crystal. The dash symbol (-) represent concentration under the detection limit of the instruments.

MRS1En - Ol 3												
Name	Distance (µm)	Na_2O	MgO	Al_2O_3	SiO_2	CaO	TiO_2	Cr_2O_3	MnO	FeO	NiO	Total
ol3-2_40	390	-	46.36	0.04	39.96	0.18	-	0.02	0.14	13.20	0.29	**100.20**
ol3-2_41	400	0.01	46.18	-	40.09	0.24	-	0.06	0.22	13.25	0.27	**100.33**
ol3-2_42	410	0.01	46.25	0.01	40.08	0.23	0.01	0.05	0.17	13.39	0.28	**100.49**
ol3-2_43	420	-	46.43	0.01	39.96	0.22	0.02	0.02	0.15	13.35	0.27	**100.42**
ol3-2_44	430	-	46.19	0.05	39.83	0.24	-	0.01	0.17	13.37	0.30	**100.15**
ol3-2_45	440	-	46.04	0.04	39.98	0.23	-	0.02	0.15	13.43	0.26	**100.15**
ol3-2_46	450	-	46.20	0.02	39.87	0.25	0.01	0.01	0.17	13.44	0.24	**100.22**
ol3-2_47	460	0.02	46.10	0.03	40.06	0.23	0.02	0.04	0.20	13.64	0.27	**100.59**
ol3-2_48	470	-	45.94	0.04	40.01	0.23	0.01	0.02	0.16	13.47	0.25	**100.12**
ol3-2_49	480	-	46.18	0.01	39.74	0.24	-	0.03	0.21	13.41	0.31	**100.12**
ol3-2_50	490	-	46.07	0.02	39.96	0.24	0.02	0.01	0.16	13.29	0.24	**100.01**
ol3-2_51	500	-	45.98	0.05	39.90	0.25	0.02	0.05	0.21	13.46	0.24	**100.16**
ol3-2_52	510	0.01	46.14	0.02	39.78	0.20	-	0.06	0.21	13.71	0.24	**100.37**
ol3-2_53	520	-	45.99	0.04	40.02	0.24	0.02	0.03	0.21	13.64	0.29	**100.48**
ol3-2_54	530	-	45.88	-	39.90	0.24	-	0.07	0.23	13.83	0.26	**100.42**
ol3-2_55	540	-	46.09	0.03	39.72	0.23	0.01	0.05	0.25	13.61	0.24	**100.23**
ol3-2_56	550	-	45.95	0.07	39.42	0.23	-	0.07	0.20	13.64	0.28	**99.84**
ol3-2_57	560	-	45.92	0.04	39.97	0.23	0.01	-	0.16	13.87	0.24	**100.45**
ol3-2_58	570	-	45.67	0.03	39.62	0.28	0.01	0.06	0.20	13.80	0.27	**99.93**
ol3-2_59	590 - Rim	-	45.48	0.06	39.40	0.27	0.02	0.05	0.21	14.80	0.24	**100.53**

Table 3: Continuation.

MRS1En - Ol 4												
Name	Distance (µm)	Na_2O	MgO	Al_2O_3	SiO_2	CaO	TiO_2	Cr_2O_3	MnO	FeO	NiO	Total
ol4-1_1	Core - 0	0.06	44.89	0.01	39.51	0.27	0.02	0.01	0.21	14.57	0.23	**99.78**
ol4-1_2	10	0.02	45.09	0.01	39.41	0.24	0.02	-	0.24	14.49	0.17	**99.68**
ol4-1_3	20	0.02	44.96	0.02	39.63	0.24	0.01	-	0.22	14.41	0.20	**99.71**
ol4-1_4	30	-	44.72	0.05	39.48	0.23	0.01	0.03	0.21	14.57	0.23	**99.55**
ol4-1_5	50	0.01	44.88	0.03	39.54	0.24	0.02	0.02	0.22	14.47	0.21	**99.66**
ol4-1_6	60	0.02	44.88	0.04	39.62	0.27	0.02	0.03	0.19	14.65	0.17	**99.86**
ol4-1_7	70	0.05	45.07	0.02	39.52	0.25	0.01	0.05	0.22	14.49	0.24	**99.91**
ol4-1_8	80	0.01	44.88	0.04	39.48	0.26	-	-	0.24	14.83	0.21	**99.95**
ol4-1_9	90	0.02	44.76	0.02	39.57	0.28	0.01	0.02	0.19	14.71	0.20	**99.78**
ol4-1_10	100	-	44.86	0.02	39.56	0.26	0.01	0.03	0.18	14.80	0.27	**99.99**
ol4-1_11	110	0.00	44.82	0.04	39.53	0.26	0.02	0.01	0.28	14.72	0.22	**99.88**
ol4-1_12	120	0.02	44.78	0.01	39.58	0.26	0.01	0.01	0.16	14.60	0.21	**99.64**
ol4-1_13	130	-	44.78	0.02	39.30	0.27	0.00	0.04	0.19	14.56	0.16	**99.33**
ol4-1_14	140	0.04	44.80	0.03	39.40	0.26	0.00	0.03	0.23	14.44	0.20	**99.42**

Table 4: EPMA analyses of the major element composition of an olivine crystal. The dash symbol (-) represent concentration under the detection limit of the instruments.

MRS1En - Ol 4												
Name	Distance (µm)	Na_2O	MgO	Al_2O_3	SiO_2	CaO	TiO_2	Cr_2O_3	MnO	FeO	NiO	Total
ol4-1_15	150	-	44.91	0.01	39.47	0.25	0.00	0.03	0.20	14.72	0.19	**99.79**
ol4-1_16	160	0.04	44.80	0.02	39.47	0.28	0.03	0.02	0.22	14.49	0.20	**99.56**
ol4-1_17	170	0.01	44.85	0.02	39.63	0.25	0.01	0.05	0.27	14.75	0.13	**99.97**
ol4-1_18	180	-	44.76	0.01	39.62	0.26	-	0.01	0.18	14.61	0.22	**99.69**
ol4-1_19	190	0.01	44.78	0.04	39.33	0.26	-	0.01	0.20	14.59	0.22	**99.43**
ol4-1_20	200	0.01	45.23	0.03	39.58	0.26	0.02	-	0.22	14.99	0.22	**100.56**
ol4-1_21	210	-	44.94	0.01	39.29	0.24	0.00	0.07	0.23	14.89	0.17	**99.84**
ol4-1_22	220	0.01	44.83	0.05	39.56	0.26	0.04	0.03	0.24	14.64	0.22	**99.89**
ol4-1_23	230	0.02	45.01	0.04	39.38	0.26	0.03	0.02	0.20	14.70	0.19	**99.86**
ol4-1_24	240	-	45.05	0.03	39.48	0.24	0.01	0.04	0.20	14.84	0.17	**100.06**
ol4-1_25	250	0.01	44.72	0.01	39.25	0.26	0.02	0.01	0.21	14.74	0.21	**99.44**
ol4-1_26	260	0.03	44.91	0.06	39.38	0.24	0.00	0.03	0.17	14.59	0.21	**99.62**
ol4-1_27	270	0.00	44.94	0.02	39.20	0.26	0.01	0.04	0.19	14.74	0.16	**99.56**
ol4-1_28	280	-	45.20	0.05	39.64	0.26	0.01	0.05	0.18	14.77	0.22	**100.37**
ol4-1_29	290	0.02	44.82	0.01	39.60	0.24	0.01	0.03	0.24	14.38	0.22	**99.59**
ol4-1_30	300	0.01	44.77	0.04	39.22	0.25	0.01	0.02	0.19	14.45	0.24	**99.19**
ol4-1_31	310	-	45.15	0.01	39.45	0.26	0.01	0.04	0.25	14.48	0.25	**99.91**
ol4-1_32	320	0.03	45.09	0.00	39.34	0.23	-	0.04	0.21	14.31	0.20	**99.45**
ol4-1_33	330	0.01	44.92	0.03	39.47	0.24	0.05	0.02	0.18	14.32	0.14	**99.38**
ol4-1_34	340	-	45.02	0.01	39.44	0.25	0.01	0.01	0.22	14.59	0.18	**99.72**
ol4-1_35	350	0.01	45.30	0.05	39.63	0.26	0.01	0.02	0.21	14.45	0.23	**100.16**
ol4-1_36	360	0.02	44.90	0.01	39.45	0.24	0.01	-	0.20	14.21	0.26	**99.31**
ol4-1_37	370	0.02	45.24	0.00	39.38	0.26	0.00	0.02	0.20	14.34	0.20	**99.67**
ol4-1_38	380	-	44.79	0.02	39.22	0.24	0.01	0.03	0.19	14.90	0.19	**99.59**
ol4-1_39	390	0.02	44.63	0.02	39.12	0.25	0.00	0.04	0.23	14.90	0.20	**99.41**

Table 4: Continuation.

MRS1EM - Ol 4									
Name	Distance (µm)	MgO	Al_2O_3	SiO_2	CaO	MnO	FeO	NiO	Total
ol4-2	Core - 0	44.5114	0.0279	39.6059	0.2628	0.2183	14.8495	0.2151	**99.69**
ol4-3	63.98	44.88	0.03	39.52	0.28	0.23	15.02	0.22	**100.17**
ol4-4	113.02	44.83	-	39.68	0.26	0.26	14.98	0.21	**100.22**
ol4-5	163.50	45.05	0.04	39.59	0.28	0.20	14.97	0.23	**100.37**
ol4-6	199.01	44.86	0.02	39.91	0.26	0.23	14.66	0.21	**100.15**
ol4-7	238.63	45.04	0.02	39.43	0.25	0.26	15.13	0.21	**100.33**
ol4-8	269.50	44.89	0.03	39.69	0.25	0.20	15.21	0.23	**100.50**
ol4-9	301.70	44.75	0.01	39.75	0.28	0.25	15.30	0.17	**100.51**
ol4-10	331.72 - Rim	46.99	0.03	38.06	0.25	0.22	15.25	0.21	**101.01**

Table 5: The major element composition of an olivine crystal from sample MRS1EM. The dash symbol (-) represent concentration under the detection limit of the instruments.

MRS1EM - Ol 7									
Name	**Distance (µm)**	**MgO**	**Al_2O_3**	**SiO_2**	**CaO**	**MnO**	**FeO**	**NiO**	**Total**
ol7-1_1	Core - 0	45.52	0.03	39.72	0.23	0.24	14.62	0.22	**100.57**
ol7-1_2	8.06	45.37	0.03	39.91	0.25	0.15	14.39	0.27	**100.36**
ol7-1_3	16.61	45.27	0.01	40.07	0.26	0.18	14.60	0.26	**100.65**
ol7-1_4	24.67	45.22	0.03	39.77	0.26	0.21	14.29	0.21	**99.99**
ol7-1_5	33.61	45.44	0.04	39.92	0.27	0.25	14.77	0.20	**100.90**
ol7-1_6	41.23	45.58	0.03	40.19	0.25	0.18	14.72	0.24	**101.18**
ol7-1_7	50.17	45.46	0.02	39.94	0.24	0.15	14.75	0.20	**100.77**
ol7-1_8	58.24	45.25	0.04	40.05	0.26	0.22	14.46	0.25	**100.53**
ol7-1_9	67.18	45.15	0.03	40.06	0.24	0.21	14.67	0.22	**100.57**
ol7-1_10	74.80	45.15	0.06	40.14	0.23	0.19	14.53	0.20	**100.51**
ol7-1_11	83.74	45.24	0.04	39.85	0.24	0.15	14.81	0.20	**100.54**
ol7-1_12	91.80	45.15	0.02	40.02	0.27	0.19	14.58	0.21	**100.44**
ol7-1_13	100.35	45.18	0.02	39.74	0.26	0.23	14.86	0.23	**100.52**
ol7-1_14	108.41	44.98	0.02	39.87	0.24	0.20	14.64	0.27	**100.23**
ol7-1_15	117.35	44.81	0.03	39.80	0.25	0.20	14.86	0.23	**100.18**
ol7-1_16	124.97	44.81	0.03	39.92	0.22	0.21	14.89	0.22	**100.31**
ol7-1_17	133.91	45.22	0.03	39.77	0.23	0.16	14.90	0.21	**100.53**
ol7-1_18	141.97	45.00	0.02	40.05	0.23	0.20	14.86	0.22	**100.58**
ol7-1_19	150.52	44.91	0.03	39.96	0.24	0.24	14.74	0.22	**100.34**
ol7-1_20	158.58	44.91	0.02	40.12	0.26	0.22	14.84	0.21	**100.58**
ol7-1_21	167.53	44.92	0.05	39.55	0.27	0.17	14.88	0.20	**100.03**
ol7-1_22	175.14	45.26	0.03	39.89	0.25	0.20	14.81	0.16	**100.61**
ol7-1_23	184.09	45.06	0.03	39.79	0.26	0.25	14.82	0.22	**100.43**
ol7-1_24	192.15	45.09	0.04	40.04	0.25	0.21	15.01	0.23	**100.87**
ol7-1_25	201.09	44.78	0.03	39.88	0.25	0.21	14.90	0.19	**100.24**
ol7-1_26	208.71	44.94	0.01	39.53	0.25	0.22	15.05	0.20	**100.20**
ol7-1_27	217.65	44.62	0.03	40.05	0.29	0.24	15.04	0.18	**100.43**
ol7-1_28	225.71	44.76	0.04	39.83	0.24	0.21	15.55	0.20	**100.82**
ol7-1_29	234.26	44.64	0.06	40.07	0.25	0.20	15.20	0.19	**100.62**
ol7-1_30	242.32 -Rim	44.90	0.00	39.79	0.27	0.22	15.45	0.20	**100.83**

Table 6: EPMA analyses of the major element composition of an olivine crystal

MRS1EM - Ol 8									
Name	**Distance (µm)**	**MgO**	**Al_2O_3**	**SiO_2**	**CaO**	**MnO**	**FeO**	**NiO**	**Total**
ol8-2_1	Core - 0	46.09	0.03	40.21	0.21	0.19	13.98	0.27	**100.98**
ol8-2_2	5.39	46.05	0.06	40.11	0.22	0.21	13.75	0.29	**100.69**
ol8-2_3	11.71	46.04	0.04	39.89	0.23	0.24	13.95	0.22	**100.61**
ol8-2_4	17.09	45.96	-	39.68	0.23	0.15	13.71	0.22	**99.95**
ol8-2_5	22.48	45.79	0.02	40.02	0.25	0.19	13.82	0.25	**100.33**
ol8-2_6	28.80	45.79	0.03	40.20	0.25	0.14	14.10	0.25	**100.77**
ol8-2_7	34.19	45.68	-	40.01	0.23	0.20	14.32	0.25	**100.71**
ol8-2_8	40.51	46.03	0.03	40.21	0.25	0.25	14.10	0.27	**101.15**
ol8-2_9	45.90	45.80	0.02	40.07	0.24	0.18	13.97	0.24	**100.51**
ol8-2_10	51.28	46.00	0.05	39.61	0.27	0.23	14.26	0.22	**100.63**
ol8-2_11	57.99	45.61	0.04	40.06	0.22	0.16	14.19	0.25	**100.53**
ol8-2_12	63.38	45.62	0.03	40.08	0.22	0.22	14.24	0.28	**100.68**
ol8-2_13	68.76	45.64	0.04	40.10	0.23	0.22	13.97	0.25	**100.46**
ol8-2_14	75.09	45.65	0.04	39.91	0.25	0.16	14.11	0.24	**100.36**
ol8-2_15	80.47	45.75	0.02	40.03	0.23	0.18	14.34	0.25	**100.81**
ol8-2_16	86.80	45.40	0.02	39.95	0.26	0.19	14.47	0.23	**100.51**
ol8-2_17	92.18	44.94	0.02	39.83	0.26	0.25	14.54	0.20	**100.04**
ol8-2_18	97.57	44.98	0.01	39.93	0.29	0.23	14.79	0.17	**100.40**
ol8-2_19	103.89 -Rim	44.63	0.02	39.98	0.31	0.23	15.69	0.16	**101.04**

Table 7: The major element composition of an olivine crystal from sample MRS1EM. The dash symbol (-) represent concentration under the detection limit of the instruments.

MRS1EM - Ol 9									
Name	**Distance (µm)**	**MgO**	**Al_2O_3**	**SiO_2**	**CaO**	**MnO**	**FeO**	**NiO**	**Total**
ol9-1	Core - 0	45.99	0.02	40.50	0.26	0.15	13.54	0.27	**100.73**
ol9-2	13.42	45.77	0.03	39.67	0.30	0.22	13.34	0.19	**99.51**
ol9-3	27.34	45.82	0.02	40.16	0.25	0.18	13.45	0.23	**100.10**
ol9-4	35.41	45.97	0.01	39.91	0.28	0.21	13.59	0.26	**100.22**
ol9-5	48.21	45.85	0.04	40.41	0.25	0.18	13.41	0.26	**100.39**
ol9-6	58.65	45.97	0.03	40.32	0.27	0.15	13.44	0.25	**100.43**
ol9-7	67.71	46.12	0.03	40.04	0.27	0.15	13.51	0.24	**100.36**
ol9-8	76.71	46.00	0.02	40.00	0.26	0.22	13.56	0.25	**100.31**
ol9-9	83.03	46.02	0.00	40.15	0.26	0.20	13.24	0.24	**100.11**
ol9-10	89.03	46.17	0.04	40.08	0.27	0.22	13.35	0.29	**100.42**
ol9-11	99.47	46.00	0.03	40.27	0.28	0.15	13.48	0.25	**100.47**
ol9-12	112.20	46.11	0.03	40.28	0.27	0.21	13.41	0.26	**100.58**
ol9-13	120.75	45.97	0.02	39.87	0.26	0.18	13.46	0.23	**99.98**
ol9-14	127.96	46.06	0.02	40.06	0.26	0.22	13.38	0.26	**100.25**
ol9-15	138.77	46.06	0.03	39.96	0.25	0.20	13.40	0.23	**100.13**
ol9-16	177.40	46.19	0.02	39.89	0.30	0.18	13.48	0.26	**100.32**
ol9-17	195.78	46.17	0.03	40.04	0.27	0.20	13.63	0.25	**100.59**
ol9-18	209.24	45.79	0.08	40.10	0.24	0.20	13.31	0.28	**100.00**
ol9-19	220.55	45.82	0.04	40.02	0.26	0.15	13.63	0.24	**100.16**
ol9-20	230.55	46.01	0.02	39.99	0.30	0.18	13.62	0.24	**100.36**

Table 8: EPMA analyses of the major element composition of an olivine crystal

MRS1EM - Ol 9									
Name	**Distance (µm)**	**MgO**	**Al_2O_3**	**SiO_2**	**CaO**	**MnO**	**FeO**	**NiO**	**Total**
ol9-21	248.04	46.11	0.05	40.06	0.26	0.20	13.48	0.29	**100.46**
ol9-22	257.48	46.03	0.04	40.04	0.26	0.20	13.63	0.26	**100.46**
ol9-23	269.52	45.92	0.04	39.69	0.22	0.21	13.58	0.28	**99.95**
ol9-24	276.52	45.60	0.03	39.90	0.29	0.20	13.32	0.24	**99.58**
ol9-25	285.74	46.90	0.02	39.84	0.29	0.19	13.68	0.23	**101.14**
ol9-26	295.74	46.11	0.01	39.90	0.26	0.17	13.56	0.26	**100.28**
ol9-27	304.74	45.83	0.03	39.95	0.26	0.23	13.45	0.24	**99.99**
ol9-28	315.92	45.96	0.04	39.94	0.26	0.18	13.21	0.24	**99.84**
ol9-29	324.17	45.81	0.04	40.28	0.26	0.16	13.45	0.26	**100.26**
ol9-30	341.17	45.95	0.02	40.18	0.25	0.15	13.60	0.27	**100.41**
ol9-31	351.98	46.00	0.02	40.31	0.28	0.22	13.72	0.23	**100.78**
ol9-32	360.23	46.32	0.07	40.01	0.26	0.14	13.90	0.30	**101.00**
ol9-33	366.23	46.23	0.06	39.91	0.25	0.19	13.66	0.26	**100.55**
ol9-34	378.44	46.14	0.05	40.21	0.26	0.19	13.62	0.24	**100.70**
ol9-35	393.67	46.12	0.04	40.13	0.22	0.18	13.86	0.31	**100.84**
ol9-36	403.67	45.66	0.01	39.94	0.27	0.19	13.78	0.22	**100.06**
ol9-37	413.96	46.03	0.03	40.28	0.23	0.19	14.08	0.24	**101.08**
ol9-38	434.58	45.96	0.02	39.90	0.25	0.26	14.02	0.22	**100.62**
ol9-39	445.40	45.56	0.02	40.15	0.25	0.14	13.76	0.24	**100.12**
ol9-40	456.03	45.54	0.04	39.93	0.29	0.19	13.79	0.27	**100.03**
ol9-41	465.46	45.65	0.01	40.23	0.24	0.18	14.19	0.28	**100.78**
ol9-42	472.46	45.63	0.01	40.04	0.24	0.17	13.97	0.20	**100.25**
ol9-43	483.46	45.71	0.05	39.98	0.21	0.18	13.85	0.26	**100.24**
ol9-44	497.06	45.72	0.02	39.95	0.22	0.24	13.68	0.24	**100.07**
ol9-45	510.06	45.22	0.05	40.00	0.22	99.97	14.02	0.25	**99.97**
ol9-46	517.34	45.39	0.05	39.65	0.23	0.16	14.30	0.21	**99.99**
ol9-47	531.55	45.19	0.03	39.89	0.25	0.19	14.29	0.20	**100.04**
ol9-48	545.77	45.40	0.02	39.54	0.25	0.21	14.26	0.24	**99.93**
ol9-49	555.77	45.01	0.05	39.83	0.26	0.21	14.56	0.22	**100.12**
ol9-50	563.77	45.20	0.05	39.86	0.28	0.22	14.45	0.21	**100.26**
ol9-51	573.77	45.19	0.03	39.86	0.22	0.22	14.90	0.20	**100.62**
ol9-52	583.77	45.09	0.03	39.14	0.26	0.18	14.80	0.20	**99.70**

Table 8: Continuation.

Appendix II – Sample MRS2A

This appendix contains the major element analyses of 4 olivines and 2 pyroxenes.

MRS2A - Ol 1												
Name	**Distance (µm)**	**Na_2O**	**MgO**	**Al_2O_3**	**SiO_2**	**CaO**	**TiO_2**	**Cr_2O_3**	**MnO**	**FeO**	**NiO**	**Total**
ol1_1	Core - 0	0.01	47.84	-	40.48	0.22	0.00	0.00	0.19	11.38	0.17	**100.29**
ol1_2	24.08	0.01	47.80	-	40.00	0.21	-	-	0.21	11.24	0.18	**99.64**
ol1_3	48.17	0.01	47.88	-	40.00	0.23	0.01	-	0.17	11.27	0.18	**99.74**
ol1_4	71.36	0.01	47.94	0.02	40.31	0.25	-	0.03	0.17	11.35	0.24	**100.31**
ol1_5	95.44	-	47.91	0.00	40.07	0.27	0.01	-	0.22	11.55	0.19	**100.22**
ol1_6	119.53	0.01	48.15	0.01	40.34	0.24	-	0.04	0.14	11.48	0.17	**100.58**
ol1_7	143.61	-	47.87	-	40.27	0.26	-	0.01	0.18	11.20	0.17	**99.95**
ol1_8	166.81	-	47.76	-	40.27	0.25	0.01	-	0.17	11.35	0.18	**99.98**
ol1_9	190.89	0.00	47.89	0.02	40.42	0.26	0.01	0.03	0.20	11.11	0.19	**100.13**
ol1_10	214.97	-	47.91	0.03	40.28	0.28	0.01	0.01	0.15	11.33	0.11	**100.10**

Table 9: The major element composition of an olivine crystal from sample MRS2A. The dash symbol (-) represent concentration under the detection limit of the instruments.

MRS2A - Ol 2									
Name	Distance (µm)	MgO	Al_2O_3	SiO_2	CaO	MnO	FeO	NiO	Total
ol-2_1	Core - 0	48.42	0.01	40.52	0.23	0.16	10.63	0.22	**100.21**
ol-2_2	12	48.62	0.01	40.47	0.21	0.20	10.66	0.21	**100.39**
ol-2_3	24	48.61	-	40.59	0.21	0.19	10.49	0.18	**100.27**
ol-2_4	36	48.96	0.03	40.75	0.23	0.12	10.64	0.24	**100.96**
ol-2_5	48	48.66	0.02	40.64	0.25	0.14	10.59	0.28	**100.59**
ol-2_6	60	48.81	0.01	40.25	0.24	0.14	10.51	0.26	**100.21**
ol-2_7	72	48.24	0.04	40.66	0.22	0.13	10.27	0.22	**99.78**
ol-2_8	84	48.72	0.04	40.73	0.23	0.18	10.48	0.21	**100.60**
ol-2_9	96	48.61	0.06	40.58	0.25	0.20	10.40	0.23	**100.32**
ol-2_10	108	48.56	0.03	40.51	0.26	0.14	10.44	0.22	**100.17**
ol-2_11	120	48.88	0.005	40.74	0.23	0.18	10.51	0.23	**100.79**
ol-2_12	132	48.75	0.004	40.89	0.21	0.20	10.48	0.19	**100.73**
ol-2_13	144	48.70	0.03	40.51	0.20	0.14	10.48	0.20	**100.25**
ol-2_14	156	48.78	0.02	40.50	0.23	0.17	10.41	0.22	**100.33**
ol-2_15	168	48.72	0.03	40.58	0.25	0.15	10.28	0.22	**100.22**
ol-2_16	180	48.73	0.01	40.59	0.21	0.16	10.40	0.21	**100.31**
ol-2_17	192	48.99	0.02	40.65	0.24	0.15	10.40	0.24	**100.70**
ol-2_18	204	49.05	0.01	40.69	0.24	0.21	10.52	0.24	**100.97**
ol-2_19	216	48.69	-	40.54	0.24	0.20	10.32	0.21	**100.20**
ol-2_20	228	48.71	0.04	40.52	0.24	0.19	10.12	0.25	**100.06**
ol-2_21	240	48.87	0.01	40.71	0.27	0.08	10.27	0.22	**100.43**
ol-2_22	252	48.86	0.03	40.91	0.22	0.22	10.29	0.26	**100.79**
ol-2_23	264	48.91	0.04	40.65	0.24	0.16	10.08	0.23	**100.30**
ol-2_24	276	48.83	0.02	40.55	0.23	0.17	10.21	0.25	**100.26**
ol-2_25	288	49.03	0.02	40.62	0.24	0.15	10.44	0.26	**100.77**
ol-2_26	300	48.93	0.03	40.48	0.23	0.16	10.06	0.25	**100.13**
ol-2_27	312	48.88	-	40.61	0.23	0.16	10.00	0.23	**100.12**
ol-2_28	324	49.00	0.001	39.46	0.26	0.16	10.15	0.18	**99.22**
ol-2_29	336	49.03	0.01	40.72	0.21	0.18	10.12	0.27	**100.54**
ol-2_30	348	48.99	0.03	40.52	0.25	0.15	9.99	0.26	**100.18**
ol-2_31	360	48.97	0.01	40.39	0.25	0.15	10.20	0.21	**100.18**
ol-2_32	372	48.93	0.003	40.47	0.24	0.21	10.32	0.29	**100.46**
ol-2_33	384	49.13	0.03	40.64	0.20	0.19	10.22	0.21	**100.63**
ol-2_34	396	48.90	0.02	40.55	0.21	0.18	10.12	0.25	**100.23**
ol-2_35	408	49.20	0.03	40.60	0.25	0.13	10.22	0.16	**100.59**
ol-2_36	420	48.92	0.003	40.58	0.23	0.22	10.03	0.22	**100.21**
ol-2_37	432	48.85	0.03	40.65	0.24	0.20	10.18	0.25	**100.41**
ol-2_38	444	48.64	0.03	40.50	0.24	0.15	10.26	0.17	**100.00**
ol-2_39	456 - Rim	48.68	0.01	40.42	0.28	0.21	10.45	0.22	**100.27**

Table 10: EPMA analyses of the major element composition of an olivine crystal. The dash symbol (-) represent concentration under the detection limit of the instruments.

MRS2A - Ol 3												
Name	Distance (µm)	Na_2O	MgO	Al_2O_3	SiO_2	CaO	TiO_2	Cr_2O_3	MnO	FeO	NiO	Total
ol3-1_1	Core - 0	-	48.87	0.03	40.39	0.22	0.007	0.013	0.14	10.25	0.24	**100.17**
ol3-1_2	10	-	48.73	0.01	40.59	0.28	0.006	0.031	0.15	10.07	0.21	**100.08**
ol3-1_3	20	-	49.12	0.03	40.47	0.25	0.009	0.024	0.15	10.30	0.24	**100.58**
ol3-1_4	30	-	49.08	0.04	40.36	0.22	0.021	0.043	0.17	10.36	0.25	**100.53**
ol3-1_5	40	-	49.03	0.03	40.43	0.22	0.015	0.015	0.18	10.33	0.18	**100.42**
ol3-1_6	50	-	48.73	0.02	40.74	0.24	-	0.059	0.14	10.24	0.20	**100.36**
ol3-1_7	60	-	48.56	0.02	40.37	0.25	0.025	0.053	0.17	10.04	0.25	**99.72**
ol3-1_8	70	0.008	48.62	0.02	40.76	0.23	0.014	0.050	0.15	10.21	0.26	**100.33**
ol3-1_9	80	-	48.91	0.02	40.38	0.22	0.025	0.005	0.15	10.16	0.16	**100.03**
ol3-1_10	90	0.001	48.71	0.03	40.49	0.22	0.004	0.011	0.16	10.22	0.22	**100.08**
ol3-1_11	100	-	48.83	0.01	40.45	0.26	0.014	0.001	0.17	10.19	0.20	**100.13**
ol3-1_12	110	-	49.02	0.03	40.56	0.23	0.004	0.037	0.18	10.26	0.22	**100.54**
ol3-1_13	120	0.029	48.62	-	40.66	0.23	0.016	0.051	0.16	10.18	0.31	**100.26**
ol3-1_14	130	-	48.52	0.03	40.36	0.24	-	0.021	0.15	10.02	0.26	**99.59**
ol3-1_15	140	0.015	48.81	0.02	40.53	0.25	-	0.038	0.16	10.28	0.23	**100.34**
ol3-1_16	150	-	48.70	0.03	40.39	0.23	0.018	0.013	0.17	10.11	0.24	**99.91**
ol3-1_17	160	-	48.74	0.01	40.45	0.22	0.003	0.050	0.11	10.31	0.23	**100.13**
ol3-1_18	170	-	48.49	0.03	40.40	0.21	0.019	0.043	0.19	10.01	0.20	**99.59**
ol3-1_19	180	-	48.62	0.03	40.27	0.24	0.010	-	0.14	10.31	0.24	**99.85**
ol3-1_20	190	0.002	48.70	0.02	40.36	0.21	0.008	0.048	0.18	10.01	0.23	**99.77**
ol3-1_21	200	-	48.57	0.03	40.57	0.21	0.017	0.002	0.16	10.11	0.18	**99.84**
ol3-1_22	210	-	48.81	0.02	40.57	0.23	0.015	0.037	0.22	10.08	0.21	**100.19**
ol3-1_23	220	-	48.80	0.01	40.64	0.24	-	0.028	0.16	10.35	0.25	**100.49**
ol3-1_24	230	0.008	48.57	0.05	40.26	0.24	0.005	0.004	0.20	10.09	0.23	**99.66**
ol3-1_25	240	-	48.46	0.02	40.47	0.23	0.024	0.001	0.18	10.18	0.19	**99.76**
ol3-1_26	250	-	48.63	0.04	40.65	0.24	0.004	0.033	0.17	10.16	0.26	**100.17**
ol3-1_27	260	0.022	48.68	0.03	40.35	0.26	0.007	0.026	0.16	10.15	0.21	**99.91**
ol3-1_28	270	0.002	48.83	-	40.48	0.24	-	-	0.12	10.15	0.20	**100.03**
ol3-1_29	280	-	48.52	0.03	40.45	0.25	0.001	0.025	0.20	10.11	0.24	**99.84**
ol3-1_30	290	-	48.73	0.04	40.50	0.24	-	0.013	0.18	9.97	0.21	**99.87**
ol3-1_31	300	-	48.66	-	40.61	0.22	0.010	0.021	0.16	9.96	0.22	**99.86**
ol3-1_32	310	0.008	48.58	0.01	40.31	0.25	0.011	0.032	0.14	10.08	0.21	**99.64**
ol3-1_33	320	0.015	48.53	0.03	40.42	0.23	0.008	0.008	0.15	10.00	0.20	**99.58**
ol3-1_34	330 - Rim	-	48.26	0.02	40.60	0.27	0.011	0.051	0.12	10.32	0.22	**99.88**

Table 11: The major element composition of an olivine crystal from sample MRS2A. The dash symbol (-) represent concentration under the detection limit of the instruments.

MRS2A - Ol 4												
Name	Distance (µm)	Na_2O	MgO	Al_2O_3	SiO_2	CaO	TiO_2	Cr_2O_3	MnO	FeO	NiO	Total
ol4-1_5	Core - 0	0.011	48.31	0.044	40.22	0.25	0.005	0.001	0.19	11.70	0.14	**100.86**
ol4-1_6	10	0.002	47.58	0.011	40.03	0.24	0.012	0.022	0.19	11.57	0.14	**99.80**
ol4-1_7	20	-	48.10	-	40.20	0.25	-	0.022	0.16	11.67	0.16	**100.56**
ol4-1_8	30	0.009	47.55	0.026	40.31	0.23	0.008	0.006	0.21	11.54	0.15	**100.03**
ol4-1_9	40	-	47.55	-	39.95	0.25	0.009	0.012	0.27	11.65	0.19	**99.88**
ol4-1_10	50	-	47.54	-	40.45	0.25	0.024	0.006	0.19	11.68	0.14	**100.27**
ol4-1_11	60	0.009	47.58	-	40.31	0.27	-	0.008	0.17	11.56	0.15	**100.05**
ol4-1_12	70	-	47.71	-	40.29	0.24	0.011	0.027	0.17	11.74	0.15	**100.34**
ol4-1_13	80	0.014	47.64	0.022	40.29	0.22	0.006	0.007	0.18	11.67	0.13	**100.18**
ol4-1_14	90	-	47.48	-	40.22	0.26	0.017	0.008	0.20	11.62	0.17	**99.99**
ol4-1_15	100	0.009	47.70	0.025	40.25	0.27	0.019	-	0.17	11.40	0.13	**99.98**
ol4-1_16	110	-	47.85	0.011	40.02	0.25	-	0.013	0.16	11.58	0.17	**100.07**
ol4-1_17	120	-	48.20	0.029	40.01	0.24	0.018	0.018	0.21	11.64	0.10	**100.48**
ol4-1_18	130	0.014	47.48	0.018	40.20	0.23	-	-	0.13	11.67	0.15	**99.90**
ol4-1_19	140	-	47.86	-	40.39	0.24	-	0.024	0.21	11.86	0.14	**100.71**
ol4-1_20	150	0.003	47.73	0.005	40.13	0.25	0.004	0.031	0.16	11.55	0.15	**100.01**
ol4-1_21	160	-	47.70	0.001	40.28	0.23	0.017	-	0.19	11.59	0.23	**100.24**
ol4-1_22	170	0.006	47.72	0.022	40.41	0.24	-	0.024	0.21	11.54	0.17	**100.35**
ol4-1_23	180	0.019	47.96	0.035	40.15	0.23	0.016	0.030	0.21	11.52	0.18	**100.35**
ol4-1_24	190	0.025	47.62	0.018	40.27	0.25	-	-	0.19	11.28	0.20	**99.85**
ol4-1_25	200	-	47.56	0.032	40.21	0.24	0.009	0.020	0.20	11.28	0.15	**99.71**
ol4-1_26	210	-	47.77	0.003	40.55	0.24	0.007	0.027	0.19	11.42	0.15	**100.37**
ol4-1_27	220	0.012	47.73	0.014	40.26	0.25	0.003	-	0.16	11.44	0.18	**100.05**
ol4-1_28	230	0.010	47.68	0.028	40.19	0.26	-	0.005	0.18	11.49	0.18	**100.03**
ol4-1_29	240 - Rim	0.017	48.09	0.038	40.50	0.29	-	0.014	0.16	11.21	0.20	**100.52**

Table 12: EPMA analyses of the major element composition of an olivine crystal. The dash symbol (-) represent concentration under the detection limit of the instruments.

MRS2A - Ol 4a												
Name	Distance (µm)	Na_2O	MgO	Al_2O_3	SiO_2	CaO	TiO_2	Cr_2O_3	MnO	FeO	NiO	Total
ol4a-1_1	Core - 0	-	48.03	0.033	40.30	0.23	-	0.022	0.19	11.48	0.17	**100.46**
ol4a-1_2	10	-	47.72	-	40.38	0.29	-	0.021	0.18	11.38	0.14	**100.10**
ol4a-1_3	20	-	47.71	0.000	40.58	0.26	0.008	0.017	0.19	11.41	0.16	**100.34**
ol4a-1_4	30	0.019	47.50	-	40.49	0.26	-	-	0.15	11.61	0.10	**100.14**
ol4a-1_5	40	-	47.66	0.018	40.32	0.22	0.005	0.014	0.23	11.38	0.14	**100.00**
ol4a-1_6	50	0.015	48.05	-	40.25	0.26	-	0.007	0.21	11.66	0.17	**100.62**
ol4a-1_7	60	0.011	47.88	0.027	40.33	0.25	0.020	0.027	0.20	11.69	0.20	**100.63**
ol4a-1_8	70	-	47.71	0.024	40.30	0.24	0.003	0.030	0.22	11.59	0.18	**100.28**
ol4a-1_9	80	-	47.83	0.035	40.29	0.23	0.015	0.032	0.20	11.44	0.13	**100.20**
ol4a-1_10	90	0.005	47.82	0.029	40.57	0.25	-	0.027	0.20	11.54	0.15	**100.59**

Table 13: The major element composition of an olivine crystal from sample MRS2A. The dash symbol (-) represent concentration under the detection limit of the instruments.

MRS2A - Ol 4a												
Name	Distance (µm)	Na_2O	MgO	Al_2O_3	SiO_2	CaO	TiO_2	Cr_2O_3	MnO	FeO	NiO	Total
ol4a-1_11	100	-	47.86	0.031	40.06	0.26	0.004	0.008	0.20	11.74	0.19	**100.34**
ol4a-1_12	110	-	47.83	-	40.19	0.25	0.005	0.033	0.20	11.38	0.17	**100.05**
ol4a-1_13	120	-	47.57	0.001	40.42	0.26	-	0.010	0.13	11.35	0.20	**99.95**
ol4a-1_14	130	-	47.60	-	40.39	0.25	0.007	-	0.18	11.49	0.15	**100.07**
ol4a-1_15	140	0.023	47.78	0.018	40.39	0.26	0.004	0.010	0.17	11.15	0.17	**99.98**
ol4a-1_16	150	-	47.71	0.005	40.43	0.20	0.010	-	0.14	11.46	0.16	**100.11**
ol4a-1_17	160	-	47.77	0.004	40.15	0.24	0.002	0.014	0.18	11.47	0.19	**100.02**
ol4a-1_18	170	0.022	47.84	-	40.41	0.26	-	0.027	0.20	11.64	0.20	**100.60**
ol4a-1_19	180	-	48.47	0.014	40.18	0.24	0.012	0.017	0.22	11.32	0.17	**100.65**
ol4a-1_20	190	0.026	47.84	0.015	40.48	0.25	-	0.006	0.15	11.56	0.19	**100.52**
ol4a-1_21	200	-	47.59	0.036	40.37	0.24	0.032	0.030	0.22	11.17	0.15	**99.83**
ol4a-1_22	210	0.017	47.89	-	40.43	0.22	0.001	0.041	0.18	11.39	0.19	**100.36**
ol4a-1_23	220	-	47.75	0.022	40.30	0.27	0.008	0.027	0.17	11.48	0.16	**100.18**
ol4a-1_24	230	-	47.79	0.019	40.15	0.25	-	0.002	0.17	11.70	0.15	**100.23**
ol4a-1_25	240	-	47.72	-	40.43	0.26	0.008	0.011	0.21	11.25	0.15	**100.03**
ol4a-1_26	250	-	48.04	-	40.52	0.22	-	0.022	0.20	11.62	0.18	**100.80**
ol4a-1_27	260	0.018	47.94	0.005	40.20	0.26	0.016	0.017	0.22	11.35	0.19	**100.21**
ol4a-1_28	270	0.011	47.87	0.003	40.42	0.25	0.007	0.017	0.23	11.57	0.17	**100.55**
ol4a-1_29	280	-	47.72	0.021	40.66	0.23	-	0.028	0.21	11.30	0.13	**100.30**
ol4a-1_30	290	-	47.88	0.046	40.42	0.20	-	0.027	0.17	11.67	0.19	**100.61**
ol4a-1_31	300	-	47.83	0.004	40.46	0.25	0.006	0.026	0.18	11.59	0.18	**100.52**
ol4a-1_32	310	-	47.59	0.021	40.30	0.23	0.001	0.010	0.14	11.36	0.17	**99.82**
ol4a-1_33	320	-	47.64	-	40.48	0.22	0.017	0.019	0.17	11.22	0.17	**99.93**
ol4a-1_34	330	-	48.90	0.060	37.94	0.26	0.006	0.001	0.17	11.30	0.19	**98.83**
ol4a-1_35	350	0.009	47.90	-	40.40	0.27	0.020	0.002	0.19	11.56	0.18	**100.52**
ol4a-1_36	360	-	47.93	0.022	40.27	0.22	0.011	0.043	0.23	11.33	0.17	**100.22**
ol4a-1_37	370	-	47.77	0.019	40.19	0.22	0.011	0.028	0.17	11.11	0.16	**99.68**
ol4a-1_38	410	-	47.71	0.009	40.14	0.23	0.014	0.006	0.18	11.34	0.15	**99.76**
ol4a-1_39	420	-	47.92	-	40.14	0.22	0.006	0.034	0.21	11.17	0.25	**99.94**
ol4a-1_40	430	0.029	48.04	0.009	40.38	0.22	0.016	0.037	0.18	11.30	0.17	**100.39**
ol4a-1_41	440	0.014	47.97	0.015	40.34	0.24	-	0.033	0.26	11.39	0.14	**100.41**
ol4a-1_42	450	-	47.79	0.016	40.52	0.24	0.008	0.025	0.16	11.23	0.18	**100.16**
ol4a-1_43	460	0.001	47.73	0.004	40.44	0.24	0.011	0.032	0.24	11.37	0.18	**100.25**
ol4a-1_44	470	-	47.60	0.020	40.27	0.28	0.009	-	0.21	11.14	0.16	**99.68**
ol4a-1_45	480	-	48.25	0.023	40.60	0.25	0.001	0.014	0.17	11.18	0.19	**100.67**
ol4a-1_46	490 - Rim	0.009	48.64	0.075	39.69	0.28	0.019	0.044	0.21	11.76	0.19	**100.91**

Table 13: Continuation.

MRS2A - Cpx 2											
Name	Distance (µm)	Na_2O	MgO	Al_2O_3	SiO_2	CaO	TiO_2	Cr_2O_3	MnO	FeO	Total
cpx2-1_1	Core - 0	0.13	15.77	4.24	50.11	22.57	0.74	0.14	0.13	5.01	**98.85**
cpx2-1_2	10	0.16	15.89	4.24	50.25	22.45	0.71	0.18	0.08	5.27	**99.24**
cpx2-1_3	20	0.20	15.63	4.48	50.31	22.58	0.67	0.05	0.12	5.30	**99.32**
cpx2-1_4	30	0.18	15.68	4.54	50.33	22.44	0.66	0.05	0.14	5.15	**99.16**
cpx2-1_5	40	0.21	16.05	4.11	50.67	22.91	0.62	0.10	0.08	5.21	**99.97**
cpx2-1_6	50	0.24	16.15	3.85	50.80	22.79	0.69	0.14	0.15	4.94	**99.75**
cpx2-1_7	60	0.22	16.22	3.72	51.04	22.74	0.64	0.16	0.10	4.74	**99.58**
cpx2-1_8	70	0.19	16.07	3.78	50.90	22.95	0.53	0.38	0.08	4.41	**99.30**
cpx2-1_9	80	0.16	15.97	4.32	50.37	23.30	0.39	0.69	0.13	4.07	**99.40**
cpx2-1_10	90	0.15	16.11	4.21	50.53	23.13	0.36	0.67	0.12	4.12	**99.41**
cpx2-1_11	100	0.16	15.82	4.94	50.13	22.83	0.41	0.61	0.09	4.01	**98.99**
cpx2-1_12	110	0.18	15.75	4.97	50.41	23.21	0.42	0.61	0.08	3.97	**99.60**
cpx2-1_13	120	0.20	15.90	4.96	50.04	22.95	0.44	0.56	0.08	4.16	**99.29**
cpx2-1_14	130	0.14	15.79	4.87	50.41	23.01	0.40	0.55	0.07	4.04	**99.29**
cpx2-1_15	140	0.17	15.84	4.94	50.21	22.84	0.39	0.56	0.09	3.86	**98.91**
cpx2-1_16	150	0.14	15.85	4.89	50.00	23.15	0.43	0.57	0.07	4.13	**99.22**
cpx2-1_17	160	0.11	15.97	4.94	50.34	23.35	0.45	0.60	0.11	4.17	**100.03**
cpx2-1_18	170	0.15	15.74	4.91	50.32	23.33	0.43	0.59	0.05	3.95	**99.49**
cpx2-1_19	180	0.16	15.81	4.94	50.27	23.08	0.41	0.55	0.08	3.96	**99.27**
cpx2-1_20	190	0.15	15.81	4.86	50.15	23.06	0.47	0.59	0.11	3.90	**99.09**
cpx2-1_21	200	0.13	15.80	4.97	50.01	22.97	0.46	0.60	0.08	4.16	**99.19**
cpx2-1_22	210	0.12	15.73	4.88	50.15	23.10	0.49	0.55	0.05	3.87	**98.95**
cpx2-1_23	220	0.15	15.71	4.86	50.08	23.20	0.44	0.59	0.08	3.97	**99.08**
cpx2-1_24	230	0.13	15.65	4.93	50.01	23.24	0.45	0.63	0.10	4.10	**99.24**
cpx2-1_25	240	0.15	15.65	4.81	50.09	23.20	0.43	0.58	0.10	3.89	**98.91**
cpx2-1_26	250	0.16	15.94	4.75	50.35	23.34	0.44	0.49	0.11	3.86	**99.45**
cpx2-1_27	260	0.13	15.83	4.46	50.49	23.30	0.41	0.58	0.10	3.91	**99.21**
cpx2-1_28	270	0.14	15.86	4.39	50.35	23.33	0.42	0.59	0.05	3.94	**99.06**
cpx2-1_29	280	0.12	15.86	4.34	50.58	23.02	0.39	0.56	0.08	3.89	**98.83**
cpx2-1_30	290	0.19	15.76	4.50	50.44	23.07	0.42	0.51	0.10	3.90	**98.89**
cpx2-1_31	300	0.14	15.72	4.76	49.87	22.94	0.41	0.57	0.09	3.99	**98.49**
cpx2-1_32	310	0.14	15.67	4.90	49.85	23.08	0.42	0.59	0.08	4.01	**98.73**
cpx2-1_33	320	0.15	15.66	4.82	50.03	22.87	0.44	0.58	0.07	4.32	**98.96**
cpx2-1_34	330	0.13	16.10	3.88	51.01	22.77	0.37	0.38	0.10	4.10	**98.84**
cpx2-1_35	340	0.12	16.66	3.45	51.25	22.86	0.35	0.26	0.12	4.03	**99.09**
cpx2-1_36	350	0.13	16.49	3.23	51.35	22.82	0.39	0.16	0.03	4.53	**99.14**
cpx2-1_37	360	0.18	16.25	3.25	51.31	23.01	0.41	0.17	0.06	4.36	**99.00**
cpx2-1_38	370	0.17	16.17	3.82	50.76	22.85	0.53	0.07	0.12	4.79	**99.27**

Table 14: EPMA analyses of the major element composition of an pyroxene crystal.

MRS2A - Cpx 2											
Name	Distance (µm)	Na_2O	MgO	Al_2O_3	SiO_2	CaO	TiO_2	Cr_2O_3	MnO	FeO	Total
cpx2-1_39	380	0.19	16.24	3.25	51.42	22.57	0.48	0.08	0.14	4.77	**99.14**
cpx2-1_40	390	0.17	16.06	3.66	50.95	22.58	0.52	0.01	0.09	5.01	**99.07**
cpx2-1_41	400	0.17	15.80	4.04	50.98	22.59	0.60	0.01	0.15	5.27	**99.62**
cpx2-1_42	410	0.14	15.90	3.68	50.78	22.78	0.56	0.04	0.11	4.89	**98.90**
cpx2-1_43	420	0.15	14.65	2.54	48.44	21.47	0.39	0.01	0.15	4.70	**92.49**
cpx2-1_44	430	0.19	15.94	3.32	51.23	22.57	0.46	0.05	0.14	5.17	**99.08**
cpx2-1_45	440	0.22	15.93	3.34	51.04	22.59	0.55	0.05	0.13	5.33	**99.18**
cpx2-1_46	450	0.15	16.54	3.29	51.41	22.50	0.46	0.28	0.15	4.39	**99.17**
cpx2-1_47	460	0.11	16.75	4.09	51.11	21.88	0.48	0.17	0.12	4.45	**99.16**
cpx2-1_48	470	0.11	17.55	3.25	52.19	21.81	0.39	0.20	0.11	4.19	**99.79**
cpx2-1_49	480	0.11	17.52	2.76	52.17	21.80	0.36	0.11	0.10	4.63	**99.57**
cpx2-1_50	490 - Rim	0.19	16.12	4.25	50.56	22.73	0.51	0.11	0.13	4.35	**98.94**

Table 14: Continuation.

MRS2A - Cpx 4											
Name	Distance (µm)	Na_2O	MgO	Al_2O_3	SiO_2	CaO	TiO_2	Cr_2O_3	MnO	FeO	Total
cpx4-1_1	Core - 0	0.18	16.96	3.01	51.73	22.74	0.33	0.33	0.08	3.56	**98.9286**
cpx4-1_2	10	0.17	16.90	3.25	51.96	22.88	0.30	0.26	0.05	3.53	**99.2981**
cpx4-1_3	20	0.16	16.85	3.18	51.42	22.88	0.30	0.28	0.08	3.57	**98.7375**
cpx4-1_4	30	0.15	16.58	3.20	51.20	22.90	0.32	0.27	0.11	3.60	**98.3406**
cpx4-1_5	40	0.17	16.97	3.25	51.65	22.87	0.34	0.37	0.04	3.65	**99.3063**
cpx4-1_6	50	0.13	16.84	3.15	51.66	23.07	0.35	0.38	0.10	3.78	**99.4658**
cpx4-1_7	60	0.20	16.83	3.26	51.52	22.91	0.37	0.42	0.08	3.76	**99.3313**
cpx4-1_8	70	0.21	16.23	3.75	50.88	22.74	0.40	0.56	0.09	3.84	**98.6927**
cpx4-1_9	80	0.17	16.74	3.77	51.37	22.87	0.35	0.24	0.08	4.00	**99.5876**
cpx4-1_10	90	0.16	16.59	3.53	51.30	23.02	0.36	0.20	0.09	3.80	**99.0484**
cpx4-1_11	100	0.18	16.44	3.62	51.30	23.07	0.34	0.16	0.12	4.03	**99.2689**
cpx4-1_12	110	0.16	16.58	3.64	51.39	22.96	0.34	0.20	0.12	3.75	**99.1284**
cpx4-1_13	120	0.19	16.59	3.57	51.28	22.98	0.32	0.21	0.08	3.82	**99.036**
cpx4-1_14	130	0.15	16.54	3.56	51.32	22.97	0.33	0.20	0.06	3.83	**98.9703**
cpx4-1_15	140	0.16	16.50	3.64	51.65	22.93	0.34	0.19	0.04	3.80	**99.2468**
cpx4-1_16	150	0.16	16.51	3.51	51.52	22.91	0.32	0.36	0.08	3.61	**98.9901**
cpx4-1_17	160	0.13	16.60	3.40	51.32	23.00	0.33	0.44	0.06	3.65	**98.9318**
cpx4-1_18	170	0.17	16.58	3.35	51.48	22.92	0.31	0.43	0.13	3.64	**99.0112**
cpx4-1_19	180	0.22	16.53	3.19	51.52	22.80	0.34	0.27	0.07	3.52	**98.4687**
cpx4-1_20	190	0.18	16.67	3.08	51.94	22.73	0.31	0.30	0.08	3.58	**98.8779**
cpx4-1_21	200	0.18	16.59	3.06	51.88	22.79	0.36	0.23	0.05	3.61	**98.7457**
cpx4-1_22	210	0.14	16.74	2.99	51.85	23.07	0.33	0.24	0.02	3.56	**98.9457**
cpx4-1_23	220	0.15	16.87	3.04	51.65	23.03	0.34	0.25	0.09	3.49	**98.9204**

Table 15: The major element composition of an pyroxene crystal from sample MRS2A.

MRS2A - Cpx 4											
Name	Distance (µm)	Na_2O	MgO	Al_2O_3	SiO_2	CaO	TiO_2	Cr_2O_3	MnO	FeO	Total
cpx4-1_24	230	0.16	16.87	2.98	51.92	23.06	0.36	0.25	0.05	3.62	**99.2708**
cpx4-1_25	240	0.17	16.83	3.13	51.74	22.83	0.35	0.24	0.09	3.65	**99.0257**
cpx4-1_26	250	0.19	16.55	3.11	51.70	22.81	0.36	0.25	0.06	3.67	**98.6948**
cpx4-1_27	260	0.16	16.63	3.12	51.32	22.91	0.35	0.29	0.09	3.64	**98.5152**
cpx4-1_28	270	0.14	16.62	3.34	51.17	22.91	0.34	0.32	0.10	3.50	**98.4433**
cpx4-1_29	280	0.19	16.42	3.35	51.27	22.81	0.34	0.44	0.08	3.49	**98.3838**
cpx4-1_30	290	0.17	16.62	3.27	51.67	22.76	0.33	0.19	0.13	3.72	**98.8441**
cpx4-1_31	300	0.15	16.49	3.72	51.31	22.83	0.33	0.19	0.08	3.94	**99.0376**
cpx4-1_32	310	0.14	16.50	3.66	51.28	22.80	0.33	0.16	0.10	3.81	**98.7823**
cpx4-1_33	320	0.19	16.51	3.67	51.08	23.01	0.36	0.22	0.10	3.99	**99.1217**
cpx4-1_34	330	0.13	16.41	3.66	51.30	22.89	0.35	0.19	0.05	3.76	**98.7548**
cpx4-1_35	340	0.12	16.58	3.39	51.37	23.00	0.34	0.14	0.14	3.70	**98.7633**
cpx4-1_36	350	0.14	16.55	3.59	51.28	22.91	0.41	0.13	0.11	3.97	**99.0875**
cpx4-1_37	360	0.13	16.43	3.57	51.24	22.85	0.35	0.16	0.09	3.81	**98.6185**
cpx4-1_38	370	0.17	16.50	3.65	51.16	23.12	0.36	0.32	0.08	3.59	**98.9655**
cpx4-1_39	380	0.15	16.67	3.33	51.56	22.93	0.30	0.48	0.06	3.61	**99.0875**
cpx4-1_40	390	0.13	16.36	4.09	50.84	22.84	0.44	0.42	0.10	3.64	**98.8464**
cpx4-1_41	400	0.16	16.37	4.06	51.44	22.75	0.38	0.35	0.13	3.73	**99.3656**
cpx4-1_42	410	0.18	16.37	3.85	51.36	22.78	0.39	0.29	0.08	3.73	**99.0308**
cpx4-1_43	420	0.15	16.38	3.98	50.98	22.90	0.38	0.36	0.05	3.83	**99.0097**
cpx4-1_44	430	0.12	16.49	3.72	51.16	22.94	0.39	0.29	0.09	3.63	**98.8465**
cpx4-1_45	440	0.14	16.61	3.72	51.33	23.14	0.37	0.30	0.07	3.65	**99.3193**
cpx4-1_46	450	0.18	16.64	3.78	51.36	23.07	0.33	0.28	0.10	3.83	**99.5652**
cpx4-1_47	460	0.15	16.61	3.68	51.24	22.94	0.37	0.24	0.04	3.94	**99.2122**
cpx4-1_48	470	0.17	16.42	4.01	50.91	22.50	0.42	0.34	0.07	4.09	**98.938**
cpx4-1_49	480	0.16	16.14	4.22	50.69	22.34	0.52	0.32	0.06	4.60	**99.0492**
cpx4-1_50	490	0.20	16.08	4.15	50.82	22.22	0.64	0.11	0.18	5.05	**99.4544**
cpx4-1_51	500	0.22	16.04	4.14	51.00	22.28	0.60	0.19	0.11	5.03	**99.6126**
cpx4-1_52	510	0.17	16.28	3.65	51.07	22.58	0.52	0.26	0.11	4.56	**99.2094**
cpx4-1_53	520	0.15	16.63	3.29	51.56	22.72	0.42	0.37	0.08	3.97	**99.1814**
cpx4-1_54	530	0.18	16.83	3.26	51.74	22.93	0.39	0.36	0.09	4.05	**99.8255**
cpx4-1_55	540	0.21	16.47	3.90	51.39	22.80	0.42	0.38	0.09	3.72	**99.3706**
cpx4-1_56	550	0.12	16.60	3.62	51.55	22.88	0.37	0.57	0.08	3.64	**99.4261**
cpx4-1_57	560	0.18	16.79	3.56	51.38	22.69	0.35	0.46	0.10	3.61	**99.1053**
cpx4-1_58	570	0.21	16.96	3.54	51.90	22.46	0.33	0.41	0.10	3.51	**99.4112**
cpx4-1_59	580	0.18	16.76	4.01	51.41	22.53	0.39	0.51	0.07	3.61	**99.4647**
cpx4-1_60	590 - Rim	0.16	16.21	5.53	49.45	22.05	0.59	0.31	0.06	4.23	**98.5921**

Table 15: Continuation.

Appendix III – Sample MRS4

This appendix contains the major element analyses of 4 olivines.

MRS4 - Ol 1									
Name	Distance (µm)	MgO	Al_2O_3	SiO_2	CaO	MnO	FeO	NiO	Total
Ol1-1_1	Core - 0	49.22	-	39.79	0.25	0.20	9.05	0.23	**98.74**
Ol1-1_2	14.21	49.50	0.027	40.89	0.27	0.17	9.13	0.27	**100.26**
Ol1-1_3	27.67	49.30	0.006	40.59	0.30	0.12	9.16	0.24	**99.71**
Ol1-1_4	41.88	49.16	0.025	40.70	0.30	0.18	8.90	0.23	**99.51**
Ol1-1_5	55.33	49.27	0.030	40.66	0.32	0.18	9.14	0.23	**99.84**
Ol1-1_6	69.55	49.31	0.011	40.78	0.29	0.16	9.19	0.24	**99.98**
Ol1-1_7	83.76	49.28	0.027	40.59	0.28	0.14	9.09	0.25	**99.67**
Ol1-1_8	97.21	49.32	0.051	40.64	0.27	0.15	9.12	0.24	**99.78**
Ol1-1_9	111.42	49.72	0.007	40.57	0.31	0.17	9.14	0.22	**100.14**
Ol1-1_10	125.64	49.36	0.033	40.71	0.28	0.13	9.26	0.25	**100.03**
Ol1-1_11	139.09	49.30	0.026	40.75	0.31	0.15	9.03	0.23	**99.79**
Ol1-1_12	153.30	49.23	-	40.55	0.28	0.16	8.91	0.23	**99.35**
Ol1-1_13	166.76	49.29	0.028	40.49	0.30	0.17	9.08	0.25	**99.60**
Ol1-1_14	180.97	49.28	0.034	40.64	0.28	0.12	9.19	0.25	**99.79**
Ol1-1_15	195.18	49.31	-	40.51	0.31	0.18	8.99	0.24	**99.54**
Ol1-1_16	208.64	49.44	-	40.59	0.27	0.16	9.13	0.23	**99.82**
Ol1-1_17	222.85	49.37	0.031	40.91	0.29	0.17	8.96	0.26	**99.98**
Ol1-1_18	236.30	49.36	0.030	40.69	0.32	0.15	9.27	0.23	**100.05**
Ol1-1_19	250.51	49.21	0.054	40.87	0.26	0.13	8.96	0.26	**99.74**
Ol1-1_20	264.73	49.60	0.008	40.53	0.29	0.17	9.31	0.20	**100.11**
Ol1-1_21	278.18	49.38	0.015	40.61	0.29	0.16	9.21	0.21	**99.89**
Ol1-1_22	292.39	49.53	0.028	40.49	0.29	0.13	8.91	0.22	**99.60**
Ol1-1_23	305.85	49.28	0.055	40.66	0.31	0.16	9.11	0.22	**99.79**
Ol1-1_24	319.45	49.38	0.012	40.63	0.28	0.15	9.15	0.21	**99.82**
Ol1-1_25	333.66	49.37	0.023	40.58	0.29	0.15	8.94	0.23	**99.58**
Ol1-1_26	347.12	49.38	-	40.76	0.27	0.17	9.16	0.23	**99.98**
Ol1-1_27	361.33	49.39	0.016	40.66	0.28	0.18	8.95	0.22	**99.69**
Ol1-1_28	375.54	49.34	0.027	40.82	0.28	0.16	9.13	0.23	**100.00**
Ol1-1_29	388.99	49.25	0.041	40.46	0.27	0.15	9.08	0.25	**99.51**
Ol1-1_30	403.21	49.16	0.016	40.48	0.26	0.16	8.94	0.21	**99.22**
Ol1-1_31	416.66	49.17	0.021	40.52	0.26	0.14	8.91	0.25	**99.26**
Ol1-1_32	430.87	49.17	0.025	40.80	0.26	0.17	9.09	0.23	**99.75**
Ol1-1_33	445.09	49.32	0.048	40.63	0.28	0.17	8.95	0.22	**99.62**
Ol1-1_34	458.54	48.93	0.042	40.84	0.26	0.14	8.97	0.23	**99.41**
Ol1-1_35	472.75	49.58	0.044	40.91	0.27	0.15	9.09	0.25	**100.30**
Ol1-1_36	486.21	49.54	0.020	40.42	0.30	0.15	8.89	0.22	**99.54**

Table 16: EPMA analyses of the major element composition of an olivine crystal. The dash symbol (-) represent concentration under the detection limit of the instruments.

MRS4 - Ol 1									
Name	Distance (µm)	MgO	Al_2O_3	SiO_2	CaO	MnO	FeO	NiO	Total
Ol1-1_37	500.42	49.29	0.018	40.65	0.28	0.13	9.14	0.22	**99.72**
Ol1-1_38	514.63	49.34	0.000	40.86	0.27	0.13	8.97	0.24	**99.81**
Ol1-1_39	528.08	49.55	0.053	40.54	0.29	0.13	8.95	0.24	**99.75**
Ol1-1_40	542.30	49.33	0.029	40.41	0.27	0.12	9.10	0.22	**99.49**
Ol1-1_41	556.51	49.21	0.053	40.55	0.29	0.12	8.98	0.22	**99.43**
Ol1-1_42	569.96	49.16	0.030	40.61	0.27	0.17	9.04	0.21	**99.49**
Ol1-1_43	584.18	49.18	0.030	40.96	0.29	0.15	8.98	0.21	**99.81**
Ol1-1_44	597.63	49.12	0.025	40.40	0.28	0.16	9.05	0.24	**99.27**
Ol1-1_45	611.84 - Rim	48.91	0.006	40.36	0.29	0.15	9.12	0.19	**99.02**

Table 16: Continuation.

MRS4 - Ol 2									
Name	Distance (µm)	MgO	Al_2O_3	SiO_2	CaO	MnO	FeO	NiO	Total
Ol2-1_1	Core - 0	49.06	0.03	39.90	0.25	0.15	9.31	0.23	**98.93**
Ol2-1_2	10.82	49.06	-	39.79	0.27	0.16	9.26	0.21	**98.75**
Ol2-1_3	23.02	49.20	0.03	39.99	0.23	0.14	9.33	0.21	**99.13**
Ol2-1_4	33.84	49.22	0.02	39.62	0.29	0.15	9.15	0.23	**98.70**
Ol2-1_5	46.05	49.46	0.01	39.67	0.29	0.19	9.33	0.22	**99.16**
Ol2-1_6	56.86	49.72	0.02	40.05	0.26	0.19	9.20	0.23	**99.65**
Ol2-1_7	67.68	49.27	0.02	39.96	0.28	0.18	9.32	0.21	**99.24**
Ol2-1_8	79.89	48.77	0.04	39.85	0.27	0.14	9.16	0.23	**98.46**
Ol2-1_9	90.70	49.37	0.06	39.86	0.27	0.13	9.41	0.23	**99.34**
Ol2-1_10	102.10	48.96	0.02	39.75	0.25	0.16	9.08	0.23	**98.44**
Ol2-1_11	113.77	49.32	0.00	39.81	0.27	0.21	9.12	0.25	**98.98**
Ol2-1_12	125.17	49.36	0.02	39.86	0.25	0.16	9.30	0.21	**99.16**
Ol2-1_13	136.83	49.33	0.03	39.64	0.30	0.13	9.25	0.24	**98.92**
Ol2-1_14	147.65	49.29	0.03	40.32	0.26	0.16	9.03	0.24	**99.32**
Ol2-1_15	159.05	49.29	0.05	39.95	0.28	0.17	9.02	0.23	**98.99**
Ol2-1_16	170.71	49.02	0.02	39.85	0.27	0.15	8.91	0.24	**98.46**
Ol2-1_17	182.11	49.27	0.01	39.91	0.25	0.14	9.29	0.22	**99.09**
Ol2-1_18	192.93	49.16	0.04	39.86	0.28	0.14	9.08	0.22	**98.77**
Ol2-1_19	204.59	49.14	0.03	39.99	0.26	0.17	9.22	0.22	**99.03**
Ol2-1_20	215.99	49.20	0.03	40.06	0.26	0.16	9.28	0.23	**99.20**
Ol2-1_21	227.65	49.18	0.04	39.92	0.29	0.12	9.06	0.21	**98.81**
Ol2-1_22	239.06	49.08	0.01	39.66	0.26	0.21	9.48	0.22	**98.93**
Ol2-1_23	249.87	49.31	-	40.21	0.26	0.19	9.14	0.22	**99.33**
Ol2-1_24	262.08	49.24	0.01	39.82	0.29	0.18	9.12	0.21	**98.87**
Ol2-1_25	272.90	49.22	0.03	39.77	0.28	0.12	9.27	0.24	**98.91**
Ol2-1_26	283.71	49.01	0.04	39.92	0.27	0.20	9.05	0.18	**98.66**
Ol2-1_27	295.92	49.23	0.04	39.96	0.31	0.17	9.17	0.24	**99.11**
Ol2-1_28	306.74	49.30	0.02	39.84	0.29	0.23	9.30	0.26	**99.25**
Ol2-1_29	318.94	48.89	0.03	39.85	0.34	0.16	9.32	0.19	**98.77**

Table 17: The major element composition of an olivine crystal from sample MRS4. The dash symbol (-) represent concentration under the detection limit of the instruments.

MRS4 - Ol 3									
Name	Distance (µm)	MgO	Al_2O_3	SiO_2	CaO	MnO	FeO	NiO	Total
Ol3-1	Core - 0	48.12	0.031	40.47	0.28	0.16	10.76	0.25	**100.07**
Ol3-1_1	38.29	47.75	0.024	40.24	0.26	0.13	10.75	0.22	**99.37**
Ol3-1_2	48.14	47.93	0.007	40.33	0.27	0.19	10.89	0.23	**99.84**
Ol3-1_3	59.32	47.90	0.038	40.56	0.26	0.19	10.75	0.25	**99.93**
Ol3-1_4	69.17	47.93	0.001	40.51	0.28	0.22	10.82	0.24	**100.00**
Ol3-1_5	80.35	48.02	-	40.40	0.30	0.20	10.82	0.25	**100.00**
Ol3-1_6	90.20	47.77	0.048	40.47	0.27	0.24	10.68	0.24	**99.73**
Ol3-1_7	100.49	48.43	0.013	40.75	0.26	0.19	11.21	0.25	**101.09**
Ol3-1_8	111.26	47.71	0.018	40.49	0.27	0.19	10.81	0.21	**99.69**
Ol3-1_9	121.56	47.76	0.032	40.55	0.27	0.20	10.80	0.26	**99.87**
Ol3-1_10	131.41	48.02	0.030	40.49	0.31	0.21	10.89	0.22	**100.17**
Ol3-1_11	142.59	47.91	0.014	40.16	0.29	0.20	10.71	0.22	**99.50**
Ol3-1_12	152.44	47.95	0.025	40.36	0.29	0.18	10.98	0.21	**99.99**
Ol3-1_13	163.21	47.78	0.035	40.44	0.29	0.19	10.96	0.25	**99.95**
Ol3-1_14	173.50	47.91	0.056	40.45	0.27	0.18	10.81	0.23	**99.90**
Ol3-1_15	183.35	47.79	0.026	40.81	0.30	0.23	11.18	0.24	**100.58**
Ol3-1_16	194.53	47.82	0.039	40.21	0.30	0.21	10.88	0.22	**99.67**
Ol3-1_17	204.38	47.73	0.037	40.25	0.27	0.19	10.77	0.21	**99.46**
Ol3-1_18	215.56	47.65	0.021	40.49	0.30	0.17	11.00	0.22	**99.85**
Ol3-1_19	225.41	47.77	0.051	40.43	0.29	0.14	10.92	0.21	**99.82**
Ol3-1_20	235.70	47.72	0.048	40.22	0.30	0.17	10.82	0.21	**99.48**
Ol3-1_21	246.47	47.76	0.002	40.41	0.29	0.16	10.98	0.26	**99.86**
Ol3-1_22	256.32	47.93	0.036	40.25	0.29	0.14	10.89	0.23	**99.78**
Ol3-1_23	267.50	47.45	0.044	40.45	0.33	0.17	10.85	0.22	**99.53**
Ol3-1_24	277.35	47.49	0.030	40.23	0.29	0.23	11.22	0.23	**99.71**
Ol3-1_25	287.65	47.73	0.032	40.39	0.28	0.21	11.19	0.21	**100.04**
Ol3-1_26	298.42	47.70	0.008	40.32	0.34	0.23	11.06	0.20	**99.85**
Ol3-1_27	308.71	47.47	0.012	40.21	0.26	0.20	10.93	0.23	**99.32**
Ol3-1_28	318.56	47.68	0.023	40.47	0.29	0.20	10.95	0.21	**99.82**
Ol3-1_29	329.74	47.72	0.021	40.55	0.32	0.25	10.67	0.24	**99.77**
Ol3-1_30	339.59	47.99	0.021	40.32	0.32	0.20	10.21	0.24	**99.30**
Ol3-1_31	350.77	47.79	-	40.30	0.33	0.17	10.50	0.26	**99.36**
Ol3-1_32	360.62	44.57	0.009	39.60	0.27	0.23	14.05	0.10	**98.83**

Table 18: EPMA analyses of the major element composition of an olivine crystal. The dash symbol (-) represent concentration under the detection limit of the instruments.

MRS4 - Ol4									
Name	Distance (µm)	MgO	Al_2O_3	SiO_2	CaO	MnO	FeO	NiO	Total
Ol4-1_1	0	47.48	0.020	40.14	0.32	0.20	10.78	0.19	**99.13**
Ol4-1_2	10	47.38	0.036	40.28	0.32	0.19	10.86	0.18	**99.25**
Ol4-1_3	20	47.41	0.052	40.45	0.31	0.24	10.76	0.18	**99.41**
Ol4-1_4	30	47.09	0.038	40.36	0.34	0.21	10.77	0.20	**99.00**
Ol4-1_5	38	47.62	0.029	40.44	0.33	0.17	11.23	0.19	**100.00**
Ol4-1_6	48	47.51	0.006	40.31	0.31	0.23	11.01	0.18	**99.55**
Ol4-1_7	58	47.24	0.033	40.64	0.34	0.18	10.79	0.20	**99.43**
Ol4-1_8	68	47.38	0.010	40.42	0.30	0.16	10.69	0.23	**99.19**
Ol4-1_9	78	47.35	0.023	40.45	0.34	0.17	10.96	0.19	**99.48**
Ol4-1_10	88	47.70	0.046	40.49	0.33	0.18	11.05	0.21	**100.01**
Ol4-1_11	97	47.44	-	40.68	0.32	0.22	10.93	0.17	**99.77**
Ol4-1_12	107	47.59	-	40.46	0.32	0.24	11.30	0.19	**100.09**
Ol4-1_13	117	47.37	0.017	40.49	0.34	0.20	11.03	0.21	**99.66**
Ol4-1_14	127	47.10	0.031	40.46	0.31	0.18	11.08	0.19	**99.35**
Ol4-1_15	137	47.30	0.021	40.67	0.33	0.21	10.86	0.23	**99.62**
Ol4-1_16	147	47.31	0.019	40.13	0.33	0.22	11.01	0.20	**99.22**
Ol4-1_17	155	47.15	0.005	40.38	0.34	0.22	11.10	0.17	**99.36**
Ol4-1_18	165	46.97	0.020	40.57	0.33	0.15	10.96	0.21	**99.21**
Ol4-1_19	175	46.41	0.010	40.62	0.31	0.23	11.96	0.18	**99.73**
Ol4-1_20	185 - Rim	44.79	0.019	40.18	0.30	0.23	14.36	0.12	**100.00**

Table 19: The major element composition of an olivine crystal from sample MRS4. The dash symbol (-) represent concentration under the detection limit of the instruments.

Appendix IV – Sample D4

This appendix contains the major element analyses of 6 olivines.

D4 - Ol 1									
Name	**Distance (µm)**	**MgO**	**Al_2O_3**	**SiO_2**	**CaO**	**MnO**	**FeO**	**NiO**	**Total**
ol1-2_1	Core - 0	37.30	0.011	37.32	0.15	0.45	24.33	0.06	**99.62**
ol1-2_2	9	37.30	-	37.73	0.15	0.42	24.09	0.08	**99.78**
ol1-2_3	19	36.98	-	37.35	0.15	0.40	23.86	0.09	**98.84**
ol1-2_4	28	37.35	-	37.63	0.13	0.47	24.16	0.07	**99.81**
ol1-2_5	37	37.24	-	37.77	0.16	0.45	24.20	0.10	**99.92**
ol1-2_6	46	37.22	0.004	37.56	0.14	0.46	23.99	0.08	**99.46**
ol1-2_7	56	37.06	-	37.63	0.14	0.45	23.69	0.07	**99.04**
ol1-2_8	65	37.24	0.000	37.54	0.17	0.41	24.24	0.06	**99.67**
ol1-2_9	74	37.16	-	37.32	0.14	0.44	24.09	0.07	**99.22**
ol1-2_10	83	37.23	-	37.08	0.14	0.37	23.81	0.11	**98.74**
ol1-2_11	93	37.20	0.027	37.22	0.16	0.45	24.06	0.08	**99.19**
ol1-2_12	102	37.40	-	37.44	0.15	0.42	24.02	0.08	**99.50**
ol1-2_13	111	37.55	0.008	37.38	0.17	0.41	23.51	0.05	**99.08**
ol1-2_14	120	37.65	-	37.46	0.15	0.43	23.49	0.08	**99.27**
ol1-2_15	130	38.08	0.019	37.50	0.13	0.41	22.99	0.06	**99.19**
ol1-2_16	139	38.10	-	37.71	0.16	0.40	22.82	0.05	**99.24**
ol1-2_17	148	38.34	0.012	37.60	0.16	0.43	22.43	0.07	**99.04**
ol1-2_18	157	38.67	-	38.06	0.16	0.33	22.49	0.05	**99.76**
ol1-2_19	167 - Rim	38.73	-	37.93	0.19	0.38	21.93	0.06	**99.23**

Table 20: EPMA analyses of the major element composition of an olivine crystal. The dash symbol (-) represent concentration under the detection limit of the instruments.

D4 - Ol 2									
Name	Distance (µm)	MgO	Al_2O_3	SiO_2	CaO	MnO	FeO	NiO	Total
ol2-2_1	Core - 0	37.15	0.008	37.34	0.15	0.43	24.28	0.07	**99.42**
ol2-2_2	8.54	37.13	-	37.02	0.12	0.41	24.33	0.04	**99.05**
ol2-2_3	18.39	37.31	0.015	37.18	0.12	0.41	24.31	0.06	**99.40**
ol2-2_4	26.94	36.94	-	36.98	0.13	0.43	23.81	0.07	**98.36**
ol2-2_5	36.79	37.17	0.003	37.36	0.16	0.51	24.16	0.07	**99.44**
ol2-2_6	45.33	37.11	-	37.21	0.15	0.42	23.82	0.08	**98.79**
ol2-2_7	55.18	37.25	-	37.16	0.13	0.41	24.16	0.05	**99.17**
ol2-2_8	63.72	36.99	0.006	37.18	0.15	0.41	23.53	0.09	**98.36**
ol2-2_9	73.57	37.27	-	37.46	0.16	0.41	23.85	0.08	**99.25**
ol2-2_10	82.12	37.20	-	37.00	0.13	0.41	23.95	0.08	**98.77**
ol2-2_11	91.60	37.15	-	37.22	0.14	0.39	23.84	0.05	**98.79**
ol2-2_12	100.55	37.31	0.005	37.20	0.13	0.40	24.07	0.06	**99.17**
ol2-2_13	110.03	37.47	-	37.32	0.13	0.45	23.67	0.06	**99.09**
ol2-2_14	118.98	37.39	-	37.34	0.13	0.50	23.95	0.09	**99.41**
ol2-2_15	128.46	37.32	-	37.30	0.15	0.43	23.38	0.06	**98.63**
ol2-2_16	137.41	37.42	-	37.30	0.14	0.43	23.52	0.09	**98.89**
ol2-2_17	146.90	37.62	-	37.38	0.13	0.47	23.61	0.09	**99.29**
ol2-2_18	155.84	37.70	-	37.78	0.16	0.35	23.69	0.06	**99.75**
ol2-2_19	165.33	37.50	0.005	37.71	0.14	0.43	23.67	0.09	**99.55**
ol2-2_20	174.27	37.72	-	37.54	0.12	0.41	23.61	0.08	**99.48**
ol2-2_21	183.76	37.98	-	37.59	0.13	0.48	23.42	0.08	**99.68**
ol2-2_22	192.30	37.62	-	37.56	0.14	0.42	23.16	0.09	**98.98**
ol2-2_23	202.15	37.88	-	37.56	0.15	0.38	23.26	0.05	**99.28**
ol2-2_24	210.69	37.89	-	37.54	0.17	0.36	23.38	0.09	**99.43**
ol2-2_25	220.54	38.06	0.031	37.75	0.13	0.40	22.93	0.08	**99.38**
ol2-2_26	229.09	38.38	0.014	37.62	0.19	0.40	22.63	0.09	**99.32**
ol2-2_27	238.94	38.55	-	37.81	0.17	0.39	22.26	0.06	**99.24**
ol2-2_28	247.48	38.58	0.010	37.67	0.17	0.39	21.98	0.06	**98.86**
ol2-2_29	257.33 - Rim	38.86	-	37.96	0.20	0.36	21.69	0.10	**99.17**

Table 21: The major element composition of an olivine crystal from sample D4. The dash symbol (-) represent concentration under the detection limit of the instruments.

D4 - Ol 3									
Name	Distance (µm)	MgO	Al_2O_3	SiO_2	CaO	MnO	FeO	NiO	Total
ol3-3_1	0	37.33	-	37.54	0.17	0.42	23.82	0.08	**99.36**
ol3-3_2	10	37.23	0.019	37.48	0.14	0.46	24.03	0.04	**99.40**
ol3-3_3	20	37.18	0.016	37.93	0.19	0.53	23.88	0.06	**99.78**
ol3-3_4	30	37.11	-	37.67	0.14	0.43	24.23	0.06	**99.64**
ol3-3_5	40	37.06	0.005	37.65	0.18	0.42	24.31	0.06	**99.69**
ol3-3_6	50	35.76	0.011	36.91	0.18	0.46	23.54	0.06	**96.93**
ol3-3_7	60	37.07	0.015	37.53	0.15	0.46	24.36	0.08	**99.67**
ol3-3_8	70	36.71	-	37.99	0.15	0.43	24.53	0.05	**99.87**
ol3-3_9	80	36.71	0.001	37.48	0.18	0.40	24.13	0.09	**98.99**
ol3-3_10	90	36.66	-	37.69	0.14	0.38	24.32	0.06	**99.25**
ol3-3_11	100	36.74	-	37.26	0.14	0.48	24.16	0.04	**98.82**
ol3-3_12	110	36.66	-	37.29	0.15	0.39	24.32	0.07	**98.88**
ol3-3_13	120	36.70	0.018	37.63	0.16	0.41	24.40	0.05	**99.37**
ol3-3_14	130	36.75	-	37.55	0.15	0.46	24.21	0.07	**99.19**
ol3-3_15	140	36.81	-	37.33	0.17	0.44	24.38	0.06	**99.19**
ol3-3_16	150	36.67	-	37.63	0.17	0.45	24.21	0.06	**99.18**
ol3-3_17	160	36.80	0.025	37.69	0.17	0.45	24.29	0.06	**99.49**
ol3-3_18	170	37.22	0.031	37.50	0.14	0.41	24.19	0.06	**99.53**
ol3-3_19	180	37.29	0.020	37.53	0.17	0.46	23.91	0.06	**99.44**
ol3-3_20	190	37.27	0.004	37.86	0.15	0.39	23.66	0.07	**99.42**
ol3-3_21	200	37.84	-	37.75	0.16	0.44	23.40	0.09	**99.68**
ol3-3_22	210	37.73	-	37.94	0.19	0.40	22.93	0.05	**99.24**
ol3-3_23	220	37.95	0.037	38.03	0.19	0.40	22.89	0.08	**99.57**
ol3-3_24	230	38.25	-	38.08	0.18	0.39	22.13	0.06	**99.08**
ol3-3_25	240 - Rim	38.71	-	38.23	0.18	0.37	21.71	0.06	**99.26**

Table 22: EPMA analyses of the major element composition of an olivine crystal. The dash symbol (-) represent concentration under the detection limit of the instruments.

D4 - Ol 3(2)									
Name	Distance (µm)	MgO	Al_2O_3	SiO_2	CaO	MnO	FeO	NiO	Total
Ol3(2)1_1	0.00	37.37	0.014	37.77	0.16	0.45	25.09	0.10	**100.95**
Ol3(2)1_2	14.14	37.33	-	38.15	0.19	0.47	24.99	0.05	**101.18**
Ol3(2)1_3	28.28	37.13	-	37.84	0.15	0.49	25.04	0.05	**100.70**
Ol3(2)1_4	43.42	37.39	-	37.90	0.16	0.45	25.01	0.06	**100.97**
Ol3(2)1_5	57.56	37.41	-	38.10	0.16	0.49	24.82	0.08	**101.06**
Ol3(2)1_6	71.70	37.78	0.005	37.73	0.17	0.44	25.36	0.09	**101.57**
Ol3(2)1_7	85.84	37.37	0.003	38.03	0.18	0.41	24.79	0.06	**100.84**
Ol3(2)1_8	99.99	37.69	-	38.19	0.18	0.49	25.04	0.06	**101.66**
Ol3(2)1_9	114.13	37.62	0.006	38.31	0.15	0.45	25.01	0.05	**101.59**
Ol3(2)1_10	129.26	37.57	0.018	38.04	0.16	0.43	24.86	0.03	**101.10**
Ol3(2)1_11	143.40	37.56	0.005	38.07	0.16	0.40	24.50	0.10	**100.79**
Ol3(2)1_12	157.54	37.73	0.004	38.01	0.18	0.41	24.62	0.05	**101.00**
Ol3(2)1_13	171.69	37.35	0.020	37.15	0.15	0.42	23.72	0.09	**98.90**
Ol3(2)1_14	185.83	37.86	-	38.05	0.17	0.47	24.28	0.09	**100.92**
Ol3(2)1_15	199.97	38.06	-	38.12	0.19	0.40	23.89	0.08	**100.73**
Ol3(2)1_16	215.10	37.35	0.197	38.46	0.23	0.42	24.07	0.03	**100.76**
Ol3(2)1_17	229.25	38.55	-	38.41	0.18	0.42	23.78	0.08	**101.43**
Ol3(2)1_18	243.39	38.63	-	38.29	0.15	0.46	23.27	0.10	**100.90**
Ol3(2)1_19	257.53	38.51	0.007	38.28	0.16	0.40	23.38	0.09	**100.83**
Ol3(2)1_20	271.67	38.89	-	38.08	0.19	0.47	23.32	0.09	**101.04**
Ol3(2)1_21	285.81	38.43	-	37.85	0.18	0.46	22.69	0.04	**99.65**
Ol3(2)1_22	300.95	39.43	-	38.46	0.17	0.38	22.78	0.08	**101.31**
Ol3(2)1_23	315.09	39.39	0.012	38.36	0.17	0.40	22.33	0.08	**100.74**
Ol3(2)1_24	329.23 - Rim	39.59	0.004	38.55	0.22	0.41	22.33	0.07	**101.17**

Table 23: The major element composition of an olivine crystal from sample D4. The dash symbol (-) represent concentration under the detection limit of the instruments.

D4 - Ol 4									
Name	Distance (µm)	MgO	Al_2O_3	SiO_2	CaO	MnO	FeO	NiO	Total
ol4-4_1	Core - 0	36.73	-	37.01	0.14	0.46	24.35	0.04	**98.74**
ol4-4_2	11.18	36.73	-	37.07	0.19	0.47	24.43	0.05	**98.95**
ol4-4_3	21.23	36.33	-	37.22	0.18	0.44	24.46	0.07	**98.71**
ol4-4_4	32.41	36.59	-	36.97	0.18	0.43	24.13	0.07	**98.36**
ol4-4_5	42.46	36.60	0.001	37.04	0.19	0.44	24.30	0.06	**98.63**
ol4-4_6	53.64	36.87	-	37.19	0.15	0.37	24.56	0.06	**99.19**
ol4-4_7	63.69	36.59	-	37.02	0.17	0.47	24.19	0.05	**98.49**
ol4-4_8	74.87	36.53	0.001	37.27	0.17	0.38	23.96	0.03	**98.35**
ol4-4_9	84.92	36.89	0.019	37.41	0.16	0.42	24.59	0.07	**99.55**
ol4-4_10	96.10	36.74	-	37.05	0.17	0.49	24.01	0.09	**98.55**
ol4-4_11	106.15	37.18	0.045	37.13	0.16	0.45	24.42	0.05	**99.44**
ol4-4_12	117.33	36.81	0.002	36.94	0.16	0.37	23.97	0.05	**98.31**
ol4-4_13	127.38	37.12	0.017	36.95	0.17	0.49	24.01	0.08	**98.84**
ol4-4_14	138.56	36.83	0.021	37.10	0.17	0.33	23.82	0.06	**98.33**
ol4-4_15	148.61	37.00	-	37.07	0.17	0.42	23.69	0.05	**98.40**
ol4-4_16	159.79	37.10	-	37.23	0.19	0.41	23.51	0.06	**98.49**
ol4-4_17	169.84	37.23	0.036	37.44	0.18	0.43	23.38	0.06	**98.75**
ol4-4_18	181.02	37.91	-	37.28	0.17	0.43	23.53	0.09	**99.41**
ol4-4_19	191.07 - Rim	37.75	0.008	37.59	0.17	0.39	23.04	0.03	**98.98**

Table 24: EPMA analyses of the major element composition of an olivine crystal. The dash symbol (-) represent concentration under the detection limit of the instruments.

D4 - Ol 5									
Name	Distance (µm)	MgO	Al_2O_3	SiO_2	CaO	MnO	FeO	NiO	Total
ol5-5_1	0.00	36.86	-	37.37	0.11	0.47	24.01	0.06	**98.88**
ol5-5_2	10.44	36.97	0.004	37.05	0.12	0.43	24.13	0.06	**98.77**
ol5-5_4	30.13	37.28	0.024	37.17	0.12	0.43	24.41	0.08	**99.52**
ol5-5_5	40.57	37.21	-	37.44	0.15	0.44	24.06	0.07	**99.37**
ol5-5_6	51.01	37.31	-	37.25	0.13	0.37	24.21	0.09	**99.36**
ol5-5_7	60.49	37.08	-	37.31	0.13	0.36	24.05	0.06	**99.00**
ol5-5_8	70.93	36.99	0.007	37.35	0.14	0.36	24.10	0.06	**99.01**
ol5-5_9	81.37	37.09	-	37.35	0.16	0.40	23.85	0.07	**98.92**
ol5-5_10	91.57	37.24	0.011	37.50	0.15	0.41	23.87	0.12	**99.31**
ol5-5_11	101.06	37.44	-	37.64	0.14	0.43	24.26	0.06	**99.97**
ol5-5_12	111.50	37.34	0.002	37.42	0.12	0.40	23.74	0.06	**99.08**
ol5-5_13	121.94	37.31	-	37.41	0.16	0.35	23.70	0.06	**98.99**
ol5-5_14	131.43	37.43	0.022	37.51	0.15	0.38	24.05	0.05	**99.60**
ol5-5_15	141.62	37.05	0.054	37.30	0.12	0.44	23.52	0.06	**98.53**
ol5-5_16	152.06	37.48	-	37.19	0.15	0.41	24.15	0.07	**99.44**

Table 25: The major element composition of an olivine crystal from sample D4. The dash symbol (-) represent concentration under the detection limit of the instruments.

D4 - Ol 5									
Name	Distance (µm)	MgO	Al_2O_3	SiO_2	CaO	MnO	FeO	NiO	Total
ol5-5_17	162.50	37.23	-	37.30	0.15	0.49	23.77	0.06	**99.00**
ol5-5_18	171.99	37.16	-	37.51	0.13	0.44	23.60	0.10	**98.94**
ol5-5_19	182.43	37.39	-	37.34	0.11	0.40	24.07	0.04	**99.35**
ol5-5_20	192.63	37.46	0.005	37.30	0.13	0.42	24.03	0.08	**99.44**
ol5-5_21	202.12	37.44	-	37.19	0.12	0.46	23.87	0.07	**99.15**
ol5-5_23	223.00	37.34	-	37.27	0.16	0.48	23.71	0.07	**99.03**
ol5-5_24	233.44	37.21	-	37.13	0.15	0.37	23.76	0.08	**98.70**
ol5-5_25	242.92	37.21	0.001	37.04	0.14	0.40	23.87	0.08	**98.74**
ol5-5_26	253.12	37.24	-	37.25	0.12	0.44	23.93	0.08	**99.07**
ol5-5_27	263.56	37.26	0.023	37.22	0.13	0.47	23.76	0.07	**98.92**
ol5-5_28	274.00	37.23	-	37.17	0.12	0.34	23.77	0.05	**98.67**
ol5-5_29	283.49	37.18	-	37.12	0.12	0.45	23.72	0.06	**98.64**
ol5-5_30	293.93	37.20	-	37.06	0.14	0.48	23.97	0.04	**98.88**
ol5-5_31	304.13	36.92	-	37.56	0.15	0.44	23.64	0.05	**98.75**
ol5-5_32	313.61	36.82	-	37.21	0.16	0.41	24.01	0.06	**98.68**
ol5-5_33	324.05	36.97	-	37.25	0.13	0.36	24.13	0.07	**98.91**
ol5-5_34	334.50	36.93	0.035	37.12	0.14	0.43	24.53	0.08	**99.26**
ol5-5_35	344.94	36.74	-	37.15	0.13	0.47	24.21	0.04	**98.74**
ol5-5_36	354.42	36.74	0.023	37.28	0.14	0.43	24.38	0.09	**99.09**
ol5-5_37	364.62	36.58	-	37.28	0.14	0.39	24.17	0.04	**98.62**
ol5-5_38	375.06	36.42	0.008	36.86	0.15	0.39	24.05	0.07	**97.95**
ol5-5_40	394.99	36.73	-	37.07	0.13	0.37	24.74	0.08	**99.13**
ol5-5_41	405.43	36.70	-	36.97	0.13	0.41	24.51	0.05	**98.77**
ol5-5_42	415.63	36.64	0.001	36.89	0.15	0.45	24.09	0.07	**98.28**
ol5-5_43	425.11	36.54	-	37.21	0.13	0.39	24.20	0.05	**98.52**
ol5-5_45	445.99	36.65	0.010	36.92	0.15	0.45	24.20	0.06	**98.45**
ol5-5_48	476.09	37.09	0.033	36.83	0.12	0.45	23.78	0.08	**98.37**
ol5-5_50	496.02	37.35	0.020	37.04	0.17	0.45	24.19	0.05	**99.28**
ol5-5_51	506.46	37.37	-	36.80	0.19	0.46	23.42	0.06	**98.29**
ol5-5_53	527.10	37.19	0.147	37.54	0.20	0.39	23.30	0.11	**98.87**
ol5-5_54	536.59	38.18	0.006	37.29	0.16	0.37	22.58	0.09	**98.66**
ol5-5_55	547.03 - Rim	38.54	0.008	37.36	0.18	0.38	22.01	0.07	**98.55**

Table 25: Continuation.

D4 - Ol 6									
Name	**Distance (µm)**	**MgO**	**Al_2O_3**	**SiO_2**	**CaO**	**MnO**	**FeO**	**NiO**	**Total**
ol6-6_4	Core - 28	37.01	0.024	37.21	0.14	0.42	23.63	0.06	**98.50**
ol6-6_6	47	37.35	-	37.24	0.16	0.44	23.68	0.06	**98.94**
ol6-6_8	66	36.96	-	37.19	0.16	0.41	23.77	0.08	**98.57**
ol6-6_9	75	37.47	0.014	37.06	0.15	0.45	23.86	0.07	**99.07**
ol6-6_11	94	37.26	0.027	36.96	0.12	0.48	23.72	0.10	**98.67**
ol6-6_12	103	37.10	0.015	37.08	0.14	0.34	23.78	0.07	**98.52**
ol6-6_13	113	37.38	0.015	37.26	0.16	0.43	24.14	0.06	**99.43**
ol6-6_16	141	37.14	0.023	37.37	0.13	0.39	23.90	0.08	**99.02**
ol6-6_17	150	37.49	-	37.62	0.16	0.38	24.11	0.08	**99.84**
ol6-6_18	160	37.22	0.016	37.08	0.16	0.42	24.00	0.06	**98.96**
ol6-6_22	197	37.28	-	37.39	0.20	0.39	23.86	0.09	**99.21**
ol6-6_23	206	37.34	0.007	37.32	0.15	0.45	23.55	0.07	**98.88**
ol6-6_24	216	37.17	-	37.41	0.16	0.39	24.04	0.06	**99.22**
ol6-6_25	225	37.03	-	37.09	0.14	0.44	23.80	0.06	**98.57**
ol6-6_26	235	37.41	0.032	37.33	0.17	0.39	23.96	0.08	**99.37**
ol6-6_27	244	37.46	-	37.47	0.17	0.40	24.08	0.05	**99.64**
ol6-6_28	253	37.45	-	37.63	0.18	0.39	23.82	0.06	**99.53**
ol6-6_29	263	37.33	0.026	37.36	0.17	0.40	23.74	0.03	**99.05**
ol6-6_30	272	37.31	-	37.16	0.16	0.38	23.90	0.05	**98.96**
ol6-6_31	282	37.51	0.015	38.00	0.14	0.39	23.63	0.08	**99.79**
ol6-6_32	291	37.49	-	37.50	0.17	0.43	23.61	0.07	**99.28**
ol6-6_33	300	37.33	-	37.28	0.18	0.40	23.39	0.07	**98.65**
ol6-6_34	310	37.71	0.011	37.49	0.16	0.41	23.68	0.08	**99.54**
ol6-6_35	319	37.42	0.006	37.20	0.17	0.43	23.25	0.07	**98.55**
ol6-6_37	338	37.85	-	37.58	0.16	0.37	23.16	0.06	**99.18**
ol6-6_38	347	38.09	-	37.62	0.20	0.38	23.15	0.06	**99.49**
ol6-6_39	357 - Rim	38.04	0.000	37.23	0.19	0.39	22.77	0.07	**98.69**

Table 26: EPMA analyses of the major element composition of an olivine crystal. The dash symbol (-) represent concentration under the detection limit of the instruments.

Appendix V – Sample D5A (1) and D5A (2)

This appendix contains the major element analyses of13 olivines and 4 pyroxenes. Moreover, in this appendix can be found the trace element analyses of 8 pyroxenes.

D5A(1) - Ol 1									
Name	**Distance (µm)**	**MgO**	**Al_2O_3**	**SiO_2**	**CaO**	**MnO**	**FeO**	**NiO**	**Total**
Ol1-2_1	Core - 0	46.53	0.002	40.39	0.20	0.19	13.20	0.20	**100.71**
Ol1-2_2	9.49	46.38	-	40.27	0.23	0.20	12.97	0.20	**100.27**
Ol1-2_3	18.97	45.96	-	40.16	0.24	0.19	12.83	0.21	**99.61**
Ol1-2_4	28.82	46.57	0.018	40.75	0.24	0.19	12.93	0.23	**100.94**
Ol1-2_5	37.37	46.13	0.017	40.17	0.24	0.19	12.95	0.19	**99.88**
Ol1-2_6	46.85	46.44	0.028	39.93	0.26	0.23	12.70	0.19	**99.78**
Ol1-2_7	56.34	46.38	0.026	40.20	0.20	0.22	12.57	0.20	**99.80**
Ol1-2_8	66.19	45.91	0.003	40.33	0.22	0.20	12.39	0.19	**99.24**
Ol1-2_9	75.68	46.32	-	40.31	0.23	0.20	12.81	0.22	**100.07**
Ol1-2_10	85.16	46.56	0.018	40.17	0.22	0.17	12.29	0.23	**99.66**
Ol1-2_11	93.71	46.35	0.025	40.33	0.22	0.19	12.53	0.21	**99.85**
Ol1-2_12	103.56	46.73	-	40.34	0.24	0.17	12.46	0.24	**100.17**
Ol1-2_13	113.04	46.77	0.028	40.27	0.23	0.20	12.35	0.23	**100.08**
Ol1-2_14	122.53	46.56	-	39.92	0.23	0.18	12.26	0.25	**99.40**
Ol1-2_15	132.02	46.70	0.018	40.48	0.26	0.22	12.46	0.25	**100.39**
Ol1-2_16	141.86	46.49	0.006	40.49	0.24	0.16	12.11	0.28	**99.78**
Ol1-2_17	150.41	46.40	0.009	40.16	0.24	0.18	12.19	0.24	**99.42**
Ol1-2_18	159.90	46.85	0.005	40.35	0.24	0.24	12.25	0.27	**100.21**
Ol1-2_19	169.38	46.29	-	40.20	0.25	0.19	12.03	0.26	**99.22**
Ol1-2_20	179.23	47.03	-	40.47	0.22	0.23	12.07	0.26	**100.28**
Ol1-2_21	188.72	46.69	0.022	40.41	0.27	0.20	12.04	0.27	**99.90**
Ol1-2_22	198.21	47.31	-	40.98	0.22	0.22	12.37	0.25	**101.34**
Ol1-2_23	206.75	47.55	-	40.91	0.26	0.16	12.23	0.27	**101.39**
Ol1-2_24	216.60	46.61	0.030	40.46	0.26	0.16	12.30	0.26	**100.09**
Ol1-2_25	226.08	46.68	-	40.78	0.26	0.25	12.17	0.27	**100.40**
Ol1-2_26	235.57	47.07	-	40.61	0.24	0.16	12.16	0.27	**100.50**
Ol1-2_27	245.06	47.02	0.005	40.76	0.27	0.19	12.43	0.30	**100.97**
Ol1-2_28	263.45	47.13	0.020	40.87	0.28	0.14	12.37	0.23	**101.03**
Ol1-2_29	272.94	47.09	0.009	40.91	0.24	0.21	12.49	0.25	**101.20**
Ol1-2_30	282.43	46.48	0.008	40.50	0.24	0.18	12.33	0.23	**99.97**
Ol1-2_31	292.27	46.86	0.047	40.52	0.25	0.23	12.46	0.23	**100.60**
Ol1-2_32	301.76	46.66	-	40.94	0.23	0.20	12.46	0.25	**100.74**
Ol1-2_33	319.79	46.76	0.012	40.54	0.24	0.27	12.50	0.25	**100.57**
Ol1-2_34	358.10	46.66	0.000	40.98	0.21	0.17	13.00	0.26	**101.28**
Ol1-2_35	376.49	46.41	0.002	41.03	0.22	0.25	13.13	0.21	**101.24**

Table 27: The major element composition of an olivine crystal from sample D5A(1).. The dash symbol (-) represent concentration under the detection limit of the instruments.

D5A(1) - Ol 1									
Name	Distance (µm)	MgO	Al_2O_3	SiO_2	CaO	MnO	FeO	NiO	Total
Ol1-2_36	385.98	46.49	-	41.06	0.23	0.22	13.11	0.22	**101.32**
Ol1-2_37	395.47	45.85	0.007	40.26	0.20	0.23	12.99	0.21	**99.74**
Ol1-2_38	424.29	46.17	0.042	40.88	0.24	0.19	13.60	0.19	**101.31**
Ol1-2_39	432.83	46.04	0.019	40.66	0.21	0.27	13.89	0.21	**101.30**
Ol1-2_40	442.68	45.82	0.006	40.54	0.21	0.21	14.11	0.20	**101.10**
Ol1-2_41	452.17	45.47	0.007	40.33	0.22	0.16	14.12	0.19	**100.51**
Ol1-2_42	461.66 - Rim	45.34	0.014	40.65	0.24	0.25	14.40	0.18	**101.08**

Table 27: Continuation.

D5A(1) - Ol 2									
Name	Distance (µm)	MgO	Al_2O_3	SiO_2	CaO	MnO	FeO	NiO	Total
Ol2-2_1	Core - 0	41.87	0.030	38.96	0.20	0.26	18.15	0.12	**99.59**
Ol2-2_2	9.90	41.75	0.020	38.80	0.18	0.29	18.22	0.15	**99.40**
Ol2-2_3	20.53	41.59	0.029	39.28	0.23	0.30	18.08	0.14	**99.64**
Ol2-2_4	30.43	42.16	-	39.44	0.21	0.34	18.49	0.15	**100.78**
Ol2-2_5	41.06	42.46	-	39.67	0.22	0.29	17.95	0.15	**100.74**
Ol2-2_6	50.96	42.27	0.022	39.49	0.22	0.27	18.15	0.15	**100.57**
Ol2-2_7	60.86	41.81	0.022	39.26	0.22	0.28	18.03	0.12	**99.74**
Ol2-2_8	71.49	41.65	0.002	38.86	0.19	0.30	17.96	0.12	**99.09**
Ol2-2_9	82.12	42.19	-	39.84	0.22	0.34	18.08	0.12	**100.80**
Ol2-2_10	92.75	42.27	-	40.03	0.20	0.27	17.87	0.15	**100.80**
Ol2-2_11	102.65	41.68	-	39.29	0.22	0.28	17.85	0.13	**99.45**
Ol2-2_12	113.28	42.37	-	39.78	0.24	0.28	17.78	0.12	**100.56**
Ol2-2_13	123.18	42.04	0.021	39.53	0.20	0.30	18.05	0.14	**100.28**
Ol2-2_14	133.08	42.73	0.008	39.90	0.20	0.29	18.25	0.14	**101.51**
Ol2-2_15	143.71	42.67	0.014	39.72	0.21	0.22	17.87	0.14	**100.85**
Ol2-2_16	153.61	42.29	0.029	39.71	0.21	0.31	17.97	0.13	**100.66**
Ol2-2_17	164.24	42.30	-	39.75	0.22	0.32	17.99	0.14	**100.71**
Ol2-2_18	174.14	42.31	-	39.58	0.20	0.28	17.81	0.10	**100.30**
Ol2-2_19	184.04	42.59	0.003	39.74	0.20	0.28	17.58	0.15	**100.55**
Ol2-2_20	194.67	42.44	-	39.83	0.20	0.31	17.84	0.15	**100.78**
Ol2-2_21	204.57	42.57	0.009	39.65	0.22	0.28	17.95	0.15	**100.83**
Ol2-2_22	215.20	42.14	-	39.72	0.20	0.27	17.44	0.11	**99.88**
Ol2-2_23	225.83	43.02	0.019	40.25	0.21	0.34	17.37	0.13	**101.34**
Ol2-2_24	236.46	42.76	-	39.87	0.21	0.32	17.35	0.14	**100.65**
Ol2-2_25	256.26	43.07	0.008	40.24	0.17	0.29	17.18	0.15	**101.10**
Ol2-2_26	266.89	43.19	-	40.40	0.21	0.31	17.11	0.15	**101.37**
Ol2-2_27	276.78	43.23	0.003	40.10	0.20	0.29	16.74	0.14	**100.71**
Ol2-2_28	297.31	42.33	0.014	40.18	0.20	0.31	17.61	0.17	**100.82**

Table 28: EPMA analyses of the major element composition of an olivine crystal. The dash symbol (-) represent concentration under the detection limit of the instruments.

D5A(1) - Ol 3 (1)									
Name	Distance (µm)	MgO	Al_2O_3	SiO_2	CaO	MnO	FeO	NiO	Total
Ol3-3_2	Core - 11	46.61	0.010	40.44	0.23	0.15	12.95	0.25	**100.63**
Ol3-3_3	21	46.57	-	40.77	0.22	0.14	12.97	0.26	**100.94**
Ol3-3_4	32	46.54	0.035	40.92	0.25	0.20	13.31	0.24	**101.51**
Ol3-3_6	53	45.64	0.003	40.65	0.24	0.23	13.85	0.29	**100.91**
Ol3-3_7	63	45.68	0.021	40.49	0.21	0.19	14.25	0.26	**101.11**
Ol3-3_8	74	44.95	0.017	40.24	0.23	0.18	14.17	0.28	**100.05**
Ol3-3_9	84	45.20	0.014	40.57	0.21	0.23	14.95	0.23	**101.41**
Ol3-3_13	127	44.23	0.002	40.25	0.22	0.25	16.02	0.23	**101.19**
Ol3-3_14	137	43.96	-	39.97	0.20	0.27	16.05	0.21	**100.66**
Ol3-3_15	148	43.90	0.008	40.27	0.20	0.26	15.95	0.24	**100.83**
Ol3-3_16	158	43.89	-	40.06	0.21	0.26	15.93	0.25	**100.59**
Ol3-3_17	169	43.61	0.005	39.95	0.20	0.17	15.76	0.22	**99.91**
Ol3-3_19	190	44.20	0.012	40.14	0.23	0.26	16.19	0.25	**101.30**
Ol3-3_20	201	44.08	0.005	40.49	0.23	0.25	16.13	0.22	**101.41**
Ol3-3_21	211	43.83	0.006	40.29	0.21	0.26	16.05	0.23	**100.87**
Ol3-3_23	232	43.81	0.011	40.43	0.20	0.31	16.18	0.22	**101.15**
Ol3-3_24	243	43.84	0.015	40.37	0.22	0.29	16.16	0.23	**101.13**
Ol3-3_25	253	43.69	0.018	40.22	0.22	0.28	16.34	0.23	**101.00**
Ol3-3_26	264	43.53	0.010	40.00	0.21	0.22	16.49	0.22	**100.67**
Ol3-3_27	275	43.36	0.018	40.16	0.21	0.22	17.02	0.20	**101.19**
Ol3-3_29	296	43.04	0.025	40.31	0.16	0.28	17.12	0.24	**101.16**
Ol3-3_30	306	42.69	-	40.09	0.18	0.29	17.58	0.23	**101.05**
Ol3-3_31	317	42.38	0.008	39.65	0.19	0.28	17.43	0.18	**100.13**
Ol3-3_32	327	41.72	0.017	39.41	0.17	0.32	17.73	0.18	**99.55**
Ol3-3_33	338	41.63	0.026	39.61	0.18	0.36	18.54	0.17	**100.51**
Ol3-3_34	348	41.63	0.014	39.38	0.17	0.34	18.94	0.14	**100.62**
Ol3-3_35	359 - Rim	41.36	0.028	39.79	0.17	0.30	19.00	0.14	**100.80**

Table 29: The major element composition of an olivine crystal from sample D5A(1).. The dash symbol (-) represent concentration under the detection limit of the instruments.

D5A(1) - Ol 3 (2)									
Name	Distance (µm)	MgO	Al_2O_3	SiO_2	CaO	MnO	FeO	NiO	Total
ol3(2)1_1	Core - 0	47.55	-	40.41	0.24	0.22	11.85	0.31	**100.57**
ol3(2)1_2	9.43	47.75	0.012	40.49	0.24	0.20	12.24	0.24	**101.16**
ol3(2)1_3	18.38	47.52	0.006	40.55	0.25	0.25	11.84	0.27	**100.69**
ol3(2)1_4	27.81	47.41	0.006	40.34	0.27	0.19	12.13	0.26	**100.61**
ol3(2)1_5	37.25	47.55	0.035	40.40	0.24	0.21	12.25	0.31	**100.99**
ol3(2)1_6	47.10	24.90	0.469	22.00	0.17	0.12	6.25	0.10	**54.01**
ol3(2)1_7	56.53	46.87	0.014	39.94	0.24	0.26	12.60	0.28	**100.19**
ol3(2)1_8	65.96	46.87	0.030	40.14	0.24	0.16	13.14	0.21	**100.78**
ol3(2)1_9	74.91	46.92	0.003	40.34	0.23	0.16	13.38	0.25	**101.28**
ol3(2)1_10	84.34	46.48	0.038	40.31	0.23	0.22	13.30	0.28	**100.86**
ol3(2)1_11	93.78	46.33	0.027	40.25	0.24	0.27	13.52	0.25	**100.89**
ol3(2)1_12	102.72	46.35	0.013	40.27	0.24	0.27	13.75	0.27	**101.15**
ol3(2)1_13	112.15	45.95	-	40.03	0.26	0.24	14.43	0.25	**101.17**
ol3(2)1_14	121.59	45.51	0.018	39.90	0.21	0.25	14.66	0.25	**100.80**
ol3(2)1_15	130.53	45.19	0.018	39.86	0.21	0.25	14.56	0.25	**100.34**
ol3(2)1_16	140.83	45.03	0.022	39.72	0.23	0.22	15.20	0.29	**100.71**
ol3(2)1_17	150.26	43.65	0.033	38.74	0.20	0.29	15.39	0.25	**98.55**
ol3(2)1_18	159.21	44.39	0.043	39.58	0.23	0.26	15.57	0.19	**100.28**
ol3(2)1_19	168.64	44.20	0.033	39.67	0.19	0.28	16.33	0.18	**100.88**
ol3(2)1_20	178.07	44.14	0.004	39.49	0.19	0.28	16.63	0.21	**100.94**
ol3(2)1_21	187.02	43.69	0.002	39.51	0.20	0.29	17.07	0.18	**100.95**
ol3(2)1_22	196.45	42.72	-	39.18	0.17	0.29	17.32	0.15	**99.83**
ol3(2)1_23	205.89	42.54	0.030	38.73	0.19	0.28	17.80	0.19	**99.75**
ol3(2)1_24	214.83	42.45	0.038	38.98	0.19	0.29	17.79	0.18	**99.92**
ol3(2)1_25	224.26	42.59	-	38.93	0.20	0.30	18.22	0.12	**100.36**
ol3(2)1_26	234.56	42.47	-	39.03	0.19	0.29	18.50	0.19	**100.67**
ol3(2)1_27	243.50	42.17	0.031	38.94	0.20	0.28	18.45	0.20	**100.27**
ol3(2)1_28	252.94	42.06	-	39.03	0.19	0.30	18.84	0.15	**100.56**
ol3(2)1_29	262.37	41.89	0.001	38.71	0.20	0.36	18.73	0.17	**100.07**
ol3(2)1_30	271.32	42.00	0.014	39.14	0.21	0.34	19.13	0.13	**100.96**
ol3(2)1_31	290.18	41.56	-	38.94	0.22	0.29	18.77	0.14	**99.92**
ol3(2)1_32	299.62	41.84	-	38.87	0.20	0.32	19.10	0.16	**100.50**
ol3(2)1_33	317.98	41.54	-	38.70	0.17	0.38	18.80	0.18	**99.76**
ol3(2)1_34	327.41	41.50	0.027	38.91	0.19	0.38	19.24	0.17	**100.42**
ol3(2)1_35	346.65	41.55	-	38.57	0.19	0.38	19.43	0.13	**100.25**
ol3(2)1_36	356.49	41.76	0.031	38.81	0.15	0.37	19.81	0.17	**101.09**
ol3(2)1_37	375.36	41.52	0.018	38.93	0.18	0.33	19.53	0.12	**100.62**
ol3(2)1_38	384.80	41.63	0.031	38.92	0.19	0.33	18.80	0.13	**100.04**
ol3(2)1_39	403.15	41.58	-	38.91	0.16	0.34	19.06	0.12	**100.18**
ol3(2)1_40	412.59 - Rim	39.99	0.003	38.50	0.20	0.36	21.01	0.09	**100.15**

Table 30: EPMA analyses of the major element composition of an olivine crystal. The dash symbol (-) represent concentration under the detection limit of the instruments.

D5A(1) - Ol 4 (2)									
Name	Distance (µm)	MgO	Al_2O_3	SiO_2	CaO	MnO	FeO	NiO	Total
ol4(2)1_1	0.00	48.56	0.010	40.44	0.21	0.21	10.45	0.27	**100.16**
ol4(2)1_2	14.14	48.59	0.030	40.66	0.20	0.18	10.41	0.30	**100.35**
ol4(2)1_3	27.48	48.65	0.014	40.45	0.24	0.18	10.29	0.35	**100.17**
ol4(2)1_4	41.63	48.51	-	40.70	0.23	0.17	10.11	0.37	**100.09**
ol4(2)1_5	55.94	48.68	0.016	40.41	0.20	0.18	10.25	0.33	**100.06**
ol4(2)1_6	70.09	49.02	0.005	40.66	0.19	0.16	9.98	0.38	**100.39**
ol4(2)1_7	83.43	48.88	0.024	40.79	0.21	0.18	10.22	0.33	**100.63**
ol4(2)1_8	97.57	48.90	0.016	40.80	0.22	0.15	10.22	0.37	**100.67**
ol4(2)1_9	111.89	48.79	0.018	40.61	0.19	0.17	9.93	0.27	**99.98**
ol4(2)1_10	126.03	48.90	0.022	40.75	0.20	0.19	10.06	0.29	**100.40**
ol4(2)1_11	139.37	48.77	0.013	40.77	0.21	0.17	9.97	0.37	**100.28**
ol4(2)1_12	153.51	49.01	0.007	40.74	0.21	0.21	10.13	0.29	**100.61**
ol4(2)1_13	167.83	48.64	0.032	40.75	0.22	0.17	9.84	0.30	**99.95**
ol4(2)1_14	181.97	49.00	0.007	40.55	0.21	0.18	9.96	0.28	**100.19**
ol4(2)1_15	195.32	50.84	0.060	42.85	0.26	0.22	9.90	0.38	**104.51**
ol4(2)1_16	209.46	48.89	0.012	40.56	0.21	0.17	9.97	0.36	**100.16**
ol4(2)1_17	223.78	48.83	0.001	40.92	0.21	0.14	9.87	0.31	**100.29**
ol4(2)1_18	236.93	48.89	0.006	40.75	0.22	0.19	9.77	0.41	**100.24**
ol4(2)1_19	251.25	48.90	0.000	40.88	0.20	0.19	9.77	0.32	**100.26**
ol4(2)1_20	265.39	48.66	0.024	40.74	0.22	0.20	10.00	0.31	**100.17**
ol4(2)1_21	279.71	48.95	0.033	40.51	0.25	0.19	9.95	0.33	**100.21**
ol4(2)1_22	292.86	48.84	-	40.78	0.18	0.19	9.73	0.38	**100.09**
ol4(2)1_23	307.18	49.01	0.027	40.62	0.20	0.15	10.12	0.32	**100.45**
ol4(2)1_24	321.32	48.72	-	40.57	0.23	0.16	9.80	0.30	**99.77**
ol4(2)1_25	335.64	48.96	0.024	40.60	0.23	0.18	9.96	0.31	**100.27**
ol4(2)1_26	348.79	48.79	0.018	40.89	0.21	0.11	9.88	0.32	**100.23**
ol4(2)1_27	363.11	48.70	0.023	40.88	0.22	0.17	9.95	0.37	**100.32**
ol4(2)1_28	377.25	48.45	0.022	40.67	0.21	0.17	9.86	0.37	**99.76**
ol4(2)1_29	391.39	48.56	0.009	40.75	0.21	0.16	10.17	0.36	**100.23**
ol4(2)1_30	404.73	48.41	-	40.65	0.21	0.12	10.14	0.28	**99.81**
ol4(2)1_31	433.18	48.46	0.012	40.95	0.20	0.16	10.21	0.31	**100.29**
ol4(2)1_32	447.49	48.59	-	40.64	0.21	0.18	10.46	0.30	**100.38**
ol4(2)1_33	474.95	48.54	0.014	40.68	0.21	0.18	10.30	0.33	**100.26**
ol4(2)1_34	489.27	48.38	0.023	40.65	0.22	0.17	10.49	0.31	**100.23**
ol4(2)1_35	517.71	48.35	0.008	40.58	0.23	0.21	10.48	0.30	**100.16**
ol4(2)1_36	532.03	48.27	0.002	40.64	0.22	0.13	10.55	0.27	**100.08**
ol4(2)1_37	559.49	48.28	0.004	40.48	0.20	0.18	10.58	0.32	**100.05**
ol4(2)1_38	573.81	48.04	0.016	40.46	0.21	0.20	10.90	0.41	**100.23**
ol4(2)1_39	602.25	48.35	0.037	40.56	0.21	0.16	10.71	0.31	**100.33**
ol4(2)1_40	616.57	48.10	0.007	40.50	0.21	0.17	11.10	0.31	**100.38**

Table 31: The major element composition of an olivine crystal from sample D5A(1).. The dash symbol (-) represent concentration under the detection limit of the instruments.

D5A(1) - Ol 4 (2)									
Name	Distance (µm)	MgO	Al_2O_3	SiO_2	CaO	MnO	FeO	NiO	Total
ol4(2)1_41	644.03	48.30	0.039	40.45	0.22	0.20	11.09	0.27	**100.57**
ol4(2)1_42	658.35	45.67	0.064	38.46	0.22	0.16	10.94	0.31	**95.83**
ol4(2)1_43	672.49	47.75	0.025	40.35	0.20	0.21	11.31	0.37	**100.21**
ol4(2)1_44	686.81	47.49	0.024	40.38	0.20	0.18	11.52	0.32	**100.12**
ol4(2)1_45	699.96	44.88	0.100	38.39	0.25	0.16	11.42	0.32	**95.52**
ol4(2)1_46	714.28	47.13	0.038	40.15	0.20	0.18	11.54	0.25	**99.48**
ol4(2)1_47	728.42	47.63	-	40.43	0.20	0.21	11.86	0.25	**100.57**
ol4(2)1_48	742.74	47.24	-	40.41	0.20	0.14	11.92	0.34	**100.24**
ol4(2)1_49	755.89	47.48	-	40.34	0.19	0.16	11.87	0.34	**100.38**
ol4(2)1_50	770.21	26.81	0.122	24.01	0.32	0.09	6.40	0.09	**57.85**
ol4(2)1_51	784.35	46.67	-	39.89	0.19	0.23	12.27	0.33	**99.58**
ol4(2)1_52	797.69	46.78	0.041	40.13	0.17	0.16	12.19	0.27	**99.74**
ol4(2)1_53	811.83	46.85	0.022	40.06	0.18	0.17	12.61	0.28	**100.17**
ol4(2)1_54	825.98	46.61	-	40.24	0.17	0.24	12.70	0.28	**100.24**
ol4(2)1_55	840.29	46.60	-	40.05	0.16	0.25	12.91	0.21	**100.18**
ol4(2)1_56	853.45	46.56	-	39.69	0.18	0.21	13.15	0.26	**100.04**
ol4(2)1_57	867.76	46.30	0.035	39.95	0.21	0.21	12.99	0.22	**99.90**
ol4(2)1_58	881.91	46.58	0.002	40.05	0.20	0.24	12.97	0.25	**100.29**
ol4(2)1_59	896.22	46.35	0.026	40.04	0.20	0.24	13.23	0.30	**100.39**
ol4(2)1_60	909.38	46.43	0.023	40.08	0.20	0.18	13.25	0.29	**100.45**
ol4(2)1_61	923.69	46.41	-	40.06	0.19	0.21	13.33	0.30	**100.52**
ol4(2)1_62	937.84	46.09	-	40.19	0.20	0.29	13.31	0.22	**100.30**
ol4(2)1_63	952.15	46.39	0.008	40.02	0.21	0.25	13.62	0.23	**100.74**
ol4(2)1_64	965.31	46.33	-	40.16	0.22	0.21	13.36	0.23	**100.53**
ol4(2)1_65	979.63	46.24	0.019	39.94	0.19	0.23	13.67	0.21	**100.50**
ol4(2)1_66	993.77	46.12	-	39.99	0.19	0.26	13.71	0.25	**100.52**
ol4(2)1_67	1007.11	45.87	0.009	40.09	0.21	0.20	13.59	0.20	**100.17**
ol4(2)1_68	1021.25	46.27	-	39.94	0.17	0.24	14.03	0.28	**100.94**
ol4(2)1_69	1035.57	45.77	0.030	39.94	0.21	0.28	13.71	0.22	**100.16**
ol4(2)1_70	1049.71	45.74	0.029	40.02	0.19	0.26	13.85	0.21	**100.30**
ol4(2)1_71	1063.05	46.07	0.005	39.88	0.20	0.26	13.95	0.23	**100.59**
ol4(2)1_72	1077.20	43.89	0.043	38.65	0.23	0.18	13.27	0.21	**96.48**
ol4(2)1_73	1091.51	45.57	-	39.95	0.22	0.22	14.09	0.23	**100.29**
ol4(2)1_74	1105.66	45.88	-	40.00	0.21	0.23	14.04	0.20	**100.56**
ol4(2)1_75	1119.00	45.90	0.025	40.08	0.23	0.23	13.97	0.22	**100.66**
ol4(2)1_76	1133.14	46.01	0.012	40.03	0.22	0.27	14.16	0.17	**100.87**
ol4(2)1_77	1147.46	45.68	0.003	39.94	0.20	0.24	13.97	0.19	**100.22**
ol4(2)1_78	1161.60	45.33	0.009	39.97	0.18	0.25	14.48	0.19	**100.41**
ol4(2)1_79	1174.94	44.82	-	39.67	0.19	0.28	15.33	0.13	**100.42**
ol4(2)1_80	1189.08	43.00	-	39.21	0.22	0.28	17.50	0.15	**100.36**

Table 31: Continuation.

D5A(1) - Ol 4 (1)									
Name	Distance (µm)	MgO	Al_2O_3	SiO_2	CaO	MnO	FeO	NiO	Total
Ol4-4_1	Core - 0	48.49	-	41.47	0.19	0.19	10.33	0.32	**100.99**
Ol4-4_2	10.20	48.59	0.003	41.53	0.22	0.16	10.42	0.36	**101.28**
Ol4-4_4	31.58	48.61	0.015	41.90	0.23	0.18	10.16	0.34	**101.43**
Ol4-4_5	42.76	48.47	0.048	41.19	0.23	0.18	10.05	0.35	**100.52**
Ol4-4_6	52.95	48.10	+	41.19	0.22	0.15	9.92	0.33	**99.91**
Ol4-4_7	64.14	48.54	0.006	41.31	0.22	0.14	10.07	0.35	**100.64**
Ol4-4_8	74.33	47.90	0.001	41.19	0.20	0.20	9.89	0.34	**99.71**
Ol4-4_9	85.51	48.26	0.003	40.97	0.22	0.16	10.11	0.35	**100.08**
Ol4-4_10	95.71	48.00	0.016	41.21	0.21	0.19	10.16	0.33	**100.12**
Ol4-4_11	105.91	47.82	0.026	41.41	0.25	0.20	10.34	0.36	**100.40**
Ol4-4_12	117.09	47.99	+	41.19	0.21	0.15	10.37	0.30	**100.21**
Ol4-4_13	127.29	47.67	0.030	41.27	0.22	0.19	10.40	0.30	**100.08**
Ol4-4_14	138.47	47.96	0.021	40.89	0.21	0.15	10.34	0.32	**99.89**
Ol4-4_15	148.67	47.76	0.001	40.87	0.22	0.18	10.61	0.31	**99.96**
Ol4-4_16	159.85	48.36	0.019	41.26	0.21	0.20	10.48	0.32	**100.84**
Ol4-4_17	170.04	48.28	0.014	41.39	0.19	0.21	10.70	0.32	**101.11**
Ol4-4_18	181.23	47.48	0.017	41.03	0.21	0.17	10.51	0.31	**99.73**
Ol4-4_19	191.42	48.26	0.002	41.51	0.22	0.17	10.56	0.34	**101.07**
Ol4-4_20	202.60	48.41	+	41.66	0.23	0.15	10.63	0.29	**101.37**
Ol4-4_21	212.80	48.01	0.004	41.14	0.21	0.16	10.47	0.32	**100.31**
Ol4-4_22	223.00	47.73	0.026	40.90	0.21	0.18	10.40	0.31	**99.76**
Ol4-4_23	234.18	47.97	0.029	41.30	0.24	0.15	10.28	0.27	**100.23**
Ol4-4_24	244.38	47.85	0.011	40.96	0.24	0.15	10.16	0.34	**99.71**
Ol4-4_25	255.56	48.28	0.024	41.33	0.21	0.14	10.24	0.31	**100.54**
Ol4-4_26	266.00	48.53	-	41.45	0.22	0.16	10.55	0.33	**101.25**
Ol4-4_27	277.18	50.00	0.016	40.32	0.21	0.23	10.39	0.35	**101.52**
Ol4-4_28	287.38	48.41	0.027	41.62	0.23	0.14	10.30	0.31	**101.03**
Ol4-4_29	298.56	48.38	0.034	41.46	0.23	0.13	10.31	0.35	**100.91**
Ol4-4_30	308.76	48.10	0.013	41.52	0.23	0.15	10.47	0.35	**100.83**
Ol4-4_31	318.95	48.28	0.008	41.22	0.25	0.15	10.49	0.33	**100.72**
Ol4-4_32	330.13	48.40	-	41.42	0.21	0.21	10.74	0.32	**101.30**
Ol4-4_34	351.51	48.17	-	41.46	0.22	0.19	10.74	0.34	**101.11**
Ol4-4_36	372.89	47.85	0.032	41.28	0.21	0.16	11.13	0.33	**101.00**
Ol4-4_37	383.09	47.55	-	41.09	0.22	0.18	11.35	0.32	**100.71**
Ol4-4_38	394.27	47.39	0.009	41.18	0.24	0.24	11.52	0.36	**100.94**
Ol4-4_39	404.47	47.32	0.015	41.38	0.21	0.17	11.53	0.34	**100.96**
Ol4-4_40	415.65	47.46	0.017	40.90	0.22	0.18	11.92	0.30	**101.00**
Ol4-4_41	425.85	47.10	-	40.86	0.20	0.20	12.14	0.36	**100.87**
Ol4-4_42	436.04	46.67	0.010	40.89	0.21	0.21	12.07	0.29	**100.34**
Ol4-4_43	447.22	46.67	0.008	40.83	0.20	0.20	12.58	0.27	**100.76**

Table 32: EPMA analyses of the major element composition of an olivine crystal. The dash symbol (-) represent concentration under the detection limit of the instruments.

D5A(1) - Ol 4 (1)									
Name	Distance (µm)	MgO	Al_2O_3	SiO_2	CaO	MnO	FeO	NiO	Total
Ol4-4_44	457.42	46.55	0.008	40.64	0.21	0.18	12.55	0.28	**100.42**
Ol4-4_45	468.60	46.59	0.027	40.94	0.20	0.19	12.90	0.26	**101.12**
Ol4-4_46	478.80	46.06	0.025	40.44	0.19	0.18	13.18	0.24	**100.31**
Ol4-4_47	489.98	46.04	0.000	40.50	0.22	0.21	13.35	0.24	**100.55**
Ol4-4_48	500.18	45.71	0.022	40.47	0.22	0.25	13.42	0.23	**100.32**
Ol4-4_49	511.36	44.81	-	40.32	0.21	0.22	15.03	0.20	**100.79**
Ol4-4_50	521.56 - Rim	41.78	0.008	39.39	0.24	0.38	18.34	0.14	**100.29**

Table 32: Continuation.

D5A(1) - Ol 5									
Name	Location	MgO	Al_2O_3	SiO_2	CaO	MnO	FeO	NiO	Total
Ol6-1	Core 1	46.79	0.01	40.83	0.25	0.21	13.13	0.28	**101.50**
Ol6-2	Core 2	46.49	0.01	40.54	0.21	0.22	12.90	0.26	**100.62**
Ol6-2	Core 3	48.74	0.03	41.77	0.17	0.19	10.24	0.25	**101.40**
Ol6-3	Core 4	45.52	0.01	40.47	0.15	0.21	13.52	0.24	**100.12**
Ol6-4	Rim 1	38.70	0.02	38.85	0.17	0.45	22.70	0.11	**101.00**
Ol6-5	Rim 2	37.95	0.01	38.50	0.16	0.42	22.21	0.09	**99.34**

Table 33: The major element composition of an olivine crystal from sample D5A(1). The dash symbol (-) represent concentration under the detection limit of the instruments.

D5A(1) - Ol 6									
Name	Distance (µm)	MgO	Al_2O_3	SiO_2	CaO	MnO	FeO	NiO	Total
Ol7-1	Core 1	36.21	-	37.23	0.14	0.58	24.86	0.04	**99.06**
Ol7- 2	Core 2	36.12	-	37.34	0.15	0.53	24.65	0.03	**98.83**
Ol7-3	Core 3	37.45	0.04	38.20	0.13	0.56	23.92	0.05	**100.37**
Ol7- 4	Rim 1	37.18	-	38.49	0.13	0.48	24.63	0.05	**100.96**
Ol7 -	Rim 2	37.37	-	38.84	0.13	0.46	24.60	0.05	**101.43**

Table 34: EPMA analyses of the major element composition of an olivine crystal. The dash symbol (-) represent concentration under the detection limit of the instruments.

D5A(1) - Ol 7									
Name	Distance (µm)	MgO	Al_2O_3	SiO_2	CaO	MnO	FeO	NiO	Total
Ol7-7_1	Core - 0	43.07	0.011	39.89	0.11	0.33	17.21	0.18	**100.80**
Ol7-7_2	9.85	42.98	0.025	40.14	0.14	0.28	17.55	0.14	**101.26**
Ol7-7_3	21.03	42.45	-	39.66	0.13	0.30	17.51	0.16	**100.21**
Ol7-7_4	30.88	42.41	0.014	39.61	0.12	0.30	17.31	0.11	**99.88**
Ol7-7_5	41.65	43.19	-	39.88	0.13	0.32	18.02	0.13	**101.66**
Ol7-7_6	51.50	42.66	-	39.96	0.14	0.32	17.39	0.15	**100.62**
Ol7-7_7	62.68	42.19	0.018	39.51	0.15	0.29	17.43	0.14	**99.72**
Ol7-7_8	72.53	41.77	0.030	39.30	0.16	0.28	17.52	0.16	**99.21**
Ol7-7_9	82.38	42.03	0.000	39.25	0.14	0.30	17.62	0.12	**99.45**
Ol7-7_10	93.15	42.38	-	39.73	0.16	0.29	18.22	0.15	**100.92**
Ol7-7_11	103.44	42.20	0.002	39.86	0.17	0.24	18.13	0.12	**100.72**
Ol7-7_12	114.21	41.97	0.002	40.25	0.15	0.34	18.11	0.12	**100.94**
Ol7-7_13	124.06	42.17	-	39.79	0.18	0.33	18.34	0.11	**100.92**
Ol7-7_14	133.91	45.37	0.046	37.03	0.18	0.27	18.11	0.11	**101.10**
Ol7-7_15	145.09	42.50	0.013	39.98	0.16	0.29	18.54	0.15	**101.64**
Ol7-7_16	154.94	42.11	0.013	39.88	0.17	0.32	17.77	0.11	**100.37**
Ol7-7_17	165.71	42.40	0.013	39.84	0.18	0.31	17.85	0.12	**100.72**
Ol7-7_18	175.56	42.40	0.007	39.88	0.21	0.30	17.84	0.13	**100.76**
Ol7-7_19	186.74	41.83	-	39.79	0.20	0.32	18.13	0.13	**100.39**
Ol7-7_20	196.59	39.76	0.016	38.81	0.23	0.40	20.75	0.09	**100.05**

Table 35: EPMA analyses of the major element composition of an olivine crystal. The dash symbol (-) represent concentration under the detection limit of the instruments.

D5A(1) - Ol 8									
Name	Distance (µm)	MgO	Al_2O_3	SiO_2	CaO	MnO	FeO	NiO	Total
Ol8-8_1	Core - 0	40.17	-	39.32	0.20	0.34	20.76	0.11	**100.90**
Ol8-8_2	9.43	40.38	0.033	39.53	0.18	0.28	20.79	0.10	**101.29**
Ol8-8_3	18.38	40.15	-	38.96	0.18	0.34	20.79	0.10	**100.51**
Ol8-8_4	27.81	40.26	-	39.46	0.16	0.33	20.90	0.10	**101.20**
Ol8-8_5	36.76	39.71	0.001	38.98	0.14	0.33	20.88	0.09	**100.13**
Ol8-8_6	46.19	40.15	-	39.37	0.17	0.27	20.92	0.11	**100.99**
Ol8-8_7	55.13	40.04	0.014	39.28	0.18	0.32	20.84	0.11	**100.79**
Ol8-8_8	64.57	40.18	0.006	39.51	0.14	0.31	21.23	0.10	**101.48**
Ol8-8_9	74.42	39.78	0.008	38.54	0.19	0.32	20.61	0.09	**99.54**
Ol8-8_10	83.85	39.86	-	39.07	0.17	0.34	20.54	0.13	**100.11**
Ol8-8_11	92.80	39.62	-	39.02	0.16	0.37	20.70	0.12	**99.99**
Ol8-8_12	102.23	40.07	-	39.14	0.13	0.32	21.31	0.10	**101.07**
Ol8-8_13	111.17	40.01	0.021	39.12	0.17	0.34	21.24	0.11	**101.01**
Ol8-8_14	120.61	39.28	0.020	38.84	0.15	0.33	20.65	0.08	**99.36**
Ol8-8_15	129.55	39.73	-	39.17	0.17	0.34	21.08	0.09	**100.57**
Ol8-8_16	138.99	39.72	-	39.11	0.19	0.34	21.24	0.12	**100.71**
Ol8-8_17	147.93	39.66	0.033	39.15	0.18	0.36	21.93	0.12	**101.42**
Ol8-8_18	157.36	39.41	-	38.90	0.19	0.33	21.34	0.09	**100.27**
Ol8-8_19	166.31	39.11	-	39.21	0.15	0.40	21.48	0.12	**100.48**
Ol8-8_20	175.74	39.19	0.029	38.91	0.20	0.37	21.18	0.10	**99.98**
Ol8-8_21	194.12	39.11	0.011	39.03	0.16	0.36	21.76	0.10	**100.54**
Ol8-8_22	203.97	39.08	-	38.98	0.16	0.37	21.55	0.13	**100.27**
Ol8-8_23	213.40	38.94	0.004	38.78	0.18	0.37	21.67	0.09	**100.04**
Ol8-8_24	222.35	39.35	-	39.14	0.18	0.34	21.43	0.10	**100.55**
Ol8-8_25	231.78	39.69	-	39.19	0.15	0.34	20.78	0.09	**100.24**
Ol8-8_26	240.73	40.50	0.013	39.36	0.18	0.40	19.61	0.12	**100.18**
Ol8-8_27	250.16	41.68	0.008	39.32	0.18	0.28	18.27	0.12	**99.85**
Ol8-8_28	259.10	39.76	0.002	39.37	0.23	0.35	21.00	0.08	**100.79**

Table 36: EPMA analyses of the major element composition of an olivine crystal. The dash symbol (-) represent concentration under the detection limit of the instruments.

D5A(2) - Ol 1												
Name	Distance (µm)	Na_2O	MgO	Al_2O_3	SiO_2	CaO	TiO_2	Cr_2O_3	MnO	FeO	NiO	Total
ol1-1_1	Core - 0	0.02	43.46	0.016	39.64	0.23	0.011	0.017	0.31	15.99	0.13	**99.83**
ol1-1_2	10	0.05	43.34	0.023	39.18	0.20	0.002	-	0.34	15.69	0.18	**99.01**
ol1-1_3	20	-	43.62	0.006	39.39	0.21	0.009	-	0.29	15.49	0.11	**99.12**
ol1-1_4	30	-	43.89	0.007	39.49	0.20	0.030	-	0.25	15.94	0.13	**99.95**
ol1-1_5	40	0.00	43.88	-	39.78	0.21	0.002	0.005	0.26	15.74	0.16	**100.04**
ol1-1_6	50	0.01	43.67	0.030	39.51	0.20	0.032	0.006	0.29	15.70	0.16	**99.60**

Table 37: EPMA of the major element composition of an olivine crystal. The dash symbol (-) represent concentration under the detection limit of the instruments.

D5A(2) - Ol 1												
Name	Distance (µm)	Na_2O	MgO	Al_2O_3	SiO_2	CaO	TiO_2	Cr_2O_3	MnO	FeO	NiO	Total
ol1-1_7	60	0.01	43.01	-	39.92	0.19	-	0.013	0.23	15.69	0.09	**99.16**
ol1-1_8	70	0.02	44.44	0.032	38.86	0.19	0.003	0.007	0.26	15.77	0.23	**99.81**
ol1-1_9	80	-	43.54	0.019	39.49	0.18	0.012	0.046	0.25	15.44	0.15	**99.11**
ol1-1_10	90	0.01	42.32	0.021	40.95	0.20	0.018	0.031	0.28	15.49	0.13	**99.45**
ol1-1_11	100	-	43.51	0.006	39.65	0.19	-	-	0.29	15.53	0.16	**99.34**
ol1-1_14	130	-	43.40	0.016	39.77	0.20	0.003	0.025	0.28	15.97	0.14	**99.81**
ol1-1_15	140	-	43.57	0.036	39.64	0.19	0.003	0.037	0.25	15.77	0.15	**99.64**
ol1-1_16	150	0.00	43.39	0.003	40.00	0.19	0.003	0.020	0.24	16.21	0.13	**100.18**
ol1-1_17	160	0.01	43.48	-	39.77	0.24	0.006	0.001	0.27	15.96	0.16	**99.88**
ol1-1_18	170	-	43.59	0.019	39.71	0.21	-	0.007	0.25	16.04	0.16	**100.00**
ol1-1_19	180	-	43.50	-	39.47	0.21	0.009	0.029	0.32	15.56	0.19	**99.28**
ol1-1_20	190	-	43.32	-	39.54	0.18	0.000	-	0.29	16.05	0.12	**99.50**
ol1-1_21	200	-	43.78	0.000	39.46	0.21	-	-	0.29	16.17	0.12	**100.03**
ol1-1_22	210	0.03	43.29	0.018	39.44	0.21	0.004	-	0.29	15.60	0.16	**99.04**
ol1-1_23	220	0.00	43.35	0.000	39.37	0.21	0.008	0.019	0.31	15.79	0.13	**99.18**
ol1-1_24	230	0.01	43.51	0.012	39.57	0.25	0.018	0.024	0.30	15.98	0.15	**99.82**
ol1-1_25	240	-	43.61	0.025	39.59	0.21	0.023	0.010	0.26	15.60	0.18	**99.51**
ol1-1_26	250	-	42.84	0.003	39.43	0.22	0.010	0.016	0.32	15.90	0.16	**98.91**
ol1-1_27	260	-	41.28	0.000	40.64	0.23	-	0.003	0.30	16.18	0.17	**98.80**
ol1-1_28	270	0.04	43.30	0.024	39.38	0.21	0.022	0.031	0.30	15.85	0.13	**99.29**
ol1-1_29	280	0.04	43.28	0.004	39.62	0.23	0.009	-	0.31	15.94	0.16	**99.59**
ol1-1_30	290	-	43.49	0.020	39.61	0.18	0.006	0.002	0.26	15.76	0.17	**99.49**
ol1-1_31	300	-	43.52	-	39.47	0.22	0.008	-	0.30	16.18	0.19	**99.88**
ol1-1_32	310	0.00	43.42	-	39.69	0.21	0.009	0.046	0.30	15.79	0.20	**99.66**
ol1-1_33	320	-	43.72	0.029	39.65	0.21	-	0.008	0.30	16.04	0.15	**100.11**
ol1-1_34	330	-	43.52	0.011	39.63	0.20	0.004	0.033	0.33	15.80	0.12	**99.65**
ol1-1_35	340	-	43.44	-	39.49	0.22	0.017	0.026	0.21	15.86	0.15	**99.42**
ol1-1_36	350	-	43.61	-	39.67	0.21	0.018	0.018	0.23	15.73	0.14	**99.62**
ol1-1_37	360	-	43.55	-	39.62	0.20	0.003	0.014	0.25	16.00	0.15	**99.79**
ol1-1_38	370	-	43.43	0.010	39.60	0.22	0.011	0.007	0.31	15.80	0.13	**99.52**
ol1-1_39	380	-	43.51	0.010	39.43	0.19	-	0.001	0.30	16.01	0.14	**99.60**
ol1-1_40	390	0.01	43.73	-	39.76	0.24	0.002	0.025	0.25	15.97	0.17	**100.15**
ol1-1_41	400	-	43.37	-	39.49	0.20	0.005	0.002	0.25	16.01	0.16	**99.49**
ol1-1_42	410	-	43.58	0.001	39.42	0.25	-	0.017	0.24	15.94	0.18	**99.61**
ol1-1_43	420	-	43.42	0.000	39.66	0.20	0.003	0.016	0.32	16.09	0.10	**99.81**
ol1-1_44	430	0.02	43.49	0.019	39.58	0.18	0.016	0.012	0.29	15.95	0.16	**99.72**
ol1-1_45	440	0.01	43.57	0.017	39.80	0.21	0.004	0.017	0.29	16.18	0.09	**100.18**
ol1-1_46	450	0.00	42.83	0.037	39.59	0.24	-	0.012	0.29	15.84	0.15	**98.99**
ol1-1_47	460	0.03	43.46	0.011	39.71	0.20	0.013	-	0.30	15.95	0.12	**99.80**
ol1-1_48	470	-	43.53	0.012	39.42	0.20	-	0.009	0.33	16.30	0.15	**99.95**
ol1-1_49	480	-	43.49	0.023	39.59	0.21	-	-	0.26	16.20	0.16	**99.94**
ol1-1_50	490 - Rim	-	43.24	-	39.35	0.19	0.008	-	0.29	16.27	0.17	**99.51**

Table 37: Continuation.

D5A(2) - Ol 1 a												
Name	Distance (µm)	Na_2O	MgO	Al_2O_3	SiO_2	CaO	TiO_2	Cr_2O_3	MnO	FeO	NiO	Total
ol1a-_1	Core - 0	0.00	43.61	0.022	39.54	0.19	0.000	0.001	0.23	16.18	0.13	**99.90**
ol1a-_2	10	0.01	43.35	-	39.48	0.20	0.002	0.017	0.25	16.13	0.19	**99.63**
ol1a-_3	20	-	43.58	0.012	39.53	0.21	0.025	0.006	0.30	16.33	0.13	**100.12**
ol1a-_4	30	0.01	43.56	0.023	39.46	0.20	0.014	0.015	0.31	16.12	0.17	**99.88**
ol1a-_5	40	-	43.73	0.005	39.39	0.19	-	0.016	0.29	16.15	0.11	**99.88**
ol1a-_6	50	-	42.75	-	39.44	0.21	-	-	0.28	15.86	0.16	**98.70**
ol1a-_7	60	-	43.31	0.024	39.69	0.19	0.002	-	0.27	16.08	0.14	**99.72**
ol1a-_8	70	-	43.01	0.037	39.33	0.20	0.028	0.023	0.31	16.04	0.15	**99.11**
ol1a-_9	80	-	43.51	-	39.72	0.20	0.014	0.020	0.31	16.18	0.12	**100.08**
ol1a-_10	90	0.00	43.29	-	39.68	0.20	-	0.018	0.26	16.14	0.16	**99.74**
ol1a-_11	100	0.04	43.52	0.001	39.57	0.22	-	-	0.26	16.17	0.12	**99.89**
ol1a-_12	110	0.00	43.35	-	39.46	0.19	0.020	-	0.35	15.99	0.12	**99.49**
ol1a-_13	120	-	43.35	0.016	39.56	0.20	0.006	-	0.30	16.06	0.14	**99.63**
ol1a-_14	130	0.00	43.45	0.004	39.61	0.19	-	0.012	0.29	15.69	0.17	**99.42**
ol1a-_15	140	-	43.34	0.011	39.74	0.19	-	0.005	0.28	15.80	0.16	**99.53**
ol1a-_17	160	-	43.67	0.003	39.64	0.22	-	0.003	0.25	15.96	0.19	**99.94**
ol1a-_18	170	0.01	43.85	0.023	39.48	0.23	-	0.003	0.33	16.07	0.19	**100.18**
ol1a-_19	180	0.00	43.85	-	39.56	0.22	0.013	-	0.31	15.98	0.15	**100.08**
ol1a-_20	190	-	43.74	-	39.48	0.21	-	-	0.25	16.00	0.16	**99.83**
ol1a-_21	200	-	43.36	-	39.84	0.20	0.012	-	0.26	15.86	0.17	**99.71**
ol1a-_22	210	0.01	43.60	-	39.68	0.21	-	0.002	0.29	15.65	0.17	**99.63**
ol1a-_23	220	0.01	43.60	0.004	39.49	0.19	0.008	-	0.32	15.72	0.10	**99.45**
ol1a-_24	230	-	43.39	0.003	39.67	0.21	0.020	0.016	0.31	15.69	0.14	**99.43**
ol1a-_25	240 - Rim	-	43.65	0.009	39.39	0.22	0.001	0.014	0.31	16.46	0.14	**100.20**

Table 38: The major element composition of an olivine crystal from sample D5A(2). The dash symbol (-) represent concentration under the detection limit of the instruments.

D5A(2) - Ol 2									
Name	**Distance (µm)**	**MgO**	**Al_2O_3**	**SiO_2**	**CaO**	**MnO**	**FeO**	**NiO**	**Total**
ol2-2	Core - 0	48.24	0.036	40.57	0.13	0.16	11.11	0.37	**100.6136**
ol2-3	38.21	48.09	0.015	40.58	0.14	0.18	11.35	0.38	**100.7377**
ol2-4	121.95	47.84	0.021	40.64	0.14	0.20	11.49	0.32	**100.6615**
ol2-5	147.19	47.73	0.063	40.08	0.14	0.15	11.77	0.37	**100.3055**
ol2-6	172.19	47.71	0.048	40.35	0.15	0.14	11.65	0.37	**100.4103**
ol2-7	187.33	47.49	0.025	40.45	0.17	0.18	11.98	0.32	**100.6214**
ol2-8	214.78	47.73	0.010	40.48	0.17	0.18	11.74	0.31	**100.6141**
ol2-9	235.78	47.23	-	40.35	0.16	0.20	11.91	0.38	**100.2156**
ol2-10	261.73	47.09	0.010	40.39	0.17	0.17	12.18	0.32	**100.3171**
ol2-11	282.12	47.42	0.028	40.20	0.18	0.16	12.21	0.29	**100.5035**
ol2-12	294.21	47.09	-	40.46	0.19	0.17	12.32	0.31	**100.5348**
ol2-13	313.23	47.03	0.012	40.39	0.17	0.21	12.65	0.34	**100.8051**
ol2-14	338.31	46.75	0.008	40.33	0.17	0.25	12.84	0.29	**100.6305**
ol2-15	362.31	46.02	0.047	40.16	0.19	0.15	13.07	0.30	**99.9309**
ol2-16	385.64	46.21	0.027	40.00	0.20	0.25	13.39	0.24	**100.3092**
ol2-17	407.84	45.89	0.012	39.85	0.21	0.27	13.78	0.27	**100.2797**
ol2-18	439.60	45.52	0.017	39.87	0.21	0.17	14.17	0.20	**100.1529**
ol2-19	453.60	45.32	0.006	40.11	0.20	0.22	14.34	0.26	**100.4566**
ol2-20	470.25	45.36	0.015	39.95	0.21	0.22	14.59	0.25	**100.5943**
ol2-21	487.94	45.11	0.028	39.88	0.21	0.22	14.89	0.26	**100.6101**
ol2-22	503.50	45.16	0.022	39.82	0.20	0.24	15.08	0.27	**100.7878**
ol2-23	519.02	44.99	0.000	39.75	0.22	0.22	15.07	0.28	**100.529**
ol2-24	533.16	44.86	0.008	39.73	0.22	0.20	15.12	0.23	**100.3662**
ol2-25	547.37	44.85	-	39.55	0.23	0.24	15.44	0.29	**100.6078**
ol2-26	580.36	44.25	0.009	39.61	0.21	0.27	15.64	0.22	**100.2056**
ol2-27	592.57	44.13	0.004	39.71	0.22	0.22	15.97	0.20	**100.4544**
ol2-28	606.57	44.20	0.010	39.62	0.21	0.30	16.03	0.18	**100.5511**
ol2-29	628.57	43.90	0.020	39.41	0.23	0.28	16.23	0.19	**100.2664**
ol2-30	644.57	44.27	0.017	39.53	0.23	0.26	16.27	0.16	**100.7356**
ol2-31	653.51	44.22	0.022	39.62	0.22	0.25	15.95	0.19	**100.4771**
ol2-32	676.07	43.90	0.016	39.41	0.21	0.24	16.39	0.19	**100.3469**
ol2-33	700.77	43.62	0.009	39.65	0.21	0.29	16.44	0.17	**100.3795**
ol2-34	721.38	43.72	0.021	39.67	0.21	0.27	16.60	0.21	**100.7041**
ol2-35	741.78	43.67	0.012	39.59	0.22	0.26	16.62	0.20	**100.5682**
ol2-36	763.37	43.87	-	39.32	0.20	0.35	16.61	0.19	**100.5392**
ol2-37	793.73	44.10	0.024	39.66	0.20	0.25	16.33	0.13	**100.6884**
ol2-38	806.54	44.23	-	39.61	0.22	0.30	16.52	0.20	**101.0828**
ol2-39	821.40	44.12	0.009	39.76	0.23	0.30	15.86	0.21	**100.4865**
ol2-40	834.21	44.19	0.006	39.46	0.21	0.31	16.41	0.16	**100.7418**
ol2-41	848.98 - Rim	43.78	0.015	39.54	0.25	0.28	16.91	0.13	**100.899**

Table 39: EPMA analyses of the major element composition of an olivine crystal. The dash symbol (-) represent concentration under the detection limit of the instruments.

D5A(2) - Ol 3									
Name	Distance (µm)	MgO	Al_2O_3	SiO_2	CaO	MnO	FeO	NiO	Total
Ol1-3_1	Core - 0	47.02	0.010	40.67	0.25	0.22	12.59	0.16	**100.92**
Ol1-3_2	12.81	46.86	-	40.71	0.24	0.22	12.57	0.16	**100.75**
Ol1-3_3	25.61	47.04	0.012	40.56	0.24	0.25	12.59	0.18	**100.86**
Ol1-3_4	37.82	46.89	0.016	40.58	0.24	0.21	12.38	0.14	**100.46**
Ol1-3_5	50.63	47.26	0.018	40.83	0.23	0.19	12.42	0.19	**101.13**
Ol1-3_6	63.43	46.94	0.009	40.86	0.22	0.25	12.35	0.18	**100.81**
Ol1-3_7	76.24	47.41	0.007	40.62	0.25	0.18	12.37	0.14	**100.99**
Ol1-3_8	89.04	47.16	0.012	40.61	0.23	0.26	12.12	0.15	**100.55**
Ol1-3_9	101.09	47.26	0.009	40.72	0.21	0.21	12.05	0.18	**100.64**
Ol1-3_10	113.29	47.13	0.016	40.73	0.24	0.23	12.14	0.16	**100.65**
Ol1-3_11	126.10	47.15	-	40.49	0.23	0.24	12.11	0.17	**100.40**
Ol1-3_12	138.90	47.19	0.019	40.97	0.21	0.20	12.05	0.18	**100.81**
Ol1-3_13	151.71	47.45	0.020	40.91	0.25	0.19	11.78	0.18	**100.79**
Ol1-3_14	164.52	47.38	0.020	40.56	0.23	0.20	12.01	0.17	**100.58**
Ol1-3_15	177.32	47.42	-	40.81	0.22	0.19	11.82	0.19	**100.65**
Ol1-3_16	189.53	47.27	0.003	40.91	0.24	0.22	12.01	0.15	**100.80**
Ol1-3_17	202.34	47.56	-	40.80	0.23	0.18	11.85	0.18	**100.80**
Ol1-3_18	215.14	47.62	0.020	40.85	0.24	0.19	11.54	0.19	**100.65**
Ol1-3_19	227.95	47.38	0.024	40.52	0.26	0.23	11.62	0.17	**100.19**
Ol1-3_20	240.75	47.19	0.005	40.92	0.26	0.26	11.54	0.18	**100.37**
Ol1-3_21	253.56	46.31	0.010	40.49	0.22	0.19	11.53	0.19	**98.95**
Ol1-3_22	265.77	47.62	-	40.66	0.27	0.21	11.87	0.18	**100.80**
Ol1-3_23	277.81	47.45	0.001	40.55	0.26	0.20	11.78	0.17	**100.42**
Ol1-3_24	290.62	47.44	0.017	40.50	0.25	0.21	11.69	0.20	**100.31**
Ol1-3_25	303.42	47.75	0.013	41.35	0.27	0.25	11.70	0.19	**101.53**
Ol1-3_26	316.23	48.57	0.019	40.02	0.26	0.18	12.13	0.19	**101.37**
Ol1-3_27	329.03	47.32	-	40.67	0.26	0.18	12.57	0.20	**101.20**
Ol1-3_28	341.24	46.92	0.002	40.69	0.25	0.20	12.80	0.21	**101.08**
Ol1-3_29	354.05	45.91	0.038	41.03	0.21	0.20	13.91	0.18	**101.48**
Ol1-3_30	366.85 - Rim	44.44	0.025	39.91	0.24	0.24	15.86	0.15	**100.86**

Table 40: The major element composition of an olivine crystal from sample D5A(2). The dash symbol (-) represent concentration under the detection limit of the instruments.

D5A(2) - Ol 4									
Name	Distance (µm)	MgO	Al_2O_3	SiO_2	CaO	MnO	FeO	NiO	Total
Ol2-4_1	Core - 0	43.95	-	40.22	0.16	0.30	16.69	0.11	**101.44**
Ol2-4_2	11	43.53	-	40.23	0.18	0.28	16.79	0.13	**101.13**
Ol2-4_3	23	43.22	-	39.88	0.20	0.25	16.81	0.10	**100.45**
Ol2-4_4	34	43.17	0.008	39.66	0.18	0.23	16.81	0.10	**100.17**
Ol2-4_5	45	43.97	-	40.60	0.19	0.24	17.15	0.14	**102.30**
Ol2-4_6	57	43.46	-	39.87	0.20	0.24	16.96	0.15	**100.88**
Ol2-4_7	68	43.19	-	39.65	0.19	0.20	16.80	0.15	**100.19**
Ol2-4_8	79	43.54	-	40.24	0.19	0.29	16.70	0.13	**101.09**
Ol2-4_9	91	43.57	0.017	39.78	0.20	0.22	16.37	0.17	**100.34**
Ol2-4_10	102	43.66	0.010	39.81	0.18	0.23	16.59	0.16	**100.64**
Ol2-4_11	113	43.80	0.000	39.62	0.19	0.26	16.39	0.16	**100.43**
Ol2-4_12	125	43.51	-	39.94	0.19	0.27	16.17	0.18	**100.26**
Ol2-4_13	136	44.14	0.003	40.13	0.21	0.25	16.35	0.16	**101.24**
Ol2-4_14	147	43.91	0.012	40.03	0.20	0.25	16.00	0.19	**100.59**
Ol2-4_15	159	43.89	0.019	39.98	0.21	0.24	15.96	0.18	**100.48**
Ol2-4_16	170	43.98	0.005	39.65	0.23	0.27	15.86	0.15	**100.14**
Ol2-4_17	182	43.94	0.022	39.82	0.23	0.25	15.76	0.17	**100.19**
Ol2-4_18	193	43.77	0.010	39.93	0.20	0.22	15.62	0.18	**99.93**
Ol2-4_19	204	44.11	-	39.94	0.24	0.20	16.05	0.16	**100.70**
Ol2-4_20	216	43.81	-	39.67	0.23	0.23	15.99	0.16	**100.10**
Ol2-4_21	227	43.50	0.026	39.61	0.23	0.24	15.96	0.18	**99.74**
Ol2-4_22	238	44.29	-	39.81	0.22	0.32	16.49	0.16	**101.29**
Ol2-4_23	250	43.66	-	40.37	0.22	0.30	16.48	0.14	**101.18**
Ol2-4_24	261	43.92	0.021	40.36	0.23	0.31	17.24	0.15	**102.22**
Ol2-4_25	272	43.73	0.013	40.13	0.22	0.24	17.31	0.13	**101.78**
Ol2-4_26	284	43.71	-	40.12	0.22	0.26	17.17	0.14	**101.62**
Ol2-4_27	295	43.73	0.007	40.02	0.22	0.29	17.36	0.15	**101.79**
Ol2-4_28	306	43.54	0.026	40.09	0.21	0.32	17.67	0.14	**101.99**
Ol2-4_29	318	43.14	0.032	39.93	0.21	0.29	17.94	0.12	**101.66**
Ol2-4_30	329 - Rim	42.77	0.002	39.53	0.23	0.33	17.63	0.12	**100.61**

Table 41: EPMA of the major element composition of an olivine crystal. The dash symbol (-) represent concentration under the detection limit of the instruments.

D5A(2) - Ol 5									
Name	Distance (µm)	MgO	Al_2O_3	SiO_2	CaO	MnO	FeO	NiO	Total
Ol5-5_2	Core - 10.120	43.52	0.008	40.19	0.21	0.23	17.19	0.15	**101.50**
Ol5-5_3	19.42	42.83	-	39.46	0.18	0.29	16.75	0.16	**99.66**
Ol5-5_4	29.62	43.14	-	39.40	0.22	0.27	16.79	0.16	**99.98**
Ol5-5_5	39.81	42.92	0.004	39.34	0.19	0.28	16.83	0.14	**99.70**
Ol5-5_8	69.43	42.83	-	39.44	0.17	0.26	17.16	0.13	**99.99**
Ol5-5_9	78.48	43.38	0.022	39.87	0.21	0.23	17.20	0.13	**101.05**
Ol5-5_11	98.88	43.21	0.010	39.89	0.19	0.28	16.96	0.13	**100.67**
Ol5-5_12	108.10	43.17	0.044	39.73	0.21	0.29	17.47	0.15	**101.06**
Ol5-5_13	118.30	42.68	0.023	39.40	0.21	0.21	17.06	0.14	**99.73**
Ol5-5_14	128.50	43.22	0.007	40.08	0.21	0.30	17.47	0.13	**101.41**
Ol5-5_15	137.72	42.72	0.011	39.31	0.21	0.29	17.16	0.15	**99.84**
Ol5-5_16	147.91	42.67	0.004	39.71	0.18	0.33	17.48	0.11	**100.50**
Ol5-5_17	157.13	42.50	0.036	39.24	0.21	0.27	17.25	0.13	**99.62**
Ol5-5_19	177.53	42.37	0.010	39.29	0.20	0.26	17.15	0.11	**99.39**
Ol5-5_20	186.75	42.53	0.022	39.21	0.21	0.27	17.53	0.11	**99.89**
Ol5-5_21	196.95	42.32	0.021	39.33	0.17	0.25	17.35	0.12	**99.55**
Ol5-5_22	207.15	42.65	0.003	39.06	0.20	0.31	17.26	0.13	**99.62**
Ol5-5_23	216.20	42.76	-	39.25	0.22	0.26	17.28	0.11	**99.88**
Ol5-5_24	226.40	42.62	0.018	39.46	0.19	0.31	17.12	0.14	**99.85**
Ol5-5_25	236.60	43.03	-	39.56	0.22	0.27	17.16	0.09	**100.33**
Ol5-5_26	245.82	43.04	0.012	39.86	0.19	0.26	17.26	0.09	**100.71**
Ol5-5_27	256.01	43.45	0.015	39.91	0.20	0.29	17.35	0.12	**101.35**
Ol5-5_28	266.21	42.65	0.014	39.55	0.23	0.25	17.37	0.14	**100.20**
Ol5-5_29	275.43	41.90	0.008	39.36	0.20	0.27	18.57	0.11	**100.41**
Ol5-5_30	285.63 - Rim	38.29	0.015	38.67	0.22	0.37	22.08	0.09	**99.74**

Table 42: The major element composition of an olivine crystal from sample D5A(2). The dash symbol (-) represent concentration under the detection limit of the instruments.

D5A(2) - Cpx 2A											
Name	Distance (µm)	Na_2O	MgO	Al_2O_3	SiO_2	CaO	TiO_2	Cr_2O_3	MnO	FeO	Total
cpx2-3_1	Core - 0	0.15	15.88	3.35	51.45	22.85	0.41	0.28	0.15	4.51	**99.03**
cpx2-3_2	13	0.19	15.94	3.36	51.42	23.03	0.43	0.31	0.10	4.55	**99.33**
cpx2-3_3	26	0.17	16.12	3.25	51.42	22.86	0.40	0.23	0.17	4.50	**99.12**
cpx2-3_4	39	0.17	15.95	3.26	51.28	22.84	0.45	0.22	0.09	4.48	**98.74**
cpx2-3_5	52	0.20	15.60	3.58	50.72	22.58	0.56	0.31	0.12	5.30	**98.97**
cpx2-3_6	65	0.16	16.62	2.38	51.93	22.83	0.36	0.18	0.12	4.72	**99.28**
cpx2-3_7	78	0.15	16.59	2.36	52.16	22.71	0.36	0.14	0.10	4.62	**99.19**
cpx2-3_8	91	0.08	16.68	2.36	52.18	22.80	0.35	0.08	0.13	4.67	**99.34**
cpx2-3_9	104	0.17	16.38	2.58	52.09	22.67	0.38	0.10	0.12	4.91	**99.39**
cpx2-3_10	117	0.13	16.24	2.66	51.60	22.75	0.39	0.14	0.11	4.70	**98.72**
cpx2-3_11	130	0.10	15.95	2.80	51.40	22.68	0.43	0.14	0.16	5.05	**98.70**
cpx2-3_12	143	0.16	15.99	2.53	51.83	22.47	0.41	0.11	0.21	5.05	**98.77**
cpx2-3_13	156	0.19	16.29	1.98	52.22	21.97	0.39	0.11	0.21	5.57	**98.93**
cpx2-3_14	169	0.16	16.09	2.26	52.12	22.11	0.40	0.14	0.16	5.65	**99.09**
cpx2-3_15	182	0.19	15.85	2.66	51.65	22.52	0.46	0.09	0.16	5.59	**99.17**
cpx2-3_16	195	0.16	16.09	2.74	51.59	22.70	0.43	0.14	0.10	5.11	**99.06**
cpx2-3_17	208	0.14	16.57	2.21	52.35	22.70	0.33	0.19	0.09	4.59	**99.18**
cpx2-3_18	221	0.14	16.44	2.53	52.15	22.83	0.32	0.17	0.12	4.73	**99.41**
cpx2-3_19	234	0.15	16.16	2.87	52.17	22.85	0.36	0.23	0.16	4.62	**99.57**
cpx2-3_20	247	0.14	16.48	2.63	52.10	22.67	0.37	0.14	0.15	4.70	**99.37**
cpx2-3_21	260	0.10	16.62	2.40	52.39	22.52	0.36	0.07	0.15	4.89	**99.49**
cpx2-3_22	273	0.09	16.50	2.72	52.22	22.61	0.34	0.21	0.13	4.63	**99.44**
cpx2-3_23	286	0.13	16.30	2.70	51.71	22.84	0.33	0.16	0.13	4.41	**98.73**
cpx2-3_24	299	0.21	16.10	2.85	51.64	23.00	0.38	0.26	0.12	4.42	**98.98**
cpx2-3_25	312	0.10	16.74	2.67	52.19	22.91	0.34	0.22	0.09	4.29	**99.55**
cpx2-3_26	325	0.11	17.25	1.82	52.84	22.73	0.22	0.38	0.08	3.82	**99.24**
cpx2-3_27	338	0.11	16.44	2.71	51.48	22.96	0.32	0.31	0.10	3.94	**98.36**
cpx2-3_28	351	0.15	16.38	3.21	51.60	23.45	0.34	0.41	0.09	4.16	**99.78**
cpx2-3_29	364	0.16	16.72	2.74	51.85	22.99	0.29	0.58	0.12	3.76	**99.21**
cpx2-3_30	377	0.14	16.92	2.50	52.56	23.28	0.24	0.42	0.09	3.49	**99.65**
cpx2-3_31	390	0.20	16.57	2.72	51.91	23.04	0.26	0.69	0.15	3.54	**99.08**
cpx2-3_32	403	0.17	16.32	3.16	51.70	23.04	0.30	0.62	0.08	3.91	**99.30**
cpx2-3_33	416	0.16	16.18	3.49	51.23	23.09	0.37	0.53	0.09	4.20	**99.34**
cpx2-3_34	429	0.17	16.19	3.00	51.72	22.39	0.50	0.28	0.12	5.06	**99.44**
cpx2-3_35	442	0.12	16.28	2.95	52.01	23.11	0.37	0.45	0.09	4.21	**99.59**
cpx2-3_36	455	0.36	13.40	4.15	33.69	15.66	0.42	0.10	0.08	4.27	**72.12**
cpx2-3_37	468	0.18	16.14	3.04	51.07	22.40	0.46	0.09	0.11	5.39	**98.89**
cpx2-3_38	481	0.15	16.18	2.76	51.65	22.75	0.40	0.10	0.14	4.94	**99.08**

Table 43: EPMA analyses of the major element composition of an pyroxene crystal. The dash symbol (-) represent concentration under the detection limit of the instruments.

D5A(2) - Cpx 2A											
Name	Distance (µm)	Na_2O	MgO	Al_2O_3	SiO_2	CaO	TiO_2	Cr_2O_3	MnO	FeO	Total
cpx2-3_39	494	0.15	15.79	3.33	51.11	22.59	0.51	0.19	0.15	5.39	**99.22**
cpx2-3_40	507	0.15	15.59	3.91	50.42	22.46	0.54	0.21	0.11	5.49	**98.89**
cpx2-3_41	520	0.20	15.70	3.75	50.61	22.52	0.59	0.14	0.12	5.61	**99.26**
cpx2-3_42	533	0.25	15.37	3.26	50.86	22.06	0.60	0.03	0.12	6.48	**99.03**
cpx2-3_43	546	0.21	15.56	2.76	50.99	21.72	0.52	0.01	0.24	7.01	**99.02**
cpx2-3_44	559	0.19	15.65	2.76	51.68	21.97	0.53	-	0.22	6.34	**99.33**
cpx2-3_45	572	0.16	16.76	2.49	52.05	22.26	0.37	0.15	0.14	4.92	**99.31**
cpx2-3_46	585	0.14	16.73	2.49	52.03	22.38	0.35	0.22	0.11	4.83	**99.27**
cpx2-3_47	598	0.11	16.54	2.52	52.14	21.66	0.37	0.12	0.15	5.45	**99.06**
cpx2-3_48	611	0.14	16.51	2.75	51.58	22.19	0.41	0.19	0.12	5.04	**98.92**
cpx2-3_49	624	0.13	16.58	2.52	52.28	22.59	0.25	0.44	0.08	4.19	**99.06**
cpx2-3_50	637 - Rim	0.10	16.78	2.36	52.22	22.69	0.27	0.41	0.12	3.83	**98.78**

Table 43: Continuation

D5A(2) - Cpx 2A											
Name	Distance (µm)	Na_2O	MgO	Al_2O_3	SiO_2	CaO	TiO_2	Cr_2O_3	MnO	FeO	Total
cpx21-1_1	Core - 0	0.20	15.81	3.68	50.74	22.86	0.45	0.50	0.10	4.45	98.7838
cpx21-1_2	12	0.13	15.57	3.91	50.64	23.08	0.43	0.64	0.12	4.43	98.9464
cpx21-1_3	24	0.14	14.87	4.92	49.45	22.59	0.55	0.11	0.10	5.61	98.3294
cpx21-1_4	36	0.26	14.40	5.28	49.28	22.21	0.65	0.05	0.13	5.93	98.1885
cpx21-1_5	48	0.16	15.31	4.13	50.25	22.50	0.57	0.07	0.14	5.88	99.0173
cpx21-1_6	60	0.19	14.75	4.48	50.14	22.26	0.67	0.02	0.16	6.47	99.1407
cpx21-1_7	72	0.23	14.71	4.60	49.75	22.25	0.66	0.06	0.05	6.44	98.7455
cpx21-1_8	84	0.23	15.07	4.08	50.51	22.40	0.60	0.11	0.16	6.38	99.5236
cpx21-1_9	96	0.28	15.15	4.45	45.96	20.97	0.70	0.03	0.20	6.72	94.4428
cpx21-1_10	108	0.25	15.07	3.66	50.13	21.79	0.65	0.02	0.16	7.05	98.7718
cpx21-1_11	120	0.23	14.63	3.79	50.54	22.00	0.68	0.05	0.16	7.27	99.3527
cpx21-1_12	132	0.25	14.99	3.58	49.96	22.07	0.68	0.01	0.14	7.28	98.9556
cpx21-1_13	144	0.25	14.41	3.58	51.00	22.01	0.65	0.00	0.20	7.15	99.2511
cpx21-1_14	156	0.24	14.86	3.59	50.30	22.02	0.68	0.03	0.18	7.13	99.0298
cpx21-1_15	168	0.25	14.70	3.76	50.24	21.83	0.72	0.03	0.17	7.31	98.9999
cpx21-1_16	180	0.20	14.86	3.65	50.24	22.22	0.67	0.06	0.15	7.03	99.0732
cpx21-1_17	192	0.26	15.54	2.94	50.94	22.02	0.57	0.14	0.15	6.20	98.7656
cpx21-1_18	204	0.28	13.78	3.65	52.66	21.38	0.60	0.07	0.17	6.38	98.9688
cpx21-1_19	216	0.21	15.61	3.66	51.08	22.29	0.47	0.33	0.15	5.49	99.2912
cpx21-1_20	228	0.12	15.55	4.12	50.60	22.42	0.46	0.60	0.12	4.84	98.8437
cpx21-1_21	240	0.18	15.84	4.08	50.39	22.82	0.46	0.55	0.10	4.92	99.358
cpx21-1_22	252	0.15	15.23	4.34	50.32	22.64	0.57	0.31	0.15	5.16	98.868

Table 44: The major element composition of an pyroxene crystal from sample D5A(2).

D5A(2) - Cpx 2A											
Name	Distance (µm)	Na_2O	MgO	Al_2O_3	SiO_2	CaO	TiO_2	Cr_2O_3	MnO	FeO	Total
cpx21-1_23	264	0.17	15.59	3.83	50.53	22.31	0.52	0.22	0.13	5.45	98.7603
cpx21-1_24	276	0.13	15.67	3.99	50.34	22.77	0.49	0.35	0.10	5.24	99.0846
cpx21-1_25	288	0.13	15.59	4.06	50.84	22.81	0.47	0.40	0.16	4.80	99.2566
cpx21-1_26	300	0.13	16.29	3.10	51.78	23.30	0.29	0.78	0.07	3.86	99.6007
cpx21-1_27	312	0.14	16.33	3.05	51.51	22.81	0.29	0.72	0.07	3.69	98.6162
cpx21-1_28	324	0.13	16.49	3.01	51.70	22.62	0.30	0.74	0.06	3.76	98.8097
cpx21-1_29	336	0.16	16.28	3.14	51.30	22.90	0.32	0.88	0.10	3.74	98.8113
cpx21-1_30	348	0.13	16.33	2.99	51.51	23.10	0.29	0.88	0.13	3.86	99.2069
cpx21-1_31	360	0.10	16.14	3.14	51.46	22.67	0.31	0.87	0.08	3.86	98.6264
cpx21-1_32	372	0.17	16.38	3.11	51.57	22.95	0.30	0.97	0.14	3.66	99.244
cpx21-1_33	384	0.18	16.27	3.50	51.21	22.75	0.33	0.67	0.09	3.99	98.9793
cpx21-1_34	396	0.17	16.12	3.69	51.13	22.69	0.38	0.65	0.09	4.11	99.0375
cpx21-1_35	408	0.14	16.11	3.38	51.24	22.90	0.32	0.90	0.10	3.67	98.7578
cpx21-1_36	420	0.16	16.12	3.39	51.19	22.69	0.34	0.90	0.10	4.07	98.9524
cpx21-1_37	432	0.10	16.13	3.46	51.15	22.74	0.34	0.83	0.08	3.81	98.6355
cpx21-1_38	444	0.17	16.48	3.30	51.44	22.80	0.29	0.79	0.07	3.93	99.2733
cpx21-1_39	456	0.17	16.35	3.21	51.58	22.77	0.33	0.68	0.03	3.93	99.0638
cpx21-1_40	468	0.17	15.99	3.19	50.96	22.52	0.29	0.64	0.08	3.74	97.5878
cpx21-1_41	480	0.15	16.38	3.21	50.79	22.65	0.32	0.80	0.13	3.84	98.2745
cpx21-1_42	492	0.16	16.34	3.23	51.40	22.98	0.31	0.85	0.09	3.77	99.1342
cpx21-1_43	504	0.19	16.62	3.09	51.36	22.89	0.30	0.85	0.09	3.68	99.0854
cpx21-1_44	516	0.17	16.42	3.02	51.48	23.05	0.30	0.80	0.07	3.59	98.8861
cpx21-1_45	528	0.14	16.19	3.45	51.11	23.00	0.34	0.74	0.08	3.99	99.0385
cpx21-1_46	540	0.18	15.88	3.89	51.06	22.97	0.45	0.57	0.06	4.18	99.2294
cpx21-1_47	552	0.18	15.71	4.06	50.58	22.60	0.40	0.95	0.06	4.09	98.6437
cpx21-1_48	564	0.21	15.60	4.36	50.05	22.60	0.53	0.54	0.09	4.92	98.8967
cpx21-1_49	576	0.21	15.46	4.32	50.68	22.73	0.50	0.63	0.06	4.72	99.3182
cpx21-1_50	588	0.22	15.35	4.40	50.46	22.07	0.57	0.62	0.11	5.26	99.0534
cpx21-1_51	600	0.21	15.63	4.01	50.53	22.26	0.55	0.57	0.10	4.83	98.6832
cpx21-1_52	612	0.20	15.42	3.95	50.41	22.02	0.63	0.50	0.14	5.56	98.829
cpx21-1_53	624	0.22	15.75	3.91	50.70	22.34	0.50	0.60	0.16	4.87	99.0465
cpx21-1_54	636	0.21	15.60	3.89	50.42	22.33	0.57	0.39	0.12	5.20	98.7375
cpx21-1_55	648	0.22	15.72	3.52	51.03	22.03	0.56	0.18	0.13	5.55	98.9494
cpx21-1_56	660	0.21	15.67	3.89	50.98	22.44	0.52	0.28	0.09	5.06	99.1451
cpx21-1_57	672	0.20	15.97	3.28	51.01	22.42	0.55	0.17	0.13	5.32	99.0599
cpx21-1_58	684	0.16	15.93	3.68	50.71	22.57	0.48	0.28	0.15	5.00	98.9563
cpx21-1_59	696	0.14	16.07	3.41	51.47	22.63	0.42	0.43	0.12	4.32	99.0188
cpx21-1_60	708 - Rim	0.13	16.67	2.80	51.67	22.87	0.30	0.55	0.11	3.77	98.8587

Table 44: Continuation.

D5A(2) - Cpx 3B											
Name	Distance (µm)	Na_2O	MgO	Al_2O_3	SiO_2	CaO	TiO_2	Cr_2O_3	MnO	FeO	Total
cpx3-1_1	Core - 0	0.12	16.13	2.78	51.87	22.77	0.33	0.12	0.11	4.56	**98.79**
cpx3-1_2	11	0.14	16.24	2.75	51.82	22.96	0.33	0.18	0.17	4.67	**99.27**
cpx3-1_3	22	0.13	16.33	2.77	51.59	22.77	0.33	0.16	0.10	4.54	**98.72**
cpx3-1_4	33	0.17	16.46	2.68	52.18	22.72	0.32	0.18	0.15	4.49	**99.33**
cpx3-1_5	44	0.15	16.19	3.05	51.48	23.02	0.37	0.21	0.11	4.64	**99.22**
cpx3-1_6	55	0.14	16.06	2.57	45.03	22.27	0.37	0.15	0.12	4.77	**91.47**
cpx3-1_7	66	0.12	16.17	3.26	51.64	22.81	0.38	0.17	0.09	4.87	**99.53**
cpx3-1_8	77	0.15	16.35	2.94	51.87	22.74	0.37	0.16	0.10	4.75	**99.44**
cpx3-1_9	88	0.15	16.15	3.06	51.82	22.80	0.35	0.16	0.15	4.61	**99.25**
cpx3-1_10	99	0.18	16.33	3.01	51.77	22.55	0.37	0.16	0.08	4.76	**99.21**
cpx3-1_11	110	0.11	17.18	1.88	52.61	23.17	0.20	0.52	0.09	3.39	**99.15**
cpx3-1_12	121	0.10	16.88	2.03	52.79	23.33	0.19	0.43	0.10	3.37	**99.22**
cpx3-1_13	132	0.13	17.04	2.00	52.39	23.31	0.22	0.38	0.08	3.25	**98.80**
cpx3-1_14	143	0.11	17.15	1.92	52.68	23.48	0.20	0.61	0.12	3.22	**99.50**
cpx3-1_15	154	0.10	16.98	1.82	52.69	23.52	0.17	0.67	0.05	3.06	**99.05**
cpx3-1_16	165	0.12	17.15	1.92	52.73	23.00	0.19	0.55	0.05	3.38	**99.09**
cpx3-1_17	176	0.13	16.99	1.85	52.67	22.97	0.21	0.57	0.11	3.40	**98.91**
cpx3-1_18	187	0.15	17.11	1.95	52.92	23.31	0.20	0.59	0.11	3.35	**99.69**
cpx3-1_19	198	0.10	17.31	1.80	53.24	23.18	0.17	0.67	0.12	3.23	**99.82**
cpx3-1_20	209	0.10	17.21	1.85	52.72	23.13	0.16	0.73	0.08	2.99	**98.97**
cpx3-1_21	220	0.11	17.34	1.72	52.91	22.79	0.19	0.60	0.09	3.32	**99.08**
cpx3-1_22	231	0.12	16.80	2.37	51.83	22.95	0.27	0.36	0.09	3.95	**98.75**
cpx3-1_23	242	0.13	16.92	2.38	52.49	23.03	0.24	0.38	0.08	3.96	**99.59**
cpx3-1_24	253	0.15	16.74	2.13	52.62	22.90	0.27	0.31	0.11	3.99	**99.21**
cpx3-1_25	264	0.12	16.85	2.27	52.40	23.06	0.27	0.39	0.06	3.73	**99.14**
cpx3-1_26	275	0.13	17.04	1.98	52.87	23.06	0.20	0.58	0.08	3.34	**99.28**
cpx3-1_27	286	0.09	17.03	1.70	52.89	23.05	0.18	0.53	0.09	3.29	**98.86**
cpx3-1_28	297	0.11	16.78	2.18	52.27	23.13	0.26	0.40	0.11	3.86	**99.10**
cpx3-1_29	308	0.11	16.58	2.23	52.42	22.58	0.31	0.15	0.13	4.64	**99.15**
cpx3-1_30	319	0.08	16.19	2.31	52.27	22.70	0.35	0.06	0.12	5.32	**99.39**
cpx3-1_31	330	0.12	16.11	2.40	51.96	22.19	0.46	0.02	0.18	5.94	**99.37**
cpx3-1_32	341	0.16	15.82	2.64	51.43	21.89	0.49	0.04	0.18	6.50	**99.15**
cpx3-1_33	352	0.20	15.69	2.85	51.32	22.15	0.51	0.09	0.15	6.34	**99.29**
cpx3-1_34	363	0.24	15.40	2.68	51.15	21.83	0.48	0.04	0.19	6.61	**98.61**
cpx3-1_35	374	0.20	15.59	2.50	51.19	22.07	0.50	0.00	0.21	6.71	**98.98**
cpx3-1_36	385	0.20	15.13	3.27	50.71	22.24	0.56	0.08	0.16	6.41	**98.75**
cpx3-1_37	396	0.20	15.23	3.46	50.66	22.49	0.51	0.12	0.12	5.99	**98.79**
cpx3-1_38	407	0.19	15.40	3.22	51.01	22.37	0.54	0.10	0.15	5.84	**98.83**
cpx3-1_39	418	0.15	16.05	2.87	51.49	22.24	0.43	0.06	0.17	5.71	**99.15**

Table 45: EPMA analyses of the major element composition of an pyroxene crystal.

D5A(2) - Cpx 3B											
Name	Distance (µm)	Na_2O	MgO	Al_2O_3	SiO_2	CaO	TiO_2	Cr_2O_3	MnO	FeO	Total
cpx3-1_40	429	0.16	16.23	2.57	51.64	22.37	0.47	0.06	0.14	5.35	**98.99**
cpx3-1_41	440	0.13	16.90	2.10	52.56	22.66	0.30	0.23	0.15	4.61	**99.63**
cpx3-1_42	451	0.15	16.41	2.60	51.81	22.39	0.39	0.09	0.12	5.17	**99.13**
cpx3-1_43	462	0.12	16.61	2.47	52.07	22.64	0.32	0.15	0.11	4.48	**98.98**
cpx3-1_44	473	0.14	16.59	2.46	52.24	22.45	0.30	0.21	0.06	4.38	**98.82**
cpx3-1_45	484	0.15	16.35	2.68	51.68	22.44	0.40	0.14	0.15	5.05	**99.04**
cpx3-1_46	495	0.14	16.26	2.57	52.13	22.66	0.39	0.19	0.12	4.71	**99.18**
cpx3-1_47	506	0.16	16.22	3.24	51.59	22.80	0.36	0.47	0.10	4.36	**99.29**
cpx3-1_48	517	0.13	16.49	3.04	51.62	22.92	0.32	0.64	0.14	3.97	**99.26**
cpx3-1_49	528	0.21	16.52	2.66	53.22	22.59	0.34	0.39	0.10	4.42	**100.46**
cpx3-1_50	539	0.17	16.46	2.62	50.45	21.86	0.39	0.22	0.12	4.89	**97.19**
cpx3-1_51	550	0.18	16.43	2.47	51.41	22.20	0.42	0.23	0.13	5.17	**98.64**
cpx3-1_52	561	0.19	16.37	2.69	51.54	22.24	0.43	0.32	0.09	5.06	**98.95**
cpx3-1_53	572	0.20	16.44	2.56	51.57	22.05	0.42	0.34	0.16	4.65	**98.39**
cpx3-1_54	583	0.17	16.16	2.73	51.26	22.52	0.38	0.46	0.14	4.69	**98.51**
cpx3-1_55	594	0.19	16.44	2.60	51.99	22.13	0.40	0.39	0.13	4.73	**98.99**
cpx3-1_56	605	0.19	16.23	2.74	51.55	22.38	0.38	0.44	0.08	4.84	**98.83**
cpx3-1_57	616	0.13	16.44	2.31	51.91	22.43	0.37	0.24	0.16	4.89	**98.89**
cpx3-1_58	627	0.18	16.36	2.71	51.62	22.50	0.42	0.24	0.11	4.93	**99.07**
cpx3-1_59	638	0.18	16.42	2.62	51.79	22.69	0.39	0.18	0.16	4.84	**99.28**
cpx3-1_60	649	0.17	16.25	2.55	51.77	22.54	0.41	0.14	0.12	4.98	**98.94**
cpx3-1_61	660	0.16	16.19	3.24	51.12	22.51	0.44	0.23	0.17	4.85	**98.92**
cpx3-1_62	671	0.15	16.27	3.03	51.20	22.75	0.45	0.24	0.14	4.82	**99.04**
cpx3-1_63	682	0.16	16.37	3.17	51.29	22.76	0.41	0.25	0.09	4.61	**99.12**
cpx3-1_64	693	0.12	16.30	3.09	50.85	22.99	0.31	0.30	0.09	4.34	**98.41**
cpx3-1_65	704	0.16	16.59	3.12	51.33	23.12	0.34	0.41	0.14	3.87	**99.09**
cpx3-1_66	715	0.12	16.23	3.02	51.39	23.04	0.34	0.41	0.13	4.01	**98.68**
cpx3-1_67	726	0.13	16.43	3.10	51.32	23.43	0.33	0.35	0.11	3.95	**99.15**
cpx3-1_68	737	0.10	16.86	2.60	51.87	22.95	0.27	0.45	0.15	3.73	**98.98**
cpx3-1_69	748	0.12	16.63	2.79	51.55	23.08	0.32	0.35	0.13	3.91	**98.88**
cpx3-1_70	759 - Rim	0.09	16.48	2.98	51.26	23.26	0.33	0.26	0.12	4.20	**98.98**

Table 45: Continuation.

D5A(2) - Cpx 3A											
Name	Distance (µm)	Na_2O	MgO	Al_2O_3	SiO_2	CaO	TiO_2	Cr_2O_3	MnO	FeO	Total
cpx31-2_1	Core - 0	0.22	15.46	3.49	50.22	22.49	0.56	0.21	0.15	5.86	**98.65**
cpx31-2_2	10	0.24	15.62	3.50	50.13	22.47	0.53	0.23	0.11	5.64	**98.47**
cpx31-2_3	20	0.19	15.94	3.09	50.63	22.77	0.54	0.21	0.15	5.24	**98.77**
cpx31-2_4	30	0.17	15.68	3.16	50.62	22.30	0.68	0.06	0.15	5.27	**98.09**
cpx31-2_5	40	0.29	14.96	3.41	51.29	21.80	0.67	0.07	0.14	5.59	**98.22**
cpx31-2_6	50	0.10	16.99	2.23	51.64	23.50	0.25	0.46	0.10	3.58	**98.86**
cpx31-2_7	60	0.10	16.97	2.13	51.68	23.28	0.22	0.43	0.07	3.83	**98.69**
cpx31-2_8	70	0.12	17.05	2.01	51.85	23.30	0.22	0.48	0.07	3.64	**98.75**
cpx31-2_9	80	0.10	16.85	2.20	51.58	23.44	0.24	0.46	0.08	3.49	**98.43**
cpx31-2_10	90	0.12	16.57	2.61	51.40	23.23	0.34	0.39	0.14	4.12	**98.92**
cpx31-2_11	100	0.15	16.43	2.62	51.14	23.14	0.36	0.32	0.11	4.20	**98.48**
cpx31-2_12	110	0.13	17.05	2.09	51.59	23.55	0.23	0.46	0.10	3.50	**98.70**
cpx31-2_13	120	0.13	17.09	2.16	51.24	23.39	0.24	0.42	0.13	3.22	**98.02**
cpx31-2_14	130	0.12	16.86	2.23	51.74	23.89	0.21	0.40	0.09	3.31	**98.85**
cpx31-2_15	140	0.13	16.90	2.15	51.68	23.62	0.22	0.37	0.08	3.49	**98.65**
cpx31-2_16	150	0.12	16.86	2.26	51.26	23.45	0.28	0.36	0.08	3.84	**98.50**
cpx31-2_17	160	0.10	16.93	2.03	51.48	23.38	0.19	0.62	0.13	3.52	**98.39**
cpx31-2_18	170	0.19	16.53	3.00	50.86	22.89	0.28	0.47	0.07	4.08	**98.38**
cpx31-2_19	180	0.22	15.87	4.01	49.63	22.83	0.46	0.50	0.10	5.13	**98.74**
cpx31-2_20	190 - Rim	0.19	15.45	4.40	49.78	22.45	0.45	0.42	0.15	5.62	**98.90**

Table 46: The major element composition of an pyroxene crystal from sample D5A(2).

Sample	Cpx 2A				Cpx 2B		
Distance (µm)	52	130	338	585	12	14	432
Elemen /Name	Cpx2A-01	Cpx2A-02	Cpx2A-03	Cpx2A-04	Cpx2B-01	Cpx2B-03	Cpx2B-04
Sc	126.54	120.58	121.71	117.19	137.63	110.70	97.44
Ti	2576.02	1908.62	2727.62	2982.49	2303.07	1647.68	1924.99
V	204.73	173.60	228.85	240.95	201.70	145.91	174.88
Cr	3322.84	5591.00	4356.21	2938.42	849.00	5190.83	3044.99
Mn	723.48	662.30	726.61	857.66	968.14	582.94	686.31
Co	28.66	26.83	25.95	27.26	30.99	24.94	25.12
Ni	160.85	187.96	152.87	144.42	171.15	165.13	160.88
Zn	15.98	13.23	17.27	17.55	20.52	7.59	20.01
Rb	-	-	0.10	-	-	-	-
Sr	31.07	29.00	28.31	29.65	28.19	26.53	26.41
Y	8.73	6.19	8.46	10.38	9.52	5.18	6.33
Zr	8.51	5.80	10.20	11.36	10.76	3.93	6.54
Nb	-	-	-	-	-	-	-
Cs	1.26	-	-	-	-	0.11	-
Ba	-	-	0.17	0.20	0.47	-	0.87
La	0.96	0.64	1.16	1.23	1.15	0.44	0.88
Ce	2.93	1.67	3.27	4.37	3.44	2.03	1.97
Pr	0.61	0.34	0.69	0.77	0.58	0.49	0.46
Nd	3.72	2.89	3.16	3.91	3.16	2.30	2.65
Sm	2.18		1.38	0.17	2.20	0.53	0.24
Eu	0.48	0.14	0.16	0.57	0.53	-	0.21
Gd	1.30	0.32	1.90	0.52	2.28	-	1.75
Tb	0.30		0.16	0.25	0.38	-	0.47
Dy	1.68	1.69	1.22	2.97	2.65	0.52	0.79
Ho	0.18	0.11	0.46	0.49	0.27	0.36	
Er	0.47	-	0.81	0.88	0.88	0.58	0.52
Tm	0.07	-	0.22	0.14		0.05	0.08
Yb	1.12	0.19	0.32	1.13	0.32	-	-
Lu	-	-	0.03	0.14	0.14	-	-
Hf	0.21	-	-	0.34	0.65	0.53	-
Ta	-	0.08	0.11	-	-	-	-
Pb	-	0.19	-	-	-	-	-
Th	0.11	-	0.14	-	-	-	-
U	-	-	-	0.11	-	-	-

Table 47: Trace element composition of sample Cpx 2. The dash symbol (-) represent concentration under the detection limit of the instruments.

Sample	Cpx 3B							Cpx 3A		
Distance (μm)	33	132	253	473	572	627	737	20	90	183
Elemen /Name	Cpx3B-01	Cpx3B-02	Cpx3B-03	Cpx3B-04	Cpx3B-05	Cpx3B-06	Cpx3B-07	Cpx3A-01	Cpx3A-02	Cpx3A-03
Sc	106.45	84.88	91.29	108.98	105.44	105.75	99.58	105.47	118.27	106.49
Ti	2004.63	967.83	1217.99	2768.48	2273.12	1952.50	1984.88	1852.83	2568.73	2121.14
V	170.15	109.49	119.66	213.04	207.95	167.74	176.82	161.59	209.32	176.12
Cr	1445.55	4195.63	3113.73	366.83	825.68	2454.82	1821.21	2446.14	739.9	2153.48
Mn	761.68	589.92	648.15	1182.88	941.31	796.75	746.51	646.8	1021.33	779.95
Co	27.47	25.56	26.43	37.81	30.37	31.48	27.60	27.17	32.52	27.25
Ni	143.84	165.98	170.68	105.21	104.53	155.22	160.19	149.36	121.97	153.78
Zn	26.15	8.85	8.96	25.92	-	8.46	14.68	10.89	18.36	17.82
Rb	0.66	-	-	0.43	-	-	-	-	-	0.161
Sr	35.48	25.14	28.42	28.68	24.68	23.15	25.79	27.15	26.6	24.42
Y	5.37	2.42	3.55	10.32	8.00	7.02	5.05	6.04	8.1	7.46
Zr	4.49	1.98	2.08	8.99	6.97	5.16	5.94	5.49	8.94	7.79
Nb	0.06	0.37	-	-	-	-	0.71	-	-	0.039
Cs	-	-	-	-	-	0.78	-	-	-	-
Ba	-	-	-	-	-	-	0.93	1.79	3.15	-
La	0.65	-	0.44	1.14	1.25	0.17	0.63	0.78	0.83	0.73
Ce	2.63	0.36	0.55	3.81	2.87	3.07	2.26	2.1	3.34	2.74
Pr	0.38	-	0.08	0.75	1.09	0.10	0.55	0.485	0.58	0.6
Nd	2.24	0.30	-	3.48	2.67	1.41	2.24	1.58	3.38	3.29
Sm	0.52	-	-	1.05	2.11	-	1.03	1.17	1.03	-
Eu	0.34	-	0.28	-	-	-	-	0.335	0.282	0.154
Gd	0.72	-	1.36	1.11		0.77	0.84	1.13	1.96	1.19
Tb	0.24	-	-	0.19	0.30	0.23	0.15	0.305	-	0.05
Dy	1.25	-	0.57	1.26	0.57	1.46	1.03	0.76	0.85	0.84
Ho	0.13	-	-	0.18	-	-	-	0.172	0.349	0.13
Er	0.25	0.25	0.24	1.95	-	0.28	-	-	0.74	0.48
Tm	-	-	0.08	0.06	0.07		0.17	0.061	0.025	0.214
Yb	0.61	-	0.77	-	-	0.89	-	-	1.01	0.63
Lu		0.07	0.24	-	-	-	-	0.135		0.022
Hf	-	-	-	-	-	-	0.61	0.75	0.29	0.28
Ta	-	-	0.21	0.17		0.21	-	-	-	-
Pb	-	-	1.17	-	0.67	0.70	0.67	-	-	-
Th	-	-	0.56	-	0.42	-	-	0.061	0.154	0.085
U	-	-	-	-	2.51	-	-	-	0.19	0.141

Table 48: Trace element composition of sample Cpx 3. The dash symbol (-) represent concentration under the detection limit of the instruments.

Sample	Cpx 7		Cpx 8				Cpx 9	
Elemen /Name	Cpx7-01	Cpx7-02	Cpx8-01	Cpx8-02	Cpx8-03	Cpx8-04	Cpx9-01	Cpx9-02
Sc	119.02	127.05	105.26	100.42	125.72	101.71	121.45	134.44
Ti	3426.35	4547.42	3725.35	2219.18	2096.20	2502.01	3365.97	5248.20
V	283.02	337.07	285.22	175.74	203.02	216.47	269.91	369.40
Cr	2017.16	560.93	-	2272.68	2130.77	1569.93	161.17	58.65
Mn	1030.85	1184.91	1716.77	826.87	843.03	836.14	1433.30	1357.57
Co	32.96	32.58	39.34	33.44	32.11	30.46	27.42	34.27
Ni	128.60	112.82	53.81	146.93	176.74	166.78	74.86	83.09
Zn	21.79	24.53	58.95	34.14	15.71	-	45.06	23.48
Rb	0.12	-	-	0.81	-	-	-	-
Sr	34.09	34.94	29.65	29.42	32.32	30.75	28.01	33.95
Y	11.87	15.01	17.22	7.96	8.92	7.90	13.45	22.65
Zr	12.10	16.63	19.83	4.01	2.66	9.15	15.07	23.51
Nb	-	-	-	0.10	-	-	0.39	0.18
Cs	-	-	-	-	-	-	-	-
Ba	-	-	-	-	-	-	-	-
La	1.70	1.93	2.71	1.04	0.77	1.18	1.86	3.70
Ce	4.68	6.86	9.47	2.69	2.11	2.00	8.32	10.35
Pr	0.89	1.44	1.97	0.44	-	1.31	1.80	1.84
Nd	5.20	7.88	11.43	4.72	-	1.08	0.81	6.65
Sm	1.48	2.50	3.56	-	-	2.15	2.89	2.33
Eu	0.70	0.94	1.42	-	0.48	0.40	-	0.72
Gd	0.63	2.70	2.68	0.54	2.55	-	3.24	-
Tb	0.25	0.32	0.55	-	0.25	0.21	1.02	0.22
Dy	2.25	3.83	3.15	-	-	-	-	2.63
Ho	0.49	0.57	0.56	0.11		0.35	0.71	0.66
Er	0.91	1.36	2.72	1.53	-	-	-	3.69
Tm	0.14	0.21	0.56	-	-	-	-	0.25
Yb	1.46	0.90	0.42	-	2.83	-	-	-
Lu	0.09	0.21	-	-	-	-	-	-
Hf	0.41	0.91	-	-	-	-	-	2.45
Ta	0.05	-	-	-	-	-	1.01	0.28
Pb	-	0.29	0.96	-	-	0.92	-	0.42
Th	0.10	-	0.35	-	-	-	-	-
U	-	-	-	-	-	0.80	-	1.16

Table 49: Trace element composition of sample Cpx 7, 8 and 9. The dash symbol (-) represent concentration under the detection limit of the instruments.

Sample	Cpx 10			
Elemen /Name	Cpx10-17	Cpx10-18	Cpx10-19	Cpx10-20
Sc	127.65	97.52	107.22	123.12
Ti	3624.78	1760.55	1781.33	2324.13
V	278.10	143.11	159.06	196.70
Cr	698.20	2833.21	1490.89	886.21
Mn	1201.60	691.87	768.48	1003.94
Co	33.88	24.79	28.37	30.80
Ni	109.45	157.24	149.50	120.29
Zn	44.29	22.72	22.26	29.78
Rb	0.30	0.14	0.26	0.13
Sr	31.20	22.44	22.34	26.11
Y	13.47	6.01	6.93	8.74
Zr	15.17	5.21	6.53	9.40
Nb	0.84	-	-	-
Cs	0.29	-	0.70	-
Ba	0.72	-	0.47	0.42
La	1.86	0.49	0.52	0.69
Ce	6.22	2.04	2.47	3.42
Pr	1.02	0.37	0.36	0.68
Nd	6.35	0.26	2.98	3.54
Sm	2.31	0.58	-	1.93
Eu	0.49	0.13	0.43	-
Gd	2.37	0.77	1.19	1.86
Tb	0.52	0.06	0.21	0.19
Dy	2.66	1.32	0.83	1.77
Ho	0.33	0.33	0.33	-
Er	1.61	0.09	0.52	0.99
Tm	0.24	-	0.03	-
Yb	1.11	-	-	0.41
Lu	0.37	0.05	-	0.18
Hf	0.83	-	-	-
Ta	-	0.10	-	0.06
Pb	-	-	0.41	0.23
Th	-	-	0.12	0.21
U	1.05	-	0.30	-

Table 50: Trace element composition of sample Cpx 10. The dash symbol (-) represent concentration under the detection limit of the instruments.

Appendix VI – Sample D6

This appendix contains the major element analyses of 5 olivines and 2 pyroxenes. Moreover, in this appendix can be found the trace element composition of 2 pyroxenes.

D6- Ol 1												
Name	Distance (µm)	Na_2O	MgO	Al_2O_3	SiO_2	CaO	TiO_2	Cr_2O_3	MnO	FeO	NiO	Total
ol1-1_1	Core - 0	0.003	46.46	-	39.82	0.15	0.018	0.062	0.22	13.65	0.25	**100.63**
ol1-1_2	15	-	46.16	0.020	39.56	0.14	0.000	0.014	0.22	13.59	0.25	**99.95**
ol1-1_3	29	-	46.24	0.010	40.03	0.15	0.009	0.026	0.20	13.54	0.17	**100.38**
ol1-1_4	44	0.016	46.28	0.005	39.92	0.15	0.009	0.062	0.24	13.31	0.23	**100.22**
ol1-1_5	59	-	46.45	-	39.63	0.14	0.002	0.034	0.26	13.55	0.22	**100.28**
ol1-1_6	73	-	46.59	-	39.68	0.15	0.036	0.017	0.20	13.49	0.22	**100.38**
ol1-1_7	88	0.035	46.47	0.010	39.63	0.14	-	-	0.20	13.33	0.24	**100.05**
ol1-1_8	103	-	46.22	0.001	39.67	0.14	-	0.026	0.21	13.07	0.22	**99.55**
ol1-1_9	117	-	46.07	0.029	39.57	0.13	0.018	-	0.27	13.30	0.19	**99.58**
ol1-1_10	132	-	46.40	0.034	39.34	0.15	-	0.017	0.20	13.53	0.23	**99.90**
ol1-1_11	147	-	46.51	0.024	39.63	0.14	-	0.048	0.18	13.56	0.23	**100.33**
ol1-1_12	161	-	46.02	0.001	39.47	0.14	0.038	0.060	0.15	13.18	0.21	**99.27**
ol1-1_13	176	-	46.15	-	39.27	0.14	-	0.014	0.24	13.44	0.21	**99.46**
ol1-1_14	191	-	46.39	0.054	39.48	0.12	0.006	0.014	0.19	13.31	0.20	**99.76**
ol1-1_15	205	-	46.22	0.013	39.30	0.12	-	-	0.21	13.17	0.18	**99.20**
ol1-1_16	220	0.004	46.63	0.003	39.25	0.14	0.034	-	0.15	13.28	0.23	**99.70**
ol1-1_17	235	-	46.27	-	39.41	0.15	0.031	0.026	0.22	13.57	0.17	**99.85**
ol1-1_18	249	0.027	46.52	0.004	39.03	0.14	0.004	0.026	0.18	13.31	0.20	**99.43**
ol1-1_19	264	0.006	46.50	0.016	39.36	0.14	0.013	0.046	0.20	13.48	0.24	**99.99**
ol1-1_20	279	-	46.36	0.007	38.98	0.16	0.004	0.002	0.19	13.18	0.20	**99.08**
ol1-1_21	293	0.007	46.44	-	39.39	0.16	0.035	-	0.21	13.48	0.19	**99.91**
ol1-1_22	308	-	46.54	0.010	38.78	0.15	0.023	0.010	0.25	13.06	0.21	**99.03**
ol1-1_23	323	-	46.29	0.017	39.24	0.13	0.022	0.026	0.18	13.42	0.24	**99.56**
ol1-1_24	337	-	46.42	0.011	39.17	0.11	0.022	0.041	0.25	13.27	0.26	**99.55**
ol1-1_25	352	-	46.55	-	39.08	0.14	0.018	-	0.16	13.54	0.19	**99.68**
ol1-1_26	367	-	46.15	0.000	39.08	0.12	-	0.017	0.29	13.22	0.21	**99.09**
ol1-1_27	381	-	46.67	-	39.20	0.15	0.008	-	0.22	13.43	0.22	**99.90**
ol1-1_28	396	-	46.31	-	38.98	0.14	-	-	0.18	13.56	0.22	**99.38**
ol1-1_29	411	0.005	46.31	0.002	38.80	0.10	-	0.002	0.21	13.31	0.21	**98.95**
ol1-1_30	425	0.010	46.32	0.013	38.88	0.15	0.018	0.010	0.22	13.27	0.19	**99.08**
ol1-1_31	455	-	46.27	0.035	38.89	0.13	-	0.029	0.23	13.20	0.21	**98.99**
ol1-1_32	470	-	46.33	0.025	38.86	0.15	0.011	-	0.21	13.30	0.22	**99.11**
ol1-1_33	484	0.014	46.03	-	38.80	0.13	0.007	0.060	0.24	13.04	0.22	**98.54**
ol1-1_34	499	-	46.24	0.015	38.81	0.14	-	0.046	0.25	13.18	0.23	**98.91**
ol1-1_35	514	-	46.48	0.017	38.79	0.14	0.018	0.031	0.14	13.47	0.22	**99.30**
ol1-1_36	528	0.008	46.42	0.027	39.19	0.13	0.022	0.022	0.21	13.04	0.18	**99.24**
ol1-1_37	543	-	46.33	0.026	39.12	0.12	-	0.031	0.22	13.09	0.21	**99.16**

Table 51: EPMA analyses of the major element composition of an olivine crystal. The dash symbol (-) represent concentration under the detection limit of the instruments.

D6- Ol 1												
Name	Distance (µm)	Na_2O	MgO	Al_2O_3	SiO_2	CaO	TiO_2	Cr_2O_3	MnO	FeO	NiO	Total
ol1-1_38	558	-	46.35	-	38.97	0.14	-	0.034	0.22	13.32	0.21	**99.26**
ol1-1_39	572	0.005	46.14	0.014	39.09	0.11	0.002	0.002	0.23	12.88	0.14	**98.62**
ol1-1_40	587	0.000	46.18	0.022	39.03	0.12	-	0.017	0.19	13.04	0.20	**98.78**
ol1-1_41	602	0.000	46.47	0.014	38.27	0.15	-	-	0.16	13.27	0.23	**98.58**
ol1-1_42	617	0.000	46.34	0.031	38.65	0.14	0.005	0.034	0.21	13.21	0.23	**98.85**
ol1-1_43	631	0.000	46.17	-	38.80	0.15	0.011	-	0.19	13.11	0.21	**98.64**
ol1-1_44	646	0.000	46.13	0.007	38.58	0.14	-	0.010	0.15	13.14	0.15	**98.30**
ol1-1_45	661	0.000	46.41	-	38.60	0.14	-	0.048	0.22	13.24	0.20	**98.85**
ol1-1_46	675	0.007	46.33	-	38.52	0.15	0.001	0.019	0.16	13.36	0.23	**98.77**
ol1-1_47	690	0.000	46.43	0.034	38.44	0.14	0.011	0.022	0.19	13.30	0.18	**98.76**
ol1-1_48	705	0.000	46.12	-	38.46	0.14	0.008	0.026	0.17	13.07	0.26	**98.26**
ol1-1_49	719	0.000	46.40	0.017	38.15	0.14	0.006	0.053	0.20	13.27	0.24	**98.48**
ol1-1_50	734	0.000	46.18	-	38.31	0.12	0.003	-	0.21	13.29	0.22	**98.34**
ol1-1_51	749	0.000	46.12	0.006	38.36	0.15	-	0.048	0.18	12.91	0.19	**97.96**
ol1-1_52	763	0.000	46.10	0.017	38.07	0.12	0.003	0.012	0.18	12.99	0.19	**97.70**
ol1-1_53	778	0.000	46.07	0.002	38.67	0.11	0.013	-	0.17	13.26	0.21	**98.51**
ol1-1_54	793	0.000	46.33	-	38.50	0.14	-	0.057	0.20	13.34	0.21	**98.78**
ol1-1_55	807	0.000	46.43	0.012	38.53	0.15	0.022	0.010	0.20	13.47	0.19	**99.00**
ol1-1_56	822	0.008	46.21	-	38.32	0.16	0.007	0.034	0.22	13.17	0.24	**98.37**
ol1-1_57	837	0.000	46.04	0.015	38.36	0.14	-	-	0.20	13.12	0.20	**98.07**
ol1-1_58	851	0.000	46.02	-	38.59	0.15	-	0.026	0.17	13.11	0.23	**98.31**
ol1-1_59	866	0.000	46.29	0.010	38.47	0.12	-	0.017	0.21	13.41	0.23	**98.77**
ol1-1_60	881	0.000	46.38	-	39.05	0.12	0.013	0.019	0.23	13.38	0.28	**99.47**
ol1-1_61	895	0.000	46.08	0.028	38.66	0.16	-	0.036	0.24	13.39	0.19	**98.77**
ol1-1_62	910	0.000	45.73	-	38.73	0.16	0.004	-	0.21	13.84	0.17	**98.85**
ol1-1_63	925	0.000	45.97	0.007	38.65	0.12	-	0.002	0.18	14.10	0.20	**99.22**
ol1-1_64	939	0.000	45.74	-	38.83	0.18	0.028	0.010	0.22	14.29	0.19	**99.49**
ol1-1_65	954	0.000	45.35	0.016	38.86	0.17	0.007	0.041	0.24	14.73	0.22	**99.63**
ol1-1_66	969	0.000	44.92	0.015	38.17	0.17	-	0.017	0.24	14.90	0.17	**98.59**
ol1-1_67	983	0.016	44.40	0.004	38.72	0.17	0.006	-	0.26	15.15	0.17	**98.90**
ol1-1_68	998	0.016	44.13	0.015	38.53	0.16	-	0.036	0.24	15.77	0.15	**99.04**
ol1-1_69	1013	0.000	44.13	0.024	38.46	0.18	-	-	0.21	15.88	0.14	**99.03**
ol1-1_70	1027	0.016	44.07	0.014	38.48	0.20	0.018	-	0.29	16.47	0.15	**99.70**
ol1-1_71	1042	0.037	44.08	0.017	38.30	0.15	0.025	-	0.25	16.51	0.12	**99.48**
ol1-1_72	1057	0.000	44.08	0.029	38.77	0.17	0.038	0.064	0.26	16.68	0.17	**100.26**
ol1-1_73	1071	0.000	43.83	0.016	38.72	0.19	0.013	-	0.23	16.60	0.15	**99.74**
ol1-1_74	1086	0.000	43.96	0.050	38.83	0.18	0.021	-	0.28	16.76	0.17	**100.24**
ol1-1_75	1101	0.000	43.85	0.059	38.72	0.18	-	-	0.25	16.76	0.13	**99.94**
ol1-1_76	1115	0.005	43.82	-	38.86	0.22	0.026	-	0.30	17.18	0.13	**100.53**
ol1-1_77	1130	0.000	43.53	0.005	38.73	0.21	-	0.040	0.28	17.26	0.12	**100.17**
ol1-1_79	1159 - Rim	0.005	42.56	0.013	38.82	0.21	-	0.021	0.28	18.05	0.10	**100.05**

Table 51: Continuation.

D6- Ol 1 (2)												
Name	Distance (µm)	Na_2O	MgO	Al_2O_3	SiO_2	CaO	TiO_2	Cr_2O_3	MnO	FeO	NiO	Total
Ol1(2)1_1	Core - 0	-	46.78	0.035	40.17	0.14	0.018	0.041	0.22	13.30	0.28	**100.99**
Ol1(2)1_2	14	-	46.73	0.026	40.46	0.13	-	0.019	0.23	13.51	0.25	**101.35**
Ol1(2)1_3	29	-	46.70	0.016	40.24	0.13	-	0.065	0.19	13.25	0.23	**100.82**
Ol1(2)1_4	43	0.017	46.78	0.007	40.21	0.13	0.001	-	0.24	13.68	0.26	**101.32**
Ol1(2)1_5	57	-	46.61	-	40.24	0.16	0.003	-	0.23	13.30	0.18	**100.72**
Ol1(2)1_6	71	-	46.77	0.004	40.29	0.14	-	0.010	0.22	13.28	0.25	**100.97**
Ol1(2)1_7	86	0.025	46.60	0.030	40.22	0.14	0.010	0.014	0.20	13.41	0.23	**100.88**
Ol1(2)1_8	100	-	46.96	0.034	40.37	0.12	-	0.002	0.24	13.79	0.24	**101.75**
Ol1(2)1_9	114	-	46.66	-	40.25	0.15	-	0.007	0.18	13.46	0.17	**100.87**
Ol1(2)1_10	129	-	46.64	0.026	40.18	0.16	0.022	0.014	0.23	13.43	0.21	**100.91**
Ol1(2)1_11	143	0.002	46.69	0.007	40.07	0.14	0.003	-	0.19	13.55	0.25	**100.91**
Ol1(2)1_12	157	-	46.84	0.017	40.47	0.16	-	0.026	0.26	13.40	0.24	**101.40**
Ol1(2)1_13	171	-	46.70	0.001	40.35	0.13	-	0.029	0.22	13.30	0.28	**101.00**
Ol1(2)1_14	186	-	46.75	0.023	40.07	0.14	-	-	0.27	13.19	0.19	**100.63**
Ol1(2)1_15	200	-	46.77	0.005	40.32	0.14	0.026	0.048	0.29	13.64	0.22	**101.45**
Ol1(2)1_16	214	0.040	46.81	0.000	40.15	0.15	-	0.074	0.26	13.45	0.18	**101.11**
Ol1(2)1_17	228	0.000	46.87	0.017	40.15	0.13	-	0.029	0.22	13.33	0.25	**101.00**
Ol1(2)1_18	243	0.003	46.83	0.021	40.09	0.13	-	0.017	0.21	13.44	0.23	**100.97**
Ol1(2)1_19	257	0.020	46.52	0.028	40.18	0.13	0.005	0.010	0.22	13.40	0.23	**100.74**
Ol1(2)1_20	271	0.000	46.67	0.017	40.24	0.12	-	0.012	0.23	13.47	0.25	**101.01**
Ol1(2)1_21	286	0.015	46.70	0.022	40.15	0.13	0.001	-	0.25	13.32	0.26	**100.84**
Ol1(2)1_22	300	0.002	46.82	0.018	40.33	0.12	-	0.048	0.25	13.48	0.23	**101.30**
Ol1(2)1_23	314	-	46.71	-	40.46	0.16	0.023	-	0.21	13.50	0.24	**101.31**
Ol1(2)1_24	328	-	46.95	-	40.29	0.13	0.027	0.014	0.21	13.51	0.21	**101.35**
Ol1(2)1_25	343	0.006	46.99	0.030	40.42	0.15	0.018	0.055	0.18	13.43	0.26	**101.53**
Ol1(2)1_26	357	0.008	46.76	-	40.37	0.18	-	0.012	0.21	13.46	0.25	**101.25**
Ol1(2)1_27	371	-	46.87	0.007	40.37	0.20	0.009	0.026	0.15	13.53	0.15	**101.30**
Ol1(2)1_28	386	-	46.81	-	40.34	0.16	-	0.019	0.22	13.25	0.21	**101.01**
Ol1(2)1_29	400	0.006	47.01	-	40.44	0.19	-	0.010	0.21	13.68	0.22	**101.76**
Ol1(2)1_30	414	-	46.59	0.032	40.42	0.19	0.011	0.046	0.23	13.37	0.26	**101.14**
Ol1(2)1_31	443	-	46.72	0.007	40.41	0.14	0.009	0.045	0.19	13.61	0.27	**101.40**
Ol1(2)1_32	458	-	46.83	0.004	40.32	0.18	-	0.067	0.21	13.50	0.26	**101.38**
Ol1(2)1_33	472	-	46.97	0.025	40.42	0.15	-	0.048	0.26	13.41	0.24	**101.52**
Ol1(2)1_34	486	-	46.62	0.018	40.31	0.17	-	0.036	0.26	13.37	0.25	**101.05**
Ol1(2)1_35	500	-	46.75	0.021	40.34	0.14	0.027	-	0.22	13.71	0.22	**101.42**
Ol1(2)1_36	515	-	46.89	0.000	40.27	0.17	0.008	-	0.22	13.52	0.29	**101.37**
Ol1(2)1_37	529	-	46.59	0.004	40.44	0.13	-	-	0.23	13.46	0.23	**101.08**
Ol1(2)1_38	558	-	46.45	-	40.35	0.15	0.025	-	0.19	13.46	0.21	**100.83**
Ol1(2)1_39	573	-	46.66	0.009	40.49	0.15	0.033	0.010	0.21	13.38	0.28	**101.23**
Ol1(2)1_40	587	0.012	46.60	0.009	40.40	0.14	-	0.029	0.26	13.50	0.29	**101.24**

Table 52: The major element composition of an olivine crystal from sample D6. The dash symbol (-) represent concentration under the detection limit of the instruments.

D6- Ol 1 (2)												
Name	Distance (µm)	Na_2O	MgO	Al_2O_3	SiO_2	CaO	TiO_2	Cr_2O_3	MnO	FeO	NiO	Total
Ol1(2)1_41	601	-	46.91	0.018	40.22	0.17	0.002	0.024	0.24	13.45	0.26	**101.28**
Ol1(2)1_42	615	0.018	46.68	0.017	40.46	0.13	-	0.012	0.23	13.49	0.22	**101.25**
Ol1(2)1_43	630	-	46.79	-	40.41	0.16	0.004	-	0.23	13.54	0.22	**101.35**
Ol1(2)1_44	644	-	46.80	-	40.07	0.14	0.001	0.041	0.19	13.60	0.25	**101.09**
Ol1(2)1_45	673	-	46.62	0.007	40.37	0.16	0.003	-	0.25	13.36	0.26	**101.03**
Ol1(2)1_46	688	0.006	46.82	0.023	40.43	0.14	0.004	-	0.24	13.66	0.29	**101.61**
Ol1(2)1_47	702	0.000	46.81	0.043	40.38	0.16	0.018	-	0.24	13.56	0.24	**101.46**
Ol1(2)1_48	716	0.008	46.73	0.031	40.49	0.14	-	0.034	0.25	13.55	0.26	**101.50**
Ol1(2)1_49	730	0.000	46.50	-	40.28	0.16	-	-	0.22	13.28	0.26	**100.71**
Ol1(2)1_50	745	0.007	47.07	-	40.30	0.16	0.001	0.033	0.24	13.81	0.26	**101.88**
Ol1(2)1_51	759	0.000	46.67	0.010	40.40	0.15	-	0.014	0.20	13.29	0.24	**100.97**
Ol1(2)1_52	787	0.013	46.71	0.000	40.51	0.17	0.006	0.002	0.26	13.54	0.21	**101.43**
Ol1(2)1_53	801	0.000	46.93	0.019	40.30	0.16	0.031	0.012	0.22	13.68	0.18	**101.52**
Ol1(2)1_54	816	0.000	46.43	0.015	40.33	0.15	0.007	0.029	0.22	13.33	0.28	**100.79**
Ol1(2)1_55	830	0.017	46.44	0.008	40.36	0.15	-	0.043	0.23	13.80	0.20	**101.25**
Ol1(2)1_56	844	0.000	46.51	-	40.56	0.16	0.030	0.007	0.16	13.59	0.27	**101.29**
Ol1(2)1_57	859	0.001	46.74	0.014	40.29	0.14	-	0.031	0.22	13.56	0.26	**101.26**
Ol1(2)1_58	873	-	46.41	0.002	40.21	0.14	0.003	0.017	0.22	13.69	0.19	**100.89**
Ol1(2)1_59	901	-	46.79	0.007	40.49	0.15	0.018	0.062	0.25	14.05	0.26	**102.07**
Ol1(2)1_60	915	-	46.61	0.028	40.23	0.15	0.004	0.012	0.24	13.83	0.24	**101.35**
Ol1(2)1_61	930	-	46.62	0.023	40.19	0.15	0.004	0.029	0.22	14.06	0.20	**101.50**
Ol1(2)1_62	944	-	46.43	-	40.44	0.13	-	0.048	0.24	13.94	0.24	**101.46**
Ol1(2)1_63	958	-	46.41	0.010	40.46	0.14	-	0.031	0.25	14.20	0.22	**101.72**
Ol1(2)1_64	973	0.017	45.67	-	40.00	0.16	0.006	-	0.21	14.60	0.23	**100.89**
Ol1(2)1_65	987	0.000	45.81	0.007	40.20	0.16	0.004	0.010	0.25	14.44	0.18	**101.07**
Ol1(2)1_66	1001	0.002	45.44	0.014	39.98	0.17	-	0.005	0.24	15.19	0.21	**101.26**
Ol1(2)1_67	1015	0.007	45.31	0.025	40.06	0.16	0.008	0.002	0.21	15.30	0.16	**101.24**
Ol1(2)1_68	1030	-	45.12	-	40.05	0.15	-	0.029	0.27	15.54	0.21	**101.37**
Ol1(2)1_69	1044	-	44.79	-	40.09	0.17	0.011	0.031	0.31	15.49	0.20	**101.10**
Ol1(2)1_70	1058	-	44.61	0.011	40.00	0.20	-	0.010	0.27	16.03	0.22	**101.35**
Ol1(2)1_71	1072	0.016	44.43	0.026	39.88	0.16	-	0.028	0.28	16.29	0.20	**101.30**
Ol1(2)1_72	1087	-	44.11	0.018	39.81	0.21	0.041	0.106	0.29	16.36	0.18	**101.12**
Ol1(2)1_73	1101	-	43.94	0.016	39.62	0.18	0.025	0.035	0.24	16.78	0.19	**101.02**
Ol1(2)1_74	1115	-	43.77	0.028	39.69	0.15	0.020	0.009	0.26	16.81	0.15	**100.88**
Ol1(2)1_75	1130	-	43.63	0.037	39.68	0.21	0.028	0.129	0.30	17.63	0.14	**101.78**
Ol1(2)1_76	1144	-	43.34	0.026	39.63	0.19	0.019	0.031	0.28	18.10	0.14	**101.76**
Ol1(2)1_78	1158	-	43.02	0.029	39.54	0.21	0.023	0.042	0.31	17.97	0.14	**101.27**
Ol1(2)1_79	1172	-	42.64	0.003	39.42	0.21	-	0.038	0.32	17.79	0.12	**100.54**
Ol1(2)1_80	1187 - Rim	-	42.42	0.003	39.44	0.23	0.035	0.028	0.37	17.84	0.13	**100.50**

Table 52: Continuation.

D6- Ol 2												
Name	Distance (µm)	Na_2O	MgO	Al_2O_3	SiO_2	CaO	TiO_2	Cr_2O_3	MnO	FeO	NiO	Total
ol2-2_1	Core - 0	0.033	44.56	0.023	38.76	0.15	0.010	0.010	0.20	15.07	0.13	**98.95**
ol2-2_2	10.77	-	44.77	0.032	38.57	0.12	0.019	0.024	0.20	15.22	0.21	**99.17**
ol2-2_3	21.21	0.012	44.69	0.007	38.88	0.15	0.001	-	0.21	14.80	0.20	**98.95**
ol2-2_4	31.98	0.014	45.03	0.033	38.59	0.13	0.020	0.005	0.25	15.33	0.14	**99.54**
ol2-2_5	42.75	-	44.79	0.009	38.82	0.15	0.018	-	0.20	14.81	0.17	**98.98**
ol2-2_6	53.52	0.025	45.06	0.057	38.70	0.13	-	0.021	0.25	15.08	0.14	**99.47**
ol2-2_7	63.96	0.003	44.88	-	38.82	0.14	-	0.017	0.24	14.89	0.17	**99.16**
ol2-2_8	74.73	-	45.01	-	38.52	0.12	-	0.024	0.25	15.11	0.18	**99.22**
ol2-2_9	85.50	-	44.92	0.018	38.67	0.14	0.025	0.033	0.25	15.06	0.14	**99.25**
ol2-2_10	96.27	0.007	44.88	-	38.89	0.15	0.000	0.031	0.26	15.45	0.19	**99.85**
ol2-2_11	106.71	0.014	44.84	0.034	38.98	0.17	0.042	0.017	0.21	15.13	0.13	**99.56**
ol2-2_12	117.48	-	44.92	-	38.62	0.15	0.003	-	0.22	15.16	0.15	**99.23**
ol2-2_13	128.25	0.022	44.79	0.038	38.78	0.12	0.016	0.036	0.23	15.19	0.08	**99.30**
ol2-2_14	139.02	-	44.87	-	38.94	0.13	-	0.033	0.23	14.94	0.17	**99.31**
ol2-2_15	149.46	-	44.67	0.041	38.94	0.15	0.006	0.012	0.23	15.08	0.16	**99.28**
ol2-2_16	160.23	-	44.84	-	38.94	0.17	-	-	0.22	14.92	0.21	**99.31**
ol2-2_17	171.01	0.012	45.02	-	38.86	0.15	0.016	0.007	0.22	15.04	0.14	**99.46**
ol2-2_18	181.45	-	44.81	-	39.09	0.14	-	-	0.25	15.15	0.13	**99.58**
ol2-2_19	192.22	-	45.03	-	39.23	0.14	0.004	0.017	0.26	15.31	0.15	**100.14**
ol2-2_20	202.99	0.026	44.80	0.032	39.02	0.16	0.011	-	0.26	15.23	0.17	**99.70**
ol2-2_21	213.76	0.032	45.00	-	39.14	0.15	-	0.021	0.20	15.31	0.18	**100.03**
ol2-2_22	224.20	-	45.06	0.013	39.07	0.14	-	-	0.23	15.60	0.19	**100.30**
ol2-2_23	234.97	-	44.95	0.024	38.93	0.15	0.030	-	0.26	14.97	0.18	**99.48**
ol2-2_24	245.74	-	44.96	0.043	39.08	0.13	0.001	-	0.21	14.99	0.13	**99.54**
ol2-2_25	256.51	-	45.38	-	39.17	0.15	-	0.002	0.24	15.31	0.16	**100.41**
ol2-2_27	276.76	0.035	43.35	0.044	40.01	0.17	0.001	-	0.25	14.75	0.18	**98.80**
ol2-2_29	298.31	0.011	45.11	-	39.14	0.15	0.001	-	0.26	15.26	0.15	**100.08**
ol2-2_30	308.75	0.001	45.23	-	39.04	0.10	0.008	-	0.20	15.33	0.16	**100.08**
ol2-2_32	330.29	-	44.99	0.037	39.22	0.11	0.033	-	0.26	14.69	0.19	**99.53**
ol2-2_33	341.06	-	45.22	-	39.23	0.13	-	0.043	0.21	14.77	0.18	**99.79**
ol2-2_34	351.50	0.012	45.05	0.002	39.24	0.13	-	0.024	0.23	14.98	0.18	**99.85**
ol2-2_35	362.27	-	45.04	0.004	39.27	0.14	0.022	0.005	0.24	15.36	0.20	**100.29**
ol2-2_36	373.04	-	45.09	0.023	39.20	0.14	0.013	0.012	0.23	14.93	0.18	**99.83**
ol2-2_37	383.48	0.028	45.12	0.018	39.31	0.16	0.000	0.045	0.28	14.83	0.15	**99.96**
ol2-2_38	394.25	0.023	45.19	0.063	39.27	0.17	0.010	0.000	0.23	14.88	0.21	**100.04**
ol2-2_39	405.02	-	45.00	-	39.37	0.14	0.000	0.031	0.24	14.76	0.14	**99.69**
ol2-2_40	415.79	0.020	45.19	0.025	39.20	0.17	0.020	0.024	0.19	14.96	0.16	**99.95**
ol2-2_41	426.23	0.003	45.19	0.009	39.10	0.15	-	-	0.24	14.95	0.20	**99.84**
ol2-2_42	437.00	0.007	44.99	0.029	39.19	0.16	-	-	0.24	14.91	0.11	**99.64**

Table 53: EPMA analyses of the major element composition of an olivine crystal. The dash symbol (-) represent concentration under the detection limit of the instruments.

D6- Ol 2												
Name	Distance (µm)	Na_2O	MgO	Al_2O_3	SiO_2	CaO	TiO_2	Cr_2O_3	MnO	FeO	NiO	Total
ol2-2_43	447.77	-	45.05	0.014	39.38	0.17	-	0.052	0.18	14.97	0.14	**99.96**
ol2-2_44	458.54	0.007	44.97	0.014	39.48	0.17	0.016	0.002	0.21	15.27	0.18	**100.33**
ol2-2_45	468.98	0.002	44.99	-	39.15	0.17	-	0.031	0.17	15.14	0.13	**99.78**
ol2-2_46	479.75	-	44.72	-	39.54	0.16	0.008	0.024	0.29	15.66	0.12	**100.52**
ol2-2_47	490.52	0.009	44.49	0.004	39.16	0.21	0.019	0.052	0.20	15.53	0.20	**99.87**
ol2-2_48	501.29	-	44.02	0.038	39.26	0.17	0.016	-	0.25	16.28	0.17	**100.21**
ol2-2_49	511.73	-	43.56	0.022	39.10	0.20	0.025	0.035	0.28	16.75	0.13	**100.09**
ol2-2_50	522.50 - Rim	-	43.29	-	39.05	0.22	0.015	0.042	0.30	17.38	0.17	**100.47**

Table 53: Continuation.

D6- Ol 3												
Name	Distance (µm)	Na_2O	MgO	Al_2O_3	SiO_2	CaO	TiO_2	Cr_2O_3	MnO	FeO	NiO	Total
ol3-3_1	Core - 0	-	44.70	-	39.95	0.17	0.018	-	0.26	15.68	0.13	**100.90**
ol3-3_2	9.85	-	44.53	-	39.67	0.18	0.037	0.047	0.28	15.80	0.13	**100.66**
ol3-3_3	20.62	0.009	44.43	-	39.96	0.16	0.020	-	0.26	15.48	0.12	**100.44**
ol3-3_4	30.47	-	44.60	0.036	39.91	0.18	-	0.017	0.29	15.59	0.13	**100.74**
ol3-3_5	40.32	-	44.91	0.014	40.13	0.17	-	0.045	0.21	15.76	0.12	**101.36**
ol3-3_6	49.80	-	44.84	0.010	39.87	0.18	0.002	0.033	0.21	15.45	0.12	**100.70**
ol3-3_7	60.57	0.003	44.84	-	39.79	0.16	0.022	0.055	0.26	15.52	0.11	**100.76**
ol3-3_8	70.42	-	44.81	-	39.78	0.17	0.016	0.033	0.22	15.52	0.20	**100.74**
ol3-3_9	80.27	-	44.89	0.066	39.68	0.17	0.018	0.024	0.24	15.54	0.11	**100.74**
ol3-3_10	90.12	0.026	44.64	0.024	39.62	0.19	0.015	0.043	0.21	15.36	0.16	**100.30**
ol3-3_11	100.89	0.026	45.06	0.047	39.85	0.17	-	0.002	0.27	15.20	0.15	**100.77**
ol3-3_12	110.74	0.023	44.86	0.029	39.98	0.20	0.018	0.029	0.25	15.38	0.16	**100.92**
ol3-3_13	120.59	0.039	44.92	-	39.77	0.17	0.006	0.024	0.29	15.26	0.13	**100.61**
ol3-3_14	130.08	0.004	45.21	0.022	40.04	0.19	0.024	0.017	0.24	15.12	0.17	**101.03**
ol3-3_15	140.85	0.003	44.84	0.044	39.86	0.17	-	0.040	0.29	15.31	0.15	**100.71**
ol3-3_16	150.69	0.001	45.02	0.040	39.73	0.20	0.036	0.021	0.25	15.47	0.14	**100.91**
ol3-3_17	160.54	0.039	44.84	0.009	39.77	0.19	-	0.017	0.26	15.28	0.15	**100.56**
ol3-3_18	170.39	0.023	45.08	-	39.85	0.17	0.023	0.050	0.24	15.43	0.20	**101.07**
ol3-3_19	181.16	0.026	44.75	-	39.77	0.19	-	0.014	0.21	15.41	0.16	**100.52**
ol3-3_20	200.86	0.014	44.57	-	39.91	0.17	-	0.048	0.25	15.44	0.18	**100.58**
ol3-3_21	211.63	-	44.43	0.015	39.68	0.20	0.004	0.036	0.26	15.41	0.17	**100.20**
ol3-3_22	221.12	-	44.60	-	40.02	0.22	0.005	0.057	0.24	15.67	0.14	**100.95**
ol3-3_23	230.97	-	44.64	0.011	40.10	0.18	0.008	0.036	0.21	15.79	0.17	**101.14**
ol3-3_24	240.82	-	44.36	0.017	39.92	0.22	0.027	0.057	0.27	15.94	0.13	**100.94**
ol3-3_25	251.59	-	44.49	0.053	39.64	0.20	-	-	0.21	15.96	0.19	**100.74**
ol3-3_26	261.43	-	44.13	0.016	39.72	0.18	0.001	-	0.27	16.07	0.13	**100.51**
ol3-3_27	271.28	0.017	44.28	0.024	39.51	0.24	-	-	0.22	16.42	0.15	**100.86**
ol3-3_28	281.13	0.010	43.89	0.026	39.81	0.19	-	0.024	0.27	16.31	0.13	**100.65**
ol3-3_29	291.90	0.017	43.96	-	39.61	0.21	0.006	0.054	0.24	16.62	0.15	**100.88**
ol3-3_31	301.39	0.004	43.12	-	39.61	0.21	-	0.024	0.33	17.23	0.14	**100.68**
ol3-3_32	311.24	-	43.20	0.025	39.46	0.22	-	0.042	0.32	17.67	0.13	**101.06**
ol3-3_33	321.09	0.024	42.95	-	39.28	0.20	0.004	0.002	0.27	17.88	0.17	**100.79**
ol3-3_34	331.86 - Rim	-	42.77	0.003	39.24	0.22	0.001	-	0.28	18.12	0.08	**100.70**

Table 54: The major element composition of an olivine crystal from sample D6. The dash symbol (-) represent concentration under the detection limit of the instruments.

D6- Ol 4									
Name	Distance (µm)	MgO	Al_2O_3	SiO_2	CaO	MnO	FeO	NiO	Total
ol4-4_1	Core - 0	41.83	-	38.73	0.17	0.26	18.44	0.10	**99.53**
ol4-4_2	9	42.15	-	38.74	0.18	0.33	18.56	0.09	**100.04**
ol4-4_3	18	42.03	0.012	38.53	0.19	0.32	18.62	0.12	**99.83**
ol4-4_4	27	42.22	0.029	38.95	0.17	0.32	18.54	0.12	**100.36**
ol4-4_5	36	41.96	-	38.64	0.16	0.32	18.33	0.13	**99.55**
ol4-4_6	45	41.96	-	38.68	0.18	0.31	18.28	0.09	**99.51**
ol4-4_7	54	41.96	0.025	38.53	0.18	0.33	18.69	0.09	**99.81**
ol4-4_8	63	42.22	-	38.60	0.19	0.32	18.74	0.12	**100.18**
ol4-4_9	72	41.95	-	38.82	0.15	0.33	18.48	0.10	**99.83**
ol4-4_10	81	41.96	0.002	39.03	0.17	0.23	18.20	0.10	**99.69**
ol4-4_11	90	42.10	-	38.57	0.21	0.27	18.85	0.11	**100.12**
ol4-4_12	99	41.98	-	38.83	0.20	0.29	18.38	0.12	**99.80**
ol4-4_13	108	41.93	-	38.85	0.19	0.30	18.68	0.14	**100.09**
ol4-4_14	117	41.91	0.007	38.62	0.17	0.26	19.03	0.13	**100.12**
ol4-4_15	126	42.03	0.001	38.65	0.16	0.32	18.64	0.09	**99.89**
ol4-4_16	135	41.86	-	39.00	0.18	0.28	18.71	0.11	**100.14**
ol4-4_17	144	41.96	0.024	38.72	0.17	0.33	19.04	0.12	**100.36**
ol4-4_18	153	41.88	-	38.75	0.19	0.31	18.88	0.12	**100.13**
ol4-4_19	162	41.62	-	38.51	0.20	0.32	19.22	0.12	**99.99**
ol4-4_20	171	41.55	0.002	38.54	0.18	0.29	19.24	0.10	**99.91**
ol4-4_21	180	41.38	-	38.60	0.19	0.36	19.74	0.15	**100.41**
ol4-4_22	189	40.98	-	38.62	0.20	0.35	19.62	0.10	**99.88**
ol4-4_23	198	40.99	-	38.57	0.15	0.33	20.05	0.11	**100.21**
ol4-4_24	207	40.53	-	38.30	0.17	0.37	20.36	0.11	**99.83**
ol4-4_25	216	40.33	0.014	38.32	0.18	0.33	20.28	0.09	**99.54**
ol4-4_26	225	40.62	0.009	38.07	0.18	0.30	21.00	0.11	**100.29**
ol4-4_27	234	40.38	0.007	38.60	0.20	0.37	20.30	0.08	**99.92**
ol4-4_28	243	40.87	0.018	38.43	0.23	0.36	19.84	0.09	**99.84**
ol4-4_29	252	41.53	0.012	38.62	0.23	0.35	19.26	0.07	**100.08**
ol4-4_30	261 - Rim	42.19	0.042	39.02	0.25	0.32	18.44	0.10	**100.37**

Table 55: EPMA analyses of the major element composition of an olivine crystal. The dash symbol (-) represent concentration under the detection limit of the instruments.

D5 Ol 4									
Name	Distance (µm)	MgO	Al_2O_3	SiO_2	CaO	MnO	FeO	NiO	Total
ol5-5_1	Core - 0	45.07	0.006	39.83	0.18	0.22	14.70	0.20	**100.21**
ol5-5_2	8	45.01	0.046	39.69	0.19	0.22	14.77	0.20	**100.12**
ol5-5_3	16	45.29	0.038	39.66	0.21	0.21	14.66	0.20	**100.27**
ol5-5_4	24	45.03	0.005	39.87	0.21	0.23	14.84	0.20	**100.39**
ol5-5_5	32	45.30	0.021	39.62	0.20	0.20	14.65	0.21	**100.20**
ol5-5_6	40	45.21	-	39.67	0.17	0.23	14.74	0.23	**100.25**
ol5-5_7	48	43.22	0.383	39.64	0.21	0.18	14.76	0.20	**98.60**
ol5-5_8	56	45.32	0.011	39.60	0.20	0.24	14.61	0.21	**100.18**
ol5-5_9	64	45.28	0.026	39.62	0.20	0.22	14.96	0.22	**100.52**
ol5-5_10	72	45.40	0.003	39.46	0.18	0.25	14.47	0.23	**99.98**
ol5-5_11	80	45.19	0.040	39.42	0.21	0.22	14.53	0.20	**99.81**
ol5-5_12	88	45.26	0.035	39.89	0.20	0.20	14.75	0.24	**100.56**
ol5-5_13	96	45.55	0.009	39.75	0.18	0.21	14.85	0.21	**100.76**
ol5-5_14	104	45.35	-	39.56	0.18	0.24	14.48	0.21	**100.03**
ol5-5_15	112	45.37	0.036	39.40	0.18	0.20	14.76	0.21	**100.15**
ol5-5_16	120	45.19	-	39.80	0.16	0.23	14.89	0.21	**100.48**
ol5-5_17	128	45.06	0.012	39.46	0.21	0.21	14.71	0.26	**99.92**
ol5-5_18	136	44.83	0.017	39.95	0.18	0.18	14.44	0.21	**99.81**
ol5-5_19	144	44.74	0.018	39.37	0.23	0.23	14.49	0.20	**99.28**
ol5-5_20	152	44.97	0.014	39.75	0.20	0.21	15.00	0.18	**100.33**
ol5-5_21	160	45.02	0.000	39.70	0.19	0.22	14.93	0.24	**100.30**
ol5-5_22	168	43.86	0.207	38.99	0.20	0.23	14.68	0.21	**98.38**
ol5-5_23	176	44.83	0.014	39.60	0.21	0.28	14.84	0.22	**99.98**
ol5-5_24	184	44.89	0.024	39.52	0.19	0.26	15.14	0.18	**100.20**
ol5-5_25	192	44.63	0.013	39.32	0.19	0.22	15.15	0.19	**99.72**
ol5-5_26	200	44.55	0.022	39.57	0.18	0.20	14.96	0.23	**99.71**
ol5-5_27	208	44.27	0.017	39.51	0.22	0.22	15.62	0.17	**100.04**
ol5-5_28	216	43.98	-	39.28	0.22	0.21	16.17	0.19	**100.05**
ol5-5_29	224	39.53	0.489	39.27	0.22	0.27	16.17	0.15	**96.09**
ol5-5_30	232 - Rim	43.07	0.007	39.22	0.22	0.34	17.15	0.15	**100.17**

Table 56: The major element composition of an olivine crystal from sample D6. The dash symbol (-) represent concentration under the detection limit of the instruments.

D6 - Cpx 21											
Name	Distance (µm)	Na_2O	MgO	Al_2O_3	SiO_2	CaO	TiO_2	Cr_2O_3	MnO	FeO	Total
cpx1-1_1	Core -0	0.37	13.94	5.93	47.80	22.46	1.22	0.72	0.12	5.84	**98.40**
cpx1-1_2	13	0.37	13.94	5.87	48.02	22.29	1.18	0.74	0.13	6.07	**98.61**
cpx1-1_3	26	0.39	14.06	5.85	48.22	22.43	1.21	0.76	0.14	5.97	**99.03**
cpx1-1_4	39	0.40	13.89	5.78	48.08	22.36	1.15	0.72	0.12	5.99	**98.49**
cpx1-1_5	52	0.41	14.00	5.76	48.33	22.50	1.19	0.71	0.10	5.94	**98.94**
cpx1-1_6	65	0.34	14.03	5.58	48.48	22.42	1.13	0.74	0.09	6.01	**98.82**
cpx1-1_7	78	0.41	11.12	4.76	38.38	18.12	0.93	0.66	0.10	4.85	**79.32**
cpx1-1_8	91	0.42	14.08	5.49	48.30	22.38	1.13	0.72	0.13	5.77	**98.44**
cpx1-1_9	104	0.37	14.09	5.53	48.26	22.39	1.12	0.69	0.12	5.90	**98.47**
cpx1-1_10	117	0.41	14.23	5.51	48.25	22.42	1.12	0.69	0.09	5.84	**98.57**
cpx1-1_11	130	0.44	14.26	5.50	48.64	22.46	1.06	0.72	0.15	5.77	**98.99**
cpx1-1_12	143	0.44	14.17	5.53	48.45	22.42	1.03	0.75	0.13	5.99	**98.90**
cpx1-1_13	156	0.43	14.11	5.54	48.73	22.43	1.04	0.72	0.13	5.76	**98.89**
cpx1-1_14	169	0.39	14.14	5.53	48.26	22.61	1.07	0.75	0.18	5.98	**98.91**
cpx1-1_15	182	0.39	14.05	5.51	48.52	22.38	1.06	0.66	0.13	6.04	**98.74**
cpx1-1_16	195	0.42	14.04	5.50	48.72	22.45	1.02	0.74	0.13	5.78	**98.81**
cpx1-1_17	208	0.37	14.17	5.46	48.43	22.30	1.06	0.74	0.11	5.92	**98.58**
cpx1-1_18	221	0.39	14.15	5.61	48.23	22.48	1.08	0.71	0.13	5.76	**98.52**
cpx1-1_19	234	0.37	14.16	5.57	48.47	22.42	1.14	0.69	0.08	6.15	**99.05**
cpx1-1_20	247	0.40	13.99	5.68	48.20	22.54	1.10	0.73	0.10	5.85	**98.60**
cpx1-1_21	260	0.43	14.07	5.64	48.43	22.59	1.08	0.73	0.14	5.95	**99.05**
cpx1-1_22	273	0.39	13.75	5.61	47.74	22.17	1.09	0.69	0.16	5.77	**97.37**
cpx1-1_23	286	0.40	14.13	5.56	48.31	22.60	1.08	0.69	0.11	5.85	**98.73**
cpx1-1_24	299	0.40	14.02	5.68	48.53	22.58	1.11	0.71	0.11	5.80	**98.95**
cpx1-1_25	312	0.38	14.03	5.57	48.40	22.35	1.15	0.68	0.10	5.83	**98.49**
cpx1-1_26	325	0.42	14.04	5.64	48.64	22.53	1.10	0.71	0.10	6.01	**99.20**
cpx1-1_27	338	0.34	11.41	5.30	43.16	19.24	0.95	0.65	0.14	5.19	**86.38**
cpx1-1_28	351	0.39	14.24	5.48	48.17	22.29	1.09	0.68	0.07	5.86	**98.27**
cpx1-1_29	364	0.46	14.10	5.47	48.57	22.40	1.10	0.65	0.07	6.02	**98.85**
cpx1-1_30	377	0.40	14.01	5.55	48.45	22.51	1.10	0.72	0.10	5.82	**98.66**
cpx1-1_31	390	0.42	14.07	5.53	48.54	22.44	1.07	0.62	0.14	6.00	**98.83**
cpx1-1_32	403	0.41	13.91	5.83	48.84	22.10	1.13	0.70	0.14	6.00	**99.06**
cpx1-1_33	416	0.33	11.46	5.24	42.26	18.91	1.01	0.62	0.07	5.04	**84.94**
cpx1-1_34	429	0.43	13.62	4.98	41.33	20.23	1.05	0.61	0.11	5.13	**87.48**
cpx1-1_35	442	0.41	14.35	5.71	48.04	22.50	1.21	0.74	0.15	5.81	**98.92**
cpx1-1_36	455	0.41	14.08	5.76	48.54	22.43	1.18	0.73	0.12	5.87	**99.11**
cpx1-1_37	468	0.39	13.99	5.64	47.81	22.49	1.17	0.70	0.16	5.92	**98.26**
cpx1-1_38	481	0.42	14.11	5.65	48.20	22.40	1.16	0.73	0.10	5.84	**98.61**
cpx1-1_39	494	0.36	14.03	5.70	48.32	22.52	1.17	0.70	0.10	5.82	**98.71**

Table 57: EPMA analyses of the major element composition of an pyroxene crystal.

D6 - Cpx 1											
Name	Distance (µm)	Na_2O	MgO	Al_2O_3	SiO_2	CaO	TiO_2	Cr_2O_3	MnO	FeO	Total
cpx1-1_40	507	0.35	14.09	5.69	48.03	22.49	1.10	0.69	0.13	5.83	**98.41**
cpx1-1_41	520	0.41	14.07	5.77	48.14	22.78	1.14	0.69	0.10	5.96	**99.05**
cpx1-1_42	533	0.39	14.11	5.72	48.06	22.48	1.22	0.72	0.13	5.95	**98.78**
cpx1-1_43	546	0.44	14.13	5.68	48.17	22.74	1.19	0.73	0.14	6.01	**99.24**
cpx1-1_44	559	0.40	13.99	5.68	48.04	22.51	1.18	0.68	0.12	5.99	**98.60**
cpx1-1_45	572	0.41	14.16	5.61	48.02	22.73	1.18	0.70	0.12	5.97	**98.90**
cpx1-1_46	585	0.40	14.22	5.68	48.10	22.36	1.21	0.72	0.11	5.96	**98.75**
cpx1-1_47	598	0.47	14.67	5.86	46.41	22.16	1.17	0.65	0.13	5.96	**97.48**
cpx1-1_48	611	0.41	14.18	5.60	48.38	22.40	1.18	0.60	0.11	5.94	**98.80**
cpx1-1_49	624	0.43	14.20	5.49	48.54	22.52	1.15	0.59	0.07	6.03	**99.01**
cpx1-1_50	637 - Rim	0.43	14.28	5.55	48.23	22.67	1.19	0.59	0.10	5.97	**99.02**

Table 57: Continuation.

D6 - Cpx 2											
Name	Distance (µm)	Na_2O	MgO	Al_2O_3	SiO_2	CaO	TiO_2	Cr_2O_3	MnO	FeO	Total
cpx2-5_1	Core - 0	0.29	14.95	4.58	49.48	22.32	0.92	0.32	0.14	5.93	**98.93**
cpx2-5_2	11	0.29	14.96	4.63	49.54	22.29	0.96	0.32	0.10	6.04	**99.13**
cpx2-5_3	22	0.37	14.67	4.87	49.33	22.29	0.98	0.22	0.14	6.16	**99.02**
cpx2-5_4	33	0.30	15.03	4.63	49.54	22.10	0.98	0.22	0.16	6.21	**99.17**
cpx2-5_5	44	0.29	14.85	4.76	49.32	22.36	1.04	0.14	0.14	6.48	**99.37**
cpx2-5_6	55	0.27	14.72	4.81	49.39	22.01	1.01	0.11	0.11	6.43	**98.86**
cpx2-5_7	66	0.37	14.71	4.77	49.26	22.11	1.03	0.11	0.18	6.45	**98.99**
cpx2-5_8	77	0.32	14.77	4.42	49.73	22.39	0.94	0.50	0.13	5.56	**98.77**
cpx2-5_9	88	0.34	14.46	5.18	48.95	21.98	1.13	0.31	0.14	6.54	**99.03**
cpx2-5_10	99	0.35	14.42	5.13	48.82	22.30	1.18	0.22	0.19	6.68	**99.28**
cpx2-5_11	110	0.36	14.48	4.96	48.87	22.12	1.21	0.19	0.17	6.63	**98.99**
cpx2-5_12	121	0.33	14.70	4.66	49.01	21.96	1.16	0.14	0.13	6.60	**98.69**
cpx2-5_13	132	0.34	14.68	4.37	49.45	22.07	1.17	0.06	0.10	6.59	**98.83**
cpx2-5_14	143	0.38	14.98	4.18	49.49	21.92	1.12	0.21	0.12	6.72	**99.13**
cpx2-5_15	154	0.36	14.57	4.36	49.39	21.96	1.21	0.13	0.15	6.69	**98.80**
cpx2-5_16	165	0.43	14.00	5.06	48.11	21.59	1.44	0.03	0.15	7.97	**98.79**
cpx2-5_17	176	0.42	14.07	4.42	49.09	21.64	1.26	0.03	0.20	7.70	**98.83**
cpx2-5_18	187	0.34	14.83	4.13	49.70	22.05	1.01	0.48	0.14	6.17	**98.86**
cpx2-5_19	198 - Rim	0.69	13.54	6.86	48.75	21.07	1.51	0.33	0.14	6.85	**99.74**

Table 58: The major element composition of a pyroxene crystal from sample D6.

Sample	Cpx 1				Cpx 2		
Elemen /Name	cpx1-01	cpx1-02	cpx1-03	cpx1-04	cpx2-01	cpx2-02	cpx2-03
Sc	146.53	167.96	154.63	148.48	189.16	190.82	167.86
Ti	5122.32	6917.40	6448.24	6449.95	5537.29	6006.90	6968.83
V	270.44	321.27	298.39	331.46	392.60	418.68	420.86
Cr	3830.99	4619.89	4180.77	2495.97	2280.21	1618.62	950.57
Mn	894.20	904.08	805.06	1003.33	1001.82	1003.99	1146.67
Co	26.88	28.27	24.73	30.79	28.26	28.00	27.97
Ni	114.01	125.29	112.81	132.93	101.50	91.96	63.97
Zn	14.94	22.70	26.42	24.37	22.49	19.58	36.18
Rb	-	-	-	-	-	-	0.53
Sr	87.56	87.22	79.85	92.85	58.85	60.26	61.01
Y	17.50	20.36	18.20	20.27	22.54	23.81	25.37
Zr	41.35	56.41	46.85	45.88	42.04	41.86	43.33
Nb	0.33	0.55	0.47	0.45	0.05	0.14	0.81
Cs	-	-	-	-	-	-	-
Ba	0.13	0.33		0.09	-	-	8.39
La	7.13	9.48	7.84	7.80	6.35	6.33	8.01
Ce	22.54	27.50	21.86	25.77	20.72	21.53	24.49
Pr	4.27	4.59	4.47	4.18	3.77	3.95	4.30
Nd	19.33	22.09	21.73	22.52	18.40	19.10	17.99
Sm	4.65	5.56	5.29	5.90	4.13	5.16	4.25
Eu	1.40	1.61	1.42	1.61	1.23	1.46	1.64
Gd	3.50	5.45	4.89	6.21	5.39	3.48	5.24
Tb	0.54	0.73	0.64	0.59	0.88	0.77	0.65
Dy	4.87	4.45	4.06	3.92	4.44	4.60	4.07
Ho	0.63	0.70	0.56	0.87	0.98	0.62	1.22
Er	1.37	2.12	1.56	1.87	2.28	3.47	2.40
Tm	0.22	0.26	0.21	0.19	0.21	0.41	0.33
Yb	0.94	0.80	1.54	1.21	1.41	0.77	1.62
Lu	0.14	0.25	0.20	0.29	0.40	-	0.21
Hf	1.47	1.57	1.62	2.02	2.20	2.16	1.88
Ta	0.07	0.36	0.17	-	0.20	0.13	0.36
Pb	-	1.57	0.10	-	-	-	-
Th	0.11	-	0.14	0.18	-	0.11	0.37
U	0.13	-	0.14	0.13	-	0.32	-

Table 59: Trace element composition from Cpx 1 and Cpx 2. The dash symbol (-) represent concentration under the detection limit of the instruments.

Sample	Cpx 1				Cpx 2		
Elemen /Name	**cpx1-01**	**cpx1-02**	**cpx1-03**	**cpx1-04**	**cpx2-01**	**cpx2-02**	**cpx2-03**
Distance (µm)	117	221	481	624	22	110	176
Sc	146.53	167.96	154.63	148.48	189.16	190.82	167.86
Ti	5122.32	6917.40	6448.24	6449.95	5537.29	6006.90	6968.83
V	270.44	321.27	298.39	331.46	392.60	418.68	420.86
Cr	3830.99	4619.89	4180.77	2495.97	2280.21	1618.62	950.57
Mn	894.20	904.08	805.06	1003.33	1001.82	1003.99	1146.67
Co	26.88	28.27	24.73	30.79	28.26	28.00	27.97
Ni	114.01	125.29	112.81	132.93	101.50	91.96	63.97
Zn	14.94	22.70	26.42	24.37	22.49	19.58	36.18
Rb	-	-	-	-	-	-	0.53
Sr	87.56	87.22	79.85	92.85	58.85	60.26	61.01
Y	17.50	20.36	18.20	20.27	22.54	23.81	25.37
Zr	41.35	56.41	46.85	45.88	42.04	41.86	43.33
Nb	0.33	0.55	0.47	0.45	0.05	0.14	0.81
Cs	-	-	-	-	-	-	-
Ba	0.13	0.33		0.09	-	-	8.39
La	7.13	9.48	7.84	7.80	6.35	6.33	8.01
Ce	22.54	27.50	21.86	25.77	20.72	21.53	24.49
Pr	4.27	4.59	4.47	4.18	3.77	3.95	4.30
Nd	19.33	22.09	21.73	22.52	18.40	19.10	17.99
Sm	4.65	5.56	5.29	5.90	4.13	5.16	4.25
Eu	1.40	1.61	1.42	1.61	1.23	1.46	1.64
Gd	3.50	5.45	4.89	6.21	5.39	3.48	5.24
Tb	0.54	0.73	0.64	0.59	0.88	0.77	0.65
Dy	4.87	4.45	4.06	3.92	4.44	4.60	4.07
Ho	0.63	0.70	0.56	0.87	0.98	0.62	1.22
Er	1.37	2.12	1.56	1.87	2.28	3.47	2.40
Tm	0.22	0.26	0.21	0.19	0.21	0.41	0.33
Yb	0.94	0.80	1.54	1.21	1.41	0.77	1.62
Lu	0.14	0.25	0.20	0.29	0.40	-	0.21
Hf	1.47	1.57	1.62	2.02	2.20	2.16	1.88
Ta	0.07	0.36	0.17	-	0.20	0.13	0.36
Pb	-	1.57	0.10	-	-	-	-
Th	0.11	-	0.14	0.18	-	0.11	0.37
U	0.13	-	0.14	0.13	-	0.32	-

Table 60: Trace element composition of Cpx1 and Cpx 2.

Appendix VII – Sample D12D2

This appendix contains the major element analyses of 7 olivines and 3 pyroxenes. Moreover, here can be found the trace element of 3 pyroxenes.

D12D2 - Ol 1(2)									
Name	Distance (µm)	MgO	Al_2O_3	SiO_2	CaO	MnO	FeO	NiO	Total
ol1(2)1_1	Core - 0	44.62	0.032	39.07	0.16	0.26	15.28	0.11	**99.53**
ol1(2)1_2	10.63015	44.50	-	38.73	0.12	0.31	15.35	0.13	**99.13**
ol1(2)1_3	22.67174	44.38	-	39.06	0.14	0.28	15.37	0.18	**99.40**
ol1(2)1_4	33.30189	44.25	0.007	39.14	0.14	0.24	15.43	0.19	**99.41**
ol1(2)1_5	44.70364	44.44	0.013	38.85	0.11	0.31	15.46	0.08	**99.27**
ol1(2)1_6	55.33379	44.48	-	38.72	0.15	0.29	15.58	0.15	**99.37**
ol1(2)1_7	66.64749	44.20	0.016	38.71	0.12	0.23	15.42	0.10	**98.80**
ol1(2)1_8	78.04925	44.31	-	38.60	0.11	0.31	15.41	0.11	**98.84**
ol1(2)1_9	88.67939	44.29	-	38.72	0.09	0.28	15.61	0.13	**99.12**
ol1(2)1_10	100.0811	44.06	0.016	38.76	0.13	0.29	15.20	0.11	**98.57**
ol1(2)1_11	111.3949	44.21	0.028	38.65	0.11	0.31	15.35	0.16	**98.82**
ol1(2)1_12	122.025	44.49	-	38.97	0.13	0.27	15.42	0.16	**99.45**
ol1(2)1_13	133.4268	44.43	0.020	38.83	0.14	0.33	15.36	0.09	**99.22**
ol1(2)1_14	144.0569	44.14	-	38.73	0.14	0.22	14.98	0.13	**98.35**
ol1(2)1_15	156.0985	44.53	-	38.75	0.13	0.27	15.61	0.11	**99.40**
ol1(2)1_16	166.7286	44.19	0.000	38.83	0.16	0.29	15.26	0.17	**98.90**
ol1(2)1_17	178.1304	44.13	-	39.00	0.13	0.25	15.30	0.14	**98.94**
ol1(2)1_18	188.7605	44.51	-	38.95	0.14	0.21	15.60	0.14	**99.56**
ol1(2)1_19	200.0743	44.45	-	38.82	0.11	0.27	15.32	0.13	**99.10**
ol1(2)1_20	211.476	44.72	-	38.99	0.13	0.26	15.35	0.13	**99.59**
ol1(2)1_21	222.1062	44.07	0.013	38.94	0.15	0.26	15.37	0.13	**98.93**
ol1(2)1_22	233.5079	44.35	-	38.97	0.13	0.29	15.41	0.21	**99.36**
ol1(2)1_23	244.8216	44.38	-	39.22	0.14	0.27	15.47	0.09	**99.57**
ol1(2)1_24	255.4518	44.54	-	39.20	0.12	0.28	15.21	0.13	**99.48**
ol1(2)1_25	266.8535	44.69	0.012	39.34	0.15	0.30	15.35	0.16	**100.00**
ol1(2)1_26	277.4837	44.72	-	39.36	0.12	0.24	15.62	0.08	**100.16**
ol1(2)1_27	289.5253	44.62	-	39.26	0.15	0.27	15.26	0.18	**99.74**
ol1(2)1_28	300.1554	44.74	0.002	39.47	0.14	0.26	15.27	0.12	**100.01**
ol1(2)1_29	310.7855	44.43	0.045	39.42	0.14	0.25	15.47	0.13	**99.89**
ol1(2)1_30	322.1873	44.57	-	39.70	0.11	0.25	15.00	0.13	**99.75**
ol1(2)1_31	344.8589	44.45	0.036	39.37	0.16	0.28	14.98	0.14	**99.41**
ol1(2)1_32	356.2606	44.68	-	39.38	0.12	0.23	15.22	0.11	**99.74**
ol1(2)1_33	366.8908	44.92	-	39.50	0.15	0.24	15.24	0.16	**100.19**
ol1(2)1_34	377.5209	44.45	0.006	39.44	0.14	0.28	14.98	0.15	**99.45**
ol1(2)1_35	389.5625	44.70	-	39.49	0.12	0.30	15.04	0.11	**99.76**
ol1(2)1_36	400.1927	44.55	0.005	39.51	0.15	0.23	15.15	0.13	**99.71**

Table 61: EPMA analyses of the major element composition of an olivine crystal. The dash symbol (-) represent concentration under the detection limit of the instruments.

D12D2 - Ol 1(2)									
Name	Distance (µm)	MgO	Al_2O_3	SiO_2	CaO	MnO	FeO	NiO	Total
ol1(2)1_37	411.5944	44.30	0.087	38.98	0.17	0.25	15.38	0.15	**99.32**
ol1(2)1_38	433.5261	44.64	-	39.73	0.14	0.25	15.18	0.13	**100.07**
ol1(2)1_39	444.8398	44.77	-	39.59	0.16	0.25	15.38	0.15	**100.30**
ol1(2)1_40	456.2416	44.65	-	39.68	0.18	0.27	15.14	0.13	**100.05**
ol1(2)1_41	466.8717	44.70	-	39.85	0.16	0.24	15.31	0.14	**100.41**
ol1(2)1_42	478.2735	44.46	0.030	39.55	0.17	0.25	15.22	0.14	**99.81**
ol1(2)1_43	489.5872	44.39	-	39.77	0.17	0.29	15.28	0.19	**100.09**
ol1(2)1_44	500.2173	44.45	0.020	39.60	0.19	0.28	15.08	0.15	**99.77**
ol1(2)1_45	522.2401	44.45	-	39.60	0.19	0.27	15.61	0.16	**100.29**
ol1(2)1_46	532.8702	44.66	-	39.53	0.21	0.26	15.69	0.18	**100.52**
ol1(2)1_47	544.9118	44.36	0.017	39.60	0.19	0.27	15.61	0.19	**100.24**
ol1(2)1_48	555.5419	44.15	0.023	39.57	0.19	0.23	15.56	0.14	**99.86**
ol1(2)1_49	566.9437	44.36	-	39.40	0.20	0.26	15.88	0.20	**100.30**
ol1(2)1_50	577.5738	44.39	0.010	39.75	0.18	0.29	15.77	0.19	**100.59**
ol1(2)1_51	588.8875	44.32	0.004	39.56	0.21	0.24	16.33	0.18	**100.84**
ol1(2)1_52	610.9103	44.40	0.011	39.62	0.20	0.27	16.48	0.17	**101.15**
ol1(2)1_53	621.5404	43.94	0.014	39.66	0.14	0.23	16.22	0.14	**100.34**
ol1(2)1_54	632.9422	43.93	0.002	39.30	0.17	0.25	15.91	0.18	**99.73**
ol1(2)1_55	644.2559	44.01	0.011	39.35	0.18	0.25	16.02	0.10	**99.92**
ol1(2)1_56	654.886	44.38	-	39.68	0.16	0.31	16.03	0.21	**100.77**
ol1(2)1_57	666.2878	44.49	0.005	39.55	0.21	0.24	15.50	0.17	**100.17**
ol1(2)1_58	676.9179	44.84	0.012	39.73	0.17	0.20	14.98	0.16	**100.08**
ol1(2)1_59	699.5895	44.89	-	39.85	0.20	0.23	15.07	0.11	**100.35**
ol1(2)1_60	710.2196	43.86	0.012	39.61	0.23	0.29	17.23	0.11	**101.34**

Table 61: Continuation.

D12D2 - Ol 1									
Name	Distance (µm)	MgO	Al_2O_3	SiO_2	CaO	MnO	FeO	NiO	Total
ol1-1_1	Core - 0	44.58	-	39.20	0.14	0.21	15.81	0.13	**100.07**
ol1-1_2	10	44.50	-	39.19	0.13	0.27	15.52	0.08	**99.68**
ol1-1_3	20	44.71	0.011	39.35	0.11	0.27	15.54	0.11	**100.11**
ol1-1_4	30	44.46	-	39.27	0.14	0.28	15.53	0.11	**99.78**
ol1-1_5	40	44.52	0.004	39.17	0.13	0.26	15.67	0.14	**99.88**
ol1-1_6	50	44.44	0.015	39.30	0.12	0.26	15.68	0.13	**99.95**
ol1-1_7	60	44.60	-	39.19	0.12	0.23	15.66	0.13	**99.94**
ol1-1_8	70	44.50	-	39.10	0.15	0.25	15.35	0.14	**99.49**
ol1-1_9	80	44.45	-	39.42	0.12	0.28	15.60	0.11	**99.98**
ol1-1_10	90	44.59	0.004	39.04	0.16	0.29	15.49	0.15	**99.72**
ol1-1_11	100	44.58	0.010	39.13	0.15	0.25	15.34	0.17	**99.64**
ol1-1_12	110	44.52	0.013	39.35	0.14	0.24	15.30	0.15	**99.72**
ol1-1_13	120	44.64	0.017	39.22	0.13	0.26	15.58	0.11	**99.96**
ol1-1_14	130	44.40	0.011	39.37	0.12	0.23	15.45	0.12	**99.70**
ol1-1_15	140	44.55	0.024	39.19	0.13	0.23	15.27	0.14	**99.52**
ol1-1_16	150	44.75	0.001	39.49	0.13	0.23	15.48	0.13	**100.19**
ol1-1_17	160	44.62	-	39.16	0.14	0.24	15.52	0.16	**99.84**
ol1-1_18	170	44.57	-	39.35	0.15	0.26	15.58	0.14	**100.05**
ol1-1_19	180	44.48	0.006	39.04	0.14	0.25	15.60	0.13	**99.65**
ol1-1_20	190	44.42	-	39.28	0.16	0.19	15.28	0.12	**99.44**
ol1-1_21	200	44.52	-	39.13	0.15	0.21	15.63	0.15	**99.79**
ol1-1_22	210	44.37	0.002	39.32	0.13	0.25	15.61	0.14	**99.83**
ol1-1_23	220	44.34	-	39.11	0.16	0.27	15.51	0.17	**99.56**
ol1-1_24	230	44.19	0.019	38.68	0.13	0.24	15.78	0.13	**99.16**
ol1-1_25	240	44.52	-	39.20	0.16	0.22	16.25	0.12	**100.46**
ol1-1_26	250	43.96	0.020	39.42	0.16	0.26	15.25	0.14	**99.21**
ol1-1_27	260	44.36	0.009	39.30	0.18	0.29	15.80	0.18	**100.12**
ol1-1_28	270	44.06	-	38.87	0.18	0.25	15.90	0.17	**99.43**
ol1-1_29	280	43.68	0.008	39.21	0.16	0.24	15.71	0.21	**99.22**
ol1-1_30	290	43.83	-	39.29	0.19	0.25	16.19	0.15	**99.90**
ol1-1_31	300	43.78	0.029	39.04	0.16	0.22	16.18	0.16	**99.57**
ol1-1_32	310	43.78	0.009	39.10	0.17	0.27	16.33	0.13	**99.79**
ol1-1_33	320	43.60	-	39.09	0.16	0.26	16.42	0.16	**99.69**
ol1-1_34	330	43.61	0.020	39.23	0.15	0.28	16.65	0.18	**100.12**
ol1-1_35	340	43.82	-	39.01	0.18	0.20	16.53	0.15	**99.89**
ol1-1_36	350	44.05	0.015	39.05	0.16	0.24	16.05	0.15	**99.71**
ol1-1_37	360	44.81	0.007	39.40	0.18	0.25	15.07	0.19	**99.91**
ol1-1_38	370	44.83	0.029	39.36	0.21	0.22	14.56	0.21	**99.43**
ol1-1_40	390 - Rim	44.18	-	39.15	0.20	0.27	15.85	0.15	**99.80**

Table 62: The major element composition of an olivine crystal from sample D12D2. The dash symbol (-) represent concentration under the detection limit of the instruments.

D12D2 - Ol 2									
Name	**Distance (µm)**	**MgO**	**Al_2O_3**	**SiO_2**	**CaO**	**MnO**	**FeO**	**NiO**	**Total**
ol2-1_1	Core - 0	46.50	0.016	39.84	0.19	0.19	13.18	0.23	**100.14**
ol2-1_2	10	46.33	-	39.71	0.21	0.20	13.02	0.20	**99.67**
ol2-1_3	20	46.55	0.007	39.74	0.19	0.20	13.10	0.22	**100.01**
ol2-1_4	30	46.45	0.034	39.87	0.20	0.26	13.19	0.21	**100.22**
ol2-1_5	40	46.34	0.017	39.68	0.17	0.24	12.90	0.18	**99.54**
ol2-1_6	50	46.36	0.020	40.16	0.23	0.20	13.05	0.22	**100.24**
ol2-1_7	60	46.52	0.005	39.77	0.18	0.26	13.44	0.20	**100.37**
ol2-1_8	70	46.18	0.024	39.77	0.20	0.19	12.84	0.21	**99.42**
ol2-1_9	80	46.47	-	39.47	0.19	0.20	12.62	0.19	**99.15**
ol2-1_10	90	46.47	0.012	39.65	0.20	0.21	12.96	0.19	**99.70**
ol2-1_11	100	46.47	0.004	40.05	0.20	0.22	12.91	0.19	**100.03**
ol2-1_12	110	46.33	0.000	40.08	0.22	0.21	12.84	0.22	**99.91**
ol2-1_13	120	46.41	0.007	39.68	0.21	0.19	12.93	0.20	**99.63**
ol2-1_14	130	46.38	0.006	39.70	0.19	0.23	12.70	0.22	**99.42**
ol2-1_15	140	46.74	-	39.94	0.18	0.21	12.85	0.18	**100.10**
ol2-1_16	150	46.37	0.027	39.78	0.18	0.21	12.73	0.22	**99.51**
ol2-1_17	160	46.39	0.029	40.03	0.20	0.23	12.89	0.23	**100.00**
ol2-1_18	170	46.15	0.005	39.73	0.18	0.21	13.17	0.19	**99.64**
ol2-1_19	180	45.50	0.031	39.45	0.23	0.25	13.32	0.21	**99.00**
ol2-1_20	190 -Rim	45.00	0.017	39.49	0.19	0.22	14.54	0.18	**99.63**

Table 63: EPMA analyses of the major element composition of an olivine crystal. The dash symbol (-) represent concentration under the detection limit of the instruments.

D12D2 - Ol 3									
Name	**Distance (µm)**	**MgO**	**Al_2O_3**	**SiO_2**	**CaO**	**MnO**	**FeO**	**NiO**	**Total**
ol3-3_1	Core - 0	46.75	0.02	40.02	0.20	0.19	12.91	0.20	**100.29**
ol3-3_2	10	46.36	0.01	40.12	0.22	0.22	12.48	0.17	**99.59**
ol3-3_3	20	46.35	0.02	40.14	0.23	0.21	12.97	0.22	**100.15**
ol3-3_4	30	46.41	0.03	40.20	0.22	0.24	12.56	0.19	**99.85**
ol3-3_5	40	47.01	0.01	39.74	0.20	0.15	12.66	0.20	**99.98**
ol3-3_6	50	46.34	0.03	40.02	0.19	0.23	12.55	0.19	**99.56**
ol3-3_7	60	46.39	0.04	40.15	0.21	0.16	12.67	0.20	**99.82**
ol3-3_8	70	46.38	0.01	39.94	0.21	0.22	12.75	0.22	**99.73**
ol3-3_9	80	46.44	0.03	39.93	0.21	0.22	12.91	0.23	**99.97**
ol3-3_10	90	46.11	-	40.02	0.20	0.21	12.93	0.18	**99.66**
ol3-3_11	100	46.19	0.03	39.98	0.21	0.21	13.33	0.23	**100.20**
ol3-3_12	110	45.86	0.03	39.80	0.21	0.17	13.44	0.19	**99.70**
ol3-3_13	120	45.80	0.01	39.97	0.21	0.17	13.75	0.20	**100.11**
ol3-3_14	130	45.60	-	39.85	0.21	0.21	13.52	0.21	**99.59**
ol3-3_15	140	45.77	-	39.98	0.22	0.20	13.75	0.20	**100.12**
ol3-3_16	150	45.54	0.02	40.02	0.20	0.23	13.55	0.19	**99.75**
ol3-3_17	160	45.78	-	40.09	0.19	0.23	14.16	0.20	**100.65**
ol3-3_18	170	45.42	0.03	39.66	0.19	0.23	14.22	0.17	**99.91**
ol3-3_19	180	45.05	0.02	39.58	0.18	0.22	14.58	0.16	**99.79**
ol3-3_20	190 - Rim	43.78	0.00	39.47	0.21	0.22	15.88	0.16	**99.73**

Table 64: The major element composition of an olivine crystal from sample D12D2. The dash symbol (-) represent concentration under the detection limit of the instruments.

D12D2 - Ol 4									
Name	Distance (µm)	MgO	Al_2O_3	SiO_2	CaO	MnO	FeO	NiO	Total
Ol4-1	Core - 0	43.61	0.020	40.05	0.11	0.31	16.31	0.11	**100.53**
Ol4-2	158.32	44.15	0.002	40.01	0.14	0.29	16.43	0.13	**101.15**
Ol4-3	180.45	44.00	0.014	39.81	0.12	0.27	16.56	0.10	**100.88**
Ol4-4	197.92	44.14	-	39.77	0.12	0.29	16.57	0.12	**101.01**
Ol4-5	222.43	43.76	0.020	40.11	0.13	0.31	16.33	0.09	**100.75**
Ol4-6	267.74	44.00	-	40.15	0.14	0.31	16.39	0.13	**101.12**
Ol4-7	290.76	42.80	0.005	39.26	0.13	0.23	16.15	0.14	**98.71**
Ol4-8	322.00	44.01	0.006	39.75	0.11	0.26	15.90	0.11	**100.15**
Ol4-9	344.14	44.73	0.016	40.11	0.15	0.24	15.61	0.10	**100.96**
Ol4-10	369.75	44.53	0.002	40.26	0.11	0.33	15.40	0.11	**100.73**
Ol4-11	392.31	44.63	-	39.72	0.12	0.21	15.35	0.09	**100.11**
Ol4-12	408.95	44.74	-	40.10	0.11	0.26	15.24	0.12	**100.57**
Ol4-13	417.44	44.92	0.010	39.89	0.15	0.30	15.07	0.10	**100.44**
Ol4-14	429.52	44.72	0.027	39.73	0.15	0.19	14.78	0.11	**99.71**
Ol4-15	437.58	45.14	0.020	39.85	0.17	0.28	15.21	0.10	**100.77**
Ol4-16	448.21	44.86	0.011	39.67	0.16	0.21	14.34	0.10	**99.36**
Ol4-17	459.53	45.68	-	39.84	0.13	0.25	14.65	0.13	**100.68**
Ol4-18	474.39	45.39	-	39.89	0.14	0.23	14.32	0.12	**100.10**
Ol4-19	487.12	45.29	0.013	39.61	0.14	0.19	14.10	0.13	**99.47**
Ol4-20	496.55	45.30	-	39.53	0.17	0.27	13.81	0.14	**99.23**
Ol4-21	510.98	45.86	0.014	39.71	0.16	0.21	13.61	0.16	**99.73**
Ol4-22	519.58	46.08	-	39.73	0.19	0.22	13.10	0.16	**99.47**
Ol4-23	530.58	45.99	-	39.75	0.17	0.28	13.09	0.16	**99.44**
Ol4-24	537.86	46.16	-	39.74	0.18	0.20	13.07	0.24	**99.58**
Ol4-25	550.86	46.12	-	39.99	0.18	0.24	12.66	0.17	**99.37**
Ol4-26	567.95	45.82	0.011	39.79	0.19	0.25	13.50	0.20	**99.76**
Ol4-27	581.40 - Rim	44.30	0.015	39.45	0.19	0.26	14.30	0.14	**98.66**

Table 65: EPMA analyses of the major element composition of an olivine crystal. The dash symbol (-) represent concentration under the detection limit of the instruments.

D12D2 - Ol 5									
Name	Distance (µm)	MgO	Al_2O_3	SiO_2	CaO	MnO	FeO	NiO	Total
Ol5-5_1	Core - 0	45.72	0.014	39.73	0.20	0.23	14.65	0.18	**100.73**
Ol5-5_2	10.20	45.88	0.019	39.42	0.21	0.23	13.20	0.25	**99.21**
Ol5-5_3	20.40	46.52	-	39.71	0.20	0.20	12.64	0.20	**99.47**
Ol5-5_4	30.59	46.77	0.020	39.71	0.20	0.25	12.35	0.19	**99.47**
Ol5-5_5	41.77	46.95	-	39.82	0.21	0.14	11.99	0.22	**99.34**
Ol5-5_6	52.21	46.74	0.005	39.82	0.18	0.20	11.90	0.27	**99.11**
Ol5-5_7	62.41	46.96	0.011	39.53	0.21	0.20	12.05	0.24	**99.20**

Table 66: The major element composition of an olivine crystal from sample D12D2. The dash symbol (-) represent concentration under the detection limit of the instruments.

D12D2 - Ol 5									
Name	Distance (µm)	MgO	Al_2O_3	SiO_2	CaO	MnO	FeO	NiO	Total
Ol5-5_8	72.61	46.68	0.012	39.72	0.19	0.22	11.69	0.23	**98.75**
Ol5-5_9	82.81	46.90	0.023	39.96	0.22	0.18	11.89	0.27	**99.44**
Ol5-5_10	93.01	46.96	-	39.76	0.19	0.17	11.94	0.25	**99.28**
Ol5-5_11	103.20	46.99	0.029	39.73	0.21	0.18	11.93	0.26	**99.32**
Ol5-5_12	114.39	47.40	0.018	39.99	0.23	0.23	12.16	0.28	**100.29**
Ol5-5_13	124.58	47.23	0.007	39.39	0.24	0.19	11.95	0.27	**99.29**
Ol5-5_14	134.78	47.29	0.030	39.21	0.21	0.16	11.84	0.23	**98.98**
Ol5-5_15	144.98	47.20	0.039	39.78	0.21	0.25	11.83	0.28	**99.60**
Ol5-5_16	155.42	47.61	0.038	40.33	0.23	0.21	11.83	0.28	**100.52**
Ol5-5_17	165.62	47.84	0.035	40.37	0.21	0.14	12.16	0.24	**100.98**
Ol5-5_18	175.82	46.78	0.238	40.35	0.24	0.20	11.93	0.24	**99.97**
Ol5-5_19	187.00	47.11	0.054	39.94	0.20	0.15	11.76	0.26	**99.48**
Ol5-5_20	197.19	47.21	0.015	39.47	0.22	0.17	12.12	0.27	**99.47**
Ol5-5_21	207.39	47.65	0.038	40.57	0.19	0.21	11.93	0.23	**100.82**
Ol5-5_22	217.59	46.81	0.056	40.19	0.22	0.20	11.68	0.24	**99.39**
Ol5-5_23	227.79	47.64	0.024	39.96	0.19	0.18	11.75	0.26	**100.00**
Ol5-5_24	237.99	47.31	0.023	40.12	0.21	0.18	11.88	0.26	**99.99**
Ol5-5_25	248.18	47.18	0.018	39.85	0.20	0.20	11.91	0.27	**99.63**
Ol5-5_26	259.59	47.60	0.011	40.46	0.20	0.18	12.02	0.25	**100.73**
Ol5-5_27	269.78	47.04	0.016	39.58	0.20	0.18	11.92	0.25	**99.18**
Ol5-5_28	279.98	47.10	0.002	39.87	0.19	0.26	12.11	0.27	**99.81**
Ol5-5_29	290.18	47.57	0.029	40.33	0.20	0.17	12.18	0.24	**100.73**
Ol5-5_30	300.38	47.04	0.030	40.01	0.22	0.18	11.80	0.26	**99.54**
Ol5-5_31	310.58	47.29	0.033	39.96	0.20	0.19	12.15	0.23	**100.06**
Ol5-5_32	320.77	47.03	0.016	39.75	0.21	0.21	11.93	0.24	**99.39**
Ol5-5_33	331.95	46.67	0.012	39.73	0.24	0.23	12.07	0.21	**99.16**
Ol5-5_34	342.15	47.02	0.025	39.94	0.19	0.21	12.08	0.21	**99.68**
Ol5-5_35	352.35	47.73	0.034	40.29	0.20	0.17	12.41	0.19	**101.02**
Ol5-5_37	372.99	47.70	0.036	39.99	0.20	0.16	12.80	0.24	**101.12**
Ol5-5_38	383.19	47.32	0.031	40.43	0.21	0.16	12.38	0.19	**100.72**
Ol5-5_39	393.39	47.10	0.017	39.86	0.21	0.18	12.17	0.22	**99.75**
Ol5-5_40	404.57	46.97	0.002	39.98	0.21	0.21	12.34	0.20	**99.91**
Ol5-5_41	414.76	47.29	0.014	40.53	0.21	0.28	12.27	0.22	**100.82**
Ol5-5_42	424.96	46.37	0.024	39.85	0.24	0.20	12.63	0.22	**99.54**
Ol5-5_43	435.16	46.49	-	40.42	0.22	0.24	13.34	0.20	**100.90**
Ol5-5_44	445.36	45.91	0.011	39.91	0.20	0.20	13.15	0.22	**99.60**
Ol5-5_45	455.56	46.33	0.012	40.30	0.20	0.20	13.88	0.19	**101.11**
Ol5-5_46	477.18	45.23	0.018	39.92	0.19	0.22	14.86	0.13	**100.58**
Ol5-5_47	487.37	44.87	-	39.85	0.15	0.25	14.67	0.17	**99.96**
Ol5-5_48	497.57 - Rim	44.75	0.016	40.11	0.21	0.26	15.62	0.16	**101.12**

Table 66: Continuation.

D12D2 - Ol 6									
Name	Distance (µm)	MgO	Al_2O_3	SiO_2	CaO	MnO	FeO	NiO	Total
Ol6-6_1	Core - 0	45.93	0.030	40.32	0.22	0.21	13.99	0.19	**100.90**
Ol6-6_2	9.85	46.62	-	40.61	0.24	0.18	13.56	0.19	**101.40**
Ol6-6_3	21.03	46.07	0.010	40.26	0.23	0.22	12.99	0.17	**99.94**
Ol6-6_4	30.88	47.28	-	40.98	0.21	0.24	13.21	0.21	**102.12**
Ol6-6_5	41.17	46.23	0.025	40.24	0.21	0.20	12.68	0.22	**99.81**
Ol6-6_6	51.02	47.00	0.017	40.94	0.22	0.16	12.84	0.20	**101.38**
Ol6-6_7	62.20	46.48	0.035	40.54	0.23	0.18	12.59	0.20	**100.24**
Ol6-6_8	72.05	46.61	0.013	40.62	0.20	0.17	12.48	0.22	**100.31**
Ol6-6_9	82.35	46.51	0.010	40.05	0.23	0.15	12.63	0.20	**99.78**
Ol6-6_11	103.41	46.56	0.023	40.52	0.23	0.24	12.43	0.24	**100.24**
Ol6-6_12	113.26	47.01	0.023	40.86	0.23	0.25	12.33	0.22	**100.92**
Ol6-6_13	124.44	46.65	-	40.66	0.19	0.17	12.37	0.22	**100.26**
Ol6-6_14	134.29	46.66	0.014	40.65	0.23	0.16	12.46	0.22	**100.39**
Ol6-6_16	154.44	47.20	0.014	41.00	0.22	0.22	12.69	0.22	**101.56**
Ol6-6_17	165.62	46.64	0.007	40.77	0.19	0.21	12.44	0.25	**100.51**
Ol6-6_18	175.47	46.38	0.021	40.45	0.21	0.14	12.31	0.21	**99.73**
Ol6-6_19	185.76	46.89	0.029	40.74	0.20	0.21	12.54	0.24	**100.85**
Ol6-6_20	196.53	46.96	0.012	40.58	0.21	0.16	12.34	0.23	**100.49**
Ol6-6_21	206.83	46.65	0.015	40.60	0.18	0.23	12.29	0.26	**100.22**
Ol6-6_22	216.68	46.66	0.005	40.78	0.22	0.22	12.61	0.20	**100.70**
Ol6-6_23	226.97	45.75	0.029	40.47	0.20	0.22	13.12	0.19	**99.98**
Ol6-6_24	237.74	45.84	0.045	40.69	0.20	0.24	14.19	0.18	**101.39**
Ol6-6_25	248.04 - Rim	44.30	0.013	39.77	0.21	0.30	15.28	0.15	**100.01**

Table 67: EPMA analyses of the major element composition of an olivine crystal. The dash symbol (-) represent concentration under the detection limit of the instruments.

D12D2 - Ol 6(2)									
Name	Distance (µm)	MgO	Al_2O_3	SiO_2	CaO	MnO	FeO	NiO	Total
ol6(2)_1	Core - 0	46.68	-	39.89	0.22	0.20	12.93	0.23	**100.20**
ol6(2)_2	15.26	46.76	0.004	40.08	0.20	0.24	12.67	0.27	**100.28**
ol6(2)_3	31.39	47.12	0.025	39.96	0.19	0.20	12.91	0.28	**100.71**
ol6(2)_4	46.65	46.93	0.038	40.10	0.22	0.21	12.47	0.20	**100.17**
ol6(2)_5	78.56	47.04	0.017	40.34	0.23	0.22	12.22	0.19	**100.31**
ol6(2)_6	94.68	46.99	0.007	39.86	0.24	0.17	12.20	0.24	**99.72**
ol6(2)_7	109.00	46.97	0.016	40.00	0.21	0.25	12.38	0.23	**100.09**
ol6(2)_8	126.49	46.83	0.022	39.89	0.20	0.21	12.48	0.25	**99.89**
ol6(2)_9	143.14	47.02	0.012	39.46	0.22	0.22	12.26	0.18	**99.43**
ol6(2)_10	160.63	47.05	-	39.40	0.21	0.17	12.14	0.28	**99.29**
ol6(2)_11	178.12	46.95	0.024	39.30	0.20	0.19	12.21	0.23	**99.13**
ol6(2)_12	195.62	46.55	0.027	39.35	0.19	0.20	12.03	0.22	**98.55**
ol6(2)_13	212.82	46.58	0.013	39.27	0.19	0.23	12.36	0.24	**98.88**
ol6(2)_14	230.31	46.57	0.022	39.15	0.18	0.25	11.85	0.28	**98.35**
ol6(2)_15	247.81	46.51	-	38.99	0.20	0.18	12.40	0.21	**98.55**
ol6(2)_16	265.30	46.51	0.005	38.83	0.21	0.20	12.41	0.23	**98.45**
ol6(2)_17	299.43 - Rim	46.08	0.033	38.51	0.16	0.22	12.89	0.22	**98.13**

Table 68: The major element composition of an olivine crystal from sample D12D2. The dash symbol (-) represent concentration under the detection limit of the instruments.

D12D2 - Ol 7									
Name	Distance (µm)	MgO	Al_2O_3	SiO_2	CaO	MnO	FeO	NiO	Total
Ol7-7_49	Core - 0	46.92	0.034	39.22	0.20	0.17	12.16	0.24	**98.94**
Ol7-7_47	11.40	46.81	0.011	39.64	0.18	0.19	11.65	0.25	**98.73**
Ol7-7_46	21.84	47.17	0.033	39.61	0.20	0.20	11.78	0.26	**99.26**
Ol7-7_45	33.24	46.74	0.001	39.26	0.20	0.15	11.84	0.27	**98.45**
Ol7-7_43	43.68	47.24	0.020	39.84	0.21	0.19	11.65	0.25	**99.40**
Ol7-7_42	55.09	47.28	0.038	39.24	0.23	0.17	11.36	0.25	**98.56**
Ol7-7_41	66.49	47.35	0.049	39.99	0.22	0.12	11.56	0.24	**99.54**
Ol7-7_40	76.69	47.25	0.002	40.00	0.19	0.21	11.39	0.27	**99.31**
Ol7-7_39	88.09	47.23	0.036	40.06	0.20	0.14	11.40	0.27	**99.33**
Ol7-7_38	98.53	47.24	0.009	39.99	0.20	0.16	11.25	0.29	**99.14**
Ol7-7_37	109.93	47.36	0.037	40.07	0.25	0.15	11.32	0.26	**99.44**
Ol7-7_36	121.33	47.27	0.033	39.97	0.25	0.20	11.54	0.26	**99.52**
Ol7-7_35	131.77	47.40	0.023	40.11	0.22	0.16	11.43	0.26	**99.60**
Ol7-7_34	143.17	47.38	0.016	40.22	0.18	0.17	11.43	0.25	**99.65**
Ol7-7_33	153.61	47.49	0.011	40.27	0.23	0.15	11.18	0.25	**99.57**
Ol7-7_32	165.02	47.42	0.013	40.13	0.21	0.19	11.33	0.25	**99.53**

Table 69: EPMA analyses of the major element composition of an olivine crystal. The dash symbol (-) represent concentration under the detection limit of the instruments.

D12D2 - Ol 7									
Name	Distance (µm)	MgO	Al_2O_3	SiO_2	CaO	MnO	FeO	NiO	Total
Ol7-7_31	175.46	47.36	0.028	40.28	0.21	0.18	11.44	0.28	**99.77**
Ol7-7_30	186.86	47.55	0.002	40.20	0.21	0.19	11.55	0.28	**99.99**
Ol7-7_29	198.26	47.44	0.019	39.98	0.20	0.19	11.68	0.24	**99.75**
Ol7-7_28	208.46	47.50	0.014	40.05	0.21	0.20	11.73	0.24	**99.94**
Ol7-7_27	219.86	47.23	0.019	40.20	0.20	0.16	11.64	0.26	**99.72**
Ol7-7_26	230.30	47.22	0.031	40.42	0.24	0.20	11.80	0.27	**100.18**
Ol7-7_25	241.70	47.14	0.022	40.47	0.22	0.19	11.72	0.29	**100.06**
Ol7-7_24	253.10	47.09	0.078	40.48	0.25	0.17	11.60	0.28	**99.94**
Ol7-7_23	263.54	47.48	0.021	40.37	0.20	0.17	12.24	0.26	**100.75**
Ol7-7_22	274.94	46.87	0.021	40.34	0.20	0.13	12.05	0.25	**99.86**
Ol7-7_21	285.39	47.10	0.027	40.70	0.22	0.17	11.87	0.24	**100.32**
Ol7-7_20	296.79	47.10	0.031	40.42	0.19	0.23	11.92	0.28	**100.17**
Ol7-7_19	308.19	47.15	0.001	40.50	0.23	0.19	11.88	0.28	**100.23**
Ol7-7_18	318.63	47.36	0.001	40.97	0.23	0.19	12.09	0.25	**101.08**
Ol7-7_17	330.03	47.09	0.011	40.67	0.21	0.20	12.03	0.25	**100.45**
Ol7-7_16	340.23	46.87	0.012	40.48	0.21	0.19	12.36	0.27	**100.38**
Ol7-7_15	351.63	46.69	0.027	40.45	0.20	0.16	12.27	0.25	**100.05**
Ol7-7_14	363.03	46.76	0.017	40.70	0.19	0.23	12.36	0.21	**100.47**
Ol7-7_13	373.47	46.69	0.015	40.64	0.22	0.18	12.25	0.26	**100.26**
Ol7-7_12	384.87	46.63	0.010	40.90	0.19	0.21	12.69	0.23	**100.85**
Ol7-7_11	395.31	46.76	-	40.69	0.20	0.22	12.90	0.26	**101.03**
Ol7-7_10	406.72	45.22	0.858	39.42	0.25	0.19	12.57	0.25	**98.76**
Ol7-7_9	417.16	46.33	0.013	40.69	0.21	0.21	12.78	0.29	**100.52**
Ol7-7_8	428.56	46.26	0.009	40.66	0.21	0.20	12.97	0.26	**100.58**
Ol7-7_7	439.96	45.95	0.025	40.74	0.22	0.19	13.02	0.27	**100.41**
Ol7-7_6	450.40	46.24	-	40.93	0.23	0.21	13.11	0.24	**100.96**
Ol7-7_5	461.80	45.99	0.008	40.45	0.21	0.16	13.46	0.24	**100.53**
Ol7-7_4	483.40	46.03	0.020	40.58	0.22	0.21	13.32	0.21	**100.59**
Ol7-7_3	494.80	45.81	0.038	40.43	0.21	0.20	13.27	0.25	**100.20**
Ol7-7_2	505.24	45.50	0.019	40.31	0.20	0.23	13.32	0.26	**99.83**
Ol7-7_1	527.09 - Rim	45.73	0.020	40.87	0.20	0.22	13.71	0.26	**101.01**

Table 69: Continuation.

D12D2 - Cpx 1											
Name	Distance (µm)	Na_2O	MgO	Al_2O_3	SiO_2	CaO	TiO_2	Cr_2O_3	MnO	FeO	Total
cpx1-1_2	Core - 0	0.25	16.95	1.98	52.49	21.13	0.52	0.13	0.21	6.14	**99.80**
cpx1-1_3	12	0.33	16.46	2.21	51.67	21.63	0.65	0.08	0.18	6.08	**99.29**
cpx1-1_4	24	0.24	16.53	2.21	51.89	21.34	0.60	0.10	0.11	5.95	**98.97**
cpx1-1_5	36	0.29	16.23	2.43	51.47	21.50	0.64	0.10	0.20	6.16	**99.01**
cpx1-1_6	48	0.27	16.42	2.25	51.57	21.75	0.60	0.09	0.16	6.11	**99.21**
cpx1-1_7	60	0.32	16.19	2.41	50.97	21.46	0.65	0.07	0.16	6.26	**98.50**
cpx1-1_8	72	0.35	16.26	2.46	51.06	21.52	0.67	0.06	0.19	5.95	**98.53**
cpx1-1_9	84	0.26	16.15	2.54	51.33	21.28	0.70	0.07	0.18	6.04	**98.55**
cpx1-1_10	96	0.33	16.66	2.88	51.37	21.66	0.66	0.07	0.19	6.09	**99.92**
cpx1-1_11	108	0.30	16.26	2.45	51.20	21.67	0.64	0.08	0.18	6.15	**98.93**
cpx1-1_12	120	0.33	16.34	2.55	51.29	21.29	0.62	0.09	0.23	6.19	**98.92**
cpx1-1_13	132	0.33	16.34	5.59	47.84	17.99	0.55	0.19	0.12	6.85	**95.80**
cpx1-1_14	144	0.26	16.56	3.43	51.31	22.01	0.51	0.60	0.12	4.80	**99.61**
cpx1-1_15	156	0.24	16.45	3.73	50.95	21.70	0.54	0.74	0.15	4.81	**99.32**
cpx1-1_16	168	0.28	16.59	3.86	51.00	21.72	0.54	0.74	0.13	4.57	**99.42**
cpx1-1_17	180	0.21	16.91	2.94	51.52	21.69	0.41	0.79	0.10	4.34	**98.91**
cpx1-1_18	192	0.25	17.14	2.90	51.96	21.34	0.45	0.51	0.14	4.66	**99.33**
cpx1-1_19	204	0.26	17.02	2.85	51.53	21.52	0.42	0.55	0.14	4.55	**98.83**
cpx1-1_20	216	0.27	16.54	3.33	51.19	21.74	0.40	0.93	0.12	4.33	**98.85**
cpx1-1_21	228	0.25	16.73	3.03	51.44	22.02	0.45	1.03	0.12	4.25	**99.32**
cpx1-1_22	240	0.24	16.38	3.33	51.11	22.21	0.50	1.14	0.14	4.29	**99.34**
cpx1-1_23	252	0.24	16.85	2.84	51.13	22.06	0.44	0.78	0.11	4.27	**98.74**
cpx1-1_24	264	0.25	16.84	2.88	51.53	22.28	0.41	0.78	0.07	4.19	**99.23**
cpx1-1_25	276	0.23	16.69	2.81	51.52	22.24	0.41	0.74	0.13	4.26	**99.04**
cpx1-1_26	288	0.20	16.61	2.81	51.48	22.40	0.43	0.61	0.07	4.42	**99.03**
cpx1-1_27	300	0.25	16.78	2.80	51.91	22.31	0.43	0.66	0.15	4.50	**99.80**
cpx1-1_28	312	0.26	16.73	2.76	51.76	22.37	0.44	0.59	0.10	4.47	**99.49**
cpx1-1_29	324	0.22	16.68	2.79	51.85	22.37	0.45	0.56	0.11	4.54	**99.58**
cpx1-1_30	336	0.23	16.62	2.77	51.33	22.40	0.47	0.55	0.14	4.55	**99.06**
cpx1-1_31	348	0.22	16.89	2.73	51.55	22.37	0.42	0.47	0.18	4.64	**99.47**
cpx1-1_32	360	0.22	16.74	2.66	51.65	22.20	0.45	0.45	0.13	4.55	**99.05**
cpx1-1_33	372	0.27	16.60	3.03	51.24	22.05	0.51	0.51	0.13	4.67	**99.01**
cpx1-1_34	384	0.22	16.62	3.08	51.09	22.14	0.54	0.44	0.16	4.74	**99.02**
cpx1-1_35	396	0.26	16.09	4.05	49.76	20.96	0.67	0.23	0.14	6.00	**98.18**
cpx1-1_36	408	0.26	16.35	3.73	50.91	22.03	0.52	0.92	0.12	4.47	**99.32**
cpx1-1_37	420	0.25	16.33	3.60	51.09	22.07	0.56	0.84	0.11	4.66	**99.50**
cpx1-1_38	432	0.31	16.45	3.80	50.59	21.47	0.58	0.57	0.11	5.03	**98.92**
cpx1-1_39	444	0.27	16.96	2.90	51.78	21.84	0.49	0.47	0.12	4.84	**99.67**
cpx1-1_40	456 - Rim	0.26	16.04	3.87	50.34	21.34	0.87	0.28	0.19	6.11	**99.31**

Table 70: The major element composition of a pyroxene crystal from sample D12D2.

D12D2 - Cpx 3											
Name	Distance (µm)	Na_2O	MgO	Al_2O_3	SiO_2	CaO	TiO_2	Cr_2O_3	MnO	FeO	Total
cpx3-1_1	0	0.24	16.49	2.20	51.73	21.80	0.57	0.01	0.18	5.80	**99.01**
cpx3-1_2	12	0.24	16.19	2.16	51.57	21.95	0.55	0.04	0.19	5.80	**98.70**
cpx3-1_3	24	0.24	16.52	2.17	51.44	22.03	0.54	0.06	0.16	5.63	**98.79**
cpx3-1_4	36	0.26	16.53	2.09	51.76	21.84	0.55	0.07	0.23	5.61	**98.94**
cpx3-1_5	48	0.25	16.32	2.17	51.81	22.09	0.56	0.02	0.16	5.66	**99.03**
cpx3-1_6	60	0.27	16.40	2.16	51.50	22.08	0.53	0.05	0.20	5.61	**98.81**
cpx3-1_7	72	0.22	16.46	2.12	51.55	21.95	0.52	0.02	0.13	5.47	**98.44**
cpx3-1_8	84	0.23	16.35	2.12	51.67	22.19	0.54	0.05	0.19	5.42	**98.75**
cpx3-1_9	96	0.23	16.55	2.11	51.42	22.33	0.53	0.04	0.21	5.40	**98.82**
cpx3-1_10	108	0.27	16.38	2.10	51.66	22.06	0.55	0.02	0.16	5.43	**98.65**
cpx3-1_11	120	0.25	16.50	2.08	51.80	21.96	0.51	0.06	0.16	5.50	**98.83**
cpx3-1_12	132	0.25	16.62	2.11	51.69	22.06	0.53	0.01	0.18	5.32	**98.77**
cpx3-1_13	144	0.24	16.51	2.09	51.41	21.80	0.51	0.01	0.14	5.52	**98.25**
cpx3-1_14	156	0.30	16.52	2.13	51.97	22.03	0.52	0.03	0.19	5.30	**98.99**
cpx3-1_15	168	0.26	16.71	2.24	51.30	22.31	0.53	0.03	0.11	5.41	**98.91**
cpx3-1_16	180	0.24	16.39	2.22	51.63	22.18	0.50	0.05	0.19	5.48	**98.89**
cpx3-1_17	192	0.23	16.41	2.16	51.62	21.96	0.48	0.08	0.13	5.46	**98.54**
cpx3-1_18	204	0.25	16.48	2.23	51.49	21.95	0.55	0.03	0.18	5.51	**98.68**
cpx3-1_19	216	0.25	16.41	2.21	51.48	21.94	0.52	0.06	0.11	5.36	**98.34**
cpx3-1_20	228	0.19	16.50	2.28	51.38	22.03	0.58	0.09	0.15	5.30	**98.50**
cpx3-1_21	240	0.26	16.38	2.23	51.58	21.99	0.54	0.12	0.18	5.36	**98.65**
cpx3-1_22	252	0.26	16.45	2.33	51.32	21.90	0.52	0.07	0.22	5.49	**98.56**
cpx3-1_23	264	0.25	16.22	2.32	51.88	21.75	0.54	0.09	0.20	5.56	**98.80**
cpx3-1_24	276	0.21	16.48	2.31	51.81	21.74	0.53	0.09	0.18	5.70	**99.04**
cpx3-1_25	288	0.23	16.55	2.31	51.56	22.03	0.56	0.08	0.15	5.39	**98.86**
cpx3-1_26	300	0.23	16.51	2.29	51.36	21.88	0.52	0.10	0.16	5.40	**98.47**
cpx3-1_27	312	0.25	16.41	2.27	51.59	21.88	0.53	0.05	0.17	5.57	**98.73**
cpx3-1_28	324	0.22	16.43	2.32	51.39	21.66	0.55	0.08	0.19	5.40	**98.25**
cpx3-1_29	336	0.22	16.47	2.32	51.73	21.87	0.52	0.06	0.16	5.54	**98.89**
cpx3-1_30	348	0.23	16.41	2.31	51.55	21.80	0.53	0.07	0.15	5.40	**98.43**
cpx3-1_31	360	0.27	16.43	2.49	51.80	21.58	0.51	0.08	0.16	5.71	**99.04**
cpx3-1_32	372	0.24	16.64	2.26	51.66	21.75	0.53	0.10	0.15	5.63	**98.95**
cpx3-1_33	384	0.29	16.44	2.22	51.90	21.68	0.52	0.10	0.18	5.45	**98.77**
cpx3-1_34	396	0.20	16.59	2.31	51.22	21.81	0.54	0.10	0.18	5.47	**98.43**
cpx3-1_35	408	0.24	16.46	2.23	51.60	22.19	0.54	0.01	0.19	5.49	**98.95**
cpx3-1_36	420	0.26	16.26	2.26	51.64	21.82	0.54	0.01	0.16	5.68	**98.62**
cpx3-1_37	432	0.25	16.22	2.33	51.33	22.10	0.60	0.03	0.18	5.62	**98.66**
cpx3-1_38	444	0.26	16.30	2.30	51.01	21.97	0.61	0.03	0.16	5.66	**98.29**
cpx3-1_39	456	0.28	16.34	2.30	51.12	21.90	0.60	0.02	0.14	6.07	**98.78**

Table 71: EPMA analyses of the major element composition of a pyroxene crystal.

D12D2 - Cpx 3											
Name	Distance (µm)	Na_2O	MgO	Al_2O_3	SiO_2	CaO	TiO_2	Cr_2O_3	MnO	FeO	Total
cpx3-1_40	468	0.24	16.36	2.24	50.67	21.99	0.66	0.07	0.17	5.71	**98.11**
cpx3-1_41	480	0.26	16.38	2.21	51.25	21.70	0.64	0.04	0.20	6.09	**98.75**
cpx3-1_42	492	0.30	16.13	2.29	50.85	21.78	0.69	0.06	0.20	6.15	**98.46**
cpx3-1_43	504	0.28	16.09	2.30	50.74	21.82	0.68	0.04	0.19	5.99	**98.13**
cpx3-1_44	516	0.28	16.16	2.34	50.92	21.70	0.69	0.05	0.18	6.06	**98.38**
cpx3-1_45	528	0.26	16.19	2.37	50.68	21.79	0.67	0.07	0.17	6.09	**98.29**
cpx3-1_46	540	0.33	15.95	2.34	50.96	21.82	0.70	0.02	0.16	6.07	**98.33**
cpx3-1_47	552	0.30	16.16	2.39	50.94	21.99	0.69	0.06	0.15	6.23	**98.91**
cpx3-1_48	564	0.28	16.39	2.29	50.84	21.88	0.67	0.08	0.16	5.85	**98.44**
cpx3-1_49	576	0.27	16.49	3.45	50.35	22.07	0.43	1.00	0.13	4.20	**98.38**
cpx3-1_50	588	0.25	16.38	3.02	50.83	22.02	0.50	0.47	0.12	4.85	**98.43**
cpx3-1_51	600	0.22	16.10	2.42	50.93	21.88	0.66	0.11	0.13	5.87	**98.32**
cpx3-1_52	612	0.22	16.47	3.26	50.46	21.94	0.54	0.57	0.14	4.82	**98.41**
cpx3-1_53	624	0.25	16.50	3.32	50.60	22.20	0.43	0.96	0.10	3.98	**98.32**
cpx3-1_54	636	0.22	16.44	3.24	50.66	22.24	0.44	0.97	0.11	4.23	**98.57**
cpx3-1_55	648	0.28	16.13	3.47	48.58	21.57	0.62	1.01	0.05	4.36	**96.08**
cpx3-1_56	660	0.22	16.38	3.29	50.52	22.07	0.45	0.99	0.16	4.19	**98.27**
cpx3-1_57	672	0.28	16.54	3.29	50.52	22.25	0.45	1.00	0.12	4.24	**98.69**
cpx3-1_58	684	0.24	16.75	3.37	50.63	21.77	0.47	0.58	0.14	4.30	**98.26**
cpx3-1_59	696	0.23	16.68	3.07	50.76	21.92	0.50	0.67	0.17	4.62	**98.62**

Table 71: Continuation.

D12D2 - Cpx 4											
Name	Distance (µm)	Na_2O	MgO	Al_2O_3	SiO_2	CaO	TiO_2	Cr_2O_3	MnO	FeO	Total
cpx4-1_1	Core - 0	0.30	16.50	4.25	50.60	22.65	0.41	1.14	0.07	3.56	**99.49**
cpx4-1_2	14	0.28	16.27	4.27	50.52	22.34	0.46	1.13	0.09	3.64	**99.01**
cpx4-1_3	28	0.27	16.41	4.18	50.18	22.41	0.47	1.11	0.11	3.46	**98.59**
cpx4-1_4	42	0.26	16.42	4.19	50.52	22.57	0.47	1.16	0.09	3.62	**99.30**
cpx4-1_5	56	0.23	16.46	4.17	50.40	22.53	0.44	1.11	0.10	3.52	**98.98**
cpx4-1_6	70	0.29	16.31	4.13	50.45	22.42	0.45	1.11	0.06	3.54	**98.77**
cpx4-1_7	84	0.29	16.35	4.11	50.44	22.26	0.47	1.17	0.09	3.57	**98.76**
cpx4-1_8	98	0.24	16.13	4.09	50.60	22.28	0.45	1.10	0.05	3.43	**98.37**
cpx4-1_9	112	0.27	16.42	4.10	50.54	22.61	0.43	1.11	0.11	3.60	**99.18**
cpx4-1_10	126	0.28	16.38	4.08	50.57	22.40	0.42	1.17	0.07	3.53	**98.89**
cpx4-1_11	140	0.25	16.45	4.17	50.53	22.37	0.44	1.11	0.11	3.61	**99.02**
cpx4-1_12	154	0.25	16.37	4.09	50.50	22.50	0.42	1.14	0.06	3.56	**98.89**
cpx4-1_13	168	0.28	16.43	4.06	50.61	22.40	0.41	1.17	0.08	3.61	**99.05**
cpx4-1_14	182	0.29	16.35	4.01	50.28	22.18	0.44	1.17	0.06	3.59	**98.38**
cpx4-1_15	196	0.29	16.19	4.04	50.59	22.36	0.44	1.12	0.10	3.74	**98.88**
cpx4-1_16	210	0.26	16.36	4.02	50.60	22.36	0.44	0.99	0.10	3.75	**98.89**
cpx4-1_17	224	0.30	16.26	4.04	50.57	22.42	0.43	1.12	0.10	3.77	**99.01**
cpx4-1_18	238	0.28	16.28	3.93	50.85	22.59	0.45	1.10	0.06	3.64	**99.18**
cpx4-1_19	252	0.29	16.35	3.99	50.38	22.37	0.46	1.10	0.09	3.76	**98.79**
cpx4-1_20	266	0.28	16.24	4.04	50.64	22.32	0.41	1.01	0.10	3.73	**98.77**
cpx4-1_21	280	0.30	16.36	3.95	50.81	22.21	0.43	1.21	0.07	3.69	**99.03**
cpx4-1_22	294	0.31	16.50	3.96	50.50	22.32	0.41	1.14	0.08	3.91	**99.14**
cpx4-1_23	308	0.36	16.24	4.01	50.92	22.30	0.44	1.12	0.10	3.76	**99.25**
cpx4-1_24	322	0.29	16.21	3.89	50.42	22.22	0.44	1.09	0.11	3.88	**98.56**
cpx4-1_25	336	0.32	16.28	3.92	50.34	22.25	0.43	1.13	0.10	3.92	**98.71**
cpx4-1_26	350	0.50	13.49	5.21	49.88	20.12	0.68	1.09	0.13	3.99	**95.09**
cpx4-1_27	364	0.79	16.66	2.71	38.58	21.90	0.44	1.03	0.14	3.82	**86.06**
cpx4-1_28	378	0.30	16.38	3.71	50.26	22.45	0.46	0.99	0.08	3.84	**98.47**
cpx4-1_29	392	0.29	16.31	3.70	50.93	22.45	0.44	0.81	0.09	4.16	**99.19**
cpx4-1_30	406	0.28	16.42	3.70	50.97	22.39	0.48	0.76	0.10	3.90	**98.99**
cpx4-1_31	420	0.30	16.61	3.66	51.00	22.13	0.46	0.71	0.08	4.15	**99.08**
cpx4-1_32	434	0.29	16.32	3.60	50.99	22.32	0.44	0.67	0.08	4.12	**98.82**
cpx4-1_33	448	0.29	16.32	3.66	51.23	22.32	0.45	0.68	0.10	4.24	**99.28**
cpx4-1_34	462	0.28	16.43	3.54	50.84	22.27	0.48	0.64	0.10	4.40	**98.98**
cpx4-1_35	476	0.29	16.46	3.54	51.17	22.14	0.46	0.69	0.15	4.44	**99.33**
cpx4-1_36	490	0.26	16.42	3.49	51.18	22.11	0.46	0.73	0.10	4.42	**99.17**
cpx4-1_37	504	0.30	16.50	3.34	51.24	22.04	0.42	0.69	0.13	4.41	**99.07**
cpx4-1_38	518	0.29	16.70	3.27	51.24	22.26	0.43	0.64	0.11	4.55	**99.48**
cpx4-1_39	532	0.28	16.64	3.06	51.28	22.09	0.40	0.56	0.09	4.60	**99.01**
cpx4-1_40	546	0.24	16.60	2.97	51.38	21.98	0.40	0.57	0.12	4.57	**98.83**

Table 72: EPMA analyses of the major element composition of a pyroxene crystal

D12D2 - Cpx 4											
Name	Distance (µm)	Na_2O	MgO	Al_2O_3	SiO_2	CaO	TiO_2	Cr_2O_3	MnO	FeO	Total
cpx4-1_41	560	0.30	16.74	2.86	51.23	21.93	0.37	0.42	0.11	4.59	**98.54**
cpx4-1_42	574	0.25	16.54	2.84	51.58	21.94	0.40	0.46	0.14	4.69	**98.84**
cpx4-1_43	588	0.27	16.61	2.90	51.63	21.83	0.41	0.50	0.09	4.68	**98.91**
cpx4-1_44	602	0.27	16.51	2.95	51.32	22.02	0.41	0.54	0.16	4.83	**99.02**
cpx4-1_45	616	0.32	16.41	3.05	51.25	21.95	0.44	0.65	0.12	4.76	**98.95**
cpx4-1_46	630	0.26	16.56	3.06	51.28	21.85	0.45	0.72	0.14	4.90	**99.22**
cpx4-1_47	644	0.30	16.17	3.21	51.04	21.93	0.45	0.79	0.11	4.77	**98.77**
cpx4-1_48	658	0.38	16.30	3.21	50.21	21.91	0.46	0.80	0.15	4.88	**98.30**
cpx4-1_49	672	0.31	16.10	3.28	50.86	21.74	0.50	0.88	0.08	4.93	**98.68**
cpx4-1_50	686	0.31	16.27	3.22	50.94	21.78	0.52	0.77	0.09	4.84	**98.76**
cpx4-1_51	700	0.37	16.24	2.99	51.11	21.73	0.53	0.71	0.13	4.86	**98.68**
cpx4-1_52	714	0.28	16.44	3.12	51.19	21.91	0.52	0.60	0.12	5.06	**99.23**
cpx4-1_53	728	0.26	15.64	3.53	51.15	21.77	0.51	0.51	0.07	4.94	**98.36**
cpx4-1_54	742	0.28	16.61	3.04	51.42	21.78	0.51	0.48	0.11	4.88	**99.12**
cpx4-1_55	756	0.24	17.09	3.74	51.00	21.47	0.38	0.70	0.11	4.30	**99.02**
cpx4-1_56	770	0.25	17.14	3.16	51.48	21.62	0.44	0.40	0.16	4.60	**99.26**
cpx4-1_57	784	0.19	17.21	2.76	51.58	21.40	0.43	0.35	0.14	4.65	**98.72**
cpx4-1_58	798	0.21	17.14	2.79	51.80	21.74	0.40	0.42	0.11	4.73	**99.34**
cpx4-1_59	812	0.23	17.13	2.82	51.60	21.50	0.40	0.41	0.16	4.56	**98.80**
cpx4-1_60	826	0.21	16.53	3.34	50.93	21.98	0.45	1.03	0.07	4.43	**98.98**
cpx4-1_61	840	0.22	16.76	2.93	51.27	22.16	0.42	0.93	0.13	4.09	**98.92**
cpx4-1_62	854	0.25	16.84	2.94	51.58	22.01	0.39	0.96	0.11	4.15	**99.25**
cpx4-1_63	868	0.23	17.04	3.37	51.37	21.35	0.37	0.83	0.13	3.84	**98.53**
cpx4-1_64	882	0.29	16.90	2.89	51.32	22.16	0.41	0.84	0.12	4.38	**99.30**
cpx4-1_65	896	0.25	16.75	2.81	51.52	21.98	0.40	0.84	0.11	4.17	**98.84**
cpx4-1_66	910	0.23	17.07	2.62	51.74	22.03	0.42	0.75	0.12	4.16	**99.14**
cpx4-1_67	924	0.24	17.09	3.23	51.20	21.73	0.37	0.91	0.09	3.91	**98.77**
cpx4-1_68	938	0.23	16.90	3.11	51.29	22.01	0.41	0.87	0.09	3.86	**98.78**
cpx4-1_69	952	0.20	16.96	2.81	51.64	22.02	0.38	0.80	0.13	4.04	**98.97**
cpx4-1_70	966 - Rim	0.23	17.30	2.45	52.02	21.50	0.40	0.55	0.15	4.50	**99.10**

Table 72: Continuation.

Sample	Cpx 1			Cpx 3				
Elemen /Name	**cpx1-01**	**cpx1-02**	**cpx1-03**	**cpx3-01**	**cpx3-02**	**cpx3-03**	**cpx3-04**	**cpx3-05**
Distance (µm)	72	228	420	36	120	264	516	636
Sc	140.10	111.80	127.55	159.18	157.12	153.85	165.59	154.02
Ti	3785.14	2934.44	3061.09	3381.65	3153.38	3036.18	3747.03	3641.4
V	376.88	348.50	333.56	368.53	340.31	327.71	418.61	388.38
Cr	663.18	4414.92	2997.66	347.83	476.25	582.80	295.36	2035.07
Mn	1390.53	1118.09	1075.59	1260.67	1213.74	1211.52	1320.47	1200.56
Co	38.45	21.46	25.31	30.79	26.79	28.90	28.73	30.82
Ni	134.95	226.54	199.16	139.20	123.21	113.19	116.32	132.64
Zn	43.01	36.70	15.57	30.16	31.45	30.19	41.76	29.17
Rb	-	-	-	-	-	-	-	-
Sr	27.85	13.68	27.07	33.04	29.42	26.51	29.44	31.28
Y	22.47	13.86	10.91	16.67	17.03	14.76	20.29	15.77
Zr	33.22	8.76	12.78	19.79	19.77	17.03	23.37	19.27
Nb	-	-	-	-	-	-	-	-
Cs	0.32	-	-	-	-	-	-	-
Ba	-	-	-	-	-	-	-	-
La	4.90	0.59	0.89	3.18	3.43	2.57	3.42	2.54
Ce	14.81	5.97	7.31	9.77	8.46	8.51	9.74	9.08
Pr	1.45	1.28	0.22	1.15	1.39	1.40	1.53	2.01
Nd	10.64	4.57	6.02	8.84	8.43	8.38	9.86	9.21
Sm	0.60	-	1.68	2.85	1.41	3.38	3.58	2.47
Eu	0.37	0.60	0.47	0.61	0.76	-	0.85	0.72
Gd	7.70	5.82	1.62	2.75	2.06	2.98	3.23	3.12
Tb	0.41	0.19	0.47	0.87	0.51	0.35	0.53	0.82
Dy	4.24	0.43	2.15	3.42	2.93	3.62	3.97	3.15
Ho	0.58	0.43	-	1.03	0.44	0.72	0.87	0.499
Er	3.02	1.48	-	1.44	2.49	1.34	1.96	1.25
Tm		0.33	-	0.14	0.42	0.08	-	0.057
Yb	3.64	-	-	-	-	1.53	0.60	-
Lu	0.35	-	-	0.39	-	0.41	0.21	0.133
Hf	1.13	-	-	0.80	-	0.15	1.96	-
Ta	-	-	-	-	-	0.09	-	0.077
Pb	0.82	-	-	-	-	-	-	0.38
Th	1.64	-	-	-	-	-	-	-
U	-	-	-	-	-	-	-	-

Table 73: Trace element analyses of Cpx 1 and 3. The dash symbol (-) represent concentration under the detection limit of the instruments.

Sample	Cpx 4							
Elemen /Name	**cpx4-01**	**cpx4-03**	**cpx4-04**	**cpx4-05**	**cpx4-06**	**cpx4-07**	**cpx4-08**	**cpx4-09**
Distance (µm)	56	336	546	700	798	826	924	952
Sc	98.94	96.06	91.91	85.23	99.21	114.26	104.96	106.81
Ti	2568.55	2473.55	2327.22	1954.56	2999.02	2610.22	2338.60	2212.53
V	233.29	230.63	246.46	230.92	309.71	295.45	258.48	260.22
Cr	7888.30	7678.41	2712.38	2175.62	3455.53	4150.46	6019.67	4648.53
Mn	733.29	788.28	896.29	1007.87	1151.32	1036.12	904.50	1095.13
Co	25.41	25.44	25.82	29.51	27.52	28.03	27.54	34.56
Ni	270.63	267.49	260.31	253.15	245.96	257.05	281.32	211.84
Zn	15.97	11.88	18.16	24.58	28.00	21.60	16.35	12.11
Rb	-	-	-	-	-	1.12	-	-
Sr	32.10	35.09	34.43	34.54	33.85	27.95	22.76	24.21
Y	8.93	9.74	9.26	10.91	13.37	13.36	9.70	10.5
Zr	12.37	10.37	11.26	10.72	16.18	11.41	7.83	9.55
Nb	-	0.13	-	0.31	0.10	-	0.06	-
Cs	5.64	0.02	0.02	-	0.08	-	0.05	-
Ba	-	-	0.15	2.28	-	-	-	-
La	1.24	1.90	1.68	2.08	2.69	1.83	0.85	1.01
Ce	4.89	5.81	7.58	8.59	9.07	5.16	3.34	3.99
Pr	0.54	1.08	0.93	0.93	1.31	0.85	0.73	0.674
Nd	4.30	5.01	5.97	5.97	8.55	3.88	4.09	3.23
Sm	1.09	-	1.50	2.36	2.12	1.89	0.68	0.34
Eu	0.59	0.53	0.56	0.36	0.94	0.53	0.48	0.54
Gd	1.64	1.75	2.01	2.34	2.10	1.98	1.52	2.36
Tb	0.39	0.34	0.26	0.19	0.42	0.60	0.35	0.266
Dy	1.02	1.41	1.25	2.17	3.51	2.11	2.12	1.76
Ho	0.39	0.33	0.41	0.52	0.44	0.46	0.25	0.358
Er	0.32	1.13	0.74	1.37	1.55	1.23	1.21	0.24
Tm	0.18	-	0.06	0.05	0.24	-	0.22	-
Yb	0.40	0.41	0.72	1.64	-	-	-	-
Lu	0.02	0.05	0.08	0.06	0.26	0.18	0.20	
Hf	0.91	-	0.64	0.14	0.22	0.29		0.16
Ta	-	-	-	-	-	-	0.19	-
Pb	-	1.86	-	0.42	0.37	-	-	-
Th	-	-	-	-	0.15	0.14	0.18	-
U	-	-	-	-	-	-	0.10	-

Table 74: Trace element analyses of Cpx 4. The dash symbol (-) represent concentration under the detection limit of the instruments.

Appendix VIII – Sample D12AB(1) and D12AB(2)

This appendix contains the major element analyses of 8 olivines and the trace elements of 6 pyroxenes.

D16AB(1) - Ol 1									
Name	Distance (µm)	MgO	Al_2O_3	SiO_2	CaO	MnO	FeO	NiO	Total
ol1-1_1	Core - 0	36.67	-	37.86	0.27	0.47	24.63	0.02	**99.92**
ol1-1_2	10.00	36.73	0.011	38.46	0.22	0.43	24.94	0.02	**100.81**
ol1-1_3	20.63	36.62	0.035	38.56	0.26	0.42	24.84	0.04	**100.77**
ol1-1_4	29.85	36.70	0.006	38.39	0.23	0.41	24.99	0.03	**100.75**
ol1-1_5	39.85	36.51	-	38.40	0.27	0.44	25.04	0.03	**100.68**
ol1-1_6	49.85	36.17	0.029	37.78	0.24	0.43	24.95	0.03	**99.63**
ol1-1_7	60.48	36.69	0.022	38.19	0.24	0.45	25.04	0.03	**100.66**
ol1-1_8	70.48	36.99	0.009	38.39	0.24	0.52	25.25	0.02	**101.43**
ol1-1_9	79.70	36.76	0.005	38.14	0.23	0.42	24.81	0.04	**100.41**
ol1-1_10	90.33	36.62	-	37.94	0.21	0.43	24.80	0.04	**100.01**
ol1-1_11	100.33	36.85	-	38.35	0.22	0.46	25.15	0.02	**101.04**
ol1-1_12	110.33	36.81	-	38.57	0.22	0.51	25.05	0.03	**101.19**
ol1-1_13	120.33	36.66	0.002	38.00	0.25	0.43	24.75	0.06	**100.15**
ol1-1_14	130.23	36.97	-	38.30	0.22	0.41	24.71	0.07	**100.68**
ol1-1_15	140.23	36.64	0.014	38.28	0.25	0.42	24.51	0.04	**100.15**
ol1-1_16	150.23	36.42	0.032	37.78	0.21	0.45	24.27	0.04	**99.21**
ol1-1_17	160.86	36.69	-	38.35	0.23	0.44	24.05	0.04	**99.79**
ol1-1_18	170.86	36.52	0.027	38.20	0.25	0.45	23.84	0.05	**99.33**
ol1-1_19	180.08	37.15	-	38.46	0.24	0.48	24.60	0.06	**100.99**
ol1-1_20	190.08	37.36	0.001	38.40	0.25	0.38	24.49	0.03	**100.91**
ol1-1_21	200.71	37.07	0.007	38.16	0.22	0.43	24.05	0.05	**99.98**
ol1-1_22	210.71	36.81	-	37.98	0.26	0.47	23.75	0.05	**99.32**
ol1-1_23	219.93	37.25	-	38.88	0.20	0.38	24.11	0.06	**100.88**
ol1-1_24	229.93	36.96	-	37.89	0.21	0.37	23.72	0.03	**99.17**
ol1-1_25	250.56	37.27	0.018	38.34	0.24	0.43	23.97	0.03	**100.30**
ol1-1_26	260.56	37.21	0.024	38.24	0.25	0.49	23.93	0.04	**100.18**
ol1-1_27	270.46	36.54	-	37.76	0.23	0.43	23.84	0.06	**98.87**
ol1-1_28	280.46	36.69	0.003	37.67	0.24	0.41	24.32	0.04	**99.37**
ol1-1_29	290.46	36.67	0.003	37.99	0.25	0.46	24.13	0.05	**99.56**
ol1-1_30	300.46	36.62	0.021	37.70	0.24	0.48	24.66	0.04	**99.76**
ol1-1_31	311.09	36.57	-	37.71	0.22	0.42	24.75	0.03	**99.70**
ol1-1_32	320.31	36.17	-	38.10	0.23	0.42	25.29	0.03	**100.25**
ol1-1_33	330.31	36.09	-	37.86	0.23	0.39	25.42	0.02	**100.02**
ol1-1_34	340.94	35.85	-	37.85	0.24	0.54	25.64	0.00	**100.11**
ol1-1_35	350.94	35.43	-	37.42	0.22	0.52	25.52	0.01	**99.13**
ol1-1_36	360.94	35.68	-	37.73	0.22	0.46	26.11	0.02	**100.21**
ol1-1_37	370.16	35.83	0.010	37.75	0.18	0.63	25.36	0.00	**99.77**
ol1-1_38	380.79 - Rim	38.36	0.007	38.10	0.24	0.38	22.65	0.01	**99.75**

Table 75: EPMA analyses of the major element composition of an olivine crystal. The dash symbol (-) represent concentration under the detection limit of the instruments.

D16AB(1) - Ol 2									
Name	Distance (µm)	MgO	Al_2O_3	SiO_2	CaO	MnO	FeO	NiO	Total
ol2-2_1	Core - 0	42.52	0.026	38.66	0.31	0.23	16.60	0.11	**98.45**
ol2-2_2	10.00	42.50	0.032	39.04	0.29	0.30	16.49	0.11	**98.76**
ol2-2_3	21.00	42.59	-	38.90	0.26	0.26	16.83	0.11	**98.96**
ol2-2_4	31.00	42.70	0.017	39.28	0.28	0.26	16.78	0.10	**99.42**
ol2-2_5	42.00	42.74	0.048	39.06	0.27	0.27	16.67	0.09	**99.15**
ol2-2_6	52.00	42.83	0.002	38.89	0.30	0.26	16.35	0.10	**98.73**
ol2-2_7	62.00	42.85	0.004	39.21	0.28	0.32	16.87	0.10	**99.64**
ol2-2_8	73.00	42.86	0.014	39.04	0.31	0.25	16.82	0.12	**99.41**
ol2-2_9	83.00	42.96	0.010	39.20	0.32	0.24	17.20	0.10	**100.03**
ol2-2_10	93.00	42.83	-	39.16	0.27	0.24	16.86	0.12	**99.48**
ol2-2_11	104.00	42.50	0.013	38.85	0.27	0.28	16.52	0.12	**98.55**
ol2-2_12	114.00	42.75	0.035	39.22	0.29	0.27	16.63	0.12	**99.33**
ol2-2_13	125.00	42.63	0.009	39.31	0.30	0.28	16.97	0.11	**99.60**
ol2-2_14	135.00	42.51	0.014	39.02	0.33	0.27	16.72	0.09	**98.95**
ol2-2_15	145.00	42.79	0.007	39.46	0.28	0.31	17.65	0.12	**100.62**
ol2-2_16	156.05	42.40	0.058	39.47	0.26	0.26	17.28	0.11	**99.83**
ol2-2_17	166.05	43.03	0.013	39.63	0.28	0.28	17.55	0.11	**100.89**
ol2-2_18	176.05	42.75	0.045	39.45	0.31	0.28	17.53	0.10	**100.45**
ol2-2_19	187.05	41.89	0.055	39.00	0.29	0.22	17.27	0.10	**98.81**
ol2-2_20	197.05	42.48	0.020	39.16	0.28	0.27	17.63	0.10	**99.94**
ol2-2_21	208.05	41.67	0.011	38.53	0.25	0.29	17.79	0.12	**98.68**
ol2-2_22	218.05	41.44	0.003	39.01	0.27	0.31	18.14	0.09	**99.26**
ol2-2_23	228.05	41.53	0.041	39.08	0.28	0.22	18.84	0.09	**100.09**
ol2-2_24	239.05	40.93	0.023	38.58	0.25	0.31	19.16	0.07	**99.32**
ol2-2_25	249.05	40.72	0.037	38.80	0.26	0.32	19.31	0.09	**99.54**
ol2-2_26	259.05	40.58	0.037	38.77	0.25	0.30	19.61	0.08	**99.63**
ol2-2_27	270.05	40.09	0.009	38.75	0.28	0.27	19.82	0.08	**99.30**
ol2-2_28	280.05	40.19	-	38.77	0.26	0.32	19.77	0.05	**99.36**
ol2-2_29	291.05	40.73	-	38.81	0.27	0.28	19.59	0.07	**99.75**
ol2-2_30	301.05	41.32	0.023	38.93	0.33	0.33	18.15	0.06	**99.15**

Table 76: The major element composition of an olivine crystal from sample D16AB(1). The dash symbol (-) represent concentration under the detection limit of the instruments.

D16AB(1) - Ol 3									
Name	**Distance (µm)**	**MgO**	**Al_2O_3**	**SiO_2**	**CaO**	**MnO**	**FeO**	**NiO**	**Total**
ol3-3_1	Core - 0	42.65	-	39.59	0.31	0.27	17.71	0.07	**100.60**
ol3-3_2	9.49	42.27	0.01	38.96	0.28	0.23	17.58	0.10	**99.43**
ol3-3_3	18.43	42.05	-	38.95	0.26	0.27	17.17	0.10	**98.80**
ol3-3_4	27.92	42.35	0.03	39.07	0.29	0.32	17.28	0.09	**99.43**
ol3-3_5	37.40	42.08	0.03	39.08	0.30	0.28	17.18	0.10	**99.05**
ol3-3_6	47.25	42.18	0.01	39.38	0.30	0.28	17.35	0.06	**99.55**
ol3-3_7	55.80	42.31	0.02	39.35	0.30	0.28	17.29	0.09	**99.63**
ol3-3_8	65.65	42.48	0.03	39.17	0.29	0.29	17.60	0.09	**99.95**
ol3-3_9	75.13	42.06	-	39.47	0.27	0.27	17.29	0.07	**99.44**
ol3-3_10	84.62	42.42	0.02	39.33	0.28	0.31	17.56	0.08	**100.00**
ol3-3_11	93.56	42.41	0.03	39.50	0.26	0.28	17.45	0.09	**100.04**
ol3-3_12	103.05	42.65	0.02	39.40	0.28	0.38	17.48	0.09	**100.28**
ol3-3_13	112.54	42.20	0.01	39.63	0.26	0.27	17.85	0.10	**100.33**
ol3-3_14	122.39	42.32	0.01	39.06	0.28	0.32	17.75	0.08	**99.82**
ol3-3_15	130.93	41.92	-	39.34	0.27	0.24	17.84	0.09	**99.71**
ol3-3_16	140.78	41.71	0.01	39.39	0.27	0.31	17.81	0.08	**99.58**
ol3-3_17	150.27	41.46	0.03	39.03	0.31	0.27	17.87	0.09	**99.07**
ol3-3_18	159.75	42.32	0.02	39.44	0.27	0.33	18.48	0.12	**100.98**
ol3-3_19	168.70	41.80	0.04	39.38	0.32	0.27	17.79	0.07	**99.67**
ol3-3_20	178.18 - Rim	42.14	0.02	39.51	0.33	0.30	18.00	0.08	**100.39**

Table 77: EPMA analyses of the major element composition of an olivine crystal. The dash symbol (-) represent concentration under the detection limit of the instruments.

D16AB(1) - Ol 4									
Name	Distance (µm)	MgO	Al_2O_3	SiO_2	CaO	MnO	FeO	NiO	Total
ol4_1	Rim - 0	42.97	0.006	39.96	0.29	0.28	17.03	0.10	**100.63**
ol4_2	9.22	44.22	0.031	39.80	0.26	0.23	15.13	0.10	**99.76**
ol4_3	17.70	44.61	0.013	39.58	0.29	0.26	14.41	0.12	**99.29**
ol4_4	26.31	45.08	0.023	40.07	0.32	0.22	14.76	0.13	**100.60**
ol4_5	34.79	45.07	0.035	40.20	0.29	0.21	14.77	0.15	**100.73**
ol4_6	44.01	44.83	0.037	39.98	0.31	0.22	14.67	0.14	**100.19**
ol4_7	52.50	44.83	0.014	39.97	0.32	0.25	14.76	0.12	**100.25**
ol4_8	61.10	44.81	0.024	39.95	0.31	0.24	14.94	0.12	**100.39**
ol4_9	70.32	44.91	0.044	39.83	0.29	0.24	14.67	0.13	**100.11**
ol4_10	78.80	44.87	0.018	40.12	0.31	0.20	14.83	0.10	**100.45**
ol4_11	88.02	44.85	0.018	39.88	0.31	0.28	14.46	0.13	**99.92**
ol4_12	95.83	44.63	0.004	40.07	0.29	0.23	14.34	0.14	**99.70**
ol4_13	105.05	45.06	0.023	40.12	0.31	0.22	14.71	0.15	**100.60**
ol4_14	113.54	44.78	0.005	40.12	0.27	0.21	14.66	0.10	**100.15**
ol4_15	122.76	44.56	0.042	39.96	0.30	0.21	14.58	0.12	**99.77**
ol4_16	131.24	44.59	0.034	40.18	0.29	0.31	14.46	0.11	**99.97**
ol4_17	139.85	44.63	0.015	40.01	0.30	0.24	14.64	0.10	**99.95**
ol4_18	149.07	44.80	0.027	39.78	0.31	0.24	14.43	0.14	**99.73**
ol4_19	157.55	44.95	0.016	40.09	0.30	0.22	14.39	0.14	**100.10**
ol4_20	166.77	44.70	0.023	39.99	0.30	0.19	14.63	0.11	**99.95**
ol4_21	174.58	44.57	0.006	39.72	0.29	0.25	14.44	0.12	**99.39**
ol4_22	183.80	44.37	0.030	39.90	0.30	0.27	14.75	0.13	**99.74**
ol4_23	192.29	44.26	0.018	39.84	0.25	0.25	14.43	0.10	**99.15**
ol4_24	201.51	44.43	0.013	40.10	0.30	0.24	14.58	0.12	**99.78**
ol4_25	210.11	45.06	0.038	40.41	0.31	0.24	14.56	0.11	**100.73**
ol4_26	218.59	44.66	0.021	40.08	0.26	0.21	14.47	0.13	**99.84**
ol4_27	227.81	45.45	0.033	40.44	0.27	0.25	15.01	0.14	**101.60**
ol4_28	236.30	44.54	0.015	39.37	0.30	0.23	14.50	0.14	**99.10**
ol4_29	245.52	44.23	0.009	39.51	0.28	0.28	14.63	0.13	**99.08**
ol4_30	253.33	44.27	0.006	39.53	0.26	0.25	14.44	0.15	**98.90**
ol4_31	262.55	44.79	0.003	40.22	0.28	0.23	14.74	0.11	**100.37**
ol4_32	271.03	45.23	-	40.35	0.32	0.22	14.45	0.11	**100.67**
ol4_33	280.25	44.80	0.008	39.92	0.29	0.28	14.53	0.15	**99.97**
ol4_34	288.85	44.30	0.009	39.57	0.29	0.25	14.32	0.14	**98.88**
ol4_35	297.34	44.50	0.025	39.74	0.27	0.21	14.50	0.12	**99.37**
ol4_36	306.56	44.97	-	40.04	0.30	0.26	14.49	0.11	**100.17**
ol4_37	315.04	44.63	0.014	39.79	0.31	0.20	14.36	0.12	**99.42**
ol4_38	323.65	44.77	0.015	39.80	0.31	0.20	14.54	0.13	**99.77**
ol4_39	332.13	45.12	-	40.45	0.30	0.26	14.89	0.12	**101.14**
ol4_40	341.35 - Rim	44.33	0.030	40.13	0.32	0.26	15.73	0.13	**100.94**

Table 78: The major element composition of an olivine crystal from sample D16AB(1). The dash symbol (-) represent concentration under the detection limit of the instruments.

D16AB(1) - Ol 4									
Name	Distance (µm)	MgO	Al_2O_3	SiO_2	CaO	MnO	FeO	NiO	Total
ol5_1	Core -0	42.66	-	39.57	0.30	0.31	17.09	0.10	**100.04**
ol5_2	9	42.91	0.02	39.77	0.28	0.31	17.03	0.11	**100.42**
ol5_3	18	42.95	0.03	40.01	0.30	0.32	17.12	0.10	**100.82**
ol5_4	28	43.09	0.02	40.07	0.28	0.28	17.23	0.09	**101.05**
ol5_5	37	42.73	-	40.16	0.29	0.33	17.24	0.10	**100.84**
ol5_6	46	42.69	0.04	39.55	0.29	0.28	17.51	0.12	**100.48**
ol5_7	55	41.89	0.02	39.53	0.30	0.29	16.99	0.10	**99.11**
ol5_8	64	42.07	0.01	39.23	0.27	0.29	17.22	0.08	**99.16**
ol5_9	73	42.12	0.02	39.00	0.30	0.27	17.28	0.11	**99.09**
ol5_10	83	42.59	0.02	39.99	0.29	0.27	17.73	0.11	**100.99**
ol5_11	92	42.09	0.01	39.39	0.30	0.31	17.32	0.10	**99.51**
ol5_12	101	42.09	0.03	39.74	0.26	0.26	17.45	0.11	**99.94**
ol5_13	110	41.90	-	39.64	0.30	0.24	17.46	0.10	**99.63**
ol5_14	119	41.62	0.01	38.83	0.26	0.30	17.41	0.08	**98.51**
ol5_15	129	40.94	0.02	41.18	0.28	0.30	17.87	0.10	**100.68**
ol5_16	138	41.99	-	39.24	0.29	0.30	18.05	0.13	**99.99**
ol5_17	147	42.23	0.01	39.05	0.27	0.31	17.94	0.09	**99.90**
ol5_18	156	43.06	0.08	38.14	0.39	0.29	17.75	0.08	**99.79**
ol5_19	165	41.42	0.02	39.62	0.30	0.30	18.04	0.08	**99.78**
ol5_20	174	40.93	0.01	39.12	0.28	0.29	17.98	0.09	**98.70**
ol5_21	193 - Rim	41.34	0.01	39.13	0.23	0.29	18.14	0.08	**99.22**

Table 79: EPMA analyses of the major element composition of an olivine crystal. The dash symbol (-) represent concentration under the detection limit of the instruments.

D16AB(2) - Ol 1												
Name	Distance (µm)	Na_2O	MgO	Al_2O_3	SiO_2	CaO	TiO_2	Cr_2O_3	MnO	FeO	NiO	Total
ol1-_1	Core - 0	0.015	43.35	0.014	39.56	0.27	-	0.017	0.31	16.73	0.11	**100.37**
ol1-_2	10	-	43.29	0.024	39.49	0.30	0.004	-	0.28	16.75	0.10	**100.25**
ol1-_3	20	-	43.08	0.028	39.50	0.27	0.023	0.033	0.24	16.43	0.14	**99.74**
ol1-_4	30	-	43.04	0.005	39.57	0.31	0.014	0.038	0.28	16.67	0.15	**100.08**
ol1-_5	40	-	43.36	0.007	39.72	0.31	-	0.027	0.31	16.54	0.09	**100.37**
ol1-_6	50	0.000	42.89	0.022	39.32	0.28	0.022	0.014	0.27	16.37	0.19	**99.37**
ol1-_7	60	0.004	43.30	0.010	39.40	0.32	-	0.007	0.28	16.74	0.09	**100.15**
ol1-_8	70	-	43.24	0.006	39.58	0.28	0.004	0.003	0.27	16.59	0.07	**100.03**
ol1-_9	80	0.014	43.06	0.045	39.50	0.30	0.009	-	0.34	16.43	0.12	**99.82**
ol1-_10	90	-	43.19	-	39.57	0.29	0.007	-	0.30	16.71	0.08	**100.14**
ol1-_11	100	-	43.26	0.012	39.54	0.26	0.015	-	0.23	16.80	0.13	**100.25**
ol1-_12	110	-	43.13	0.032	39.55	0.25	0.012	0.019	0.26	16.93	0.15	**100.34**
ol1-_13	120	0.018	42.82	0.036	39.52	0.27	0.002	0.023	0.26	16.70	0.17	**99.83**
ol1-_14	130	-	43.02	0.007	39.56	0.30	-	0.020	0.34	16.76	0.08	**100.09**
ol1-_15	140	0.004	43.35	0.019	39.43	0.32	-	0.024	0.35	16.49	0.07	**100.06**
ol1-_16	150	0.003	42.99	0.018	39.05	0.30	0.006	-	0.26	16.88	0.13	**99.64**
ol1-_17	170	-	42.54	0.025	39.38	0.27	0.009	0.010	0.27	17.24	0.10	**99.85**
ol1-_18	180	0.011	42.93	0.007	39.55	0.29	-	0.011	0.28	17.33	0.04	**100.44**
ol1-_19	190	0.039	42.59	0.018	39.43	0.26	0.011	0.011	0.30	17.22	0.07	**99.94**
ol1-_20	200	0.001	42.34	0.051	39.56	0.28	0.001	0.027	0.32	17.36	0.13	**100.07**
ol1-_21	210	-	42.69	0.006	39.28	0.28	-	0.026	0.26	17.37	0.08	**100.00**
ol1-_22	220	-	42.53	0.013	39.30	0.28	0.013	0.011	0.32	17.41	0.15	**100.02**
ol1-_23	230	-	42.09	0.033	39.28	0.26	0.012	0.016	0.33	17.72	0.07	**99.81**
ol1-_24	240	-	42.24	0.012	39.40	0.28	0.010	-	0.34	17.64	0.09	**100.01**
ol1-_25	250	-	41.87	0.017	39.24	0.31	0.018	0.006	0.28	18.04	0.12	**99.90**
ol1-_26	260	-	41.80	0.026	39.11	0.27	0.023	-	0.33	18.03	0.10	**99.68**
ol1-_27	270	-	41.45	-	39.12	0.29	0.020	-	0.35	18.30	0.07	**99.60**
ol1-_28	280	-	41.27	0.025	38.96	0.29	0.008	0.048	0.37	18.80	0.12	**99.89**
ol1-_29	290 - Rim	0.006	41.71	0.015	39.09	0.32	0.018	0.011	0.35	17.82	0.07	**99.41**

Table 80: The major element composition of an olivine crystal from sample D16AB(2). The dash symbol (-) represent concentration under the detection limit of the instruments.

D16AB(2) - Ol 1												
Name	Distance (µm)	Na_2O	MgO	Al_2O_3	SiO_2	CaO	TiO_2	Cr_2O_3	MnO	FeO	NiO	Total
ol2_1	Core - 0	-	42.47	0.010	38.96	0.26	0.019	0.017	0.29	17.14	0.11	**99.28**
ol2_2	10	-	42.10	-	39.02	0.29	0.018	0.037	0.27	17.22	0.10	**99.06**
ol2_3	20	-	42.31	0.006	38.96	0.29	0.009	0.012	0.28	17.11	0.10	**99.08**
ol2_4	30	-	42.26	-	38.97	0.26	0.013	-	0.27	17.01	0.11	**98.88**
ol2_5	40	-	42.48	0.010	38.94	0.26	0.021	0.010	0.29	17.34	0.12	**99.48**
ol2_6	50	-	42.31	0.014	39.03	0.28	0.001	-	0.28	16.87	0.07	**98.85**
ol2_7	60	0.020	42.50	0.021	39.06	0.30	-	0.038	0.28	17.21	0.11	**99.54**
ol2_8	70	-	42.43	0.012	39.05	0.26	0.009	0.008	0.31	16.86	0.11	**99.05**
ol2_9	80	-	42.50	0.020	39.19	0.26	0.027	0.028	0.25	17.02	0.15	**99.44**
ol2_10	100	-	42.44	0.008	38.91	0.30	0.011	0.014	0.30	17.03	0.10	**99.11**
ol2_11	110	-	42.27	0.016	38.94	0.30	0.026	0.019	0.25	17.02	0.03	**98.87**
ol2_12	120	0.009	42.31	0.023	39.16	0.32	0.005	0.016	0.28	16.97	0.12	**99.21**
ol2_13	130	-	42.45	0.022	38.98	0.28	0.020	0.012	0.32	16.84	0.10	**99.03**
ol2_14	140	0.009	42.13	0.040	39.24	0.30	0.014	0.008	0.29	17.01	0.10	**99.15**
ol2_15	150	0.010	42.23	0.028	39.16	0.30	-	0.023	0.29	16.70	0.10	**98.84**
ol2_16	160	0.008	41.55	0.087	39.24	0.32	0.022	-	0.34	16.93	0.10	**98.60**
ol2_17	170	0.001	42.56	0.026	39.14	0.27	0.017	-	0.33	17.36	0.11	**99.82**
ol2_18	180	0.005	42.52	0.014	39.38	0.29	0.029	0.026	0.23	17.19	0.08	**99.77**
ol2_19	190	-	42.29	0.029	39.21	0.31	0.016	-	0.31	16.90	0.11	**99.16**
ol2_20	200	0.015	42.57	0.023	39.05	0.28	0.031	0.033	0.27	16.95	0.09	**99.31**
ol2_21	210	-	42.51	0.023	38.90	0.29	0.002	0.030	0.31	16.84	0.09	**98.99**
ol2_22	220	0.016	42.31	0.045	39.17	0.30	0.026	0.015	0.24	17.05	0.11	**99.27**
ol2_23	230	-	42.65	0.018	39.24	0.29	-	0.007	0.28	16.95	0.10	**99.55**
ol2_24	240	0.030	42.33	-	39.09	0.30	0.033	-	0.28	16.95	0.13	**99.14**
ol2_25	250	0.011	42.22	0.043	39.11	0.30	-	0.021	0.21	17.03	0.09	**99.03**
ol2_26	260	-	42.53	0.043	39.22	0.31	0.022	0.006	0.25	16.90	0.10	**99.40**
ol2_27	270	-	42.26	0.024	39.07	0.31	0.016	0.020	0.29	16.64	0.14	**98.77**
ol2_28	280	-	42.44	0.037	39.06	0.29	0.029	0.012	0.29	17.17	0.18	**99.52**
ol2_29	290	-	42.16	0.022	39.24	0.28	0.008	0.008	0.29	16.87	0.10	**98.99**
ol2_30	300	-	42.40	0.053	39.28	0.28	-	0.029	0.25	17.35	0.09	**99.72**
ol2_31	310	-	42.04	0.027	39.04	0.26	-	0.018	0.32	17.04	0.10	**98.85**
ol2_32	320	-	42.15	0.003	38.85	0.27	0.009	-	0.32	17.24	0.07	**98.92**
ol2_33	330	-	42.07	0.027	39.25	0.28	0.006	0.005	0.27	17.09	0.09	**99.10**
ol2_34	340	-	42.19	-	38.90	0.28	0.015	0.034	0.27	17.09	0.12	**98.89**
ol2_35	350	0.004	42.26	0.019	38.86	0.29	0.003	0.025	0.28	17.30	0.11	**99.14**
ol2_36	360	-	42.07	0.031	38.94	0.28	0.023	0.018	0.26	17.49	0.09	**99.20**
ol2_37	380	-	42.04	0.034	39.14	0.29	0.001	-	0.31	17.12	0.11	**99.05**

Table 81: EPMA analyses of the major element composition of an olivine crystal. The dash symbol (-) represent concentration under the detection limit of the instruments

D16AB(2) - Ol 1												
Name	Distance (µm)	Na_2O	MgO	Al_2O_3	SiO_2	CaO	TiO_2	Cr_2O_3	MnO	FeO	NiO	Total
ol2_38	390	0.024	41.96	-	39.14	0.26	0.005	-	0.29	17.76	0.06	**99.50**
ol2_39	410	-	41.72	0.009	38.64	0.31	0.009	0.036	0.28	17.69	0.07	**98.78**
ol2_40	420	0.015	41.68	0.027	38.91	0.26	0.036	-	0.27	17.15	0.12	**98.47**
ol2_41	430	0.009	41.65	0.016	38.76	0.24	0.005	-	0.39	17.49	0.11	**98.68**
ol2_42	440	0.016	41.70	-	38.91	0.26	0.019	0.007	0.32	17.62	0.09	**98.93**
ol2_43	450	-	42.00	-	38.76	0.29	0.020	0.017	0.27	17.81	0.08	**99.24**
ol2_44	460	-	41.83	0.004	38.89	0.26	0.014	0.006	0.31	17.40	0.09	**98.80**
ol2_45	470	0.022	41.96	0.029	38.88	0.27	0.015	0.016	0.28	17.57	0.05	**99.09**
ol2_46	480	-	42.00	0.015	39.14	0.30	0.010	0.008	0.30	17.55	0.12	**99.45**
ol2_47	490 - Rim	-	42.34	0.025	39.23	0.29	0.029	0.020	0.32	16.96	0.11	**99.32**

Table 82: Continuation.

D16AB(2) - Ol 1												
Name	Distance (µm)	Na_2O	MgO	Al_2O_3	SiO_2	CaO	TiO_2	Cr_2O_3	MnO	FeO	NiO	Total
ol3-1_1	cire - 0	0.025	41.00	0.014	38.84	0.18	0.02	-	0.33	18.68	0.13	**99.23**
ol3-1_2	10	-	40.98	0.019	39.01	0.17	0.02	0.028	0.43	18.50	0.05	**99.21**
ol3-1_3	20	0.001	40.81	0.026	38.77	0.16	0.00	0.032	0.44	18.81	0.08	**99.13**
ol3-1_4	30	0.003	40.96	-	38.87	0.19	0.01	0.006	0.44	18.90	0.11	**99.48**
ol3-1_5	40	0.059	40.47	-	38.89	0.17	0.03	0.034	0.42	18.94	0.11	**99.13**
ol3-1_6	50	0.027	40.82	0.030	38.82	0.16	0.01	0.003	0.38	19.03	0.11	**99.39**
ol3-1_7	60	-	40.80	0.021	38.80	0.16	0.02	-	0.43	18.71	0.15	**99.08**
ol3-1_8	70	0.013	40.53	-	38.97	0.20	0.01	0.025	0.40	18.83	0.09	**99.06**
ol3-1_9	80	0.004	40.76	0.005	38.80	0.16	0.01	0.019	0.38	18.91	0.08	**99.13**
ol3-1_10	90	-	41.00	0.025	38.84	0.13	0.02	0.005	0.41	18.76	0.12	**99.31**
ol3-1_11	100	-	40.86	-	39.03	0.14	0.01	0.027	0.42	19.09	0.11	**99.68**
ol3-1_12	110	0.028	40.76	0.005	38.66	0.16	0.02	0.027	0.41	18.76	0.15	**98.97**
ol3-1_13	120	0.000	40.98	0.005	38.93	0.17	0.03	0.012	0.44	18.92	0.07	**99.55**
ol3-1_14	130	0.033	41.20	0.011	39.09	0.16	0.03	0.001	0.40	19.03	0.09	**100.05**
ol3-1_15	140	-	40.82	0.035	38.94	0.18	0.01	0.010	0.47	18.54	0.15	**99.14**
ol3-1_16	150	-	41.17	0.007	38.69	0.18	0.03	0.011	0.37	18.92	0.06	**99.43**
ol3-1_17	160	-	41.03	0.005	38.91	0.18	0.03	-	0.38	18.48	0.11	**99.12**
ol3-1_18	170	-	41.17	0.022	39.37	0.16	0.02	0.009	0.35	18.48	0.14	**99.73**
ol3-1_19	180	0.021	41.49	0.024	39.15	0.16	0.04	0.021	0.43	18.11	0.14	**99.58**
ol3-1_20	190	0.017	41.63	0.015	39.11	0.13	0.01	0.049	0.41	18.32	0.11	**99.81**
ol3-1_21	200	0.051	41.61	0.013	38.85	0.15	0.01	0.002	0.38	18.41	0.04	**99.51**
ol3-1_22	210	-	41.60	0.000	39.12	0.20	0.01	0.028	0.37	17.71	0.07	**99.09**
ol3-1_23	220	-	41.77	0.026	39.12	0.20	0.01	0.024	0.44	17.83	0.12	**99.55**
ol3-1_24	250	0.021	44.04	0.020	37.71	0.21	0.03	0.028	0.35	17.40	0.11	**99.92**
ol3-1_25	260	-	42.04	0.016	39.11	0.17	0.01	0.026	0.38	17.07	0.10	**98.91**
ol3-1_26	270	0.002	42.23	0.009	39.35	0.22	0.01	0.033	0.36	17.05	0.08	**99.34**
ol3-1_27	280	0.002	42.17	0.018	39.34	0.22	0.02	0.030	0.34	17.00	0.11	**99.24**
ol3-1_28	290 - Rim	-	42.14	0.008	39.69	0.25	0.03	0.018	0.29	17.13	0.13	**99.70**

Table 83: The major element composition of an olivine crystal from sample D16AB(2). The dash symbol (-) represent concentration under the detection limit of the instruments.

D12D2 - Cpx 1											
Name	Distance (µm)	Na_2O	MgO	Al_2O_3	SiO_2	CaO	TiO_2	Cr_2O_3	MnO	FeO	Total
cpx1-1	Core - 0	0.40	15.74	1.50	51.59	20.98	0.53	0.02	0.30	7.49	98.55
cpx1-2	61.10	0.24	16.23	3.28	51.30	22.28	0.54	0.33	0.13	4.91	99.24
cpx1-3	185.42	0.30	16.50	3.15	51.99	22.60	0.55	0.54	0.10	4.66	100.39
cpx1-4	220.14	0.26	16.52	2.91	51.60	22.16	0.51	0.45	0.08	4.70	99.20
cpx1-5	344.42	0.29	16.43	3.31	51.02	21.86	0.58	0.66	0.13	4.98	99.25
cpx1-6	379.13	0.24	16.23	3.18	51.37	22.17	0.55	0.42	0.08	4.66	98.88
cpx1-7	402.15	0.30	16.40	3.06	51.79	22.35	0.53	0.33	0.10	4.80	99.66
cpx1-8	431.31	0.25	16.19	3.11	51.34	22.30	0.51	0.32	0.11	4.76	98.87
cpx1-9	448.33	0.25	16.16	3.03	51.28	22.12	0.53	0.30	0.10	4.81	98.59
cpx1-10	472.75	0.31	16.29	3.22	51.13	22.43	0.57	0.31	0.16	4.86	99.28
cpx1-11	502.48	0.27	16.19	3.13	51.32	22.32	0.57	0.29	0.10	4.99	99.17
cpx1-12	526.33	0.31	16.32	3.11	51.30	22.30	0.54	0.23	0.14	5.14	99.39
cpx1-13	554.51	0.27	15.84	3.84	50.56	21.76	0.72	0.13	0.15	5.71	98.98
cpx1-14	570.79	0.31	16.23	2.93	51.29	22.26	0.58	0.23	0.18	5.28	99.31
cpx1-15	600.79	0.26	16.27	3.00	51.46	22.29	0.59	0.24	0.14	5.04	99.29
cpx1-16	626.79	0.26	16.13	2.75	51.38	21.95	0.65	0.04	0.12	5.69	98.97

Table 84: EPMA analyses of the major element composition of a pyroxene crystal.

D12D2 - Cpx 2											
Name	Distance (µm)	Na_2O	MgO	Al_2O_3	SiO_2	CaO	TiO_2	Cr_2O_3	MnO	FeO	Total
cpx2-2_1	Core - 0	0.32	17.04	2.21	52.01	20.18	0.58	0.09	0.16	6.62	99.22
cpx2-2_2	9	0.25	16.52	2.26	52.15	20.74	0.58	0.09	0.18	6.68	99.45
cpx2-2_3	18	0.27	16.96	2.21	51.62	20.29	0.59	0.10	0.19	6.75	98.97
cpx2-2_4	27	0.24	17.13	2.41	51.76	19.67	0.59	0.10	0.22	7.08	99.19
cpx2-2_5	36	0.25	16.77	2.60	51.46	19.75	0.60	0.12	0.15	6.93	98.63
cpx2-2_6	45	0.27	16.59	2.71	52.66	20.17	0.55	0.08	0.19	7.01	100.23
cpx2-2_7	54	0.31	16.33	2.32	50.84	19.55	0.57	0.09	0.17	6.93	97.12
cpx2-2_8	63	0.26	17.05	2.28	51.53	20.00	0.58	0.06	0.17	6.87	98.80
cpx2-2_9	72	0.27	16.86	2.22	51.89	20.30	0.54	0.09	0.17	6.75	99.10
cpx2-2_10	81	0.30	16.87	2.32	52.56	20.36	0.57	0.10	0.21	6.77	100.07
cpx2-2_11	90	0.45	16.58	2.13	49.07	18.90	0.48	0.12	0.18	6.62	94.52
cpx2-2_12	99	0.32	16.84	2.22	52.14	20.85	0.56	0.17	0.13	6.29	99.51
cpx2-2_13	108	0.32	16.77	2.22	51.98	21.05	0.55	0.13	0.16	6.14	99.31
cpx2-2_14	117	0.30	16.53	2.31	51.88	21.14	0.50	0.19	0.17	5.94	98.97
cpx2-2_15	126	0.29	16.43	2.42	51.78	21.33	0.52	0.12	0.16	6.15	99.20
cpx2-2_16	135	0.29	16.74	2.26	51.68	21.34	0.56	0.10	0.11	6.09	99.18
cpx2-2_17	144	0.30	16.24	2.32	51.87	21.26	0.55	0.10	0.21	6.06	98.91
cpx2-2_18	153	0.27	16.42	2.31	51.92	21.29	0.50	0.15	0.18	6.07	99.11
cpx2-2_19	162	0.31	16.55	2.29	51.73	21.28	0.56	0.11	0.13	6.10	99.06
cpx2-2_20	171	0.30	16.35	2.29	51.84	21.45	0.57	0.11	0.11	6.04	99.07
cpx2-2_21	180	0.32	16.58	2.26	51.82	21.27	0.53	0.13	0.17	6.08	99.15
cpx2-2_22	189	0.28	16.55	2.30	51.54	21.37	0.54	0.14	0.14	6.15	99.01
cpx2-2_23	198	0.29	16.27	2.43	51.83	21.64	0.52	0.17	0.15	5.81	99.12
cpx2-2_24	207	0.27	16.50	2.25	51.90	21.38	0.51	0.12	0.18	6.02	99.13
cpx2-2_25	216	0.26	16.55	2.21	51.80	20.99	0.55	0.14	0.15	6.13	98.77
cpx2-2_26	225	0.32	16.56	2.20	51.92	21.14	0.56	0.11	0.18	6.27	99.26
cpx2-2_27	234	0.30	16.54	2.33	52.18	21.39	0.51	0.12	0.17	5.94	99.48
cpx2-2_28	243	0.28	16.41	2.51	51.74	21.38	0.51	0.25	0.15	5.85	99.09
cpx2-2_29	252	0.28	16.65	2.60	51.58	21.75	0.50	0.35	0.15	5.28	99.13
cpx2-2_30	261	0.25	16.62	2.45	51.83	21.55	0.46	0.43	0.11	5.07	98.77
cpx2-2_31	270	0.25	16.92	2.46	52.02	21.43	0.48	0.35	0.08	5.00	98.98
cpx2-2_32	279	0.30	16.18	3.04	51.42	21.75	0.56	0.34	0.09	5.07	98.75
cpx2-2_33	288	0.32	11.14	2.85	48.47	19.59	0.53	0.28	0.11	5.72	89.01
cpx2-2_34	297	0.28	16.28	2.77	51.20	21.89	0.59	0.21	0.16	5.40	98.79
cpx2-2_35	306	0.31	16.18	2.76	51.71	21.93	0.57	0.24	0.14	5.51	99.34
cpx2-2_36	315	0.28	15.98	2.71	51.37	22.03	0.59	0.14	0.14	5.50	98.74
cpx2-2_37	324	0.31	16.17	2.74	51.73	21.94	0.57	0.18	0.15	5.45	99.24
cpx2-2_38	333	0.29	16.32	2.59	51.47	21.80	0.52	0.13	0.18	5.65	98.95
cpx2-2_39	342	0.24	16.48	2.38	51.50	21.69	0.56	0.46	0.12	5.44	98.88
cpx2-2_40	351 - Rim	0.23	16.41	2.22	51.89	21.33	0.59	0.18	0.19	6.12	99.15

Table 85: The major element composition of a pyroxene crystal from sample D16AB(2)

D12D2 - Cpx 3											
Name	Distance (µm)	Na_2O	MgO	Al_2O_3	SiO_2	CaO	TiO_2	Cr_2O_3	MnO	FeO	Total
cpx3-3_1	Core -0	0.31	15.74	1.96	50.72	19.84	0.68	0.01	0.25	8.21	97.41
cpx3-3_2	9	0.32	15.57	1.99	50.45	19.93	0.70	0.04	0.26	8.06	97.00
cpx3-3_3	18	0.32	15.58	2.01	50.33	20.15	0.71	0.02	0.20	8.20	97.21
cpx3-3_4	27	0.36	15.78	2.02	50.52	20.13	0.69	0.04	0.21	8.20	97.60
cpx3-3_5	36	0.28	15.67	1.91	50.23	19.75	0.69	0.02	0.24	8.11	96.62
cpx3-3_6	45	0.33	15.59	2.10	49.65	19.77	0.66	0.02	0.21	8.24	96.23
cpx3-3_7	54	0.29	15.72	2.20	50.25	19.91	0.71	0.05	0.23	8.06	97.14
cpx3-3_8	63	0.31	15.63	2.13	50.24	20.32	0.70	0.00	0.27	7.75	97.04
cpx3-3_9	72	0.32	15.71	2.09	50.31	20.19	0.67	0.03	0.20	8.02	97.22
cpx3-3_10	81	0.34	15.94	2.11	50.47	19.95	0.69	0.04	0.23	7.97	97.40
cpx3-3_11	90	0.32	15.90	2.08	50.27	19.73	0.67	0.02	0.27	8.34	97.29
cpx3-3_12	99	0.32	15.81	2.01	50.44	20.00	0.72	0.03	0.27	8.21	97.49
cpx3-3_13	108	0.38	15.79	2.04	50.44	19.84	0.70	0.02	0.24	8.10	97.18
cpx3-3_14	117	0.29	15.92	2.06	50.55	20.02	0.70	0.02	0.29	8.65	98.20
cpx3-3_15	126	0.29	15.58	1.95	50.69	20.05	0.71	0.05	0.27	8.42	97.72
cpx3-3_16	135	0.34	15.60	2.02	50.20	20.20	0.70	0.03	0.26	8.12	97.12
cpx3-3_17	144	0.34	15.69	2.00	50.34	19.88	0.66	0.00	0.28	8.24	97.09
cpx3-3_18	153	0.39	10.72	1.66	35.40	12.90	0.51	0.04	0.18	6.19	67.59
cpx3-3_19	162	0.36	15.67	2.12	50.30	20.02	0.63	0.05	0.23	8.09	97.09
cpx3-3_20	171	0.33	15.85	2.14	50.22	20.06	0.71	0.03	0.18	8.07	97.26
cpx3-3_21	180	0.35	15.74	2.03	50.40	19.73	0.71	0.03	0.22	8.08	96.94
cpx3-3_22	189	0.36	14.91	3.15	49.34	20.18	1.07	0.03	0.26	8.60	97.52
cpx3-3_23	198	0.45	14.27	3.87	48.19	20.21	1.25	0.03	0.19	8.84	96.84
cpx3-3_24	207	0.43	14.12	4.23	47.93	19.76	1.34	0.07	0.25	8.97	96.66
cpx3-3_25	216	0.44	14.40	3.78	48.57	20.35	1.21	0.05	0.22	8.59	97.18
cpx3-3_26	225	0.41	14.44	3.87	48.39	20.13	1.20	0.06	0.25	8.56	96.89
cpx3-3_27	234	0.46	14.45	3.62	48.47	20.48	1.11	0.06	0.25	8.31	96.74
cpx3-3_28	243	0.38	15.18	3.01	49.59	21.03	0.88	0.06	0.22	7.53	97.49
cpx3-3_29	252	0.42	14.80	3.39	48.96	20.92	0.93	0.06	0.13	7.72	96.90
cpx3-3_30	261	0.42	14.92	3.40	49.32	20.92	0.94	0.03	0.20	7.68	97.39
cpx3-3_31	270	0.38	15.06	3.29	49.57	20.83	0.90	0.04	0.20	7.68	97.56
cpx3-3_32	279	0.38	14.96	3.20	49.23	21.24	0.92	0.06	0.18	7.48	97.27
cpx3-3_33	288	0.33	14.93	3.31	49.24	21.06	0.88	0.05	0.18	7.28	96.92
cpx3-3_34	297	0.38	15.16	3.20	49.33	21.06	0.84	0.05	0.14	6.89	96.66
cpx3-3_35	306	0.35	15.35	4.03	49.13	21.43	0.82	0.70	0.16	5.55	97.16
cpx3-3_36	315	0.34	15.52	4.08	49.17	21.49	0.81	0.72	0.11	5.57	97.48
cpx3-3_37	324	0.37	15.51	3.94	49.33	21.46	0.80	0.64	0.14	5.70	97.51
cpx3-3_38	333	0.35	15.60	3.83	49.33	21.32	0.75	0.65	0.12	5.68	97.28

Table 86: EPMA analyses of the major element composition of a pyroxene crystal.

Sample	Cpx 1 - D16Ab(2)		Cpx 1 - D16AB(1)			Cpx 6 - D16AB(1)		
Elemen /Name	cpx1-01	cpx1-02	12-D16AB1-cpx1-74	cpx1-75	cpx1-76	cpx6-69	cpx6-70	cpx6-71
Sc	128.74	06-D16AB2-cpx2-03	131.21	107.49	131.64	167.79	152.67	159.18
Ti	3578.02	130.36	4392.79	3765.05	3068.77	5930.78	7361.02	6540.11
V	246.61	3542.10	227.15	262.94	223.82	345.85	382.17	351.1
Cr	1070.33	246.77	1092.23	41.30	884.20	1218.27	299.05	649.14
Mn	1299.70	1551.63	1308.50	1404.34	948.98	1145.46	1235.94	1190.38
Co	46.40	1059.14	37.59	47.90	36.45	36.35	35.09	36.56
Ni	105.33	36.58	57.02	9.75	91.70	94.98	73.13	76.21
Zn	39.14	112.31	-	16.91	6.84	24.04	30.87	34.78
Rb	-	24.62	-	1.71	-	0.23	-	0.40
Sr	28.73	-	29.63	34.18	25.94	25.09	28.10	32.22
Y	17.23	31.23	20.15	15.78	17.94	20.33	22.68	22.77
Zr	17.95	13.22	21.71	25.13	14.65	32.22	41.54	36.46
Nb	0.06	16.06	0.66	-	-	-	0.06	0.20
Cs	-	0.07	-	-	-	-	-	-
Ba	-	-	-	-	-	-	-	2.18
La	1.24	0.42	2.01	1.83	0.37	1.32	1.38	1.81
Ce	4.83	0.97	4.75	5.88	3.68	4.74	7.33	6.75
Pr	0.87	3.39	0.90	0.63	0.91	0.90	1.28	0.89
Nd	6.04	0.75	-	-	-	5.28	6.59	5.59
Sm	2.79	5.19	4.14	2.98	-	1.28	1.25	2.63
Eu	0.63	-	-	3.33	1.06	0.76	0.43	1.32
Gd	3.19	0.44	7.09	-	-	1.80	0.94	6
Tb	0.71	3.06	0.52	0.43	-	0.58	0.41	0.5
Dy	4.21	0.28		3.69	2.97	5.27	5.52	4.63
Ho	0.67	3.12	-	-	-	0.78	0.94	1.21
Er	1.67	0.53	-	-	-	3.25	2.26	3.24
Tm	0.24	2.65	-	-	-		0.16	0.137
Yb	2.10	0.26	-	-	-	1.64	3.02	2.5
Lu	0.15	0.19	0.34	-	-	0.11	-	0.45
Hf	-	0.07	1.70	-	-	-	1.88	-
Ta	0.04	1.28	-	-	0.44	0.15	1.09	0.084
Pb	-	-	-	-	-	-	-	0.25
Th	-	0.22	-	0.90	-	-	0.37	0.58
U	-	-	-	-	-	0.24	-	0.64

Table 87: Trace elements of a pyroxene from D16AB(1) and D16AB(2).

Sample	Cpx 2 - D16AB(1)				
Elemen /Name	cpx1-01	cpx1-02	cpx1-03	cpx1-04	cpx1-05
Sc	187.50	147.71	130.94	124.42	119.30
Ti	7380.38	3978.69	3477.03	3218.41	3174.53
V	501.61	292.48	267.27	208.75	224.62
Cr	3448.54	1230.82	1461.83	1651.40	1434.07
Mn	1505.22	1307.06	1131.79	982.78	942.46
Co	68.26	58.41	35.70	36.56	31.59
Ni	136.66	167.07	165.95	120.20	92.13
Zn	12.17	48.01	35.38	26.99	19.92
Rb	-	-	-	1.17	-
Sr	56.04	40.52	28.19	23.61	22.11
Y	40.63	18.30	12.88	13.36	11.07
Zr	55.69	18.53	18.51	16.49	14.38
Nb	0.71	0.65	-	-	-
Cs	-	-	0.27	-	-
Ba	-	-	-	2.19	2.78
La	4.53	4.07	-	1.28	0.74
Ce	10.27	5.46	4.66	3.52	
Pr	2.58	0.72	0.47	0.23	1.14
Nd	12.27	3.36	2.84	1.97	10.68
Sm	10.60	12.09	-	-	-
Eu	1.08	-	-	-	0.64
Gd	16.92	-	-	-	1.85
Tb	0.93	1.26	-	-	-
Dy	9.26	4.03		2.25	
Ho	1.24	1.48		0.59	0.37
Er	10.13	-	-	-	-
Tm	-	-	-	-	-
Yb	2.16	-	-	2.03	
Lu	-	0.84	-	-	0.44
Hf	-	-	1.78	-	-
Ta	-	-	0.67	-	-
Pb	-	1.78	2.66	-	-
Th	1.40	-	-	0.67	-
U	0.86	-	-	-	-

Table 88: Trace elements of a pyroxene from D16AB(1).